The University Of Sheffield.

Dynamic regulation of endothelial P2X7 receptors by blood flow patterns associated with atherosclerosis

Jack Green

A thesis submitted in partial fulfilment of the requirements for the degree of Doctor of Philosophy

Department of Infection, Immunity and Cardiovascular Disease

School of Medicine

The University of Sheffield

December 2016

Declaration

All the work presented in this thesis was my own and I confirm that approximately 95% of the experiments were carried out by myself.

Help was greatly appreciated by **Neil Bowden** who performed the sacrifice and dissection of murine aortae; from **Professor Paul Evans' group** for use of their mRNA isolated from endothelial cells from the porcine aorta; and by **Kajus Baidžajevas** and **Yang Li** who gladly shared their isolated peripheral blood monocytes.

Acknowledgements

The work in this thesis would not have been possible without the help of several people over the past 3 years.

Firstly, I am indebted to my PhD supervisor Dr Heather Wilson for her invaluable support and guidance during my PhD. Her kind encouragement and patience allowed me to pursue my ideas and develop myself as a scientist. I'd like to thank Professor Paul Evans for his critical insight and useful discussions which helped direct this work. I am grateful to everyone in the O-floor office for putting up with me and for always being willing to listen to my scientific ramblings. You were always a welcome break and I am glad for all the laughs we shared. I am especially thankful to Neil for his friendship, constant company in the lab (Friday evening tissue culture parties won't be the same) and for all the fun we had during the many trips to conferences.

Finally to my family that have supported me not just for the last 3 years, but the last 24 years, for which I am eternally grateful. Without your encouragement, I would not be the person I am today. Especially to my Mum, I am thankful for the love and support you have shown me throughout my life. Last but not least, I cannot thank Charlotte enough for always being there for me and cheering me on. Words cannot explain how much you've done for me, so all I will say is that I am truly glad to be with you and thank you for everything.

Table of Contents

Table of Figures

Table of Tables

List of Abbreviations

5'NT (CD73)	5'-nucleotidase
ADP	Adenosine diphosphate
AMP	Adenosine monophosphate
ApoE	Apolipoprotein E
ASC	Apotosis-associated speck-like protein containing a CARD
ATF2	Activated transcription factor 2
ATP	Adenosine triphosphate
BzATP	2'(3')-O-(4-Benzoylbenzoyl) adenosine-5'-triphosphate
CASP1	Caspase-1
CFD	Computational fluid dynamics
CRAC	Calcium release-activated channel
DAG	Diacylglycerol
DAMP	Damage-associated molecular pattern
ECM	Extracellular matrix
EGTA	Ethylene glycol-bis(β-aminoethyl ether)-N,N,N',N'-tetraacetic acid
EMP1	Epithelial membrane protein-1
EMP2	Epithelial membrane protein 2
EMP3	Epithelial membrane protein-3
eNOS	Endothelial nitric oxide synthase
ENTPD1 (CD39)	Ectonucleoside Triphosphate Diphosphohydrolase 1
ER	Endoplasmic reticulum
ERK	Extracellular signal-regulated kinase
E-selectin	Endothelial-selectin
GAS3	Growth arrest specific 3
GPCR	G-protein coupled receptor
HEK-293	Human embyronic kidney-293
HSP90	Heat shock protein 90
HUVEC	Human umbilical vein endothelial cells
ICAM-1	Intercellular cell adhesion molecule-1
IFNγ	Interferon gamma
IκB	Inhibitor of kappa B
IL-1	Interleukin-1
IL-18	Interleukin-18
IL-1α	Interleukin-1 alpha
IL-1β	Interleukin-1 beta
IL-1ra	Interleukin-1 receptor antagonist
IL-6	Interleukin-6
IL-8	Interleukin-8
IP3	Inositol triphosphate
JNK	c-Jun N-terminal kinases
KLF2	Krüppel-like Factor 2
LDL	Low density lipoprotein

LDLR	Low density lipoprotein receptor
LPS	Lipopolysaccharide
MAPK	Mitogen activated protein kinase
MCP-1	Monocyte chemoattractant protein-1
MDMs	Monocyte derived macrophages
MKP-1	Mitogen activated protein kinase phosphatase-1
NF-κB	Nuclear factor of kappa B
NLRP3	NACHT, LRR and PYD domains-containing protein 3
NO	Nitric oxide
NOS3	Nitric oxide synthase 3
oxLDL	Oxidised low density lipoprotein
P1	Purinergic 1
P2X	Purinergic 2X
P2Y	Purinergic 2Y
PAH	Pulmonary arterial hypertension
PBMCs	Peripheral blood mononuclear cells
PECAM-1	Platelet-endothelial cell adhesion molecule-1
PIP2	Phosphatidylinositol 4,5-bisphosphate
PLC	Phospholipase C
PMP22	Peripheral myeloid protein-22
PNGase	Peptide N-Glycosidase F
P-selectin	Platelet-selectin
ROS	Reactive oxygen species
RTK	Receptor tyrosine kinase
SERCA	Sarco/endoplasmic recticulum Ca2+-ATPase
SOCE	Store-operated calcium entry
TNF	Tumour necrosis factor
UDP	Uridine diphosphate
UTP	Uridine triphosphate
VCAM-1	Vascular cell adhesion molecule-1
VE-cadherin	Vascular endothelium cadherin
VSMC	Vascular smooth muscle cell

Abstract

Aims: Atherosclerosis occurs predominantly at arterial branches and bends that are exposed to disturbed patterns of blood flow. These sites show augmented endothelial inflammatory signalling. Endothelial cells release ATP in response to acute high shear stress but the role of ATP during chronic exposure to low oscillatory shear stress (atheroprone flow) has not been investigated. ATP signalling has been demonstrated to regulate pro-inflammatory signalling. This present study proposes that ATP signalling is enhanced at sites of atheroprone flow and aims to investigate this in endothelial cells subjected to shear stress patterns associated with atherosclerosis and atheroprotection.

Methods and Results: Human umbilical vein endothelial cells (HUVEC) were cultured under physiological atheroprotective or atheroprone flow for 72 hours and endothelial ATP-mediated responses were measured using live cell calcium imaging. Atheroprone flow-conditioned HUVEC exhibited an enhanced ATP-mediated calcium response, which was dependent on calcium influx from the extracellular space through the ATP-gated P2X7 ion channels. Endothelial P2X7 receptor expression was enhanced *in vitro* under atheroprone flow conditions and *in vivo* at atherosusceptible sites of the murine aorta. Furthermore, the ATPase CD39 was up-regulated under atheroprotective flow and this enhanced CD39 activity regulated ATP-induced calcium responses. P2X7 inhibitors were used to evaluate the role of P2X7 under atheroprone flow. P2X7 activation mediated the induction of pro-atherosclerotic interleukin-8 and E-selectin due to disturbed flow. EMP2 was identified as a regulator of macrophage P2X7 responses and its expression was enhanced in endothelial cells under atheroprotective flow patterns, suggesting further regulatory mechanisms of P2X7 signalling may occur in the endothelium.

Conclusion: P2X7 receptors are selectively activated in endothelial cells under atheroprone flow and contribute to the endothelial dysfunction associated with atherogenesis at arterial sites of disturbed flow.

Chapter 1

General Introduction

1.1 Atherosclerosis

Atherosclerosis is an irreversible chronic inflammatory disease which develops over several decades. It is the leading cause of cardiovascular disease, such as myocardial infarction and stroke, responsible for 27% of all deaths in the UK (Townsend et al. 2015). Atherosclerosis develops in the sub-endothelial layer of arteries and leads to occlusion of the vessel, restricting the flow of blood and resulting in infarction (Libby 2002). Due to the seriousness and prevalence of atherosclerosis, extensive research has been carried out characterising the disease process in an attempt to identify therapeutic targets. Figure 1.1 shows a simple schematic illustrating the development of atherosclerosis. The disease process initially occurs following endothelial damage, which is induced by a variety of conditions such as cigarette smoke, hypertension, hypercholesterolemia, diabetes and numerous other stimuli (Nayler 1995), resulting in activation of endothelial cells. This causes release of chemotactic signals, expression of adhesion molecules and an increase in endothelial permeability promoting the migration of circulating immune cells, such as monocytes and T-lymphocytes, from the blood stream into the sub-endothelial space (Hansson & Libby 2006). Increased endothelial permeability, evoked by endothelial-mesenchymal transition (Gasparics et al. 2016) or endothelial damage (von Eckardstein & Rohrer 2009), also enhances transport of circulating LDL across the endothelium. LDL is subsequently oxidised by high levels of reactive oxygen species (ROS) to oxidised LDL and is rapidly taken up by macrophages, converting them into foam cells. Foam cells and activated T-cells release a plethora of cytokines and chemokines perpetuating the inflammatory response (Hansson & Libby 2006). As the disease develops, more lipid-rich LDL and immune cells accumulate in the sub-endothelial layer, creating a lipid rich necrotic core. Increased cytokine release also alters the behaviour of the underlying vascular smooth muscle cells (VSMC), driving VSMC dysfunction. They adopt a 'non-contractile' phenotype, resulting in the increased production of extracellular matrix (ECM)

components and cytokines rather than regulation of vascular constriction. Moreover, they rapidly proliferate and migrate into the sub-endothelial layer where they contribute, along with foam cells and T-cells, to the advancement of the lipid rich necrotic core (Rudijanto 2007). These 'non-contractile/synthetic' cells expressing VSMC markers have been proposed to originate from a variety of cell types within the plaque, not just VSMCs (Bennett et al. 2016). Lineage studies have reported that myeloid and stem cell populations within the arterial wall can adopt expression of SMC markers within the plaque (Bennett et al. 2016). A fibrous cap develops above the lipid rich core and stabilises the atherosclerotic plaque, preventing exposure of the thrombogenic core to the blood stream. However, as the atheroma progresses, plaque rupture can occur resulting in exposure of the core. Exposure of ECM components initiates recruitment of platelets and subsequent thrombus development, which can further occlude the vessel and cause an infarction, starving downstream tissues of nutrients (Libby 2002). As endothelial cell activation is responsible for the initiation of atherosclerosis, their involvement in this process has been extensively researched in the hope of developing preventative therapeutics.

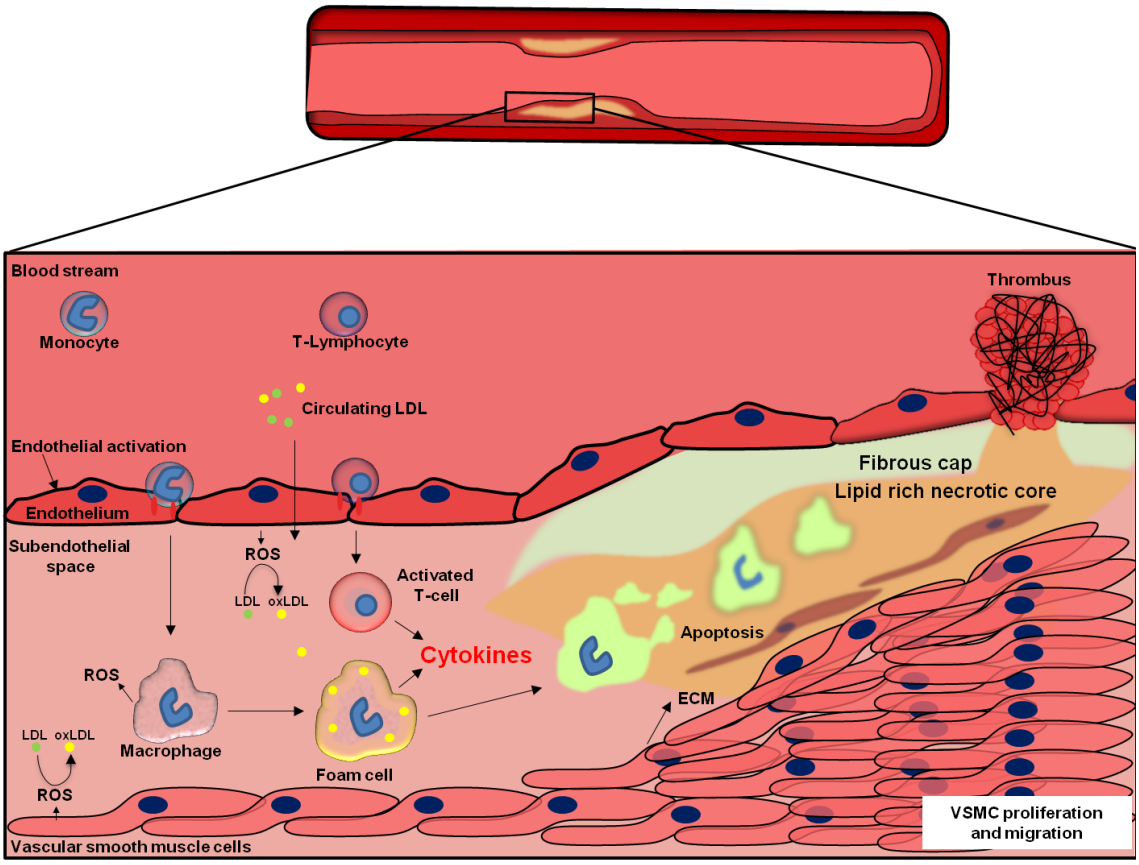

Figure 1.1 – A schematic outlining progression of the atherosclerotic plaque.

Monocytes and T-lymphocytes adhere to activated endothelial cells and migrate into the subendothelial space. Accumulation of immune cells and oxidised low density lipoprotein (oxLDL) induces local inflammatory signalling in the subendothelial space. Vascular smooth muscle cells adopt a 'synthetic' phenotype, where they proliferate rapidly and produce extracellular matrix (ECM) components and cytokines into the subendothelial layer. As the disease progresses, a lipid rich necrotic core develops from accumulation of lipids and dying cells which causes a reduction in the lumen area of the vessel. A fibrous cap of ECM components may lie above the lipid rich necrotic core, which can stimulate thrombus formation following further endothelial damage. Development of the thrombus can result in occlusion of the vessel, leading to a cessation of blood flow and infarction.

1.2 The focal nature of atherosclerosis

Despite the systemic nature of well established risk factors of atherosclerosis, including older age, diabetes and smoking (Hjermann et al. 1981), atherosclerotic lesions develop predominantly at bends and branch points of arteries. This phenomenon has been observed by researchers for centuries, resulting in a greater appreciation of the effect that vessel geometry has on blood flow and atherosclerosis development. Studies have identified two main mechanisms explaining the focal nature of atherosclerosis; mass transport of circulating mediators and differential wall shear stress (Caro 2009). In the vasculature, wall shear stress is the pressure applied tangentially to the endothelium generated by the flow of blood along the vessel. Studies examining the fluid dynamics of arteries have shown that at regions where atherosclerosis develops, blood flow is complex, producing oscillatory flow patterns with low wall shear stress (Caro et al. 1971). Conversely, regions protected from atherosclerosis are subjected to a unidirectional fluid flow with high wall shear stress (Figure 1.2). The mass transport theory proposes that this blood flow pattern within arteries leads to a preferential deposition of components within the blood including immune cells, cytokines and lipids to accumulate at bends and branch points (Warboys et al. 2011). The shear stress theory proposes that since endothelial cells lining the vessel are constantly in physical contact with flowing blood, that their phenotype is altered as a result of differential flow patterns. There is likely crosstalk between these two mechanisms *in vivo* contributing towards the focal nature of atherosclerosis. Numerous studies have therefore examined the role of shear stresses associated with 'atheroprone' and 'atheroprotective' flow patterns on endothelial function. These studies have shown that atheroprone flow is capable of activating the endothelium, inducing the expression of adhesion molecules (such as vascular cell adhesion molecule-1 (VCAM-1), intercellular adhesion molecule-1 (ICAM-1), E-selectin) and chemokines (such as monocyte chemoattractant protein-1 (MCP-1) and interleukin-8) and therefore

plays a key role in the initiation in the atherosclerotic plaque (Figure 1.3) by assisting in the recruitment of leukocytes to the vessel wall (Warboys et al. 2011; Chiu & Chien 2011). Moreover, atheroprone flow has also been reported to promote the production of reactive oxygen species (Heo et al. 2011) and endothelial-mesenchymal transition (Mahmoud et al. 2016), further inducing endothelial dysfunction. Conversely, atheroprotective flow promotes endothelial quiescence through activation of alternative pathways, such as Krüppel like factor 2 (KLF2) and endothelial nitric oxide synthase (eNOS), which effectively promote an anti-inflammatory phenotype and prevents atherosclerosis development (van Thienen et al. 2006; Berk 2008).

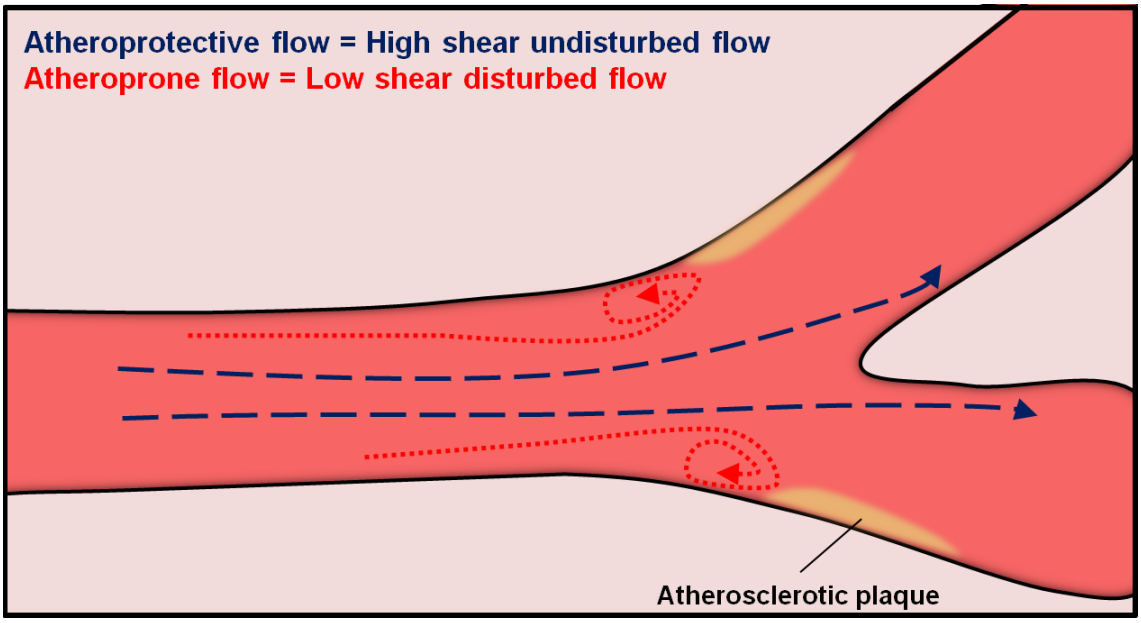

Figure 1.2 – Atherosclerosis is a focal disease.

Atherosclerosis occurs predominantly at regions of the arterial tree influenced by disturbed blood flow with low wall shear stress, whereas sites influenced by undisturbed blood flow with high wall shear stress are protected against atherosclerosis development.

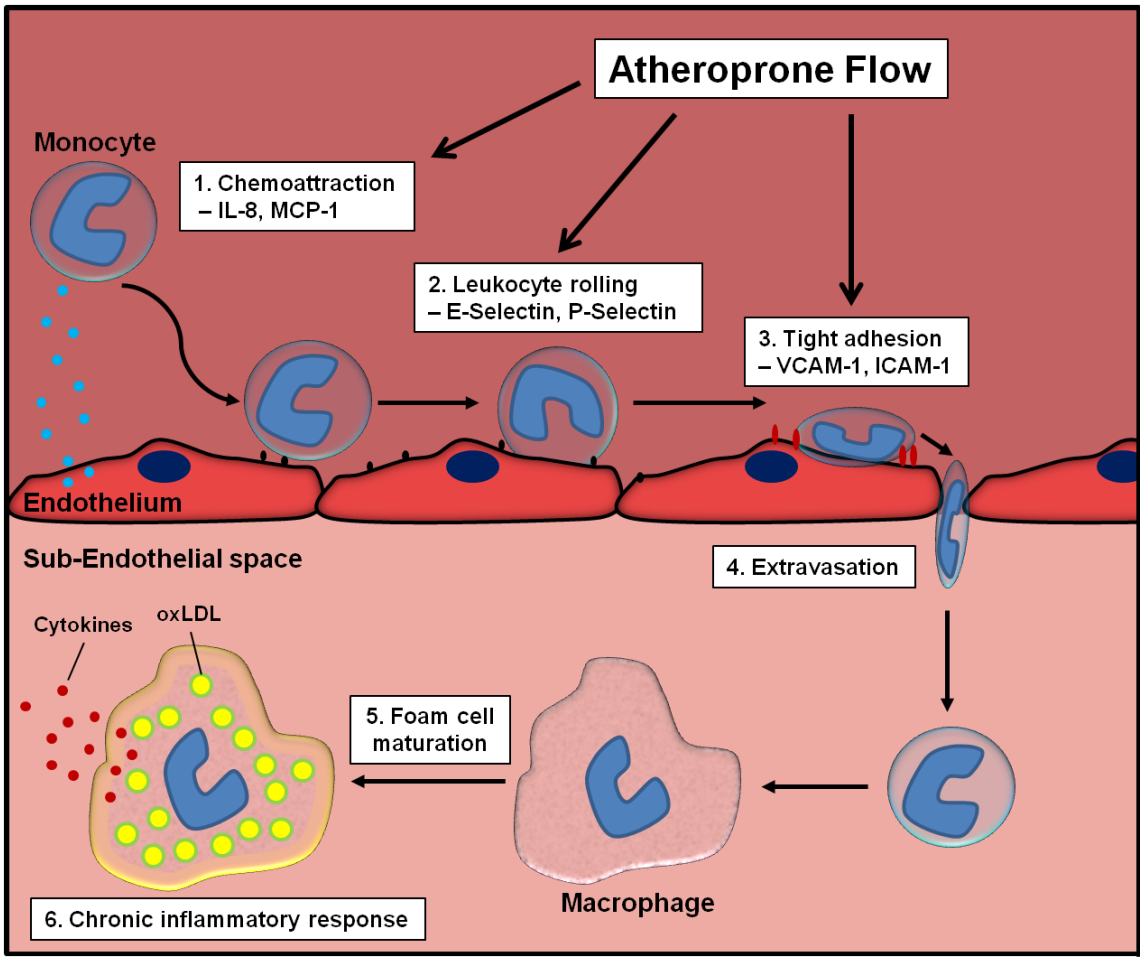

Figure 1.3 – Atheroprone flow primes the endothelium to facilitate monocyte migration in atherosclerosis.

Disturbed blood flow with low wall shear stress (atheroprone flow) induces the endothelial expression of chemokines (IL-8, MCP-1) and adhesion molecules (E-selectin, P-selectin, VCAM-1, ICAM-1), which aid in the recruitment and trapping of circulating monocytes. Once in the subendothelial layer, monocytes differentiate into macrophages and engulf surrounding oxidised low density lipoprotein (oxLDL) to become foam cells. Foam cells are pro-inflammatory and release a range of cytokines (TNF, IL-1, IFNγ), activating the endothelial cells to further up-regulate chemokines and adhesion molecules to enhance monocyte recruitment.

One mechanism in which atheroprone flow induces the expression of adhesion molecules and chemokines occurs through an increase in mitogen activated protein kinases (MAPK) and nuclear factor of κB (NF-κB) signalling (Figure 1.4). Endothelial cells influenced by atheroprone flow show enhanced c-Jun N-terminal kinase (JNK) and p38 activity resulting in an enhancement in c-Jun and ATF2 signalling, leading to increased transcription of NF-κB subunit p65, adhesion molecules and chemokines (Warboys et al. 2011; Cuhlmann et al. 2011). Moreover, atheroprone flow also primes the endothelium to cytokine induced signalling due to the enhanced expression of p65, promoting an augmented response to the presence of cytokines such as TNF, LPS or IL-1 (Hajra et al. 2000). This pathway is inhibited under atheroprotective flow, in part due to an increase in expression of MAPK phosphatase 1 (MKP-1). Increased endothelial MKP-1 expression has been shown to reduce phosphorylation of JNK and p38, reducing the activity of this pathway and as a result suppressing the expression of adhesion molecules and chemokines under atheroprotective flow (Zakkar et al. 2008); this suppression is even maintained in the presence of exogenous cytokines (Partridge et al. 2007). Mass-transport theory demonstrates that circulating cytokines are also preferentially delivered to sites of disturbed flow and since atheroprone flow primes endothelial cells for cytokine signalling, shear stress and mass transport models work synergistically to promote atherosclerosis development.

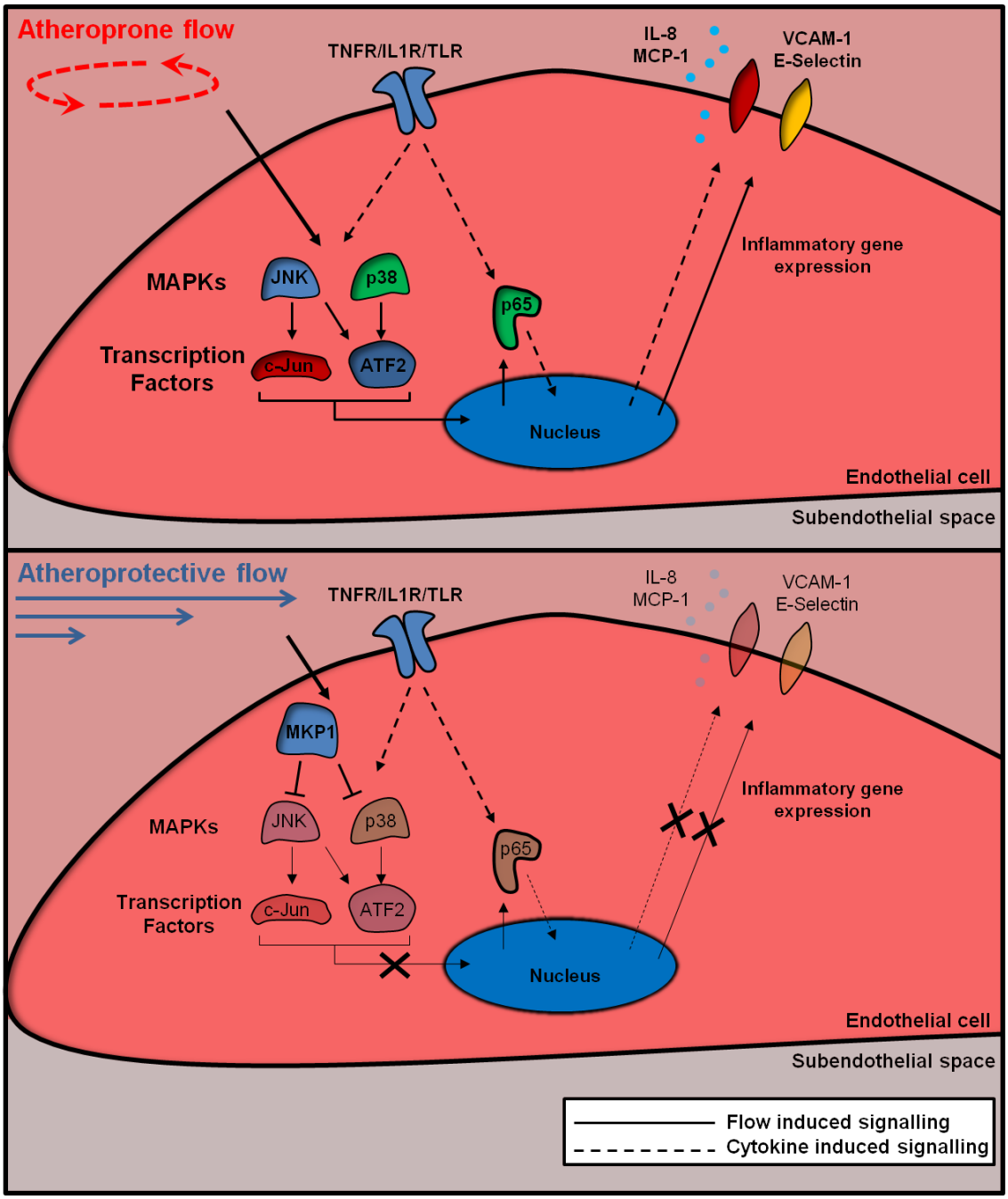

Figure 1.4 – Atheroprone flow induces MAPK and NF-κB signalling leading to endothelial inflammation.

Atheroprone flow induces activation of c-Jun N-terminal kinase (JNK) and p38, leading c-Jun and ATF2 signalling and transcription of target genes, including RelA (p65), IL-8, MCP-1, VCAM-1 and E-selectin. As p65 is up-regulated, atheroprone flow also enhances cytokine mediated signalling. These pathways are effectively inhibited under atheroprotective flow by the induction of MAP kinase phosphatase 1 (MKP1), which blocks activation of JNK and p38, subsequently reducing downstream inflammatory signalling.

In order for these differential responses to occur, endothelial cells must have mechanisms in place which 'sense' blood flow, which are proposed to be altered between atheroprotective and atheroprone flow patterns. Several mechanisms for mechanosensing have been identified which are outlined in Figure 1.5 (Chen et al. 2016). Plasma membrane structures including caveolae, the primary cilium, the glycocalyx and the plasma membrane itself have been implicated in mechanotransduction. Moreover plasma membrane receptors such as ion channels, G-protein coupled receptors (GPCRs), receptor tyrosine kinases (RTKs), specific proteins such as platelet endothelial cell adhesion molecule 1 (PECAM-1) and integrins have been implicated in shear-sensing. The plasma membrane is not the only mechanosensitive component, with evidence also suggesting that the cytoskeleton, cell-cell junctions and the nucleus are also responsible for endothelial responses to flow. Several studies have been performed examining how these pathways are regulated at the onset of atheroprotective flow, and how differential responses are activated upon exposure to atheroprone flow. One example of this is the endothelial glycocalyx, which has been shown to transduce shear stress signals into nitric oxide signalling (Florian et al. 2003). The glycocalyx is thicker on endothelial cells cultured under atheroprotective flow and at sites protected from atherosclerosis than those at atherosusceptible sites (Koo et al. 2013; Cancel et al. 2016; Gouverneur et al. 2006). As a result, this differential expression of the glycocalyx between atheroprotective and atheroprone flow patterns is in part responsible for the augmented nitric oxide signalling response in atheroprotected endothelial cells. It therefore is speculated that further mechanoresponsive pathways could also exhibit differential regulation between atheroprotective and atheroprone flow patterns. An additional proposed mechanism of mechanotransduction is the shear stress-induced extracellular release of adenosine triphosphate (ATP) (Yamamoto et al. 2003; Bodin & Burnstock 2001) which has been shown to act in an autocrine and paracrine fashion to activate endothelial ATP-gated receptors, including the P2 family of purinergic receptors (P2 receptors).

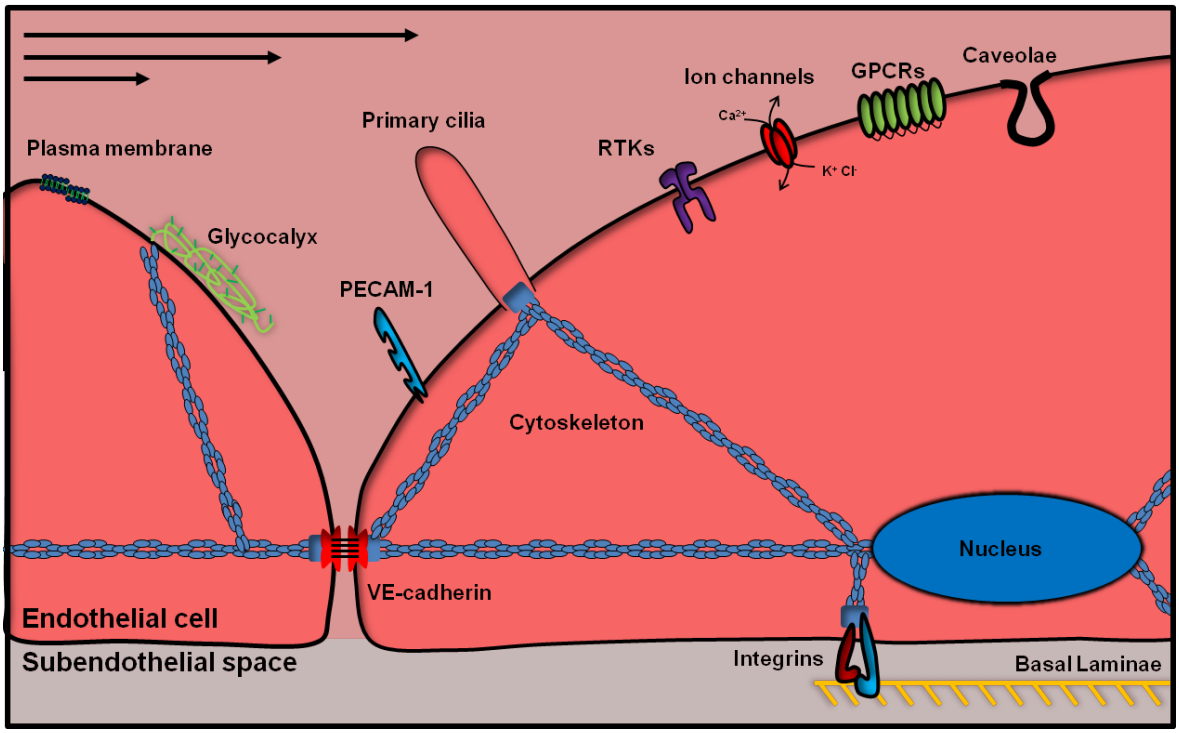

Figure 1.5 – Endothelial cells have several mechanisms of mechanosensation.

Endothelial cells can sense blood flow through a variety of mechanisms including: displacement of the plasma membrane; the glycocalyx; the primary cilium; receptor tyrosine kinases (RTKs); ion channels; G-protein coupled receptors (GPCRs); caveolae; integrins; PECAM-1; the cytoskeleton; or cell-cell junctions (such as through VE-cadherin).

1.3 Purinergic signalling and P2 receptors

Extracellular signalling of purine nucleotides and nucleosides, known as purinergic signalling, is a form of cell-cell communication which occurs through-out the body. Extracellular nucleotides are detected at the cell surface by a range of purinergic receptors, initiating intracellular signalling. There are 2 families of purinergic receptors: the P1 nucleoside and P2 nucleotide receptors (Ralevic & Burnstock 1998). The P2 receptor family is further split into two subfamilies, the P2X ion channels and the P2Y G-protein coupled receptors (GPCRs) (Weisman et al. 2006). There are seven P2X receptor (P2X1-7) and 8 P2Y receptor (P2Y1,2,4,6,11-14) subtypes. P2X receptors are activated exclusively by ATP and as a trimeric complex form a cation permeable channel causing Ca^{2+}/Na^{+} influx and K^{+} efflux (North 2002). Conversely, P2Y receptor subtypes are activated by either ATP, adenosine diphosphate (ADP), uridine triphosphate (UTP) or uridine diphosphate (UDP) and signal via G-proteins to activate phospholipase C (PLC), resulting in cleavage of phosphatidylinositol 4,5-bisphosphate (PIP_2) to inositol 1,4,5-trisphosphate (IP_3) and diacylglycerol (DAG), leading to release of Ca^{2+} from intracellular endoplasmic reticulum stores (Communi et al. 2000) (Figure 1.6). Activation of either receptor subfamily results in an increase in cytosolic Ca^{2+}, which can then evoke further downstream signalling. Each subtype exhibits different pharmacological profiles (Kügelgen 2008) activating discrete intracellular signalling pathways (Erb et al. 2006) and since different cell types express different combinations of P2 receptors, there are a wide variety of cellular responses resulting from extracellular nucleotide activation. Endothelial cells have been reported to express a range of P2 receptors; including the ATP gated P2X4, P2X7, P2Y2 and P2Y11, the ADP gated P2Y1 and the UTP/UDP gated P2Y4 and P2Y6 (K Yamamoto et al. 2000; Wang et al. 2002; Wilson et al. 2007).

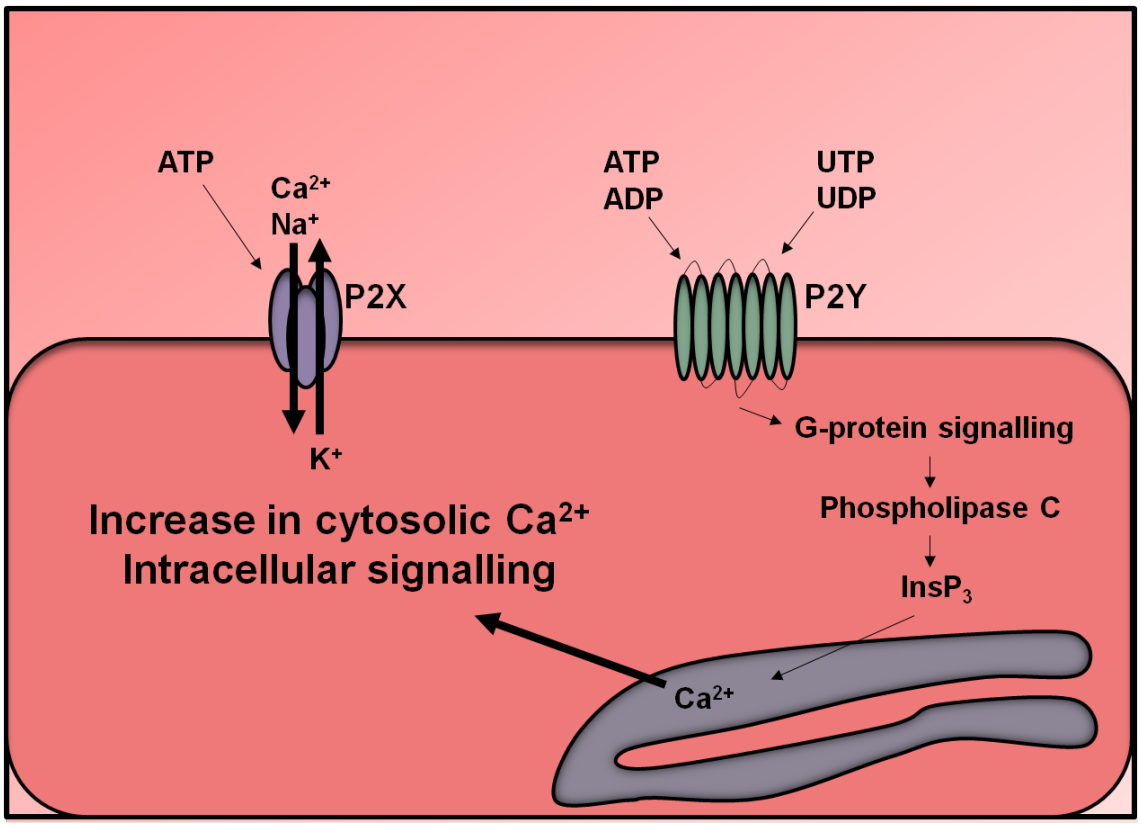

Figure 1.6 – A schematic of the signalling pathways following activation of P2X and P2Y receptors.

P2X receptors are non-selective cation channels activated exclusively by adenosine triphosphate (ATP), mediating Ca^{2+} and Na^{+} influx and K^{+} efflux. P2Y receptors are GPCRs that may be activated by ATP, adenosine diphosphate (ADP), uridine triphosphate (UTP) or uridine diphosphate (UDP), depending on subtype. Activation of P2Y receptors results in G-protein signalling, activation of phospholipase C and generation of inositol triphosphate ($InsP_3$). InsP3 binds to corresponding receptors on the endoplasmic reticulum, resulting in release of stored Ca^{2+}. Both receptor subfamilies can mediate downstream intracellular signalling as a result of mobilisation of cytosolic Ca^{2+}.

1.4 Role of adenine based nucleotides in endothelial responses

Purinergic signalling is a well recognised process in the vasculature. ATP is released extracellularly from endothelial cells in response to shear stress (Bodin & Burnstock 2001; Yamamoto et al. 2003) and acts as an autocrine/paracrine signal, activating local P2 receptors (Wang et al. 2015; Yamamoto et al. 2011). Extracellular nucleotides, such as ATP and UTP have been characterised to mediate vasodilation of blood vessels (Taylor et al. 1989; Guns et al. 2005; Guns et al. 2006). ATP, ADP and UTP induced vasodilation occurs through endothelial stimulation of P2Y receptors, whereas ATP released from nerve terminals innervating the vessel are proposed to induce vasoconstriction by P2X mediated vascular smooth muscle cell contraction (Hopwood & Burnstock 1987; Brizzolara & Burnstock 1991; Guns et al. 2005). This endothelial vasodilation is mediated through activation of endothelial nitric oxide synthase (eNOS) and the subsequent generation of the potent vasodilator nitric oxide (NO) (Gonçalves Da Silva et al. 2009; Bender et al. 2011; Guns et al. 2005).

P2 receptor subtypes exhibit different affinities to extracellular ATP and therefore the activation of specific P2 receptors can be modulated by altered concentrations of extracellular ATP. Plasma levels of ATP in the circulation are roughly 1μM/L (Forrester & Lind 1969; Jabs et al. 1977; Harkness et al. 1984), but ATP concentrations are thought be much higher at the endothelial surface with values as high as 30μM reported under shear stress conditions (Yamamoto et al. 2011). Furthermore, additional stimuli such as inflammation can modulate extracellular ATP. As a result, different P2 receptors are activated under different circumstances; this contributes to the diverse range of cellular responses to ATP.

As well as mediating vasodilation, purinergic signalling is also implicated in the induction of endothelial dysfunction. Figure 1.7 summarises all reported effects of ATP on endothelial function, highlighting its documented roles in mediating endothelial inflammation. Excess ATP signalling on endothelial cells induces an up-regulation in

the expression of adhesion molecules and chemokines. As a result of these inflammatory processes, ATP has been shown to induce leukocyte rolling and adhesion *in vitro* (Smedlund & Vazquez 2008; Sathanoori et al. 2015; Dawicki et al. 1995) and *in vivo* (Stachon et al. 2016), suggesting that extracellular ATP may be a factor in mediating leukocyte migration and atherosclerosis development. Indeed, routine exogenous ATP addition to $ApoE^{-/-}$ mice (which are pre-disposed to atherosclerosis) exacerbates atherosclerosis development (Stachon et al. 2016). Moreover inflammatory stimuli such as LPS (Bodin & Burnstock 1998), TNF (Lohman et al. 2015), hypoxia (Lim To et al. 2015) and high glucose/palmitate (Sathanoori et al. 2015) all increase extracellular ATP release from endothelial cells, further supporting a role of extracellular ATP in endothelial inflammatory responses.

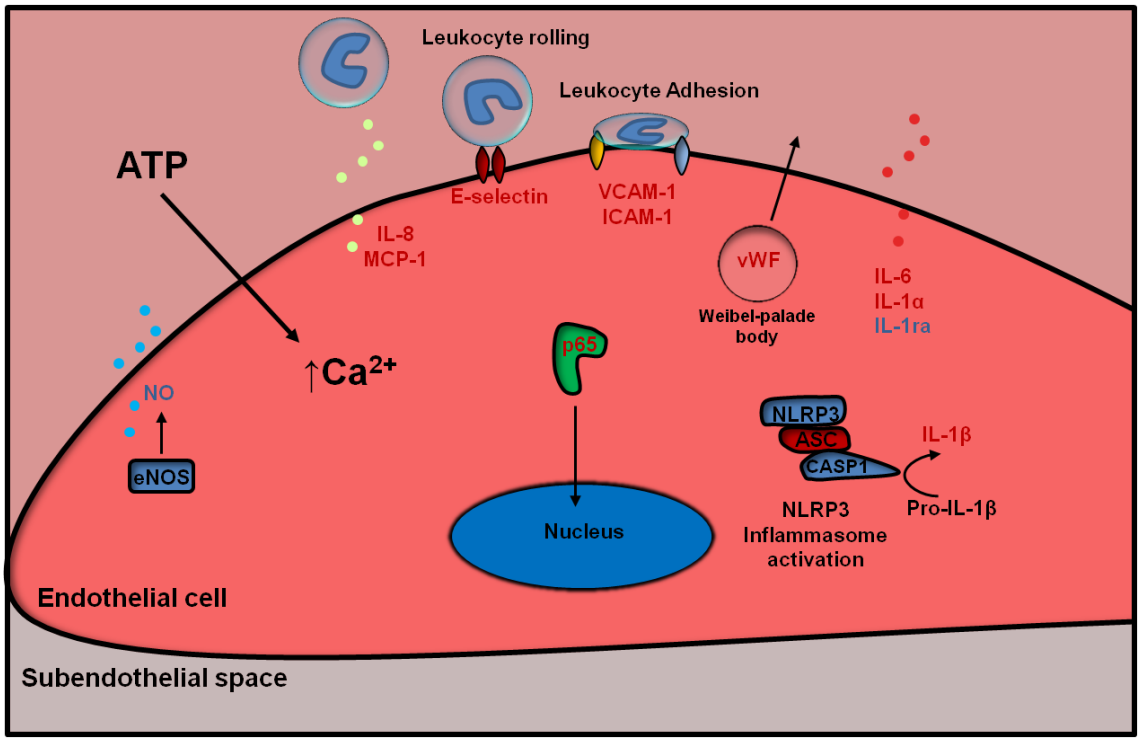

Figure 1.7 – ATP induces endothelial inflammation.

ATP signalling has been reported to have several inflammatory effects on endothelial cells as well as Ca^{2+} influx and nitric oxide (NO) production[1]. ATP stimulation causes: p65 translocation to the nucleus[2,3] and induction of IL-8[5,10], MCP-1[7,10], E-selectin[2,3], VCAM-1[4,5], ICAM-1[5,10], IL-6[5,10], IL-1α[8] and IL-1ra[9]. Exogenous ATP also induces of vWF release[2] and activates the NACHT, LRR and PYD domains-containing protein 3 (NLRP3) inflammasome, which processes IL-1β to its active form[5,6,7]. As a result, ATP increases leukocyte rolling and adhesion to endothelial cells. For simplicity, blue represents anti-inflammatory processes, whereas red denotes inflammatory actions.

1=Gonçalves Da Silva et al. 2009 , 2=von Albertini et al. 1998, 3=Goepfert et al. 2000, 4=Smedlund & Vazquez 2008, 5=Sathanoori et al. 2015, 6=Wilson et al. 2007, 7=Li et al. 2016 8=Imai et al. 2000, 9=Wilson et al. 2004, 10=Seiffert et al. 2006

Endothelial cells have several mechanisms to mediate release of extracellular ATP in response to shear stress or inflammatory stimuli, (Figure 1.8). These include; *de novo* synthesis from the ecto-F_1F_0 ATP synthase (Yamamoto et al. 2007), release through pannexin-1 (Bao et al. 2004; Lohman et al. 2015; Gödecke et al. 2012; Wang et al. 2016) and connexin channels, (D'hondt et al. 2013) and exocytosis of ATP rich vesicles (Bodin & Burnstock 2001; Lim To et al. 2015). Extracellular ATP is considered an important signalling molecule and can mediate a range of different intracellular processes and as such, mechanisms must exist to strictly regulate extracellular ATP concentrations to avoid inappropriate activation. This is achieved by the presence of several cell surface ATPases, which catalyse the breakdown of extracellular ATP (Antonioli et al. 2013). Ectonucleoside triphosphate diphosphohydrolase-1 (ENTPD1), more commonly known as CD39, hydrolyses ATP to ADP+free phosphate (Pi) and then immediately to AMP+Pi (Heine et al. 1999). 5'-nucleotidase (5'-NT), or CD73, finally catalyses the breakdown of AMP to adenosine+Pi. These ATPases can reduce P2 receptor activity by removing the active form of the ligand and are therefore considered important regulators of purinergic signalling. Furthermore, increasing evidence suggests that these mechanisms of ATP release, regulation and signalling occur within caveolae, a type of plasma membrane microdomain. Caveolae are small invaginations of the plasma membrane that have been suggested to contain mechanosensitive components and mediate intracellular signalling. Interestingly, the ecto-F_1F_0 ATP synthase (Yamamoto et al. 2007), CD39 (Koziak et al. 2000) and P2X receptors (Weinhold et al. 2010; Pfleger et al. 2012; Gangadharan et al. 2015) have been reported to localise within caveolae, providing ideal conditions for regulation of localised ATP signalling.

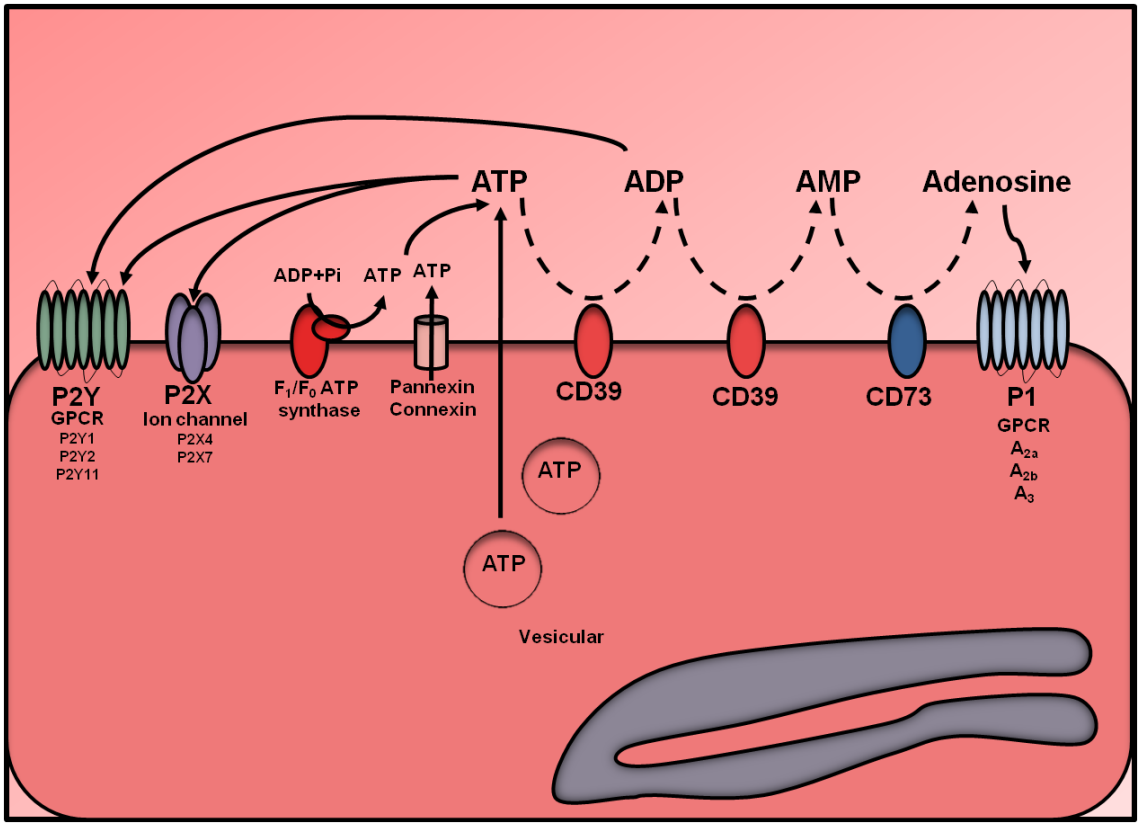

Figure 1.8 – Mechanisms of extracellular ATP release and regulation in endothelial cells.

ATP accumulates extracellularly by: release of cytosolic ATP through pannexin or connexin channels; release of ATP-rich vesicles; or *de novo* synthesis of ATP by ecto-F_1/F_0 ATP synthase. Extracellular ATP can activate P2X or P2Y receptors or is hydrolysed to ADP by ectonucleoside triphosphate diphosphohydrolase-1 (CD39). ADP can activate P2Y receptors, or is further hydrolysed by CD39. AMP is broken down to adenosine by 5'-nucleotidase (CD73), which can activate adenosine receptors.

These endothelial mechanisms of regulating extracellular ATP were recently shown to be altered by shear stress (Figure 1.9). Endothelial cell surface expression of the F_1/F_0 ATP synthase is increased under atheroprone flow conditions and at sites susceptible to atherosclerosis (Fu et al. 2011). Moreover expression of the extracellular ATPase CD39 has been proposed as an important regulator of atherosclerosis development. *In vitro,* CD39 overexpression in endothelial cells reduced ATP-induced NF-κB (P65) activation and E-selectin induction (Goepfert et al. 2000). *In vivo,* $CD39^{-/+}/ApoE^{-/-}$ mice had increased atherosclerosis (Kanthi et al. 2015) and mature (20-30 weeks) $ApoE^{-/-}$ mice, which are prone to atherosclerosis, had diminished vascular ATPase activity and increased circulating ATP levels (Mercier et al. 2012). Kanthi et al revealed stark localisation differences in endothelial CD39 expression, with predominant expression at sites of atheroprotection and diminished expression at atheroprone regions of the murine aorta (Kanthi et al. 2015), suggesting regional differences in ATP hydrolysis. As well as regulating development of atherosclerosis, CD39 activity is also important in preventing vascular dysfunction associated with pulmonary arterial hypertension (PAH). Endothelial CD39 was down-regulated in patients with PAH (Helenius et al. 2015) and $CD39^{-/-}$ mice exhibited exacerbated PAH accredited to dysregulation of purinergic signalling (Visovatti et al. 2016). This suggests that extracellular ATP is tightly regulated by endothelial cells to prevent vascular dysfunction. As a result, in circumstances where degradation of extracellular ATP is lost, such as at endothelial sites susceptible to atherosclerosis, vascular inflammation occurs promoting disease progression.

Expression of CD73, which catalyses breakdown of AMP to adenosine, is also up-regulated by atheroprotective flow, resulting in an increase of extracellular adenosine (Li et al. 2010). Adenosine is a potent vasodilator of arteries mediating production of nitric oxide through endothelial A_2 receptors (Hein & Kuo 1999; Sobrevia et al. 1997; Li et al. 1998), which unlike ATP is independent of intracellular calcium signalling (Wyatt

et al. 2002). Furthermore, CD73 has been reported to be required for ATP-mediated vasodilation (Ohta et al. 2013), suggesting that adenosine might be mediating some of the vasodilatory response after ATP addition. $CD73^{-/-}$ mice, which have a deficiency in adenosine production, have exacerbated atherosclerosis driven by an enhancement in endothelial VCAM-1 and MCP-1 expression resulting in increased leukocyte attraction and migration (Zernecke et al. 2006; Buchheiser et al. 2011), suggesting that adenosine protects against atherosclerotic plaque development.

In summary, traditionally extracellular ATP signalling has been associated with vasodilation and protection of the endothelium. However, increasing evidence suggests that if not strictly regulated, extracellular ATP can induce pro-inflammatory signalling in endothelial cells and assist in the development of vascular dysfunction preceding cardiovascular disease. Since evidence suggests regulation of extracellular ATP may be dysregulated at sites susceptible to atherosclerosis, it is proposed that purinergic signalling may be altered at these sites, meditating endothelial inflammation and contributing to atherosclerosis initiation.

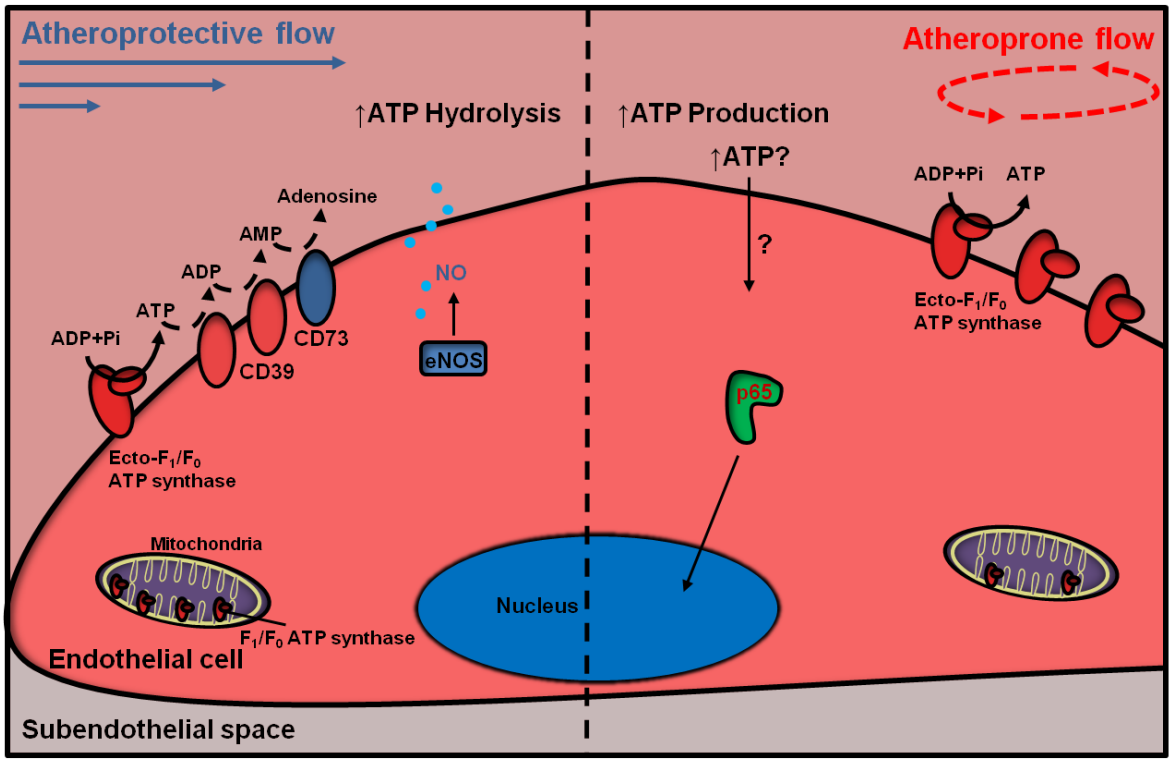

Figure 1.9 – Regulation of extracellular ATP is altered by differential shear stress in the endothelium.

Atheroprotective flow up-regulates the ecto-nucleotidases CD39 and CD73 resulting in enhanced ATP breakdown. Atheroprone flow up-regulates plasma membrane expression of the ecto-F_1/F_0 ATP synthase, speculating that extracellular ATP levels are higher.

1.5 P2 receptors respond to shear stress-induced ATP release

Since endothelial cells release ATP extracellularly in response to shear stress, the role of P2 receptors in mechanosensing in the endothelium has been studied (Figure 1.10). Over the past decade, the Ando group has demonstrated activation of endothelial P2X4 receptors by shear stress-induced released ATP and the subsequent effect on vasodilation. P2X4 is the predominant P2 receptor expressed in endothelial cells from a range of vascular beds (Ramirez & Kunze 2002; Wilson et al. 2007; Wang et al. 2002; Yamamoto et al. 2000) and indeed was found to be responsible for calcium influx after unidirectional flow application (Yamamoto et al. 2000). Moreover, $P2X4^{-/-}$ mice exhibited several vascular defects, including a lack of vasodilatory response to ATP or flow, attributed to a defect in production of the potent vasodilator nitric oxide (Yamamoto et al. 2006). More recently *in vitro* studies have also provided evidence that activation of P2X4 by atheroprotective flow patterns activates KLF2 signalling, an important upstream regulator of the atheroprotective endothelial phenotype (Sathanoori et al. 2015). However, conflicting reports question the role of P2X4, as other studies indicate that P2Y2 signalling is responsible, and not P2X4. P2Y2 receptors have been shown to be activated by ATP released under high shear unidirectional flow, contributing to eNOS activation and flow dependent vasodilation independently of P2X4 (Wang et al. 2015; Wang et al. 2016). P2Y2 has also recently been reported to contribute to shear stress induced endothelial cell migration and realignment under atheroprotective flow conditions (Sathanoori et al. 2016). Furthermore, adenosine diphosphate (ADP), the partially hydrolysed form of ATP, is considered a more potent vasodilator (Taylor et al. 1989). ADP is selective for only a subset of P2Y receptors, with P2X receptors considered insensitive to ADP (North & Surprenant 2001). ADP-gated P2Y1 receptors have been shown to be responsible for a large proportion of ATP-induced vasodilation (Bender et al. 2011), achieved through enhanced nitric oxide production (Buvinic et al. 2002).

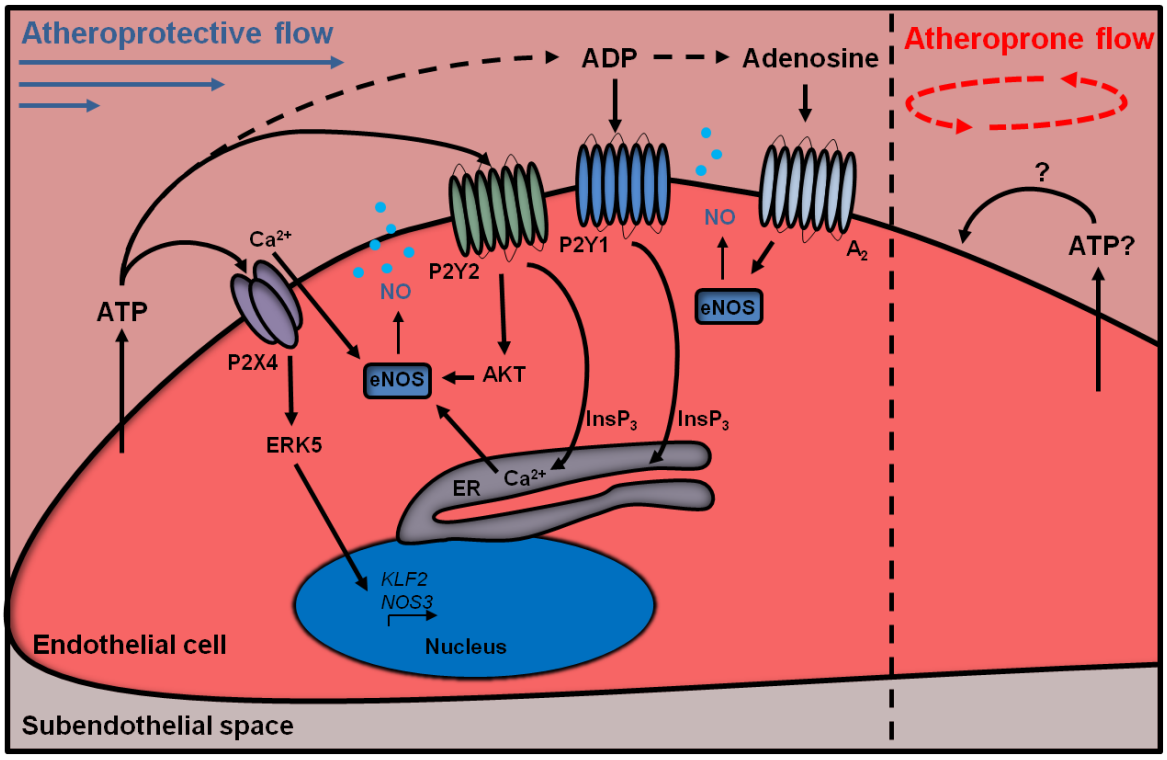

Figure 1.10 – Endothelial P2 receptors are activated by shear stress-induced ATP release.

Shear stress-induced ATP release activates nearby purinergic receptors to mediate nitric oxide (NO) production. P2X4 induces expression of atheroprotective genes *KLF2* and *NOS3*, which codes for eNOS, by ERK5 as well as activating eNOS. P2Y2 activates AKT signalling and release of ER calcium stores to activate eNOS. Partial hydrolysis of ATP to ADP also activates P2Y1 receptors, which activate eNOS by depletion of ER calcium stores. Further hydrolysis of ATP to adenosine mediates vasodilation through A_2 receptor-induced activation of eNOS. The role of ATP release and subsequent signalling is currently unknown under atheroprone flow patterns.

Endothelial cells also express the ATP gated P2X7 receptor, but its role in the endothelium responding to shear stress-induced released ATP has not been studied. P2X7 activity is associated with inflammatory signalling; activation of this receptor typically requires higher concentrations of ATP compared to other P2 receptors, likely in order to avoid inappropriate inflammatory responses. Interestingly, several studies have demonstrated activation of P2X7 in response to mechanical stress in osteoblasts and osteocytes. Similar to the endothelium, fluid shear stress, caused by the movement of the skeleton, induces extracellular ATP release from osteocytes and osteoblasts (Genetos et al. 2005). This fluid shear stress-induced ATP release was found to activate P2X7 receptors and subsequently mediate: enhanced NF-κB activity (Genetos et al. 2011); Prostaglandin E_2 release (Genetos et al. 2005) (Li et al. 2005); formation of the P2X7 associated pore (Li et al. 2005); and P2X7 dependent IL-1β secretion (Kanjanamekanant et al. 2014). Since P2X7 responses occur in osteocytes following shear stress, this suggests the possibility that P2X7 responses may also occur in response to flow in endothelial cells.

P2 receptors therefore have important roles in mediating cellular responses to shear stress. However, their functionality under flow patterns associated with atherosclerosis has not yet been studied, with studies predominantly exposing static endothelial cells to acute uniform high shear stress, characteristics of atheroprotective flow. Interestingly, many of the pathways induced by ATP in endothelial cells mirror those present under atheroprone flow. As ATP is associated with inflammatory signalling as well as nitric oxide production, P2 receptors could be differentially activated between atheroprotective and atheroprone flow conditions and contribute to the atheroprone flow-induced signalling. Indeed, despite the established role for ATP inducing nitric oxide production, a pathway associated with prevention of atherosclerosis development, knockout models for P2 receptors are universally protected against atherosclerosis. $P2Y1^{-/-}/ApoE^{-/-}$ mice and $P2Y6^{-/-}/LDLR^{-/--}$ mice exhibited a reduced

atherosclerosis burden, which is dependent on non-myeloid cells (Hechler et al. 2008; Stachon et al. 2014). $P2Y2^{-/-}$ mice showed an ~80% reduction in endothelial expression of adhesion molecule VCAM-1 in the murine aortic arch (Qian et al. 2016) and $P2Y2^{-/-}$ /$LDLR^{-/-}$ mice had reduced ATP-induced atherosclerosis (Stachon et al. 2016). P2X7 receptor expression was increased in murine (Peng et al. 2015) and human (Peng et al. 2015; Piscopiello et al. 2013) atherosclerotic plaques and aortic atherosclerotic plaque development was also reduced in $ApoE^{-/-}$ mice treated with a lentivirus containing P2X7 siRNA (Peng et al. 2015). It must be noted that these studies were not performed on endothelial specific knockouts and other cells will be contributing to the phenotype. Moreover, the studies which examined the role of P2X7 used a C57BL/6 mouse model, which has reduced functioning P2X7 receptors due to a single nucleotide polymorphism (SNP) P451L (Adriouch et al. 2002; Syberg et al. 2012), Regardless, since ATP is linked with endothelial inflammation and dysregulation of extracellular ATP occurs at sites of atheroprone flow, endothelial P2 receptors are likely candidates in mediating these effects.

1.6 P2X receptors and inflammatory signalling

Extracellular ATP acts as a damage-associated molecular pattern (DAMP), as it is maintained at milimolar concentrations intracellularly and as mentioned previously, strictly regulated extracellularly. As such, following cell damage and death, high concentrations of extracellular ATP accumulate and can signal to nearby cells as a 'danger signal' through P2 receptors (Burnstock 2016; Newton & Dixit 2012). The P2X7 receptor is most commonly studied in this response, as unlike other P2 receptors, low milimolar concentrations of ATP are required for full activation of P2X7 (Surprenant et al. 1996), a situation that occurs most often following infection or cell damage. In contrast to the other P2X receptors (P2X1-6), P2X7 has an extended intracellular C-terminal tail which is considered responsible for its distinct inflammatory properties (Costa-Junior et al. 2011). As well as functioning as a non-selective cation channel, P2X7 receptor activation is also associated with some unique functional responses including: the induction of a 900 dalton pore in the plasma membrane (Coutinho-Silva & Persechini 1997); membrane blebbing (Virginio et al. 1999); microvesicle shedding (Solini et al. 1999); MAPK and NF-κB signalling (Skaper et al. 2010); ROS generation (Suh et al. 2001); cell death (Virginio et al. 1999) and activation of the NACHT, LRR and PYD domains-containing protein 3 (NLRP3) inflammasome (Dubyak 2012) (Figure 1.11). The NLRP3 inflammasome is the molecular component responsible for the processing the pro-inflammatory cytokines IL-1β and IL-18 to their biologically active forms (Schroder & Tschopp 2010). Therefore the role of P2X7 in inflammatory conditions has been extensively studied, particularly in macrophage-like cells, as a potential therapeutic target for chronic inflammatory conditions.

However, the existence of P2X7 mediated inflammatory responses in endothelial cells shows conflicting reports, despite consensus for P2X7 receptor expression in endothelial cells. P2X7-induced cell membrane pore formation was absent in unstimulated HUVEC (H.Wilson group, unpublished) and in bovine aortic endothelial

cells (Ramirez & Kunze 2002), but did occur in murine mesenteric artery endothelial cells (Oliveira et al. 2013). ATP induced cell death, a characteristic of P2X7 activation (Virginio et al. 1999), has been reported to occur in unstimulated HUVEC (von Albertini et al. 1998; Goepfert et al. 2000), but was absent when tested by the Wilson group, even after inflammatory stimulus (Wilson et al. 2007). Moreover, even in the presence of high concentrations of ATP, endothelial cells did not bleb or form microvesicles (Wilson et al. 2007). As most of the studies on P2X7 function have been carried out in cells of myeloid origin, it is possible that endothelial P2X7 is regulated differently and as such mediates different cellular responses following activation. Indeed, much like the other endothelial P2 receptors, exogenous ATP-activated endothelial P2X7 induces the production of nitric oxide (Oliveira et al. 2013). However P2X7 is also thought to be one of the main receptors involved in ATP induced vascular dysfunction in static endothelial cells challenged with inflammatory stimuli. Endothelial P2X7 has been reported to be up-regulated by a range of inflammatory mediators and to stimulate the processing of pro-IL-1β (Wilson et al. 2007) and release of IL-1ra (Wilson et al. 2004). Moreover, endothelial inflammation induced by high glucose and palmitate is dependent on increased extracellular ATP release and P2X7 dependent expression of IL-1β, IL-6, IL-8, ICAM-1, VCAM-1 as well as increased ROS generation, p38 signalling and monocyte adhesion (Sathanoori et al. 2015). Interestingly, these are all pathways up-regulated under atheroprone flow, and seeing as P2X7 knockdown also reduces atherosclerotic plaque development in $ApoE^{-/-}$ mice (Peng et al. 2015), this suggests that endothelial P2X7 may be involved in atheroprone flow-induced inflammatory signalling.

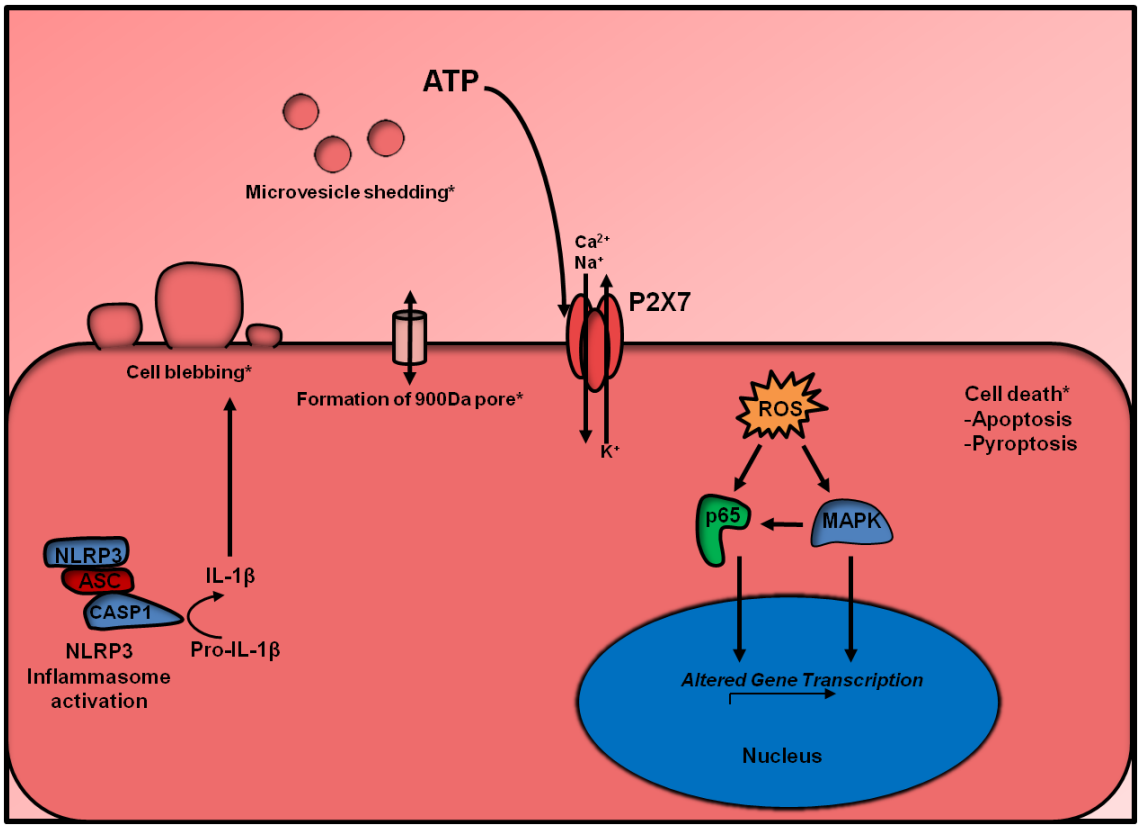

Figure 1.11 – P2X7 receptors mediate a range of intracellular responses.

Activation of P2X7 receptors evokes: Ca^{2+} and Na^{+} influx, K^{+} efflux, formation of a 900 dalton pore in the plasma membrane, activation of the NACHT, LRR and PYD domains-containing protein 3 (NLRP3) inflammasome and subsequent cleavage of pro-IL-1β, cell blebbing, microvesicle shedding, generation of reactive oxygen species (ROS), cell death through apoptosis or pyroptosis, MAPK and NF-κB (p65) signalling and subsequent effects on gene transcription.

* indicates responses absent in endothelial cells following P2X7 receptor activation.

More recently, the role of P2X4 in inflammatory signalling has been described. P2X4 is the most homologous P2X receptor to P2X7 (Kaczmarek-Hájek et al. 2012) and they are commonly co-expressed in numerous different cell types, including the endothelium (Wang et al. 2002; Wilson et al. 2007; Yamamoto et al. 2000). Recent evidence suggests P2X4 and P2X7 can directly interact in variety of cell types (Guo et al. 2007; Antonio et al. 2011; Boumechache et al. 2009; Weinhold et al. 2010; Hung et al. 2013). Furthermore, activation of classical P2X7 pathways with high concentrations of extracellular ATP have been reported to be altered by P2X4 manipulation. ATP induced IL-1β production was reduced following P2X4 knockdown in the macrophage cell line RAW264.7 (Kawano et al. 2012), bone marrow-derived dendritic cells (Sakaki et al. 2013) and microglia (Burm et al. 2016). This suggests that P2X4 can act synergistically with P2X7 to co-ordinate inflammatory responses to extracellular ATP. Endothelial P2X4 is up-regulated concomitantly with P2X7 in response to inflammatory stimuli (Wilson et al. 2007; Sathanoori et al. 2015) and despite their clear association with inflammatory signalling, limited studies are available describing the role they play in mediating vascular inflammation. Since P2X4 is already implicated in endothelial mechanosensing under atheroprotective flow conditions (Figure1.10), this receptor may also be involved in mediating cellular responses to atheroprone flow.

1.7 Regulation of P2X7 receptors

P2X7 receptors are well-described for their role in inflammation, capable of activating numerous intracellular signalling pathways. As such, extensive research has been carried out identifying mechanisms of regulation. These include processes such as alternative splicing events, plasma membrane trafficking and identification of interacting proteins.

1.7.1 Alternative splicing

Splicing is a post-transcriptional event in which introns, the non-coding regions of mRNA, are removed from RNA before exiting the nucleus. Alternative splicing is a phenomenon where some exons, the coding regions of mRNA, are skipped or introns are retained, resulting in an altered mRNA transcript and ultimately translation of a different protein (Roy et al. 2013).

Numerous alternatively spliced P2X7 receptors have been identified. Splicing occurs extensively in P2X7 transcripts, with to date 11 alternatively spliced human transcripts documented (P2X7a-j) (Sluyter & Stokes 2011). P2X7a, the classical and most studied variant, has been reported to have vastly different functional responses compared to other characterised P2X7 splice variants. P2X7b is the most extensively studied alternate variant and has been shown to be expressed endogenously in a variety of tissues (Adinolfi et al. 2010). P2X7b is especially interesting as it a truncated protein lacking the C-terminal tail associated with inflammatory signalling characteristics (Adinolfi et al. 2010). Indeed, heterologously expressed P2X7b functions as a ion channel, but could not mediate P2X7-induced pore formation, apoptosis or membrane blebbing (Cheewatrakoolpong et al. 2005). Interestingly, despite the inability of P2X7b to mediate pore formation, co-expression of P2X7a and P2X7b resulted in a potentiation of P2X7 responses, including enhanced calcium influx, pore formation and plasma membrane blebbing (Adinolfi et al. 2010). Moreover an additional variant, P2X7j, has been reported to act as a dominant negative regulator of P2X7a responses

at an endogenous level (Feng et al. 2006; Mankus et al. 2011). These studies provide examples of the complex interactions occurring between P2X7 variants to fine-tune responses, offering a further layer in P2X7 regulation. More recently, P2X7 receptor splice variants have been implicated in many disease processes (Sluyter & Stokes 2011), highlighting their importance for future studies examining P2X7. However, many of these splice variants have not been fully investigated and suggests the possibility of further regulation of uncharacterised splice variants.

1.7.2 Trafficking

Since extracellular ATP activates P2X7 receptors, controlling cell surface expression can effectively modulate receptor activity. They are predominantly expressed intracellularly within the ER/golgi apparatus due to their relatively slow trafficking pathway to the plasma membrane (Robinson & Murrell-Lagnado 2013). Moreover, cell surface expression is tightly regulated in certain cell types. Monocytes express predominantly intracellular P2X7 receptors, which upon differentiation to macrophages are trafficked to the cell surface (Gudipaty et al. 2001). Therefore, regulatory pathways must exist to control P2X7 responses by regulating its subcellular location.

Aside from trafficking to the cell surface, expression of P2X7 within discrete microdomains within the plasma membrane has been reported to extensively alter P2X7 responses. P2X7 has been found to be loosely associated with lipid rich caveolae through an interaction with the caveolae scaffold protein caveolin-1 (Barth et al. 2007; Barth et al. 2008; Weinhold et al. 2010). Evidence suggests that two separate populations of P2X7 receptors exist in the plasma membrane which display different intracellular signalling in response to ATP (Garcia-Marcos et al. 2006; Gonnord et al. 2008); plasma membrane cholesterol is a potent negative regulator of some canonical P2X7 functions (Robinson et al. 2014), indicating that P2X7 can be regulated by trafficking between normal and lipid rich plasma membrane microdomains.

1.7.3 Interacting proteins

A number of proteins have been reported to influence P2X7 function. The C-terminal tail of P2X7 is thought to account for its distinct functional and inflammatory properties (Costa-Junior et al. 2011). Therefore our group sought to identify proteins that interact with this C-terminus using yeast two hybrid and immunoprecpitation approaches. As a result, the growth arrest specific 3 (GAS3) family of proteins was found to be directly interacting with the c-terminal tail of heterologous rat P2X7 in HEK-293 cells (Wilson et al. 2002). The GAS3 family consists of four members; epithelial membrane protein 1 (EMP1), EMP2, EMP3 and peripheral myelin protein 22 (PMP22). Of these family members, EMP2 was the strongest interacting protein and subsequent work in the Wilson lab identified EMP2 as a regulator of P2X7 functions (H.Wilson group, unpublished). P2X7 can associate with caveolae through an interaction with caveolin-1 which has been shown to regulate P2X7 responses (Gangadharan et al. 2015), most likely due to associating P2X7 to lipid rafts. Pannexin-1 forms a hemi-channel linking intracellular and extracellular spaces. Pannexin-1 interacts with the P2X7 receptor and is proposed as responsible formation of the P2X7-pore and subsequent NLRP3 inflammasome activation (Pelegrin & Surprenant 2006). Moreover, pannexin-1 has also been implicated in mediating extracellular release of ATP, including in response to mechanical stimuli (Bao et al. 2004). CD39, an ecto-ATPase, is also a critical regulator of P2X7 function by limiting agonist availability (Antonioli et al. 2013). Several studies have shown that enhanced CD39 activity directly impacts P2X7 function (Kuhny et al. 2014; Goepfert et al. 2000; Nie et al. 2005). Therefore, P2X7 responses can be regulated by other proteins in a variety of different ways: by controlling the amount of available ATP, regulating the subcellular location, by direct protein interactions and potentially further unexplored mechanisms. Identification of interacting proteins and determining their role in regulating P2X7 receptor function is critical to improve our understanding of inflammation and shear stress processes.

1.8 Summary of background

In summary, atheroprone flow promotes inflammatory signalling in endothelial cells resulting in leukocyte recruitment preceding atherosclerotic plaque development. Despite the traditional atheroprotective view of extracellular ATP on endothelial cells, excess ATP can mediate vascular dysfunction through P2 receptors and assist in atherosclerosis development. Since endothelial cells release extracellular ATP in response to blood flow and recent reports suggest that extracellular ATP levels may be dysregulated at sites susceptible to atherosclerosis, an increase in ATP-induced inflammatory signalling at these areas may contribute to the initiation of the atherosclerotic plaque. However, shear-stress induced ATP signalling has currently not been studied in long-term flow culture models, which fully represents the endothelial adaptation to flow. Furthermore, despite the similarity between ATP signalling and atheroprone flow in mediating inflammatory signalling, ATP signalling has not been researched in endothelial cells under atheroprone flow conditions. P2X receptors, particularly P2X7 and P2X4, have established links in mediating ATP-induced inflammatory responses and have been reported to be activated by shear stress-induced released ATP. Moreover, endothelial P2X4 and P2X7 are up-regulated in static endothelial cells under inflammatory conditions. However, the majority of studies examining endothelial P2X receptor responses are either under static or acute atheroprotective flow conditions; the role of P2X receptors under atheroprone flow has currently not been assessed.

1.9 Hypothesis

ATP signalling and P2 receptor activity is altered in endothelial cells at sites of the vasculature influenced by atheroprotective or atheroprone flow. ATP-signalling under atheroprone flow conditions promotes endothelial inflammation through enhanced activation of P2X receptors and as a result contributes to the endothelial cell activation preceding atherosclerosis development. Figure 1.12 provides a schematic of the hypothesis.

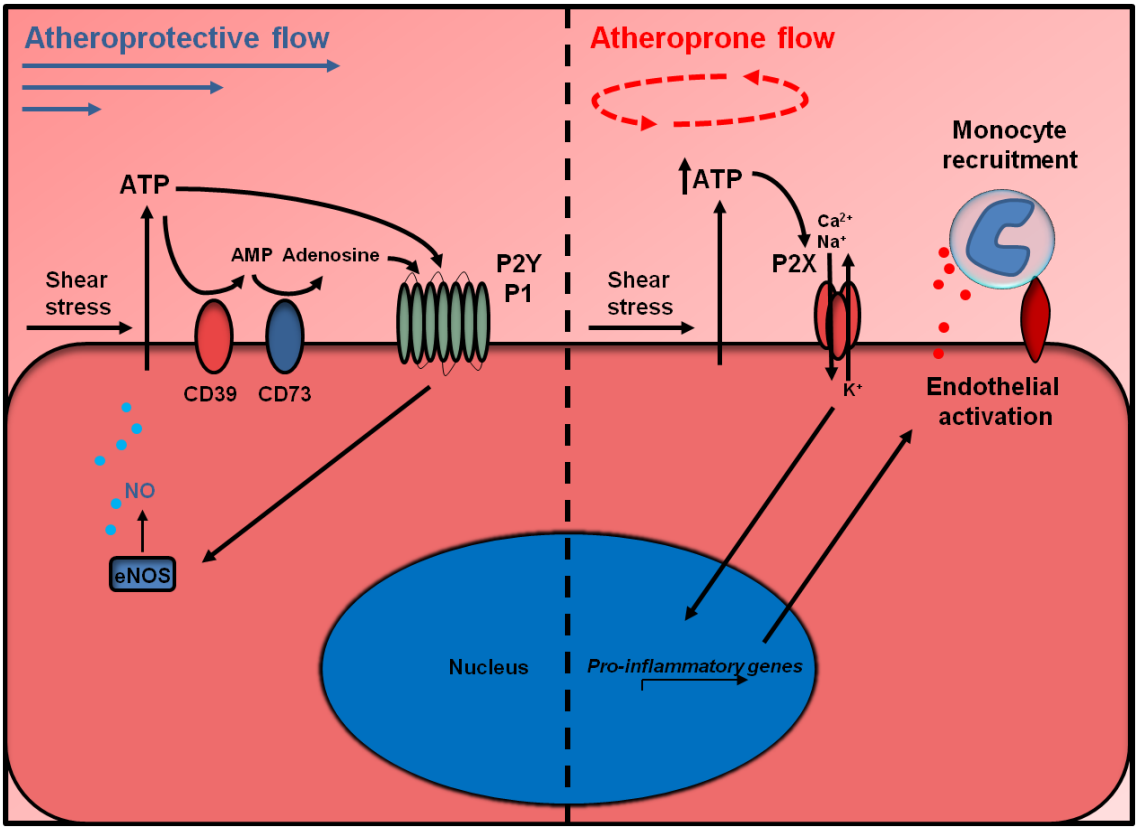

Figure 1.12 – Hypothesis: ATP signalling mediates atheroprone flow-induced inflammatory signalling through P2X receptor activation

A schematic representing the hypothesis of this research. Shear stress mediates extracellular release of ATP which activates local purinergic receptors. Under atheroprotective flow conditions, enhanced ATPase activity hydrolyses extracellular ATP, strictly regulating its levels. Activation of P2Y and P1 receptors activates eNOS and mediates atheroprotection through nitric oxide production. Conversely, ATP levels are dysregulated at vascular sites influenced by atheroprone flow. Activation of P2X receptors leads to pro-inflammatory signalling and promotes vascular dysfunction and monocyte recruitment, ultimately contributing to atherosclerosis development.

1.10 Aims

To address the hypothesis the following aims were investigated:

1) Identify if ATP-mediated signalling is altered between endothelial cells cultured under atheroprotective or atheroprone flow conditions.

2) Determine expression and possible regulatory mechanism of P2X receptors in the endothelium cultured under atheroprotective or atheroprone flow conditions.

3) Examine the role of P2X receptors in atheroprone flow-induced inflammatory signalling.

.

Chapter 2

Materials and Methods

2.1 List of reagents

Reagent	Catalog number	Vendor
A438079 hydrochloride	ab120413	Abcam
Adenosine 5′-triphosphate disodium salt hydrate (ATP)	A6419	Sigma
Amphotericin B	BP2645-50	Thermo Fisher
Anhydrous DMSO	276855	Sigma
ARL 67156 trisodium salt	1283	Tocris
ATP Determination kit	A22066	Life Technologies
AZ10606120	3323	Tocris
AZ11645373	A7321	Sigma
Bioline Isolate II RNA mini kit	BIO-52073	Bioline
Bovine Serum Albumin	A7906	Sigma
2'(3')-O-(4-Benzoylbenzoyl)adenosine 5'-triphosphate triethylammonium salt (BzATP)	B6396	Sigma
Cal-520, AM	21130-AAT	Stratech
CD14 Microbeads, human	130-050-201	Miltenyl Biotec
Collagenase from Clostridium histolyticum	C5138	Sigma
Corning® 96 well EIA/RIA plates	CLS3590	Sigma
Deoxynucleotides (dNTPs)	U1511	Promega
Endothelial Cell Growth Supplement	02-101	Merck Millipore
ECL Select Western Blotting Detection Reagent	RPN2235	GE-Healthcare
Ethylenediamine Tetraacetate Acid (EDTA)	BP2482-500	Thermo Fisher
ELISA Substrate Reagent Pack	DY999	R&D systems
Ethidium Bromide	46067	Sigma
Ethylene glycol-bis(2-aminoethylether)-N,N,N′,N′-tetraacetic acid (EGTA)	E3889	Sigma
FBS	10500	Life Technologies
FBS Ultralow endotoxin	S1860-500	VWR
Ficoll-Paque PLUS	17-1440-03	GE-Healthcare
Gelatin from bovine skin	G9391	Sigma
GeneRuler 100bp plus DNA ladder	SM0321	Thermo Fisher
Glycerol	G5516	Sigma
Go-Taq G2 Flexi (100u)	M7801	Promega
Goat serum	G6767	Sigma
Heparin sodium salt from porcine intestinal mucosa	H3149	Sigma
Human CCL2/MCP-1 DuoSet ELISA	DY279	R&D systems
Human CXCL8/IL-8 DuoSet ELISA	DY208	R&D systems
Human IL-1 alpha/IL-1F1 DuoSet	DY200	R&D systems

ELISA		
Human IL-1 beta/IL-1F2 DuoSet ELISA	DY201	R&D systems
Human IL-6 DuoSet ELISA	DY206	R&D systems
Immobilon-P PVDF membrane (0.45µm)	IPVH00010	Merck Millipore
iScript cDNA synthesis kit	170-8891	Biorad
iTaq universal SYBR supermix	172-5122	Biorad
KN-62	422706	Calbiochem
L-glutamine	BE17-605E	Lonza
Lipofectamine® RNAiMAX Transfection Reagent	1E+07	Life Techonologies
LPS from E.coli, Serotype R515	ALX-581-007-L002	Enzo
LS columns	130-042-401	Miltenyl Biotec
Medium 199	21180-021	Life Technologies
N-methyl-D-glucamine	M-2004	Sigma
NBCS	16010-159	Life Techologies
Nigericin sodium salt	N7143	Sigma
NuPage Antioxidant	NP0005	Life Technologies
NuPAGE MES running buffer (20x)	NP0002	Life Technologies
NuPAGE Transfer buffer (20X)	NP0006-1	Life Technologies
NuPAGE® Novex® 4-12% Bis-Tris Protein Gels, 1.0 mm, 10 well	NP0321BOX	Life Technologies
NuPAGE® Novex® 4-12% Bis-Tris Protein Gels, 1.0 mm, 12 well -	NP0322BOX	Life Technologies
ON-TARGETplus Non-targeting Pool	D-001810	Thermo Fisher
OptiMEM	3E+07	Life Technologies
Penicillin/Streptomycin	15140-122	Life Technologies
Perfusion set, 15cm, ID 1.6mm, 10ml, Red, pk/3	IB-10962	Thistle Scientific
Phosphatase inhibitor cocktail (100x)	5870	Cell Signalling Technologies
Pierce™ BCA Protein Assay Kit	23227	Life Technologies
Pluoronic F-127	P3000MP	Life Technologies
PNGase F	P0705	New England Biolabs
ProLong Gold antifade reagent	P36930	Life Technologies
Protease inhibitor cocktail (100x)	P8340	Sigma
PSB-12062	SML0753	Sigma
QIAquick gel extraction kit	28704	Qiagen
Recombinant Human IFN-γ	300-02	Peprotech
Recombinant Human M-CSF	300-25	Peprotech
Recombinant Human TNF	BMS301	eBioscience
Rhodamine Griffonia (Bandeirea) Simplicifolia Lectin I	RL-1102	Vector
RIPA Lysis buffer (10x)	20-188	Merck Millipore

RPMI 1640	31870-025	Life Technologies
siGLO Green Transfection Indicator	D-001630	Thermo Fisher
SMARTpool: ON-TARGETplus P2RX7 siRNA	L-003728	Thermo Fisher
SMARTpool:ON-TARGETplus EMP2 siRNA	L-016226	Thermo Fisher
Sodium bicarbonate	S5761	Sigma
Sodium deoxycholate	D6750	Sigma
Sodium dodecyl sulfate	L3771	Sigma
Suramin hexasodium salt	1472	Tocris
Thapsigargin	T9033	Sigma
TO-PRO®-3 Iodide	T3605	Life Technologies
Triton X-100	T8787	Sigma
Trypsin-EDTA	25200056	Life Technologies
Tween20	P1379	Sigma
u-Slide I (0.4) LUER, T/C treated, sterile,	IB-80176	Thistle Scientific
Viromer Green	VG-01LB-01	Cambridge Bioscience
YO-PRO®-1 Iodide	Y3603	Life Technologies
Zombie UV™ Fixable Viability Kit	423107	Biolegend
β-mercaptoethanol	M3701	Sigma
All other reagents described were from Sigma Aldrich where the source is not specified.		

Table 2.1 - List of reagents

2.2 List of antibodies

Target	Catalog number/*Clone*	Vendor
AlexaFluor488 anti-mouse CD31	102514/*MEC13.3*	Biolegend
AlexaFluor488 donkey anti-rat IgG	A21208	Life Tech
AlexaFluor568 goat anti-rabbit IgG	A11036	Life Tech
ATF-2	sc-6233 (N-96)	Santa Cruz
ATP synthase (β-subunit)	A21351/*3D5*	Life Tech
c-Jun	sc-45 (N)	Santa Cruz
Caveolin-1	610406/*2297*	BD bioscience
Caveolin-2	610684	BD bioscience
EMP2 (C-terminal)	SAB1307053	Sigma
EMP2 (HPA)	HPA014711	Sigma
FITC anti-human CD39	328205/*A1*	Biolegend
GAPDH	sc-47724 (0411)	Santa Cruz
HSP90α	ab2928	Abcam
HSP90β	ab154511	Abcam
IκB	9242	Cell Signalling Technologies
Normal Rabbit IgG	10500C	Life Tech
phospho-ATF2 (Thr71)	9221	Cell Signalling Technologies
phospho-c-Jun	sc-822 (KM-1)	Santa Cruz
phospho-p38 (Thr180,Tyr182)	28B10	Cell Signalling Technologies
phospho-p65 (Ser536)	ab86299	Abcam
P2X4	APR-002	Alomone
P2X7 (C-terminus)	APR-004	Alomone
P2X7 (Extracellular)	APR-008 (AN16)	Alomone
P2X7 (N-terminus)	sc-31499 (Y-14)	Santa Cruz
p38	9212	Cell Signalling Technologies
p65 (NF-κB)	sc-372 (C-20)	Santa Cruz
PDHX (E3BP)	M-110 sc-98751	Santa Cruz
Polyclonal Goat Anti-mouse IgG-HRP	P0447	Dako
Polyclonal Goat Anti-rabbit IgG-HRP	P0448	Dako

Table 2.2 - List of antibodies

2.3 Bioinformatics

Sequences for human P2X7 splice variants were obtained from Genbank. Genebank accession numbers; P2X7a (GQ180122.1), P2X7b (AY847298.1), P2X7c (AY847299.1), P2X7d (AY847300.1), P2X7e (AY847301.1), P2X7f (AY847302.1), P2X7g (AY847303.1), P2X7h (AY847304.1), P2X7i (NM_177427.2), P2X7j (DQ399293.1), P2X7tv4 (NR_033950.1). Sequences were aligned using Clustal Omega to identify novel exon-exon boundaries exploited to design splice variant specific primers. Specificity of primers was validated using NCBI primer blast to ensure no off-target sequences would be amplified. Predicted amino acid sequences were generated using ExPASy translate tool to identify predicted amino acid weights and antibody binding sites.

2.4 Cell Culture and reagents

2.4.1 Human Umbilical Vein Endothelial Cell (HUVEC)

Human Umbilical Vein Endothelial Cells (HUVEC) were isolated from donated umbilical cords (ethical approval: Sheffield REC 10/H1308/25) through incubation of the vein with collagenase (0.1% w/v) for 20 minutes. Isolated cells were cultured in gelatin (1% w/v) coated culture flasks in M199 media supplemented with foetal bovine serum (10% v/v), new-born bovine serum (10% v/v), 0.4mM L-glutamine, 100U/ml penicillin, 100µg/ml streptomycin, 2.5µg/ml amphotericin-B, 90µg/ml heparin and 10µg/ml endothelial cell growth supplement. HUVEC were used for experiments at P3 or P4. When appropriate HUVEC were treated with: 10ng/ml TNF, 100ng/ml IFNγ, 10µM A438079 hydrochloride or 10µM PSB-12062.

2.4.1.1 Orbital shaking model of atheroprone and atheroprotective flow

The orbital shaker system, as previously described (Warboys et al. 2014), involves culturing HUVEC using a orbital shaking platform (PSU-10i; Grant Instruments) to simulate physiological flow patterns. The radius of the orbital shaker was 10mm and

the rotation rate was set to 210rpm, with 3ml of media added per well. As a result of this rotation of the platform, a shear stress profile is generated within the well of a 6 well plate, where a pulsatile, unidirectional flow pattern of ~+13 dyn/cm^2 is created in the periphery, whereas a tangential flow pattern of ~+4dyn/cm^2 is generated in the centre of the well. Figure 2.1A shows the computational fluid dynamics (CFD) generated from the orbital shaker system. The orbital shaker platform was enclosed inside a cell culture incubator at 37°C and 5% CO_2.

HUVEC were seeded out into pre-gelatinised (1% w/v) 6 well plates at a density of 400,000 cells per well. Once a confluent adherent monolayer was reached, cells were washed once with phospho-buffered saline (PBS) and placed in 3ml of supplemented M199 media (as mentioned in 2.3.1). Cultures were then incubated at 37°C and 5% CO_2 whilst orbited at 210rpm for 72 hours. After 72 hours, cells were washed twice in ice cold PBS before cells were collected from the periphery of the well into PBS by scraping with the rubber stopper of a 1ml syringe, which removes specifically the cells at the periphery of the well. After a further two washes per well, the centre was then scraped and collected. A template was used to ensure consistency in scraping the periphery and centre of the well between experiments (Figure 2.1B). Collected cells from the respected regions were pelleted by centrifugation at 4000x*g* for 5 minutes. Cell pellets were frozen dry at -80°C until treated for RNA or protein extraction. Alternatively, the periphery of the well was collected as before, but the rest of the cells were scraped and discarded apart from the centre. The centre was then lysed directly in 40µl of Laemlli buffer and the pelleted periphery in 200µl Laemlli buffer.

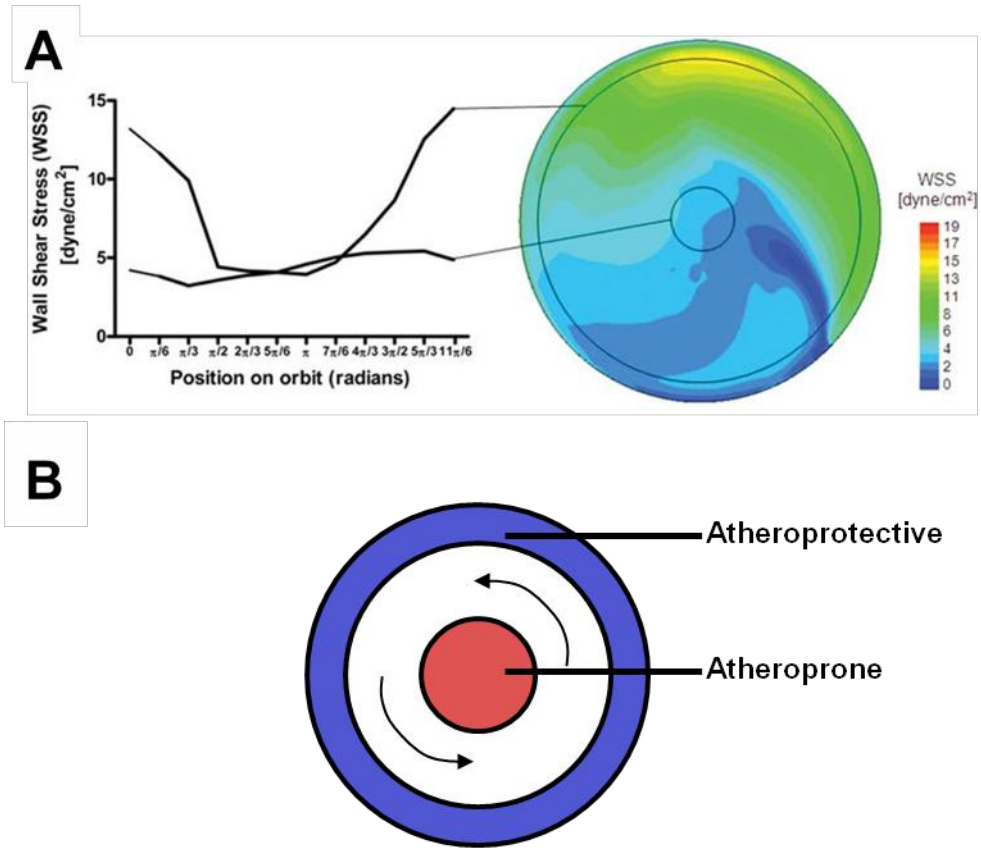

Figure 2.1 - Computational fluid dynamics of the orbital shaker model of flow.

(A) The orbital shaker generates two distinct flow patterns within a well of a 6 well plate when orbited at 210rpm with 3ml of media per well. The cells lining the periphery of the well are subjected to a pulsatile flow pattern reaching wall shear stress values of +13dynes, whereas those in the centre are influenced by disturbed flow and a low wall shear stress value of +4dynes. (B) A template used to consistently collect endothelial cells influenced by atheroprotective or atheroprone flow.

Figure (A) used with permission from: Warboys et al, Disturbed flow promotes endothelial senescence via a p53-dependent pathway, Arteriosclerosis, Thrombosis and Vascular Biology, 2014;34:985-995

(http://atvb.ahajournals.org/content/34/5/985)

2.4.1.2 ibidi flow pump model of atheroprone and atheroprotective flow

ibidi preparation: Before setting up the ibidi flow pumps system, perfusion sets were sterilised before each use with the following protocol. Immediately after use with the ibidi, the perfusion set was flushed once with bleach, and then rinsed three times with water. The perfusion sets were then autoclaved and allowed to dry. Silicon beads, which are used to dry the air before it enters the pump, were baked at 180°C for 6 hours to remove water residue. Syringes were sterilised with alcohol on the day of set up and allowed to dry in the laminar flow hood. Air filters were dried and wiped with alcohol disinfectant wipes and kept in the laminar flow hood.

Cell seeding and fluidic unit set up: 150µl of HUVEC were seeded out at a density of $1.3x10^6$/ml (200,000 cells/slide) on pre-gelatinised ibidi slides. Cells were left to adhere for 2 hours before refreshing the media and attaching the slide to the perfusion set. Sterilised syringes connected to sterilised perfusion sets and were clipped into the fluidic units.10ml of complete media was added to the syringes and air bubbles were removed from the perfusion set using a Pasteur pipette. The bottom of the perfusion set was then clamped off and the slide was attached, ensuring no air bubbles were introduced. The air filters were connected and the fluidic unit was placed in the incubator.

Shear stress parameters: Cells were cultured under flow conditions for 72 hours to simulate atheroprotective or atheroprone flow. For atheroprotective flow, +4 dyn/cm^2 for 5 minutes, +8 dyn/cm^2 for 5 minutes, then +13 dyn/cm^2 for the remainder of the experiment. Cells were gradually exposed to increasing shear stress to allow them to acclimatise to flow conditions. For atheroprone flow; a repeated cycle of +4 dyn/cm^2 for 5 minutes, then ±4dyn/cm^2 oscillating every second (0.5hz) for 2 hours. This ensures replenishment of nutrients every two hours.

After 72 hours of flow, slides containing HUVEC were detached from the ibidi system and used for calcium imaging (2.9) or the entire slide was lysed directly.

Figure 2.2 shows a schematic of the ibidi pump system. Figure 2.3 summarises the flow patterns generated by the ibidi or orbital pump system to simulate atheroprotective and atheroprone flow patterns.

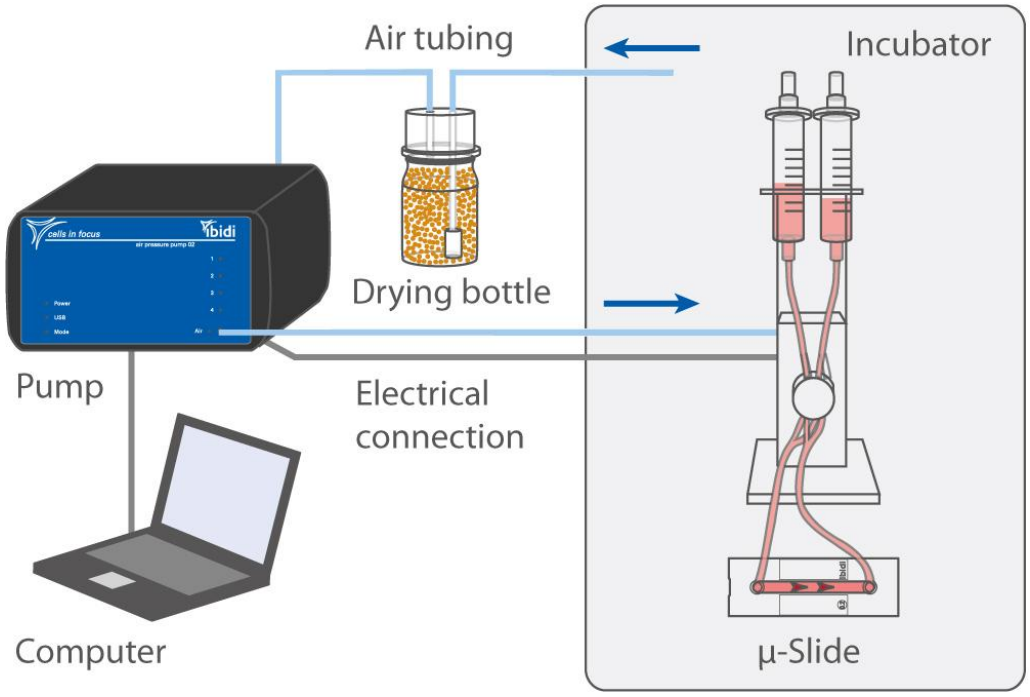

Figure 2.2 - A schematic of the ibidi pump system.

Precise flow patterns can be generated using the ibidi pump system. The ibidi pump controls the pressure inside a closed system to direct the movement of media, and as a result wall shear stress, across cells cultured on a slide. A valve dictates the directionality of flow, allowing unidirectional and bidirectional flow patterns.

Image was supplied courtesy of ibidi.

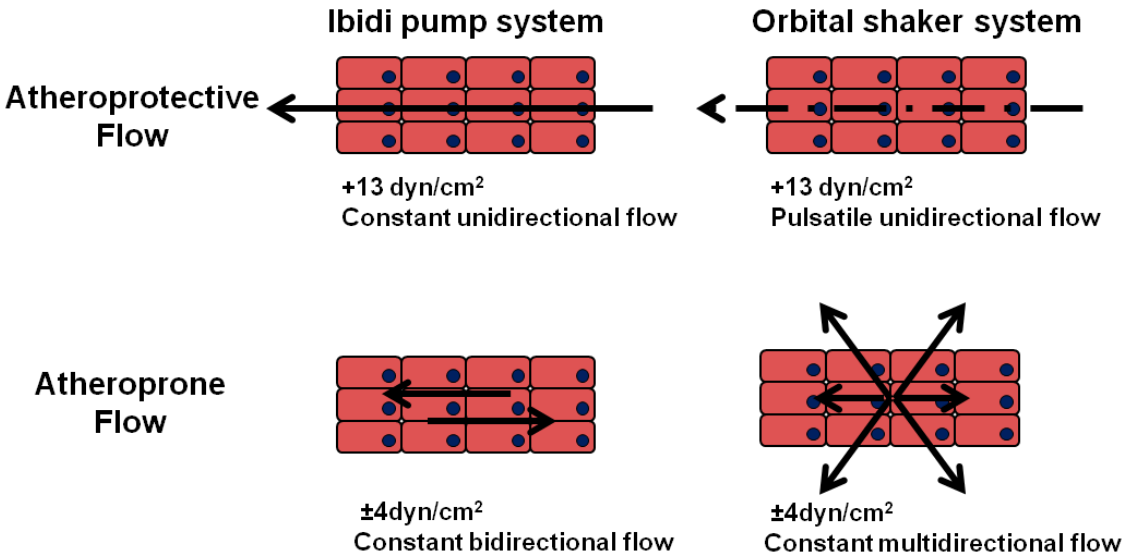

Figure 2.3 - Comparison of flow patterns generated using the ibidi pump system vs the orbital shaker system

The ibidi pump system produces a constant unidirectional flow of +13 dyn/cm^2 to mimic atheroprotective flow, whereas the orbital shaker generates a pulsatile flow pattern. The ibidi pump system can only generate bidirectional flow with low wall shear stress, whereas the orbital shaker generates multidirectional flow with transverse wall shear stress.

2.4.2 Human peripheral blood monocyte derived macrophages (MDMs)

Peripheral blood monocytes were isolated from donated human blood (Ethical approval: University of Sheffield, SMBRER310). In brief, peripheral blood mononuclear cells (PBMCs) were separated from whole blood by centrifugation using the Ficoll-Paque method. Erythrocytes were lysed from PBMCs using a 5 minute incubation of PBMC isolated cells with an erythrocyte lysis buffer (155mM NH_4Cl, 10mM $KHCO_3$, 0.1mM EDTA). CD14+ve monocytes were then purified by positive selection using magnetic CD14+ve microbeads. CD14+ve monocytes were then differentiated *in vitro* to monocyte derived macrophages (MDMs) through culture for 1 week in RPMI 1640 supplemented with 10% (v/v) ultralow endotoxin FBS, 0.05mM L-glutamine, 2U/ml Pen/Strep and 100ng/ml M-CSF. Monocytes were seeded out a $1x10^6$ in 3ml of media per 6 well plate, scaled down appropriately for smaller plates.

2.5 PCR

RNA was extracted using Isolate II RNA extraction kit and according to the manufacturer's protocol. Extracted RNA was checked for yield and purity using the Nanodrop 1000 before cDNA was synthesised from the RNA using iScript cDNA synthesis kit, according to the manufacturer's protocol.

2.5.1 Standard PCR and gel electrophoresis

cDNA was amplified by a standard polymerase chain reaction (PCR) using GoTaq G2 Flexi DNA polymerase and primers designed to amplify specific sequences (Table 2.3) according to the manufacturer's protocol, for 40 cycles. PCR products were then separated by agarose gel electrophoresis. Agarose gels (1% or 2% (w/v)) were made in TAE (Tris-Acetate-EDTA) buffer with 0.5µg/ml ethidium bromide. PCR products were loaded and ran at 100V until they had reached 2/3rds of the length of the gel. DNA was then visualised using the Bio-Rad UV imager. If one dominant band was present at the predicted size, PCR products were also sequenced by the core genomic facility (University of Sheffield) to confirm the identity of the PCR product. When more than

one band was present, DNA was extracted from the gel using QIAquick gel extraction kit, according to the manufacturer's protocol, before sequencing.

Gene target	Primer Sequences
P2X7c	*FWD: GTTGTGTCCCGAGGAATTCAGA* *REV: ACTGTATTTGGGATGGCAGTGATG*
P2X7d	*FWD: TTGACACCGCAGACTACACC* *REV: TGTTCAAGAGAGCAGGCCTTT*
P2X7e	*FWD: CCGGAAGGTGTGTAGGCAT* *REV: ACTTGGCGTATGTGGTGTAGTTG*
P2X7f	*FWD: GTTGTGTCCCGAGGAATTCAGA* *REV: CTTGGCGTATCTGAATTGCC*
P2X7g	*FWD: CCTTTGCAGCTTTTTAGACGCAC* *REV:CGCTGCGTTAGTCACTTCCTT*
P2X7h	*FWD:CCTTTGCAGCTTTTTAGACGCAC* *REV:CGCTGCGTTAGTCACTTCCTT*
P2X7i	*FWD:TTCCTACGTTTGGGGAACTCTTT* *REV:TCTCGTGGTGTAGTTGTGGC*
P2X7j	*FWD:GACCCGCAGAGCAAAGGAAT* *REV:CTTGGCGTATCTGAATTGCC*
P2X7tv4	*FWD:ACGTCCTCTCCGCAGTTCTT* *REV:TGGCGTATCTGAATTGCCAC*
P2X7 entire transcript-spanning	*FWD:GCAGTGATGTTTTCCAGTATGAGACG* *REV:GTAAGTGTCGATGAGGAAGTCGATG*

Table 2.3 - Primer sequences to human P2X7 transcripts, used for standard PCR.

2.5.2 qRT-PCR

Relative gene expression was measured by quantitative real time PCR (qRT-PCR) using gene specific primers (Table 2.4). iTaq universal SYBR green supermix and corresponding manufacturer's instructions were used to perform qRT-PCR using a CFX384 touch reach time PCR detection system (BioRad). 3.125ng of cDNA was used per reaction. Each reaction was performed in triplicate, with the Ct value averaged. Ct values were normalised using the Ct value of the flow unresponsive housekeeper gene HPRT to generate ΔCT values, as previously used in these models of endothelial flow (Mahmoud et al. 2016). Statistics were performed on ΔCT values, but fold changes are shown, calculated using the $2^{-\Delta\Delta CT}$ method.

Gene target	Primer Sequences
P2X7 (Total)	*FWD: GTCTGCAAGATGTCAAGGGC* *REV: AGCTTCCTGAACAGCTCTGA*
P2X4	*FWD: AGGACAACAGTTTCCAGGACA* *REV: CCTGCCTTCCCAAACACAAT*
Caveolin-1	*FWD: GAGAAGCAAGTGTACGACGC* *REV: ATGGCGAAGTAAATGCCCCA*
EMP-1	*FWD: GCCAATGTCTGGTTGGTTTCC* *REV: GAGGGCATCTTCACTGGCATA*
EMP-2	*FWD: CCTAACCTCCATCATCCA* *REV: TTCACGCCTGTCTGTATA*
EMP-3	*FWD: GGACAAGTCCTGGTGGACTC* *REV: ACATTACTGCAGGCCCATGT*
PMP-22	*FWD: AATTCTTGCTGGTCTGTGCG* *REV: TGTAGGCGAAACCGTAGGAG*
Pannexin-1	*FWD: GGATTCATATTGCTGGGCGG* *REV: AGCAGGCTCCATCTCTCATG*
HSP90α	*FWD: GCAGCAAAGAAACACCTGGA* *REV: CCTTCAAGGGGTGGCATTTC*
HSP90β	*FWD: ACATCATCCCCAACCCTCAG* *REV: AGCAGAAGACTCCCAAGCAT*
HPRT	*FWD: TTGGTCAGGCAGTATAATCC* *REV: GGGCATATCCTACAACAAAC*
MCP-1	*FWD: TGGGTTGTGGAGTGAGTGTT* *REV: GCAGAAGTGGGTTCAGGATT*
eNOS	*FWD: TGAAGCACCTGGAGAATGAG* *REV: TTGACCATCTCCTGATGGAA*
Interleukin-8	*FWD: GGCACAAACTTTCAGAGACAG* *REV: ACACAGAGCTGCAGAAATCAGG*
Interleukin-6	*FWD: GACAGCCACTCACCTCTTCA* *REV: CCTCTTTGCTGCTTTCACAC*
E-selectin	*FWD: GCTCTGCAGCTCGGACAT* *REV: GAAAGTCCAGCTACCAAGGGAAT*
VCAM-1	*FWD: CATTGACTTGCAGCACCACA* *REV: AGATGTGGTCCCCTCATTCG*
ICAM-1	*FWD: CACAAGCCACGCCTCCTGAACCTA* *REV: TGTGGGCCTTTGTGTTTTGATGCTA*
KLF-2	*FWD: GCACGCACACAGGTGAGAAG* *REV: ACCAGTCACAGTTTGGGAGGG*
RelA	*FWD: TCAAGATCTGCCGAGTGAAC* *REV: TGTCCTCTTTCTGCACCTTG*

Table 2.4 - Primer sequences used for qRT-PCR, to probe human cDNA.

2.6 Western blotting

HUVEC were lysed directly in Laemlli buffer (2% (w/v) SDS, 5% (v/v) β-mercaptoethanol, 10% (v/v) glycerol in 60mM Tris-HCL, pH 6.8) or in RIPA buffer (0.5% (w/v) SDS, supplemented with protease inhibitor cocktail and phosphatase inhibitors. From ibidi slides, 150µl of Laemlli buffer was added to each chamber whereas from the orbital shaker, cells were lysed in a fixed volume of lysis buffer at a ratio of 5:1 for the periphery and centre cells respectively, equating to approximately equal cell number / loading. Lysates were vortexed vigorously and subjected to one freeze-thaw cycle before being boiled at 95°C for 5 minutes. Westerns were performed using the XCell *SureLock*® Mini-Cell (Life Technologies). Protein was then resolved on a 4-12% bis-tris gel in MES buffer at 200V for 35 minutes. Proteins were then transferred onto a PVDF membrane at 35V for 1 hour at room temperature. After blocking for 1 hour in 5% (w/v) milk in Tris buffered saline (0.1% (v/v) Tween) (TBS-T) or 5% (w/v) BSA TBS-T, membranes were incubated with primary antibodies on a rotator overnight at 4°C. Blots were washed 3 times for 10 minutes in TBS-T then incubated for 1 hour with appropriate HRP-conjugated secondary antibodies. Membranes were washed 3 more times for 10 minutes in TBS-T before visualised by chemi-illuminescence using ECL-select. Chemi-illuminescence was detected using a LiCOR c-digit blot scanner and densitometry was determined using Image Studio (LiCOR Biosciences). Alternatively, HRP staining was visualised using the Bio-Rad imager and Image lab software (BioRad). Band intensities were normalised against PDHX or GAPDH.

Antibodies and dilutions used were: P2X7 1:1000 (APR-008, Alomone); P2X4 1:3000 (APR-002, Alomone); Caveolin-1 1:3000 (clone 2297, BD biosciences); Caveolin-2 1:1000 (610684, BD Biosciences); β-subunit ATP synthase 1:3000 (Clone 3D5, Molecular probes); HSP90α 1:3000 (ab2928, Abcam); HSP90β 1:3000 (ab154511, Abcam); ATF-2 1:1000 (N-96, Santa Cruz); p-ATF2 Thr71 1:1000 (9221, Cell Signalling

Technologies); p38 1:1000 (9212, Cell Signalling Technlogies); p-p38 Thr180/Tyr182 1:1000 (28B10, Cell Signalling Technologies); c-Jun 1:1000 (sc-45, Santa Cruz); p-c-Jun 1:1000 (KM-1, Santa Cruz); p65 1:3000 (C-20, Santa Cruz); p-p65 Ser536 1:3000 (ab86299, Abcam); IkB 1:1000 (9242, Cell Signalling Technologies); and EMP2 1:500 (SAB1307053, Sigma). Expression was normalized to that of GAPDH 1:10,000 (0411, Santa Cruz) or PDHX 1:6000 (M-110, Santa Cruz).

2.6.1 Deglycosylation treatment

Cell lysates were deglycosylated using PNGase-F. 1-20µg of protein in Laemlli lysis buffer was first denatured by boiling at 100°C for 10 minutes. Samples was then briefly cooled before the addition of 1x G7 reaction buffer, 1% (v/v) NP-40 and PNGase-F, or H_2O in the case of negative controls. The reaction was then incubated for at least 1 hour at 37°C before the addition of extra 5x Laemlli buffer and processing for western blotting as described above.

2.6.2 Isolation of Triton X-100 soluble and insoluble fractions

Triton X-100 soluble and insoluble protein fractions were isolated from human MDMs. Scraped MDMs were lysed in Triton X-100 soluble lysis buffer (50mM Tris, 150mM NaCl, 1% (v/v) Triton X-100, protease inhibitors, pH 6.5) for 30 minutes at 4°C. The resulting lysate was centrifuged at 9000x*g* for 30 minutes at 4°C. The supernatant was collected as the Triton X-100 soluble lysate and the pellet was further lysed in Triton X-100 insoluble lysis buffer (50mM Tris, 150mM NaCl, 0.5% (w/v) sodium deoxycholate, 1% (w/v) sodium dodecyl sulfate, 1% (v/v) Triton, protease inhibitors, pH 6.5). Triton X-100 insolute lysates were vortexed, passed through a 30 gauge needle five times and placed in a sonicated water bath for 15 minutes, before insoluble membrane fragments were removed by a 10 minute centrifugation at 10000x*g*. Samples were processed for western blotting as described in 2.5.

2.7 Gene Knockdown

2.7.1 HUVEC knockdown

P2X7 mRNA was silenced in HUVEC using a mixed pool of 4 siRNAs and compared to controls treated with non-targeting siRNA, which has been previously shown to knockdown P2X7 in human cells (Shishikura et al. 2016; Gicquel et al. 2015). HUVEC were transfected using the Lipofectamine® RNAiMAX transfection reagent. HUVEC were seeded into 6 well plates at a density of 100,000 cells per well in antibiotic-free media. The following day, when cells were between 30%-50% confluence, they were treated for transfection according to the recommended protocol for HUVEC. In brief, HUVEC were washed once in PBS before 1.6ml of antibiotic- and antifungal-free supplemented M199 was added. siRNA and RNAiMAX mixes were made individually in 200µl optiMEM (Life Technologies). The siRNA and RNAiMAX solutions were combined, incubated at room temperature for 20 minutes, and added to cells. 4-6 hours after transfection, the media was replaced with supplemented M199 (2.4.1) and incubated under static conditions for the desired time. P2X7 knockdown was determined to be optimal following 50nM siRNA treatment, 5µl RNAiMAX/well and 72 hour incubation, as decided by performing a time course.

2.7.2 Human blood monocyte derived macrophage (MDM) knockdown

After 1 week of culture with M-CSF, gene silencing was performed in macrophages using SMARTpool siRNAs and Viromer green using the manufacturer's recommended protocol. In brief, for a 6 well plate, siRNA was diluted from 20µM to 2.8µM in Buffer GREEN and mixed with the Viromer-containing solution. After 15 minutes incubation at room temperature, 200µl of the transfection mix was added drop-wise onto macrophages in 1.8ml of complete macrophage growth media (2.4.2). This equates to 25nM siRNA transfection and gene knockdown was analysed 48 hours post transfection. EMP2 knockdown was best achieved after 48 hours, determined by a time course. For calcium imaging and dye uptake experiments, macrophages were scraped

24 hours after transfection and re-seeded into 96 well plates at a density of 50,000/well, and then used 24 hours later.

2.8 Flow Cytometry

After flow conditioning with the ibidi flow system, HUVEC were detached using a diluted trypsin solution (1:5 in PBS) at room temperature for 5 minutes. Detached HUVEC were incubated with CD39-FITC (Clone A1, Biolegend) and Zombie UV viability dye in Ca^{2+}/Mg^{2+} free phosphate buffered saline (0.25% foetal bovine serum v/v) for 40 minutes at 4°C. Cells were pelleted by 5 minutes centrifugation at 1000x*g* and washed twice by re-suspension. Fluorescence was measured using a LSRII flow cytometer (BD Bioscience), with the median fluorescent intensity measured on live cells.

2.9 Calcium Imaging

Cal-520AM was used to fluorescently label intracellular calcium. On the day of the experiment, 50µg of Cal-520AM was made up to 5mM in anhydrous DMSO. Cal-520 solution was then mixed at a ratio of 1:1 with pluoronic acid F-127 and then diluted in supplemented M199 to make a 5µM Cal-520AM solution. Cells were incubated for 90 minutes in the dark at 37°C and 5% CO_2 to allow dye loading. Cells were then washed twice with a physiological Ca^{2+} extracellular imaging buffer (134.3mM NaCl, 5mM KCl, 1.2mM MgCl2, 1.5mM $CaCl_2$, 10mM HEPES, 8mM Glucose, sterile filtered and at pH 7.4), and incubated in this solution until used for imaging. For experiments requiring depletion of extracellular calcium, 1.5mM $CaCl_2$ was replaced with 0.4mM EGTA. Cells were washed three times with the EGTA containing solution and incubated for 5 minutes prior to BzATP stimulation. To deplete intracellular calcium stores, Thapsigargin was used. Thapsigargin is an inhibitor of the sarco/endoplasmic recticulum Ca^{2+} ATPases (SERCA) pump (Lytton et al. 1991), which act to regulate cytosolic calcium levels by actively pumping calcium into the endoplasmic reticulum.

Inhibition of SERCA pumps therefore lead to passive diffusion of calcium out of the endoplasmic reticulum (Sabala et al. 1993). 10μM Thapsigargin was applied for 3 minutes, over which time the calcium response to thapsigargin treatment had returned to baseline. 10μM A438079 hydrochloride (P2X7 antagonist) and 10μM PSB-12062 (P2X4 antagonist) were incubated with cells in extracellular imaging buffer for 5 minutes before BzATP stimulation. 100μM ARL-67156 (ATPase inhibitor) was added in combination with BzATP.

2.9.1 Calcium responses measured using a plate reader

Calcium responses were measured using the BMG labtech FLUOstar OPTIMA plate reader for static endothelial and macrophage cells. Cells in 96 well plates were loaded as described above (2.9), and incubated in 90μl of Ca^{2+} extracellular imaging buffer. Buffers were changed as appropriate immediately before imaging. Cells were stimulated with 10μl of stock BzATP/ATP in a Ca^{2+} and EGTA free solution by injection using the plate reader, with measurements recorded every second.

2.9.2 Calcium responses measured using microscopy

Endothelial cells preconditioned under flow using the ibidi flow pump system (2.4.1.2) were loaded under static conditions as described above (2.9). Calcium imaging was performed by epifluorescence microscopy using a Nikon Eclipse T*i* and recorded using a photometrics CoolSnap MYO. Figure 2.4 shows a schematic of how calcium imaging was performed. Slides were clipped onto the microscopy stage to keep the specimen in focus during stimulation. Cells were washed once with Ca^{2+} extracellular buffer immediately before recording. 150μl of working solution of compounds was flushed across the cells, in the same direction as the flow they were preconditioned under. Measurements were taken every second.

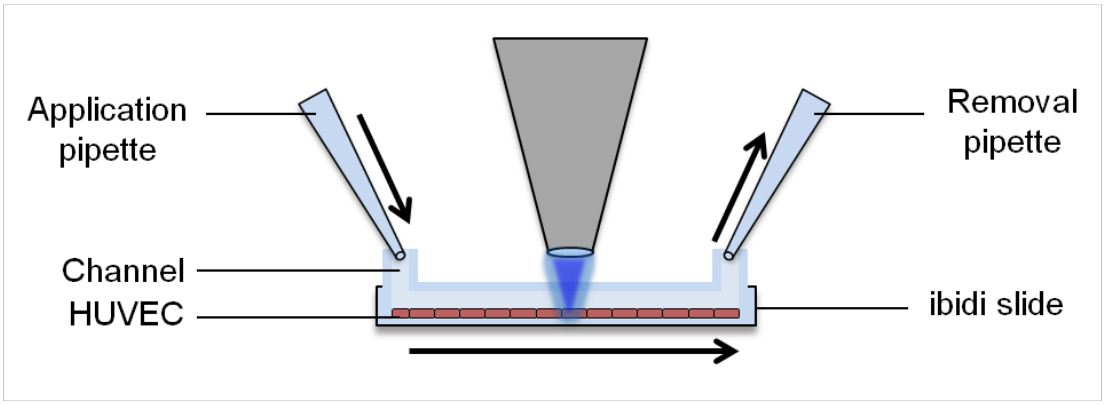

Figure 2.4 - Schematic of system used to record calcium responses in HUVEC.

HUVEC cultured on ibidi slides were clipped to the microscope stage and imaged by epifluorescence microscopy. Cells were stimulated or washed by adding 150µl of the desired solution into the inlet of the slide using the application pipette, which is then transferred across the cells by removing 150µl from the outlet of the slide. As a result, the desired solution submerges the cells of interest being recorded.

2.10 ELISA

Enzyme-linked immunosorbent assays (ELISA) were used to quantify cytokine and chemokine release from cells. HUVEC supernatant was obtained from ibidi experiments after 72 hours of culture and frozen at -80°C until used. HUVEC supernatant was diluted 1:5 for IL-8 ELISAs and concentrated 8 times for IL-1 ELISAs using microsep centrifugal concentrators, 10kDa cut off (Pall).

IL-1β ELISAs were also performed on MDM supernatants. MDMs were primed for 3 hours with 1ng/ml Lipopolysaccharide before stimulation with 300μM BzATP in vesicle shedding buffer (147mM *N*-methyl-D-glucamine, 10mM HEPES, 12mM Glucose, 2mM KCl, 2mM $CaCl_2$, 1mM $MgCl_2$, sterile filtered, pH 7.3) for 30 minutes at 37°C. When appropriate, MDMs were pre-incubated for 30 minutes with 10μM A438079 (P2X7 antagonist), which was present for the duration of BzATP stimulation. Supernatants were collected and spun at 1500x*g* for 5 minutes before freezing at -80°C. Samples were diluted 1:5 for IL-1β ELISA.

IL-1, IL-6 and IL-8 ELISAs were performed using R&D ELISA kits and according to the manufacter's protocol. The plates were washed using a BioTek El*x*50 washer, where 400μl of wash buffer (PBS 0.5% (v/v) Tween20) was added and removed 3 times. Antibody dilutions and standard curve concentrations can be found in Table 2.5. 96 well EIA/RIA plates were incubated overnight with capture antibody at room temperature. Plates were then washed and blocked for at least 1 hour with 1% (w/v) BSA-PBS, and then washed. Recombinant human standards of the protein of interest were used to generate a standard curve in 1% (w/v) BSA-PBS, which was serially diluted according to Table 2.5. Samples were incubated for 2 hours at room temperature before washing and a further 2 hours incubation with detection antibody. Plates were washed and incubated with Streptavidin-HRP for 20 minutes. After washing again, the substrate was added for 20 minutes before the reaction was stopped with 1M H_2SO_4. Standards and samples were run in duplicate and optical

density absorbance was measured at 450nm using an absorbance plate reader (Thermo Scientific Varioskan Flash). Concentrations of samples were determined by interpolation from a four-parameter logistic standard calibration curve. Data were analysed as pg/ml, and presented as fold change where appropriate.

ELISA	Reagents
IL-1α	Capture antibody: 2µg/ml Standard: 250pg/ml to 1.9pg/ml Detection antibody: 50ng/ml
IL-1β	Capture antibody: 4µg/ml Standard: 1000pg/ml to 3.906pg/ml Detection antibody: 200ng/ml
IL-6	Capture antibody: 2µg/ml Standard: 1350pg/ml to 5.273pg/ml Detection antibody: 50ng/ml
IL-8	Capture antibody: 2µg/ml Standard: 2000pg/ml to 7.813pg/ml Detection antibody: 10ng/ml

Table 2.5 - Concentrations of antibodies and recombinant standards used for ELISA analysis.

2.11 ATP detection assay

ATP was measured using a commercially available ATP determination assay. This assay uses the luciferase enzyme, which uses ATP and its substrate $_{D}$-luciferin to produce light. Since ATP is a limiting factor in this reaction, combining luciferase and $_{D}$-luciferin with a solution containing ATP will produce light proportional to the ATP concentration. HUVEC were cultured for 72 hours in supplemented M199 media under static conditions or exposed to flow by the orbital shaker. After 72 hours, cells were washed once in Ca^{2+} extracellular imaging buffer (see 2.8). HUVEC were then incubated for a further 4 hours in Ca^{2+} extracellular imaging buffer under static conditions ±10ng/ml TNF, or exposed to flow. Supernatants were collected and used immediately for ATP determination following the manufacturer's instructions. ATP determination assays were also performed on both fresh and frozen supernatants obtained from HUVEC cultured using the ibidi pump system.

2.12 Dye uptake assay

P2X7 dye uptake was assessed using the BMG labtech FLUOstar OPTIMA plate reader. As P2X7 activation causes a ~900 dalton sized pore in the membrane, small membrane impermeable nuclear dyes can pass the membrane through these pores and bind to DNA. Therefore, measurement of dye uptake in response ATP is an indicator of P2X7 receptor activity. Cells were grown in 96 well plates prior to imaging. Dye uptake was performed in a sucrose dye uptake buffer (280mM sucrose, 5.6mM KCl, 0.5mM $CaCl_2$, 10mM Glucose, 10mM HEPES, 5mM *N*-methyl-D-glucamine, 300nM Yo-Pro-1, pH 7.4), as described previously (Allsopp & Evans 2015). 90µl of sucrose dye uptake buffer was added to each well, and 10µl of 3mM BzATP was injected using the plate reader. When used, 10µM A438079 hydrochloride (P2X7 antagonist) was pre-incubated with the cells prior to BzATP addition.

2.13 *En face* immunostaining of the murine aorta

Mice were housed under specific-pathogen free conditions and studied according to UK Home Office Regulations and the UK Animals (Scientific Procedures) Act 1986. 6 week old female wild type C57BL/6 mice were sacrificed by intraperitoneal injection of pentobarbital. Exsanguination was performed via cardiac puncture before the aorta was perfused *in situ* with PBS followed by perfusion-fixation with 4% (v/v) paraformaldehyde (PFA) before harvesting. Ribcage segments, including the aorta, were further fixed for 1 hour in 2% (v/v) PFA at room temperature. Sacrifice of mice and dissection was performed by Neil Bowden (P.Evans Group). The mouse aorta has been mapped by computation fluid dynamics where the outer curvature, considered an atheroprotected site, is exposed to high shear stress, and the inner curvature, exposed to disturbed flow is an atheroprone site (Suo et al. 2007). Aortae were dissected, then blocked and permeabilised in PBS (20% (v/v) goat serum, 0.5% (v/v) triton x-100) overnight at 4°C. Primary antibodies were incubated in PBS-T (5% (w/v) BSA, 0.1% (v/v) tween-20) overnight at 4°C. Aortae segments were washed 3 times in PBS before incubation with appropriate AlexaFluor conjugated secondary antibodies in PBS-T (5% (w/v) BSA, 0.1% (v/v) tween-20) at room temperature for 5 hours. After a further 3 washes in PBS, aortae were stained with TO-PRO3 for 1 hour at room temperature. Samples were washed 3 more times in PBS before being mounted. Fully stained vessels were visualised using confocal laser-scanning microscopy (Zeiss LSM510 NLO inverted microscope), where endothelial cells were identified by strong CD31 immunostaining. Sites influenced by atheroprone and atheroprotected flow were identified by their location on the aorta as well as by cell morphology determined by CD31 staining. IgG isotype control staining was performed for each mouse on sections of the descending aorta to determine antibody specificity. 3 fields of view were taken from the atheroprotected and atheroprone site in each mouse. Images were analysed using Image J software, where the expression of the protein of interest was quantified

by measuring fluorescence intensity and averaging the measurements from the 3 fields of view. Fluorescence measurements from the IgG control were subtracted from the stains in the aorta, since this represented a non-specific or autofluorescent component. Cell surface quantification was achieved by creating a mask from the cell surface CD31 staining and measuring only the fluorescence intensity of P2X7 within this mask.

2.14 Isolation of atheroprotected and atherosusceptible sites of the porcine aorta

Sites of the porcine aorta influenced by atheroprotective or atheroprone flow patterns have been identified by computational fluid dynamics (CFD) (Serbanovic-Canic et al. 2016) and as such can be used *ex vivo*. Porcine aortae were obtained from a local reputable abattoir shortly after slaughter. Atheroprotected or atheroprone sites, identified from the CFD, were dissected out and the endothelium was studied. For calcium imaging studies, sections were placed face-down in supplemented M199 (2.4.1) with 5μM Cal-520AM (2.9) and 20μg/ml Rhodamine Griffonia (Bandeirea) Simplicifolia Lectin I, which labels the endothelium, for 90 minutes at 37°C. Sections were briefly washed and then pinned face-up in paraffin wax and imaged via confocal laser-scanning microscopy (Zeiss LSM510 NLO upright microscope). For RNA isolation, sections were incubated face-down in collagenase (0.1% w/v) in supplemented M199 media (2.4.1) for 20 minutes. Endothelial cells were gently scraped into PBS and pelleted by centrifugation at 1500x*g* for 5 minutes. RNA isolation was performed as described previously (2.5). RNA samples isolated from porcine scrapes used in this study were obtained from Professor Paul Evans' group.

2.14 Statistics

Where possible, data were checked for normal distribution. Differences between samples were analysed using a paired Students *t*-test, one way or two way ANOVA, followed by Tukey's or Sidaks post hoc analysis using Graphpad Prism software.

(*=p<0.05, **=p<0.01, ***=p<0.001, ****=p<0.0001). Each n-number represents cells isolated from different donors.

Chapter 3

ATP induced calcium responses are enhanced under atheroprone flow

3.1 Introduction

Shear stress has been established to evoke the release of adenosine triphosphate (ATP) from endothelial cells into the blood stream and activate endothelial purinergic receptors (Bodin & Burnstock 2001; Yamamoto et al. 2003). Shear stress induced ATP release has only been previously studied in endothelial cells under atheroprotective flow patterns, where it has been shown to induce nitric oxide production and vasodilation by acutely activating P2X4 (Yamamoto et al. 2006) and P2Y2 receptors (Wang et al. 2015; Sathanoori et al. 2016). In contrast to providing a protective role, extracellular ATP triggers inflammatory signalling in a number of cell types including the endothelium (von Albertini et al. 1998; Stachon et al. 2016); its levels are therefore tightly regulated under normal physiological conditions. Recent evidence have shown an association with dysregulated extracellular ATP in the induction of atherosclerosis (Mercier et al. 2012). Cell surface expression of F_1/F_0 ATP synthase, a source of shear stress induced ATP release (Yamamoto et al. 2007), is enhanced in under atheroprone flow (Fu et al. 2011) whereas the ATPase CD39, which hydrolyses extracellular ATP, is highly expressed in endothelial cells at atheroprotected regions (Kanthi et al. 2015). This indicates that extracellular ATP regulation may be altered under atheroprone flow and plays a role in promoting atherosclerosis.

The ATP gated P2 receptors are split broadly into 2 main families, the P2X ion channels and the P2Y G-protein coupled receptors (GPCRs). There are 7 P2X receptor subtypes (P2X1-7) and 8 P2Y receptor subtypes (P2Y1,2,4,6,11-14). P2X receptors respond exclusively to ATP, whereas only a fraction of P2Y receptors respond to ATP, with subtypes activated by ADP, UTP or UDP. Inflammatory stimuli has been reported to up-regulate endothelial expression of P2X4 and P2X7 receptors and activation of ATP mediated inflammatory signalling (Wilson et al. 2007; Sathanoori et al. 2015). Since P2X4 and P2X7 receptors have established links with inflammatory signalling pathways (Burnstock 2016) and extracellular ATP levels may be dysregulated under

atheroprone flow, it was proposed that these receptors mediate atheroprone flow associated inflammation signalling. Since increased intracellular calcium is the first event that occurs following P2 receptor activation, calcium imaging was used as a tool to measure purinergic responses in endothelial cells cultured under flow.

3.2 Hypothesis

Endothelial ATP responses are altered between cells conditioned with atheroprone or atheroprotective flow, mediated through activation of P2X receptors.

3.3 Aims

1) Determine if preconditioning with atheroprone or atheroprotective flow alters BzATP induced calcium signalling.
2) Identify the proportion of the BzATP response dependent on extracellular calcium.
3) Identify the proportion of the BzATP response dependent on intracellular calcium stores.
4) Evaluate the role of CD39 in BzATP induced calcium responses.

3.4 Optimisation of ATP induced calcium imaging

Before the aims were addressed, calcium imaging was optimised on static HUVEC to generate dose response curves for ATP and its modified derivative, 3'-O-(4-benzoyl)benzoyl adenosine 5'-triphosphate (BzATP). Static HUVEC were initially used as a higher throughput could be achieved. BzATP is structurally different to ATP and as a consequence it has different potencies for different P2 receptors. Interestingly, BzATP has been reported to activate P2X4 and P2X7 receptors potently, but only a subset of P2Y receptors (Table 3.1), so is a useful tool to investigate P2X receptor function. Table 3.1 shows a comparison of endothelial expressed P2 receptors and the efficacy of ATP and BzATP. BzATP is also the agonist of choice for studying P2X7 receptors, as it actually more potent at the P2X7 receptor than ATP. For this reason, BzATP is commonly misconceived as a P2X7 specific agonist, but actually activates a range of P2 receptors (Jarvis & Khakh 2009; Jacobson et al. 2002). Ionotropic P2X receptors and metabotropic P2Y receptors mobilise calcium from spatially distinct regions, with P2X receptors triggering extracellular calcium influx into the cell and P2Y receptors evoking release of intracellular calcium stores. Therefore some experiments were performed using the calcium chelator EGTA in the extracellular imaging buffer instead of calcium, as this blocks P2X mediated calcium influx but does not alter P2Y mediated calcium release.

P2 Receptor	EC50 ATP (μM)	EC50 BzATP (μM)	Relative endothelial expression (compared to P2X4)
P2X1	0.07 [1,8]	0.003[1,8]	Low/absent [2,3,4,5]
P2X4	10 [1,8]	7[1,8]	High (100)[2,3,4,5]
P2X5	10 [1,8]	>500[1,8]	Low (1)[2,4,5]
P2X7	100 [1,8]	20[1,8]	Moderate (15)[2,3,4,5]
P2Y1	1.5 (Partial) [6,8]	✘	Moderate (7)[3]
P2Y2	2.7[7,8]	4.7[7]	Moderate (5)[3]
P2Y4	Antagonist [7,10]	Antagonist[7] (IC50=150μM)	Low (1) [3]
P2Y6	✘ [8]	✘ [8]	Low (2)[3]
P2Y11	10.5[8,9]	65[8,9]	Moderate (9)[3]
References: 1 = (Jarvis & Khakh 2009), 2= (Yamamoto et al. 2000), 3= (Wang et al. 2002), 4 = (Ramirez & Kunze 2002), 5 = (Wilson et al. 2007), 6 = (Schachter & Harden 1997), 7 = (Wildman et al. 2003), 8 = (Jacobson et al. 2002), 9 = (Communi et al. 1999), 10 = (Kennedy et al. 2000)			

Table 3.1 - Comparison of endothelial P2 receptors and their approximate affinities to ATP and BzATP.

✘ indicates no evidence of activity currently reported

To determine the optimal concentration to maximise the sensitivity of our assays, a dose response curve for ATP and BzATP was generated using calcium imaging on static HUVEC. Increasing concentrations of ATP evoked larger calcium responses in static endothelial cells, which reached a maximal response at a concentration of 30μM (Figure 3.1). Depletion of extracellular calcium with EGTA indicated a larger role for extracellular calcium influx at higher ATP concentrations, as the maximal response was ~50% reduced at a concentration of 30μM and above. Stimulation with BzATP produced a smaller calcium response compared to ATP (data not shown), with 300μM BzATP producing the maximal response (Figure 3.2). When extracellular calcium was chelated with EGTA, the maximal response to 300μM BzATP was also ~50% reduced. This suggests that in endothelial cells under static conditions, the ATP and BzATP-mediated calcium responses are co-ordinated evenly between P2X and P2Y receptors.

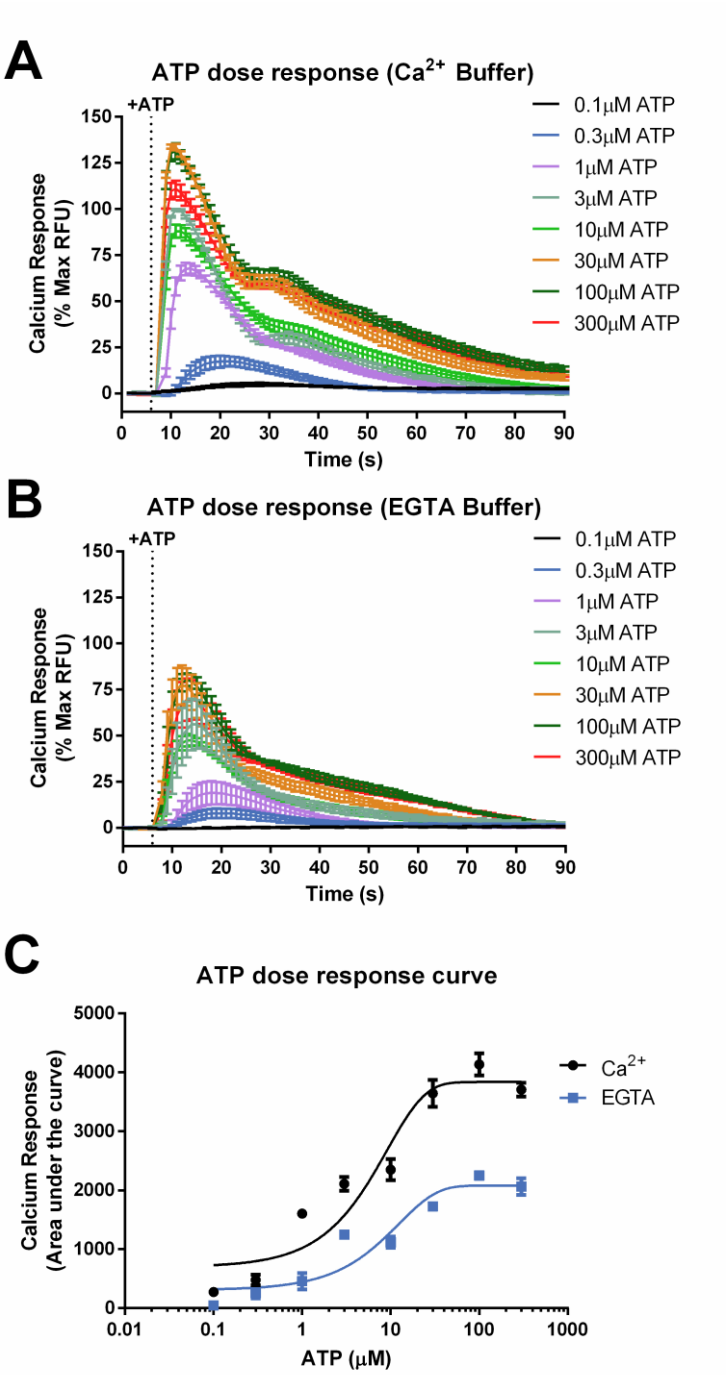

Figure 3.1 - ATP dose response curves for static HUVEC in physiological Ca^{2+} or Ca^{2+} free (EGTA) extracellular solution.

Calcium response curves for ATP generated in static HUVEC in physiological extracellular Ca^{2+} (A) or EGTA (B) containing imaging buffer (n=3). (C) Dose response curve generated from A+B. Values are ± SEM.

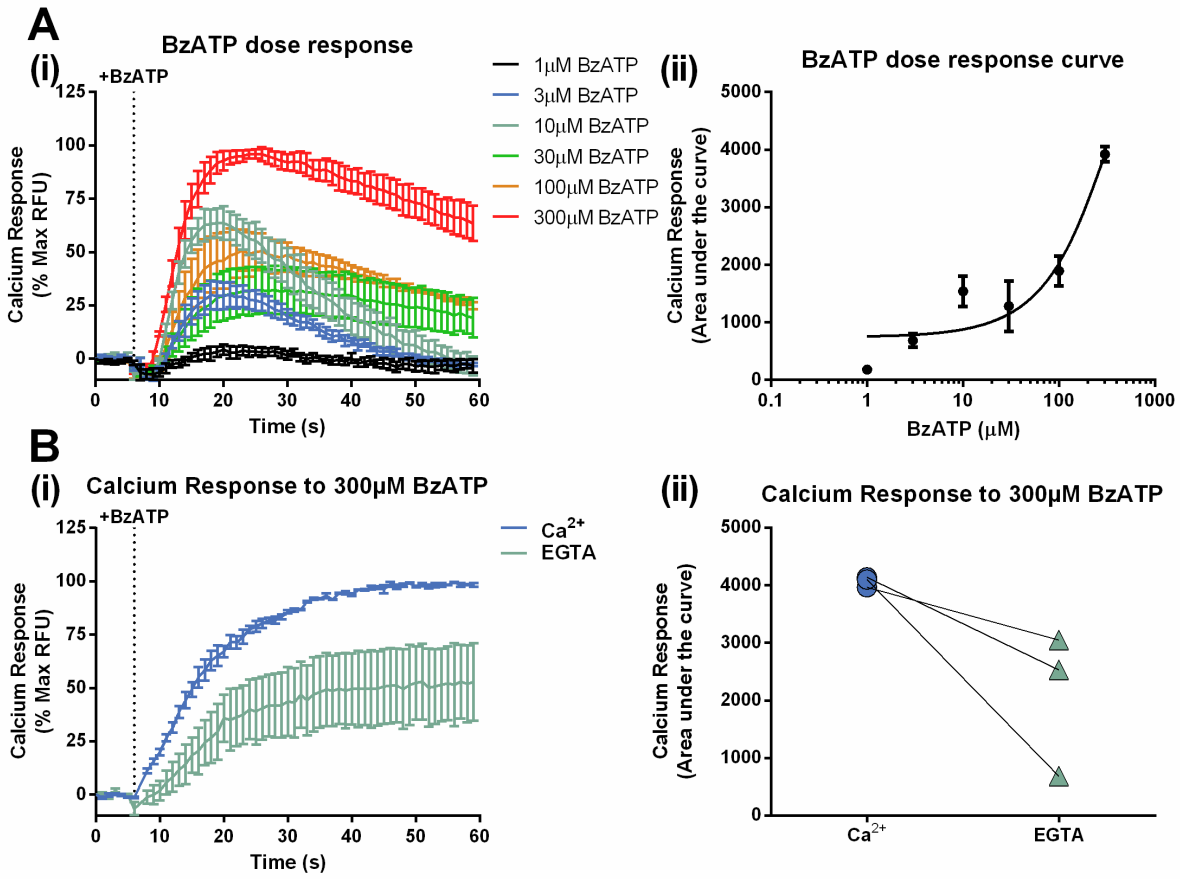

Figure 3.2 - BzATP dose response curves in static HUVEC.

(A) Calcium response curves for BzATP generated in static HUVEC in physiological extracellular Ca^{2+} imaging buffer (i) and dose response curve (ii) (n=3). (B) Calcium response curve after 300μM BzATP stimulation generated in physiological extracellular Ca^{2+} or EGTA imaging buffer (i) and area under the curve analysis (ii) (n=3). Values are ± SEM.

Previous research from the Wilson group has shown that a combination of TNF and IFNγ enhances the expression of P2X4 and P2X7 in the endothelial cells cultured under static conditions (Wilson et al., 2007). Therefore, calcium imaging was performed on TNF/IFNγ stimulated HUVEC to determine whether increased expression is also associated with an increase in P2X receptor function. Matching these observations, stimulation with TNF and IFNγ strongly induced the expression of both P2X7 (80.76± 38.73 fold) and P2X4 (80.34±35.95 fold) (Figure 3.3A). The calcium response to 300μM BzATP was also enhanced (No TNF/IFNγ=4067±53.14 vs +TNF/IFNγ=17506±2497) (Figure 3.3B), particularly with respect to extracellular calcium influx response (Ca2+ TNF/IFNγ=17506±2497 vs EGTA TNF/IFNγ= 3744±1682), suggesting an enhancement in P2X receptor functional activity due to TNF/IFNγ treatment.

BzATP exhibits a higher potency at P2X4 and P2X7, but is less potent at P2Y1, P2Y2 and P2Y11 receptors, than ATP (Table 3.1). Moreover BzATP is considered more stable and less pH sensitive than ATP. Endothelial P2X receptor expression is also predominantly P2X4 and P2X7 (Ramirez & Kunze 2002; Wilson et al. 2007; Wang et al. 2002; Yamamoto et al. 2000). Since it was proposed that P2X receptor activity was altered between atheroprone and atheroprotective flow, BzATP was used as an exogenous agonist as it is a more efficacious agonist of human P2X4 and P2X7 receptors.

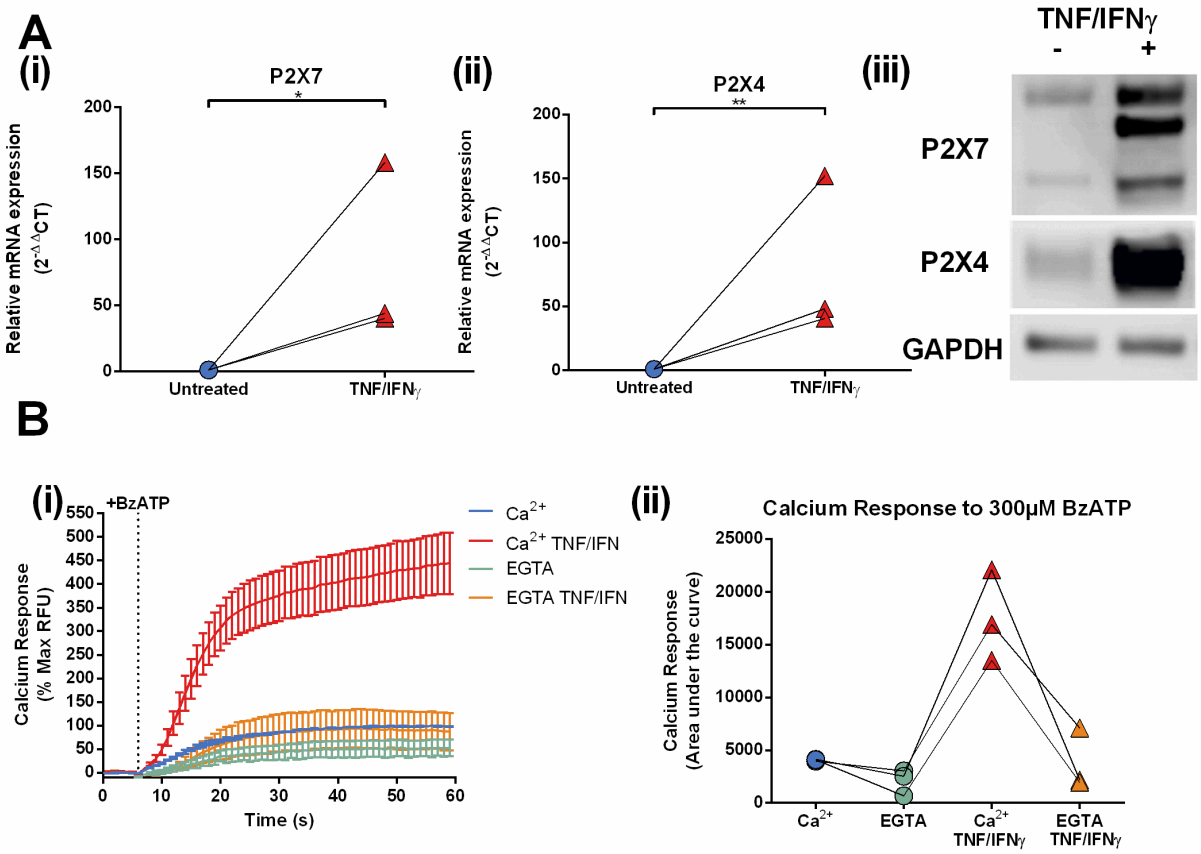

Figure 3.3 - TNF and IFNγ enhance the BzATP calcium response through extracellular calcium influx.

(A) Incubation with 10ng/ml TNF and 100ng/ml IFNγ for 48 hours up-regulates the expression of P2X4 and P2X7 mRNA and protein in static HUVEC. (B) Calcium response curves after stimulation of 300μM BzATP in static HUVEC ±TNF/IFNγ in physiological Ca^{2+} or EGTA containing extracellular buffer (i) and area under the curve analysis (ii) (n=3). * indicates p=<0.05 and ** indicates p<0.01 using a paired *t*-test. n=3. For qPCR analysis, statistical analysis was performed on the ΔCT values. Values are ± SEM.

It is well documented that extracellular ATP release occurs in response to shear stress (Bodin & Burnstock 2001; Yamamoto et al. 2007; Wang et al. 2015). To confirm this, a luminescence based ATP determination assay was performed on the supernatants of HUVEC–preconditioned under static or flow conditions using the orbital shaker model for 72 hours, before the media was replaced. HUVEC were then incubated for a further 4 hours under static conditions ±TNF, or exposed to flow. Luminescence, which relates to ATP concentration, was increased after exposure to TNF or flow (Static=2040±145.4, TNF=4829, Flow=7124±909.9) (Figure 3.4) matching previous literature (Lohman et al. 2015; Yamamoto et al. 2003; Wang et al. 2015). As this was performed in the orbital shaker model, it could not be discriminated between atheroprotective and atheroprone flow patterns as HUVEC between these populations share the same culture media. Therefore, ATP release was measured from HUVEC cultured under atheroprotective or atheroprone flow using the ibidi pump system, where endothelial cells are only influenced by one flow pattern. However a requirement for this system is an excess of 10ml of media per slide containing 250,000 endothelial cells, and as such was too dilute to detect ATP released into the supernatant.

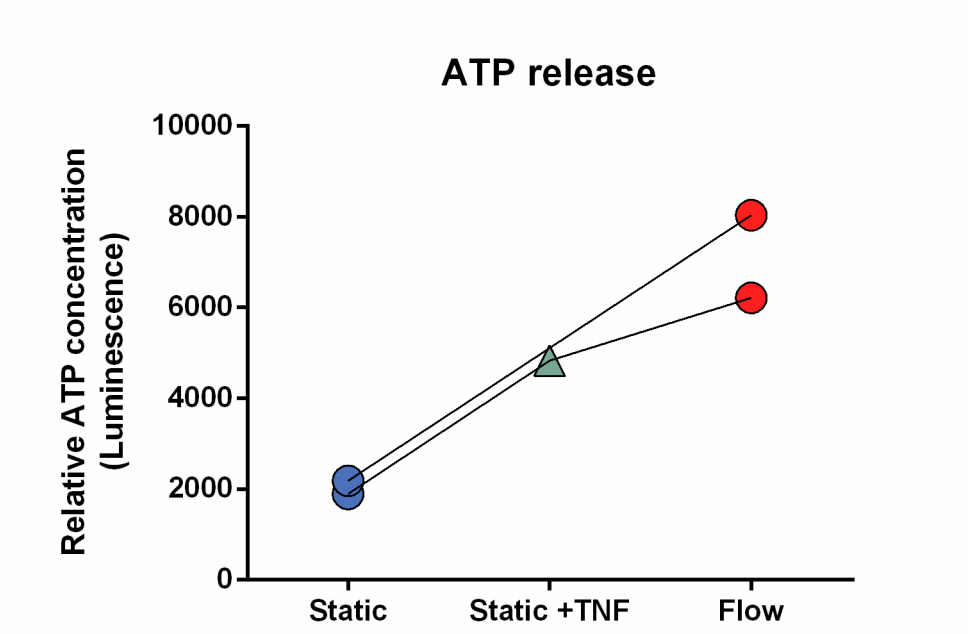

Figure 3.4 - HUVEC release ATP in response to flow.

HUVEC were preconditioned to static or flow conditions for 72 hours before the media was changed. Following 4 hours incubation under static ± 10ng/ml TNF, or flow conditions using the orbital shaker, an ATP determination assay performed on supernatants. (Static and flow, n=2. Static +TNF, n=1).

3.5 Atheroprone flow enhances calcium responses to BzATP

After characterising the calcium responses to BzATP in static endothelial cells, the calcium response was then measured in HUVEC preconditioned with either atheroprotective or atheroprone flow for 72 hours. In the arterial tree, endothelial cells are constantly under the influence of blood flow. Atherosclerosis develops at regions where endothelial cells are influenced by a complex blood flow with low wall shear stress, whereas regions under uniform blood flow with high shear stress are protected against plaque formation. Therefore these experiments were decided to be performed without static endothelial cells as this does not represent a physiological relevant condition related to our hypothesis. HUVEC were cultured under unidirectional +13 dyn/cm^2 flow to mimic atheroprotective flow or bidirectional ±4 dyn/cm^2 flow to mimic atheroprone flow. After flow conditioning on ibidi slides, cells were then loaded with a calcium dye and then imaged via epifluorescent microscopy. BzATP was applied by pipetting the BzATP solution into the inlet, then the same volume was pipetted out from the outlet (Figure 2.4). BzATP-induced calcium responses were more sustained in HUVEC preconditioned under atheroprone flow compared to cells preconditioned to atheroprotective flow (Figure 3.5). The entire calcium response, quantified by measuring the area under the curve, was significantly enhanced under atheroprone flow conditions compared to atheroprotective flow (atheroprotective=2936±197.9 vs atheroprone=5403±342.9) (Figure 3.5B). Application of an ATP-free solution produced a minimal response (210.9±32.04) demonstrating that it was not the flow of fluid generating the calcium responses (Figure 3.5A). These data suggest that atheroprone flow has conditioned the endothelial cells to be more responsive to ATP stimulation.

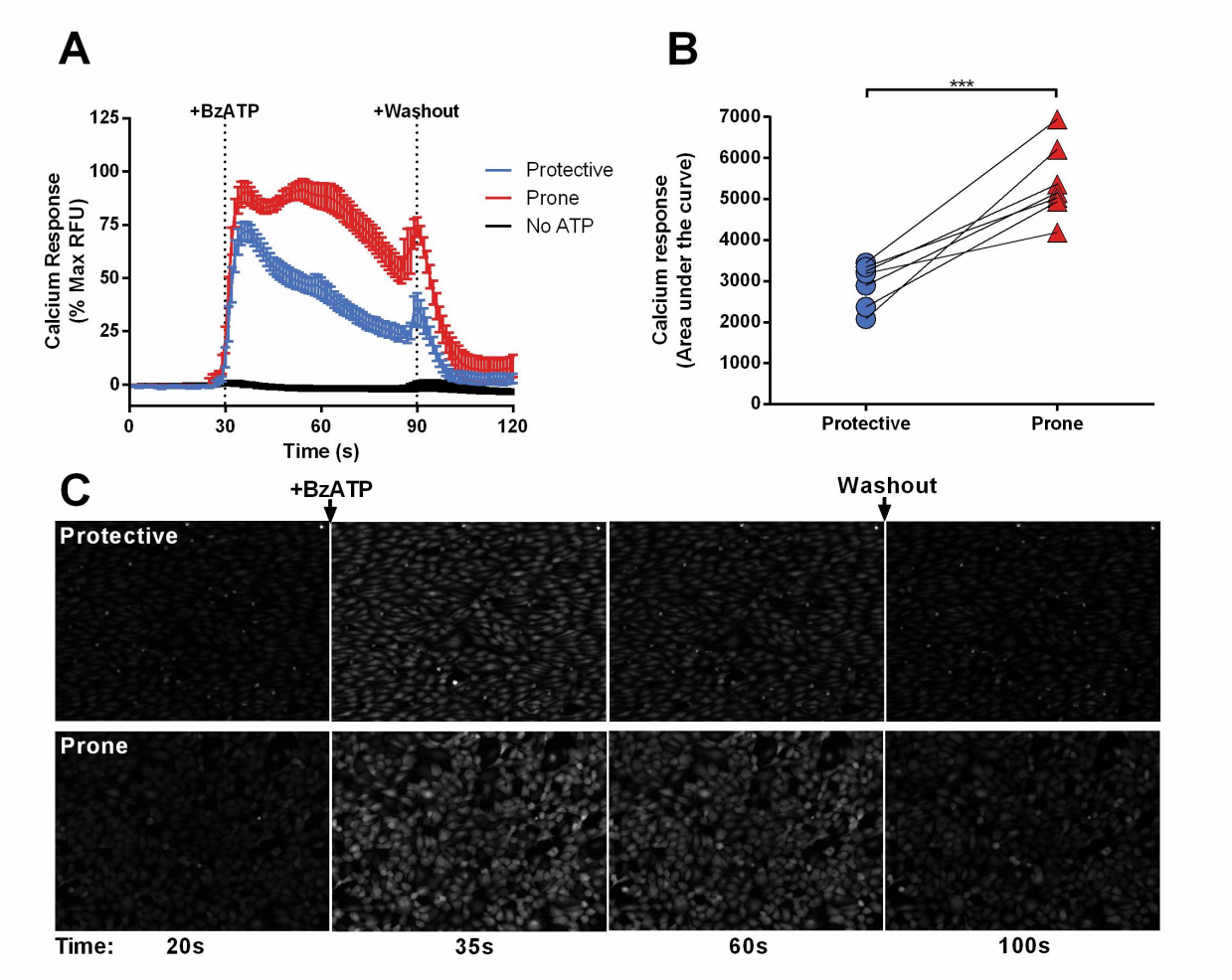

Figure 3.5 - HUVEC preconditioned under atheroprone flow exhibit an enhanced BzATP-induced calcium response.

(A) 300μM BzATP induced calcium response traces in HUVEC preconditioned with atheroprone or atheroprotective flow for 72 hours, normalised to the peak response of atheroprone flow conditioned HUVEC (A) and analysed by measuring the area under the curve (B) (n=7). (C) Representative screenshots display the change in calcium response over time before and after 300μM BzATP treatment. *** indicates p=<0.001 using a paired *t*-test. Values are ± SEM.

3.6 The Ecto-Nucleotidase CD39 is more active under atheroprotective flow

As the ecto-ATPase CD39 has been implicated in protection from atherosclerosis and has been shown to be up-regulated by shear stress (Kanthi et al. 2015), cell surface CD39 expression was assessed in HUVEC cultured under atheroprone and atheroprotective flow by flow cytometry. CD39 was strongly induced in endothelial cells cultured under atheroprotective flow compared to atheroprone flow (atheroprotective=8943±2230 vs atheroprone=3456±694) (Figure 3.6A). As well as hydrolysing ATP, CD39 has been shown to rapidly hydrolyse BzATP (Kukley et al. 2004). Therefore, it was hypothesised that the reduced BzATP-induced calcium response in atheroprotective flow conditioned HUVEC is in part controlled by an enhanced CD39 expression. To test this, flow conditioned HUVEC were stimulated with BzATP in the presence of a chemical inhibitor of CD39, ARL67156. Inhibition of CD39 enhanced the BzATP-induced calcium response in HUVEC preconditioned with atheroprotective flow (2020±300.3 to 2830±467.4) (Figure 3.6B), but not atheroprone flow (4468±431.2 to 4298±224.6) (Figure 3.6C), indicating that CD39 activity is higher under atheroprotective flow and reduces sensitivity to BzATP. However, other mechanisms must be in place explaining the difference between atheroprone and atheroprotective flow conditioned endothelial cells as inhibition only partly altered the BzATP calcium response.

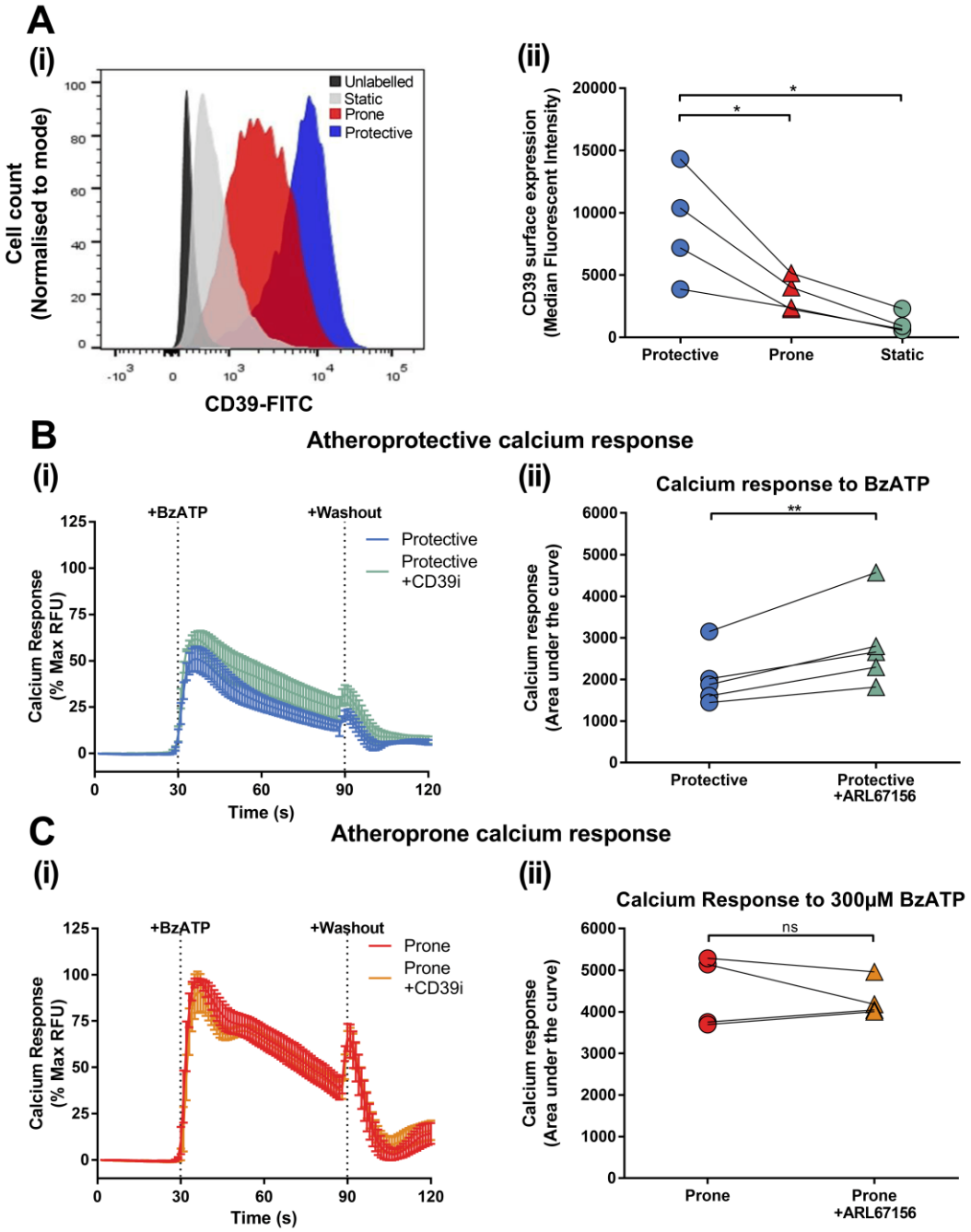

Figure 3.6 - Enhanced CD39 expression suppresses BzATP induced calcium responses in HUVEC under atheroprotective flow.

(A) Cell surface CD39 expression in HUVEC was analysed by flow cytometry. (i) Representative histograms of CD39 staining in flow conditioned HUVEC. (ii) Median fluorescent intensity of CD39 staining on flow conditioned HUVEC (n=4, * indicates p=<0.05 using a paired *t*-test). (B) BzATP induced calcium responses in atheroprotective HUVEC ± the CD39 inhibitor ARL67156 (CD39i) (i) and analysed by measuring the area under the curve (ii) (n=5 ** indicates p=<0.01 using a paired *t*-test). (C) BzATP induced calcium responses in atheroprone HUVEC ± the CD39 inhibitor ARL67156 (CD39i) (i) and analysed by measuring the area under the curve (ii) (n=4). Values are ± SEM.

3.7 Extracellular calcium is necessary for the enhanced BzATP calcium response in atheroprone flow conditioned HUVEC

BzATP generated a larger calcium response in HUVEC preconditioned under atheroprone flow, suggesting differential involvement of P2 receptors between atheroprotective and atheroprone flow. P2X receptors are ion channels evoking calcium influx from the extracellular space into the cytosol. P2Y receptors are G-Protein Coupled Receptors (GPCRs) and activate a series of intracellular signalling pathways, resulting in the release of calcium from the intracellular endoplasmic reticulum calcium stores. Therefore, to determine the role of P2Y and P2X receptors in this enhanced ATP response, experiments manipulating extracellular or intracellular calcium stores were performed. Replacement of calcium with the calcium chelator EGTA in the extracellular imaging buffer prevents calcium influx through P2X receptors following ATP stimulation (Figure 3.7A). Therefore P2X mediated calcium influx cannot occur and contribute to the calcium response while P2Y receptor activation can still trigger release of intracellular calcium stores and would remain unaltered. To complement, calcium store depletion can be achieved using thapsigargin, an irreversible inhibitor of the sarco/endoplasmic reticulum Ca^{2+} ATPase (SERCA). SERCA acts to keep cytoplasmic calcium levels low by actively pumping calcium into the endoplasmic reticulum. Thapsigagin inhibition of SERCA causes calcium to passively diffuse from the ER into the cytoplasm. Following such depletion of calcium stores, stimulation with BzATP would result in only P2X-mediated extracellular calcium influx while P2Y-mediated intracellular calcium release would be prevented (Figure 3.7B).

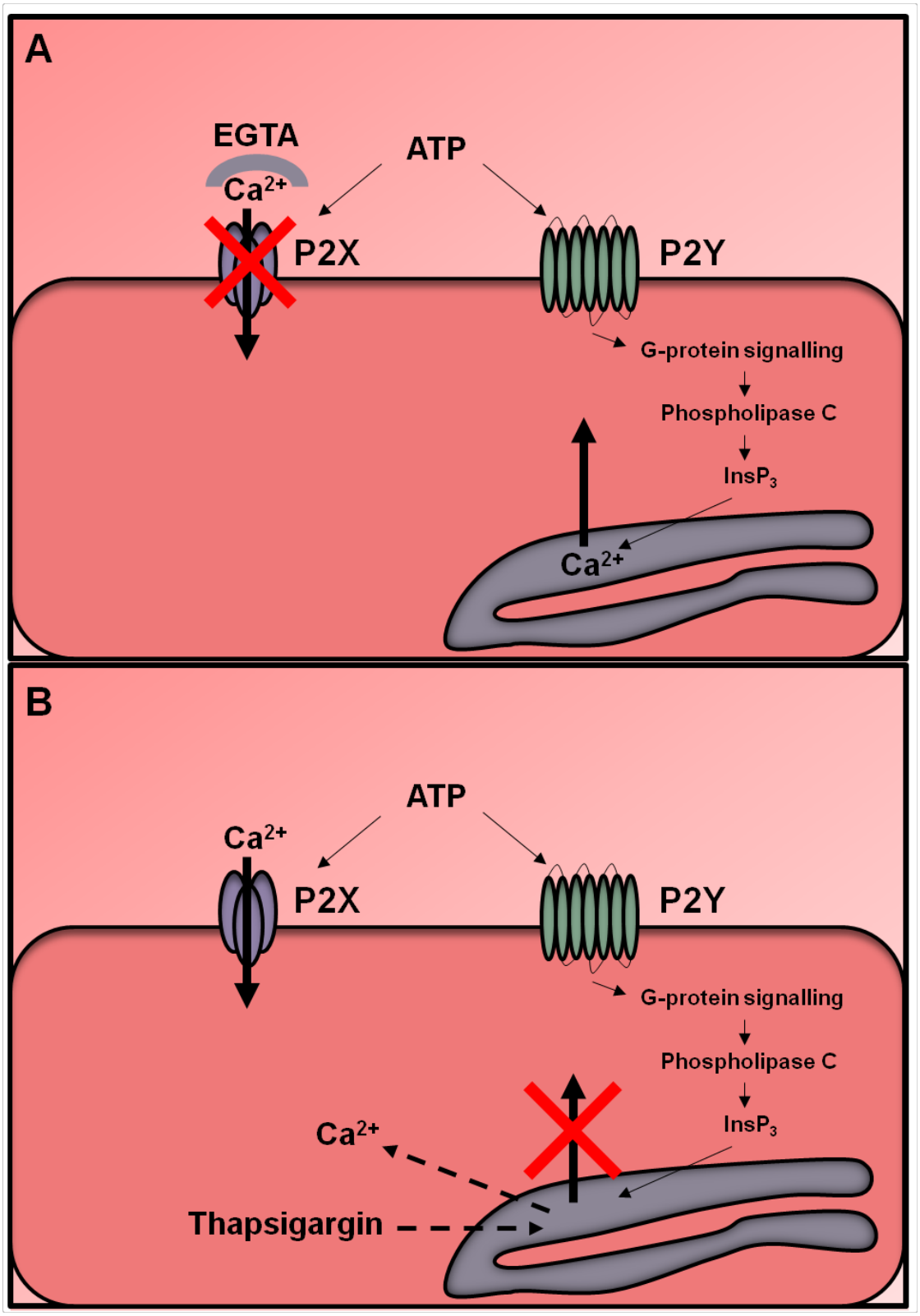

Figure 3.7 - A schematic showing the effects of either chelating extracellular calcium with EGTA on P2X and P2Y receptor mediated calcium responses.

(A) Chelation of extracellular calcium using EGTA prevents calcium influx through P2X receptors in response to extracellular ATP, but does not affect P2Y receptor mediated responses. (B) Depletion of intracellular calcium stores with thapsigargin prevents ATP triggered P2Y mediated release of calcium stores, but does not affect calcium influx through P2X receptors.

HUVEC were cultured under either atheroprotective or atheroprone flow and then stimulated with 300μM BzATP in either calcium or EGTA containing extracellular imaging buffer. In these experiments; BzATP stimulation in calcium containing extracellular imaging buffer shows the entire purinergic response, BzATP stimulation in EGTA containing extracellular imaging buffer shows the store (P2Y) response and the difference between them is due to extracellular calcium influx (P2X). Matching previous literature, the majority of the response in either condition was not inhibited by EGTA, indicating a major role for P2Y receptors in the calcium response (Gifford et al. 2004). In HUVEC preconditioned with atheroprotective flow, the entire calcium response to BzATP was unaffected by extracellular calcium depletion (Ca^{2+}=2947±214.4 vs EGTA=2613±299.6) (Figure 3.8A). In contrast, there was a significant decrease in the calcium response in HUVEC preconditioned with atheroprone flow in EGTA containing extracellular imaging buffer (Ca^{2+}=4826±218.2 vs EGTA=3504±388.7) (Figure 3.8B). This indicates that there is a selective role for extracellular calcium influx in the BzATP calcium responses in HUVEC when preconditioned with atheroprone flow, but not atheroprotective flow.

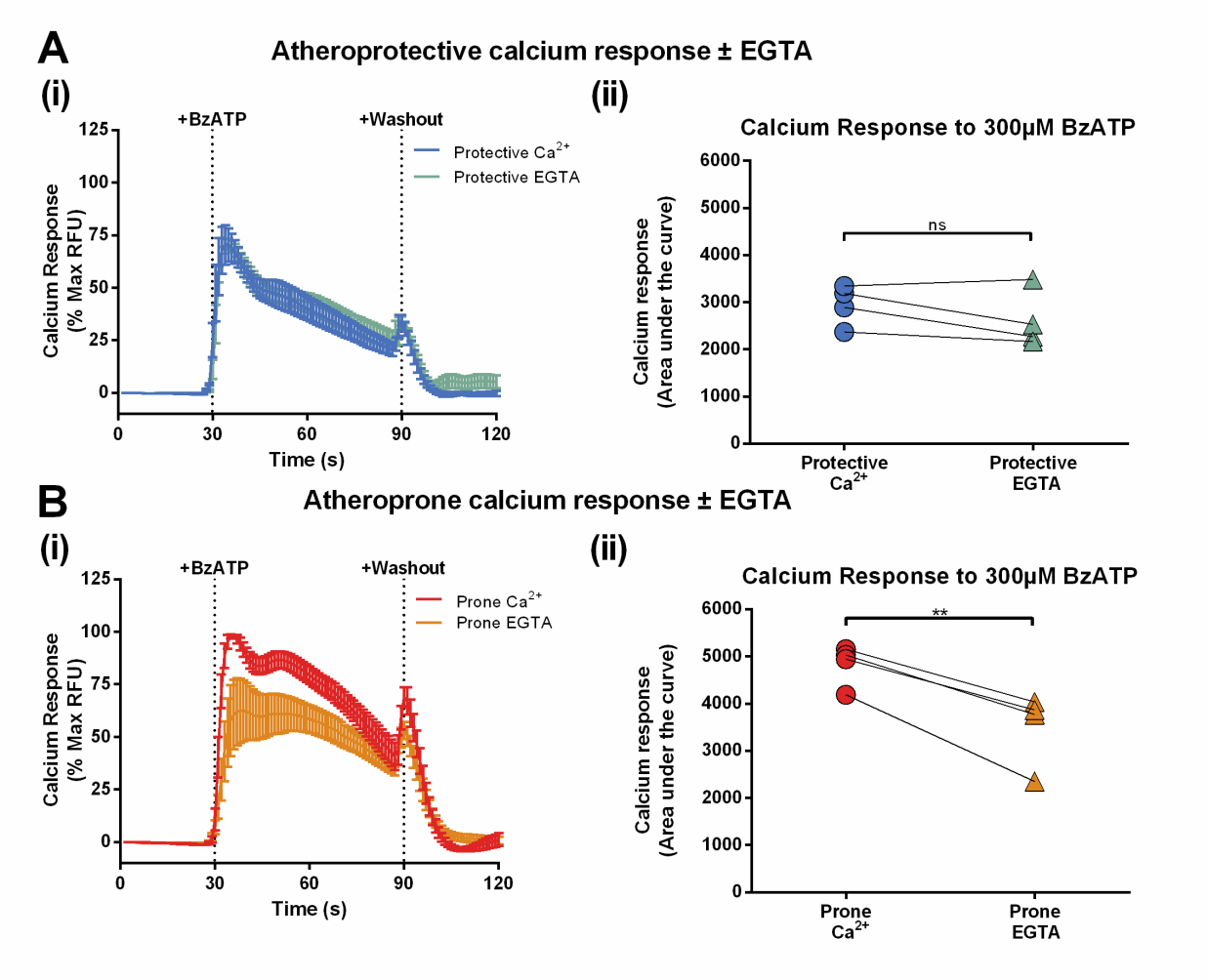

Figure 3.8 - Extracellular calcium influx in response to BzATP is increased under atheroprone flow.

(A) BzATP-induced calcium responses in HUVEC preconditioned with atheroprotective flow and in the presence of physiological extracellular calcium or EGTA over time (i) and analysed by measuring area under the curve (ii) (n=4). (B) BzATP-induced calcium responses in HUVEC preconditioned with atheroprone flow and in the presence of physiological extracellular calcium or EGTA over time (i) and analysed by measuring area under the curve (ii) (n=4). ** indicates p=<0.01 using a paired *t*-test. Values are ± SEM.

To substantiate this finding, the inverse experiment was performed where intracellular stores were pre-depleted before stimulation with BzATP. However, depletion of intracellular stores can activate an alternative extracellular calcium influx pathway known as store-operated calcium entry (SOCE). Calcium depletion from the ER activates the ER resident protein stromal interaction molecule 1 (STIM-1) that then interacts with plasma membrane calcium release-activated calcium (CRAC) channels, resulting in extracellular calcium influx. As there is evidence that this occurs in endothelial cells (Antigny et al. 2011), static HUVEC were first used to determine the duration of thapsigargin treatment required to fully deplete calcium stores and for stabilisation of SOCE. This would ensure that addition of BzATP would not coincide with the effects of store depletion or SOCE. Static HUVEC were stimulated with 10μM thapsigargin in either physiological extracellular Ca^{2+} or EGTA containing imaging buffer to fully determine the contribution of the response by store-operated calcium entry (SOCE) (Figure 3.9A). In both cases, thapsigargin treatment induced a large calcium response that slowly returned to a resting baseline after approximately 3 minutes. Thapsigargin stimulation in calcium containing extracellular buffer did produce a larger response due to SOCE (Ca^{2+}=9865±1555 vs EGTA=5212±169.5), which also persisted as an elevated baseline. The baseline, although elevated, was stable after 3 minutes. Therefore, 3 minutes pre-treatment with thapsigargin was selected as suitable for assessing the role of BzATP in extracellular calcium influx, as the stores were depleted and SOCE was stable at this time point. Thapsigargin treatment of flow conditioned HUVEC showed differences in the kinetics of calcium release (Figure 3.9Bi), but no significant difference in the area under the curve was detected (atheroprotective=8132±709.6 vs atheroprone=10352±712.4) (Figure 3.9Bii). As the area under the curve was unaffected, this indicates that the amount of calcium was unaltered, but perhaps the regulation of ER calcium stores is different, for example due to differences in expression levels of SERCA, but this was not tested.

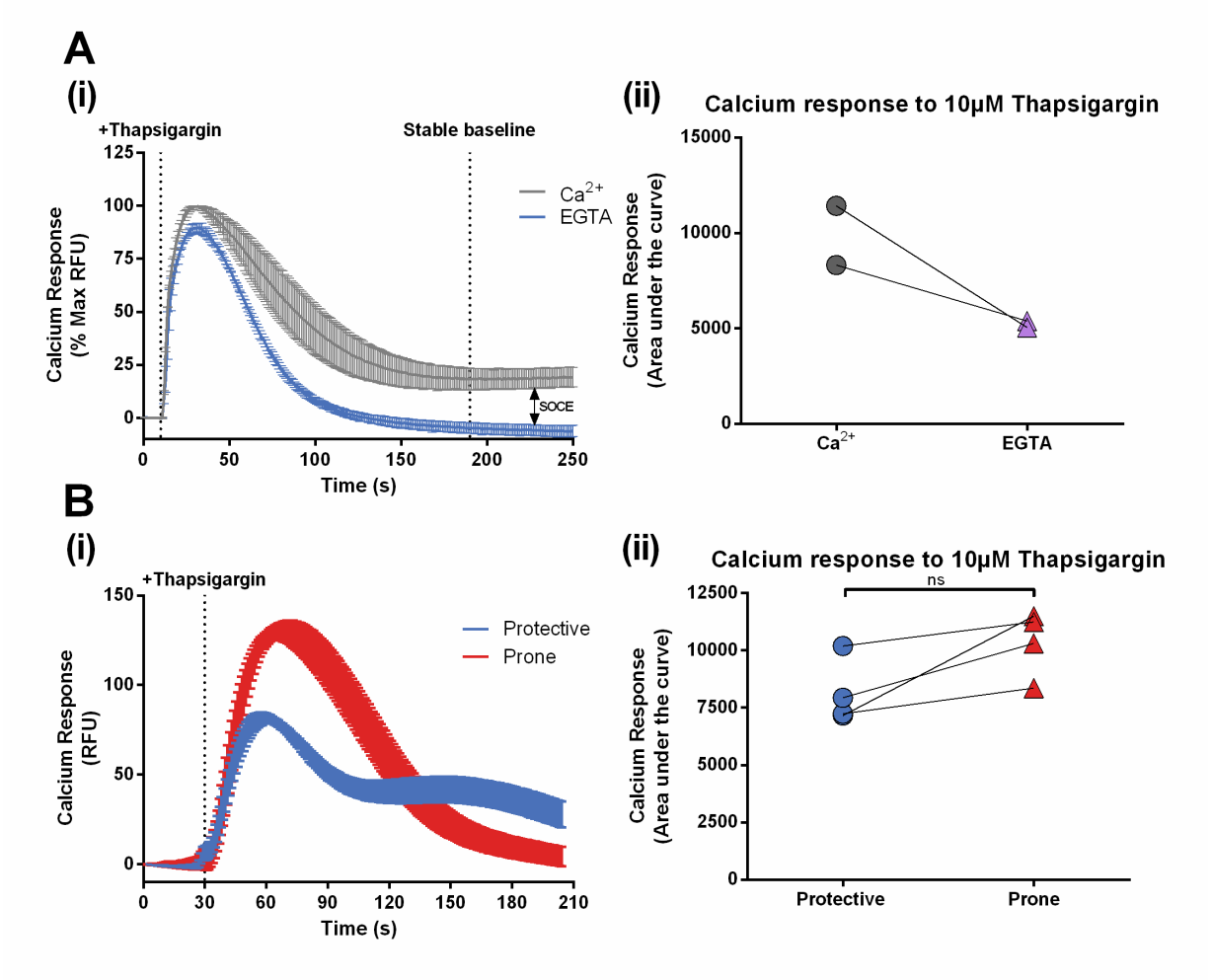

Figure 3.9 - Optimisation of thapsigargin treatment for store depletion in HUVEC.

(A) Calcium response in static HUVEC treated with 10μM thapsigargin in physiological extracellular Ca^{2+} or EGTA containing extracellular buffer over time (Ai). SOCE marks the proportion of the response dependent on extracellular calcium influx (n=2). (Aii) Area under the curve analysis of Ai (n=2). (B) Calcium response over time in HUVEC preconditioned under atheroprone or atheroprotective flow treated with 10μM thapsigargin (i) (n=4) and area under the curve analysis (ii) (n=4). Values are ± SEM.

After pre-depleting intracellular stores with thapsigargin, flow conditioned HUVEC were stimulated with BzATP and their calcium response was recorded. Matching our previous results indicating that the majority of the BzATP calcium response was from intracellular stores, the resulting calcium response was much smaller and not every cell responded. Therefore, single cell analysis was used to take into account this heterogeneity in response. Interestingly, despite being much smaller, these calcium responses were only seen in HUVEC preconditioned with atheroprone flow, with atheroprotective flow conditioned HUVEC lacking any significant calcium response (atheroprotective=17.04±14.19 vs atheroprone=263.1±97.61) (Figure 3.10). Therefore, these assays have demonstrated that HUVEC can initiate extracellular calcium influx in response to ATP under atheroprone flow conditions. Although these calcium responses were small, it should be noted that these experiments only represented calcium influx at one time point following stimulation. Therefore, it is possible that since these endothelial cells are capable of initiating extracellular calcium influx in response to ATP, potential downstream effects could accumulate over time under atheroprone flow conditions. These data further support that atheroprone flow conditioned HUVEC exhibit extracellular calcium influx responses to BzATP, which are absent in atheroprotective flow conditioned HUVEC. As P2X receptors are implicated in extracellular calcium influx in response to BzATP, they are most likely involved in this selective response due to atheroprone flow conditioning.

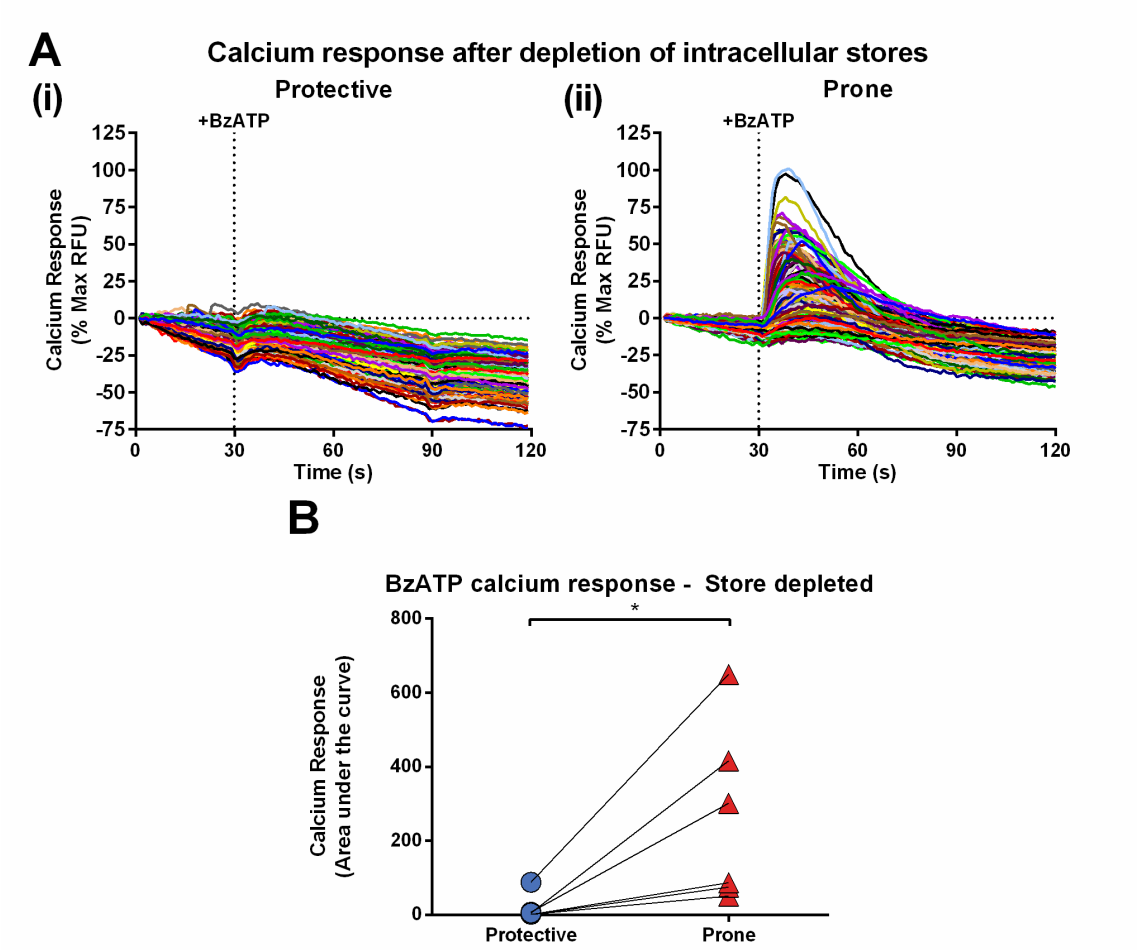

Figure 3.10 - Extracellular calcium influx in response to BzATP is increased under atheroprone flow.

(A) Representative single cell traces of BzATP-induced calcium responses in atheroprotective (i) or atheroprone (ii) flow conditioned HUVEC after 10μM thapsigargin pre-treatment and analysed by measuring the average area under the curve per donor (B) (n=6). * indicates p=<0.05 using a paired *t*-test).

3.8 Optimising ATP mediated calcium responses in *ex vivo* porcine aorta

Since atheroprone flow enhances ATP-induced calcium responses, which was proposed to be through enhanced P2X receptor activity *in vitro*, an *in vivo* approach was used to determine if altered P2X responsiveness also occurred physiologically at different sites of the arterial tree. To assess this, calcium imaging was optimised for the porcine aorta. This would be advantageous, as it would provide data on arterial cells and *ex vivo.* Porcine aortas were collected from a reputable local abattoir shortly after slaughter. Sites of the aorta influenced by atheroprone or atheroprotective flow were isolated, as determined from a computational fluid dynamics model of the porcine aorta (Serbanovic-Canic et al. 2016). These ex vivo samples were incubated with a fluorescent calcium dye and rhodamine conjugated *Griffonia simplicifolia* lectin, a specific marker of endothelial cells (Plendl et al., 1996). Sections were pinned flat in paraffin wax, endothelium facing upwards, immersed in calcium imaging buffer. Upright confocal laser scanning microscopy was used to image, as shown in Figure 3.11A. Using this technique, lectin-labelled endothelial cells were identified and shown as successfully labelled with calcium dye (Figure 3.11B). In order to see if these cells were still functional, the calcium response to 5mM ATP was tested. 5mM ATP was used as ATP is remarkably conserved signalling molecule (Fountain 2013) and should maximally activate all ATP-gated receptors at this concentration (Jacobson et al. 2002). Calcium responses could be identified in response to ATP within these cells (Figure 3.11C), but these were inconsistent and addition of agonists was technically challenging. Agonists were added by pipetting a concentrated stock solution of ATP into the calcium solution surrounding the section, but it was difficult not to accidently move the sample out of the plane of focus during pipetting, causing artefact signals. Moreover, the sections were not completely flat causing portions of the field of view to be out of focus, complicating analysis. Attempts to reliably measure ATP responses at

atheroprotective and atheroprone sites were unsuccessful due to these challenges. However, if further optimised, this technique may provide a novel approach to study endothelial calcium responses *ex vivo.*

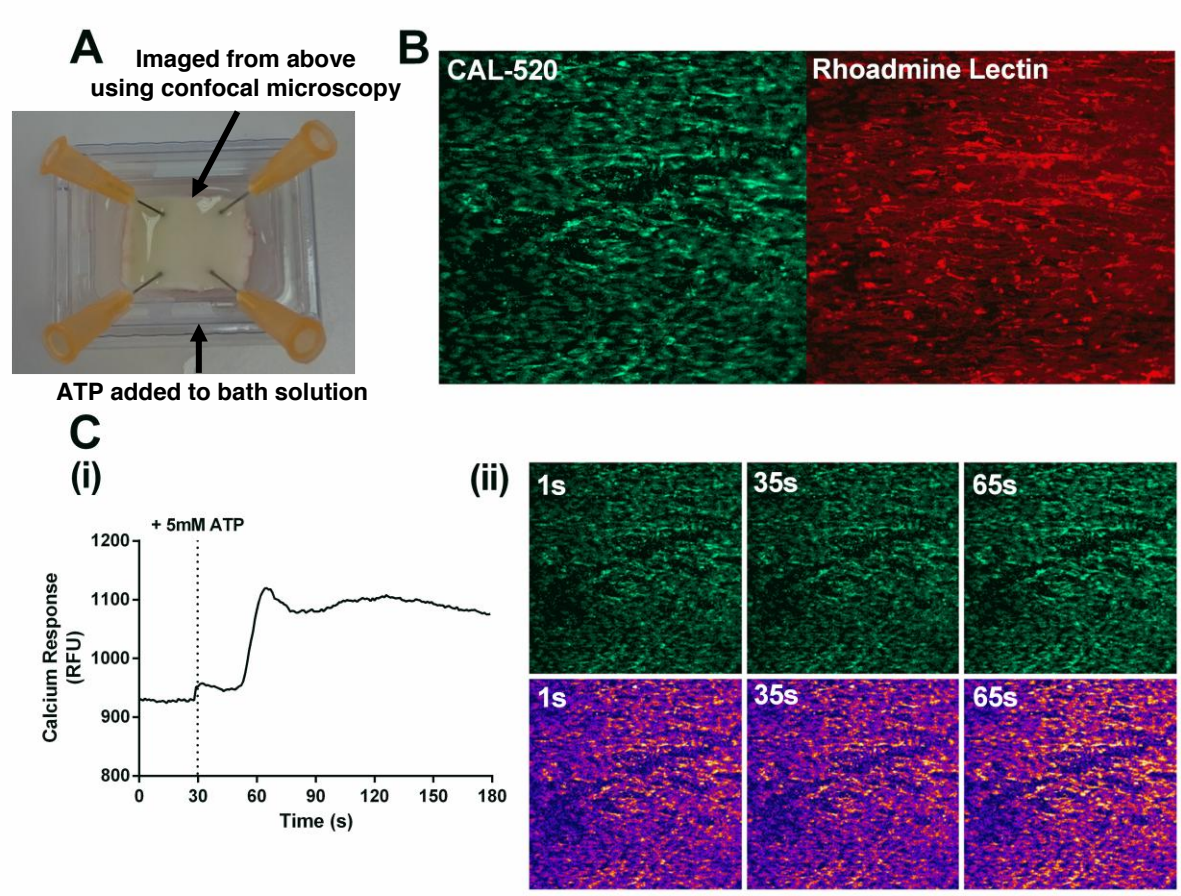

Figure 3.11 - Optimisation of *ex vivo* calcium imaging in endothelial cells lining the pig aorta.

(A) Representative image showing how porcine aortic sections were prepared for calcium imaging. (B) Representative image of rhodamine lectin (endothelial) and CAL-520 (calcium) labelling in endothelial cells of the porcine descending aorta. (C) Calcium response measured in response to 5mM ATP (i) and corresponding images taken at specific time points (ii). The upper panels display the calcium signal; the lower panels display the same signal but using a more sensitive filter.

3.9 Conclusions

These experiments investigated if ATP signalling was altered in endothelial cells under atheroprone or atheroprotective flow. Atheroprone flow conditioned endothelial cells were more responsive to BzATP, exhibiting increased extracellular calcium influx. The reduced calcium response in atheroprotective conditioned HUVEC was controlled in part by increased ATP hydrolysis driven by enhanced CD39 function. Although these experiments were performed in the presence of exogenous ATP, it provides a useful insight to understand how ATP signalling is altered in endothelial cells at atherosusceptible sites.

3.10 Discussion and future work

This study is the first to examine the role of ATP *in vitro* on endothelial cells pre-exposed to flow for 72 hours in order to simulate endothelial cells under physiologically relevant conditions. The majority of the ATP response in endothelial cells was controlled by intracellular stores, in agreement with previous studies (Gifford et al. 2004). After 72 hours of atheroprotective flow, BzATP-induced calcium responses were entirely from intracellular calcium stores, implying differential regulation of P2 receptors between atheroprone and atheroprotective flow. This indicates that after 72 hours of atheroprotective flow, only P2Y receptors were responding. This fits with the traditional view that endothelial P2Y receptors mediate vasodilation in response to ATP, an atheroprotective feature (Hopwood & Burnstock 1987). This also adds to recent accumulating evidence against P2X receptor activity under high shear stress conditions. P2X4 receptors have been reported to be activated under high shear stress conditions and contribute to KLF2 and nitric oxide signalling (Sathanoori et al. 2015; Yamamoto et al. 2000), which are typical endothelial characteristics of atheroprotection. However, these in vitro studies had examined the role of P2X4 in the onset of flow and therefore it is possible that P2X4 is present in static cells and responds to flow initially before downregulation. In fact, P2X4 expression has been

reported to be slightly downregulated over time following high shear flow compared to static cultures (Sathanoori et al. 2015; Korenaga et al. 2000). Furthermore, the experiments performed as part of my research used endothelial cells conditioned to flow for a relatively long time (>72hrs), suggesting that P2 receptor responses, including that of P2X4, may be altered after chronic exposure to flow compared these previous studies examining acute exposure to flow (<24hrs). Our experiments in HUVEC under static conditions showed that roughly half of the ATP and BzATP induced calcium response was dependent on calcium influx, providing further evidence that P2X receptor responses are down-regulated by atheroprotective flow. Furthermore, recent studies have also shown that ATP induced nitric oxide synthesis is P2Y2 dependent and that P2X4 is not involved (Raqeeb et al. 2011; Wang et al. 2015). Interestingly, global $P2X4^{-/-}$ mice do have defective adaptive vascular remodelling attributed to a reduction in nitric oxide production (Yamamoto et al. 2006), but as P2X4 is expressed in many other tissues and cell types, further work is needed to determine if endothelial P2X4 receptors are responsible.

These data suggest a potentially novel role for P2X receptor responses in endothelial cells preconditioned under atheroprone flow, as ATP induced extracellular calcium influx occurred exclusively in atheroprone flow conditioned HUVEC. These studies should be extended to make use of specific antagonist and/or knock down strategies in order to identify which specific receptors are involved in this response. As individual P2 receptor subtypes can mediate different cellular responses to ATP, potentially endothelial cells could be responding to the same stimulus with vastly different consequences between atheroprone and atheroprotected flow conditions.

Several studies have shown that ATP release occurs in response to shear stress and it is becoming more evident that there are multiple mechanisms involved in regulating ATP levels and signalling. Several mechanisms of shear stress-mediated ATP release have been proposed, including: exocytosis of ATP-rich vesicles (Bodin & Burnstock

2001); expression of a cell surface F_1/F_0 ATP synthase (Yamamoto et al. 2007); release through connexin hemichannels (D'hondt et al. 2013); and pannexin channels (Gödecke et al. 2012; Wang et al. 2016). However, the contribution of each remains unclear. In this study ATP release into the cell supernatant was increased in the presence of flow using the orbital shaker system. However, experiments using the ibidi pump system, which would allow discrimination between atheroprotective and atheroprone flow, did not detect any ATP release, most likely due to the large volume of media relative to cell number required per slide. Alternative approaches could be used to identify if localised concentrations of ATP differ between endothelial cells under atheroprone or atheroprotective flow. The Ando group were successful at measuring localised concentrations of ATP up to 30μM from endothelial cells cultured under high shear stress conditions using a live cell imaging approach (Nakamura et al. 2006; Yamamoto et al. 2011). This involves exploiting the biotin-streptavidin association, where the cells are first coated with biotin, which binds to cell surface proteins, and then streptavidin is bound to the biotin. Further addition of luciferase conjugated to biotin, which uses nearby ATP to produce light, will bind to streptavidin at the cell surface, effectively allowing determination of ATP concentrations at the cell surface. Alternatively, commercial probes (Sarissa biomedical) are available that can detect ATP concentrations in real time. Either of these approaches would be more sensitive and be able to detect ATP concentrations close to the cell surface, and determine if ATP concentrations are altered by atheroprotective or atheroprone flow patterns. Nevertheless, there is indirect evidence that suggests regulation of extracellular ATP is altered at sites of the arterial tree subjected to atheroprotective of atheroprone flow. Endothelial expression of the cell surface F_1/F_0 ATP synthase is increased under low shear oscillatory shear *in vitro*, at sites of atheroprone flow *in vivo,* (Fu et al. 2011) and following cholesterol loading (Wang et al. 2006), a risk factor for atherosclerosis development. Moreover, expression of the ecto-ATPase CD39, which is responsible for the hydrolysis of extracellular ATP, exhibits enhanced endothelial expression at sites of

atheroprotection and diminished expression in atheroprone regions of the murine aorta (Kanthi et al. 2015). The data presented here highlights that differential shear stress patterns regulate the cell surface expression of CD39 in HUVEC, suggesting that enhanced ATP breakdown may contribute to the atheroprotective phenotype of endothelial cells. Indeed, aged ApoE$^{-/-}$ mice, which are predisposed to atherosclerosis, have increased circulating ATP levels due to diminished vascular ATPase activity (Mercier et al. 2012). CD39 overexpression in HUVEC reduces ATP-induced E-selectin induction (Goepfert et al. 2000) and *in vivo*, CD39$^{-/+}$/ApoE$^{-/-}$ mice have increased atherosclerosis (Kanthi et al. 2015). The increased activity of CD39 could be responsible for the lack of P2X receptor activity under atheroprotective flow, as P2X receptors respond exclusively to ATP-based compounds and not ADP or AMP (North 2002). Therefore accumulation of extracellular ATP at sites of atheroprone flow due to increased ATP synthesis and decreased ATP hydrolysis could allow activation of P2X receptors. Indeed, CD39 has been reported to be a negative regulator of P2X7 receptor responses (Kuhny et al. 2014), and could be responsible for the lack of extracellular calcium influx under atheroprotective flow conditions. Moreover, ATP signalling is likely to occur within a closed caveolae system, since ecto-F_1F_0 ATP synthase (Yamamoto et al. 2007), CD39 (Koziak et al. 2000) and P2X receptors (Weinhold et al. 2010; Pfleger et al. 2012; Gangadharan et al. 2015) have all been reported to localise to caveolae. Indeed, shear stress-induced ATP release and subsequent calcium signalling has been reported to occur exclusively in caveolae (Yamamoto et al. 2011), suggesting that these structures do regulate purinergic signalling in response to shear stress. Further studies focused on examining the mechanisms of extracellular ATP regulation between atheroprotective and atheroprone flow would be very informative in understanding the importance of purinergic signalling in endothelial physiology.

Depletion of intracellular ER calcium stores leads to store operated calcium entry (SOCE) through calcium release-activated calcium (CRAC) channels. The calcium dynamics in response to thapsigargin treatment were different in endothelial cells preconditioned with atheroprone or atheroprotective flow, suggesting that some aspects of either ER calcium homeostasis or SOCE are altered after preconditioning to flow. Indeed, SOCE has been reported to be activated in endothelial cells on the onset of flow (Jafarnejad et al. 2015). Furthermore, it is possible that the reduced ATP-induced calcium influx observed in atheroprone flow conditioned HUVEC in the EGTA solution could, in part, result from decreased SOCE. P2Y receptor stimulation with ATP has been reported to trigger SOCE (Chang et al. 2007; Govindan & Taylor 2012), suggesting that SOCE may be increased under atheroprone flow. However, in experiments where ER Ca^{2+} stores were depleted prior to ATP addition, SOCE was stabilised to ensure it did not influence the ATP-induced calcium response. In these experiments, calcium influx only occurred after pre-conditioning to atheroprone flow, suggesting that P2X receptor responses are up-regulated. Nonetheless, the contribution of SOCE in endothelial calcium responses between conditioned atheroprone and atheroprotective flow has not been investigated. ER calcium homeostasis is important for many integral cellular processes. For example, the unfolded protein response, which can be induced by dysregulation of ER calcium stores, is up-regulated in endothelial cells at sites prone to atherosclerosis (Civelek et al. 2009). Therefore, differential regulation of intracellular calcium stores could be responsible for some atheroprone traits. However this was not studied further as it was beyond the scope of the current project, but could provide an interesting area for future investigation.

Despite the evidence suggesting the selective enhancement in P2X receptor responses under atheroprone flow compared to atheroprotective flow, the majority of the ATP-induced calcium response in either conditions was composed predominantly

of an intracellular calcium response, indicative of P2Y receptors. Therefore, the role of endothelial P2Y receptors in ATP-mediated cellular responses is likely to be very important. P2Y receptors have also been reported to be activated by mechanically released ATP, with P2Y receptors implicated in atheroprotective flow-mediated signalling. Evidence has described P2Y2 involvement in eNOS activation, NO signalling (Wang et al. 2015; Wang et al. 2016) and in the shear stress induced alignment of endothelial cells (Sathanoori et al. 2016) suggesting these receptors are protective against atherosclerosis. However, P2Y2 receptors have been associated with endothelial inflammation; deletion of P2Y2 reduces VCAM-1 expression at atheroprone sites (Qian et al. 2016), reduces atherosclerotic burden and promotes plaque stability (Stachon et al. 2016; Xingjuan et al. 2016). Similarly to P2X receptors, no study to date has examined P2Y receptor responses under atheroprone flow conditions. Therefore, despite no atheroprone-mediated enhancement in intracellular calcium responses to ATP detected in this study, the pro-atherosclerotic role of P2Y2 receptors in atheroprone flow-mediated signalling also warrants investigation, but is outside of the scope of this work..

The use of the porcine aorta for *ex vivo* studies is a potential tool to understand purinergic signalling at sites of atheroprone and atheroprotective flow. The porcine model has some advantages over commonly used murine systems. The geometry and shear stress values generated in the porcine aorta are much closer to that of humans (Serbanovic-Canic et al. 2016) whereas the murine aorta is exposed to shear stress values ~10 fold higher (Suo et al. 2007). Calcium imaging in response to ATP on the porcine aorta showed promising results with endothelial cells successfully labelled and loaded with a calcium dye. However technical difficulties were present in experiments recording ATP-induced calcium responses, which could be largely overcome by further optimising the microscopy procedures, particularly by ensuring application of ATP does not disrupt the sample. This could be achieved by using equipment such as an

automated pump system to deliver the ATP consistently and remove the potential disruption caused by human error. Further optimisation of calcium imaging on the porcine aorta would be advantageous over murine models for several reasons. Live cell calcium imaging in response to ATP on atherosusceptible and atheroprotected regions of the murine aorta would be very technically challenging due to the small size of murine aortas, whereas porcine aortas provide regions >1cm^2 exposed to atheroprone or atheroprotected flow, allowing easy manipulation of live tissue. Furthermore, porcine P2X receptors are more similar to human P2X receptors as, evolutionary speaking, pigs are closer relatives to humans than mice. This may be particularly useful as striking differences in regulation of P2X receptors, particularly P2X7, is evident between human and murine orthologues (Donnelly-Roberts et al. 2009). There are limitations to using porcine tissue however, such as a lack of knowledge of porcine P2 receptor pharmacology and antibody availability, which has been extensively characterised in murine models. However, unmodified ATP is a remarkably conserved signalling molecule, even activating P2X receptors in a range of invertebrate and single cell systems (Fountain 2013), suggesting that despite a lack of pharmacological knowledge of porcine P2X receptors, that their activity should remain suitable for study.

Chapter 4

P2X receptor activity is increased under atheroprone flow

4.1 Introduction

The previous chapter found that atheroprone flow conditioned HUVEC exhibited a selective increase in calcium influx from the extracellular space in response to BzATP. This suggests increased involvement of the P2X family of ATP-gated cation channels under these conditions. P2X4 and P2X7 are the most abundantly expressed P2X receptor subtypes expressed in the endothelium (Wang et al., 2002; Yamamoto et al., 2000) and P2X4 and P2X7 have been reported to respond to shear stress induced ATP release in endothelial cells (Yamamoto et al., 2000) and osteoblasts (Li et al., 2005), respectively. Moreover, expression of P2X4 and P2X7 is increased under inflammatory conditions *in vitro* (Sathanoori et al., 2015; Wilson et al., 2007) and P2X7 is up-regulated in the atherosclerotic plaque *in vivo* (Piscopiello et al., 2013; Peng et al., 2015), suggesting their involvement in vascular inflammation. However, no study to date has examined the role of P2X4 and P2X7 in endothelial cells influenced by atheroprone flow conditions. Therefore, it was proposed that P2X receptor signalling is increased under atheroprone flow conditions contributing to inflammatory signalling and endothelial cell activation.

The regulation and function of the P2X7 receptor has been extensively characterised in several cell types. P2X7 has been extensively studied, revealing a range of mechanisms to regulate its function. As endothelial cells do not display classical P2X7-like responses when stimulated, such as dye uptake, cell morphological changes and IL-1 secretion (Ramirez & Kunze 2002; Wilson et al. 2007), it was proposed that regulation of P2X7 receptors is altered in endothelial cells, such as by altered expression of interacting proteins or alternative splicing events. Numerous interacting proteins have been identified that regulate P2X7 function. Moreover, P2X7 is alternatively spliced, producing translated variants which exhibit very different functions (Sluyter & Stokes 2011). Therefore, the role of P2X receptors in ATP-induced calcium signalling and potential mechanisms of P2X4 and P2X7 regulation was assessed.

4.2 Hypothesis

P2X4 and P2X7 receptors are active under atheroprone flow, but not under atheroprotective flow. This activity is mediated in part by alterations in P2X4 and P2X7 regulation.

4.3 Aims

1) Determine the effect of P2X receptor antagonism on the BzATP induced calcium response.
2) Determine gene expression of P2X4 and P2X7 and known interacting proteins in endothelial cells cultured under atheroprotective or atheroprone flow.
3) Identify splice variants of P2X4 and P2X7 in the endothelium and determine their regulation by flow.

4.4 The role of P2 receptors in BzATP induced calcium responses in flow conditioned HUVEC

P2 receptors are split broadly into 2 main families, the P2X ion channels and the P2Y G-protein coupled receptors (GPCRs), which are further split into 7 P2X receptor and 8 P2Y receptor subtypes. The previous chapter found that in response to BzATP, endothelial cell calcium responses were mainly mediated by intracellular stores, indicative of P2Y receptors. However, extracellular calcium influx in response to BzATP, indicative of P2X receptor activation, occurred exclusively under atheroprone flow conditions. Since the predominant P2X receptors expressed under static conditions are P2X4 and P2X7 (Yamamoto et al. 2000; Wang et al. 2002; Wilson et al. 2007), it was proposed that these receptors contributed to ATP-induced extracellular calcium influx under atheroprone flow. Therefore, the role of these receptors was assessed using chemical inhibitors of P2 receptors. There are several commercial compounds which have shown to inhibit specific subtypes, or combinations of subtypes, and are widely used as tools to investigate the involvement of P2 receptors in research. One of these compounds, suramin, has been characterised over the past 30 years as a non-selective P2 receptor antagonist, due to its inhibitory effects on the entire P2 receptor family. However, suramin is much more potent at some receptor subtypes than others (See table 4.1). In the endothelium; P2X1 and P2Y11 are susceptible to low doses of suramin (<10μM) , P2Y2 is at a moderate dose (<100μM), but interestingly P2X7 is relatively insensitive and P2X4 is considered to be unaffected by suramin concentrations lower than 500μM. Therefore, performing calcium imaging in the presence of increasing doses of suramin provides a useful insight into the involvement of P2 receptor subtypes. HUVEC were preconditioned with atheroprone flow for 72 hours before the calcium response to 300μM BzATP was measured by calcium imaging in the presence of suramin (Figure 4.1). Treatment with 10μM suramin evoked a small (DMSO=4626±323.5, 10μM suramin=4083±425.9), but insignificant,

decrease in the calcium response, indicating that P2Y1 and P2Y11 did not contribute significantly to this response. 100μM suramin, which would fully inhibit P2Y2 receptors and potentially reduce but not abolish P2X7 receptor responses, caused a ~50% reduction in the response (DMSO=4626±323.5, 100μM suramin=2083±268.7) suggesting a significant role for endothelial P2Y2 receptors. Interestingly, a proportion of the response was unaffected by 100μM suramin treatment, suggesting that a suramin insensitive purinergic component remained active in endothelial cells, which likely represents P2X receptors.

P2 Receptor	IC50 Suramin (μM)	EC50 BzATP(μM)
P2X1	1	0.003
P2X4	>500	7
P2X5	4	>500
P2X7	78-500	20
P2Y1	3	✘
P2Y2	50	4.7
P2Y4	>300	✘
P2Y6	>100	✘
P2Y11	0.8	65
References: (Kügelgen 2008; Jarvis & Khakh 2009; Jacobson et al. 2002)		

Table 4.1 - The subunit specific potencies of suramin and BzATP on endothelial P2 receptors

✘ indicates no evidence of activity currently reported

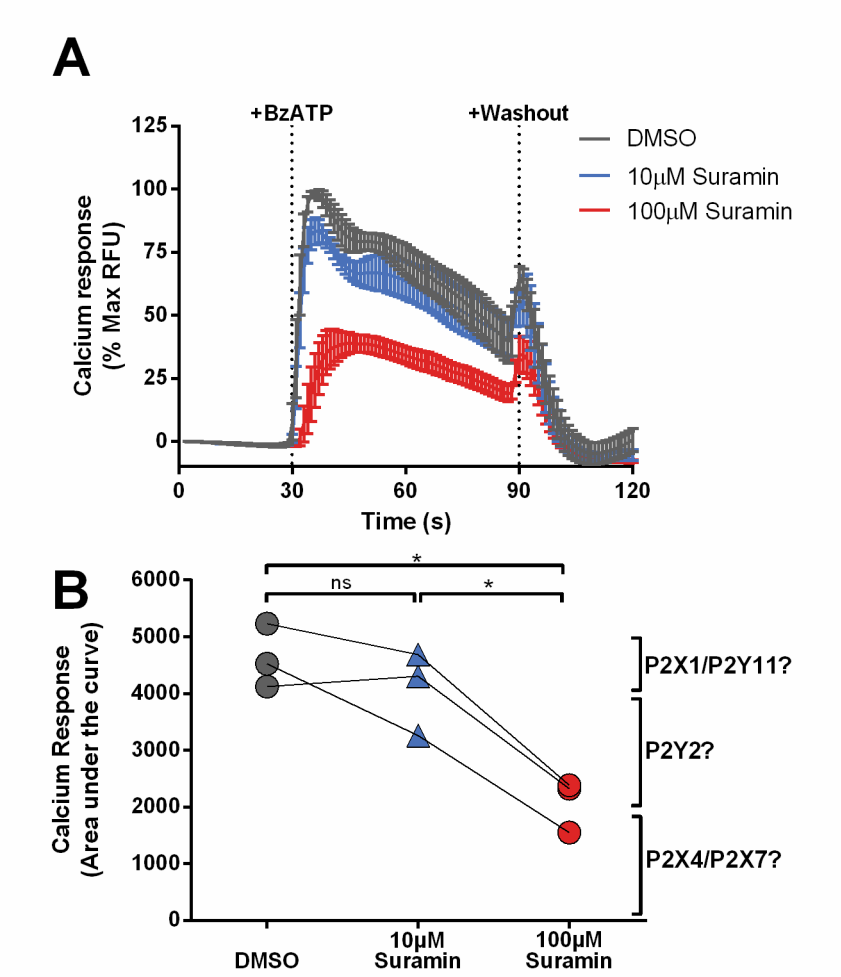

Figure 4.1 – The BzATP-induced calcium response is reduced by the non-selective P2 receptor antagonist suramin in atheroprone flow conditioned HUVEC.

(A) BzATP (300μM) induced calcium response in atheroprone flow conditioned HUVEC in the presence of increasing suramin concentrations (n=3). (B) Area under the curve of A. The relative proportion of the response suggested to be attributed to certain P2 receptors is indicated to the right of the graph based on table 4.1. * indicates p=<0.05 using a one way ANOVA. Values are ± SEM.

To further investigate P2X receptor involvement, specific antagonists acting on P2X7 and P2X4 were used, since these are the P2X subtypes predominantly expressed in the endothelium. In these experiments; the established P2X7 receptor antagonist A438079 hydrochloride, the highly potent human-specific P2X7 receptor antagonist AZ11645373 and the new P2X4 antagonist PSB-12062 were used (Bartlett et al. 2014; Hernandez-Olmos et al. 2012). The effect of these compounds on the BzATP-induced calcium response was tested on endothelial cells preconditioned with atheroprone flow. However, at doses reported to effectively inhibit P2X7 and P2X4 (Coddou et al. 2011; Hernandez-Olmos et al. 2012), no substantial decrease was observed in the calcium response (DMSO=4532±408.5 vs A438079=4393±287; DMSO= 4878±352.2 vs AZ11645373=4355±263; DMSO=4626±323.5 vs PSB12062=4711±539.7) (Figure 4.2). Further optimisation using the P2X7 antagonists A438079 and KN62 on static HUVEC revealed significantly enhanced BzATP calcium responses (DMSO=3831±127.4 vs 10μM A438079=5193±147.1 vs 50μM A438079=5655±236.3; DMSO=4067±53.14 vs KN62=7254±602.2) (Figure 4.3), the opposite of what was expected. This suggests that perhaps compensatory mechanisms, such as potential up-regulation of other P2 receptor activity in the absence of P2X7 responses, or off-target effects altering the entire calcium response. Interestingly, such enhancement was not present in endothelial cells preconditioned with atheroprone flow (Figure 4.2).

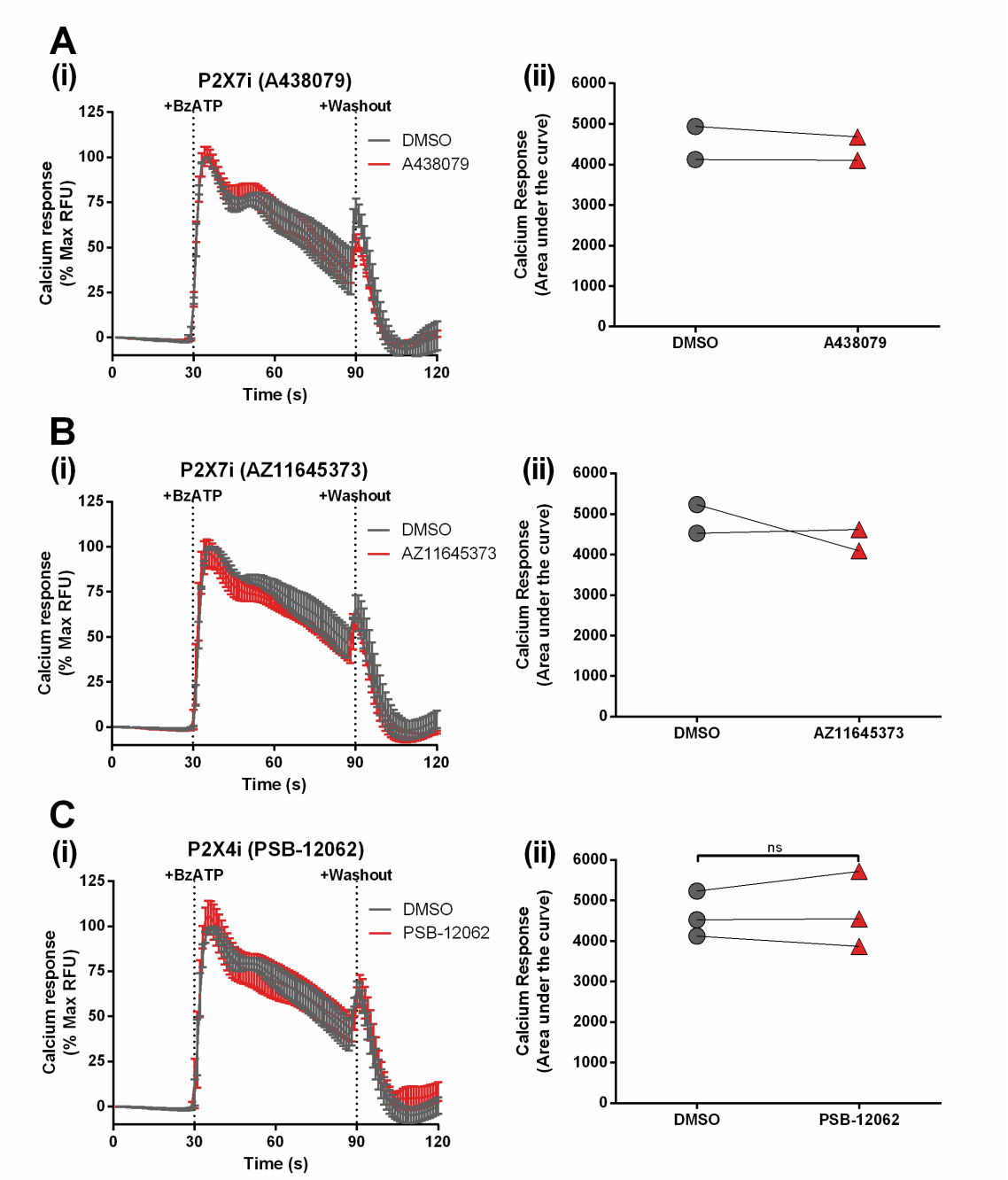

Figure 4.2 – P2X7 and P2X4 inhibitors do not alter BzATP-induced calcium responses in atheroprone flow conditioned HUVEC.

300μM BzATP-induced calcium responses (i) and area under the curve (ii) in atheroprone flow conditioned HUVEC following pre-incubation of the P2X7 antagonists A438079 (10μM) (A) (n=2), AZ11645373 (100nM) (B) (n=2), or the P2X4 antagonist PSB-12062 (10μM) (C) (n=3). Values are ± SEM.

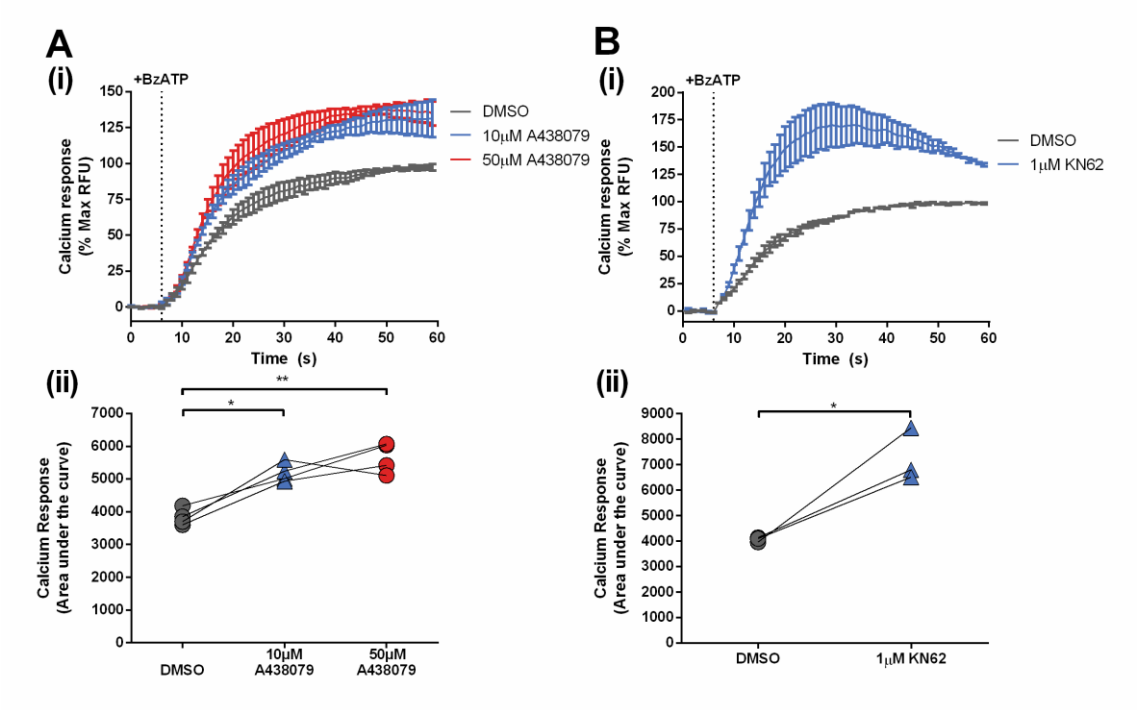

Figure 4.3 – P2X7 inhibitors increase BzATP-induced calcium responses in static HUVEC.

300μM BzATP-induced calcium response (i) and area under the curve (ii) for static HUVEC ± pre-incubation with the P2X7 antagonists A438079 (10μM or 50μM) (A) (n=4) or KN62 (1μM) (B) (n=3). * indicates p=<0.05 and ** indicates p=<0.01 using a paired *t*-test or one way ANOVA where appropriate. Values are ± SEM.

The effect of A438079 and PSB-12062 was then examined on extracellular calcium influx only, achieved by pre-depleting intracellular stores with thapsigargin, as described previously (Figure 3.7). The purpose of this was to prevent calcium responses to P2Y receptor stimulation, providing a more selective assay to study P2X receptors. Under these conditions, the calcium response was significantly reduced in atheroprone flow conditioned HUVEC following pre-treatment with the P2X7 specific antagonist A438079 (Figure 4.4A), but not the P2X4 antagonist PSB-12062 (Figure 4.4B). Analysis of the average area under the curve was significantly decreased after P2X7 inhibition (Untreated=354.2±124.5 vs A438079=219.8±86.99), but no decrease was seen after P2X4 inhibition (DMSO=168.5±76.40 vs PSB-12062=178.8± 35.24) (Figure 4.C). No response was measured in HUVEC preconditioned with atheroprotective flow, which was unaltered by addition of A438079 (data not shown). Therefore, this suggests that P2X7 receptor-mediated calcium responses are only present in HUVEC preconditioned with atheroprone flow.

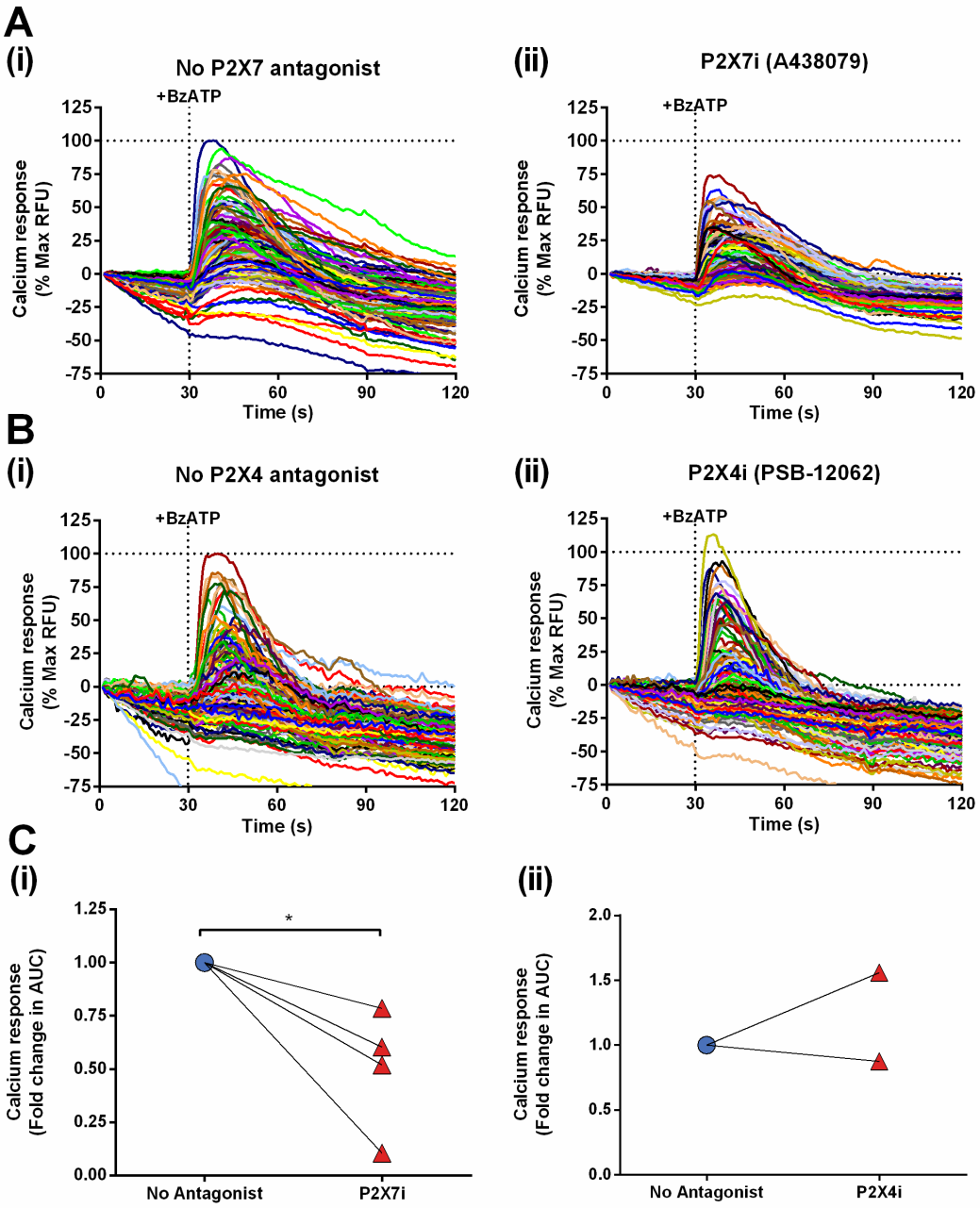

Figure 4.4 – P2X7 inhibition, but not P2X4, reduce BzATP-induced extracellular calcium influx in atheroprone flow conditioned HUVEC.

Calcium influx responses from atheroprone conditioned HUVEC in response to 300μM BzATP after store depletion using a 3 minute incubation with 10μM thapsigargin. Each line represents a single cell (170 cells). Response-curves were normalised against the peak of the largest responding cells. (A) Representative calcium response to 300μM BzATP ± the P2X7 antagonist A438079 (10μM). (B) Representative calcium response to 300μM BzATP ± the P2X4 antagonist PSB-12062 (10μM). (C) Fold change in the average area under the curve from A (P2X7i) (n=4), and (P2X4i) B (n=2). * indicates p=<0.05 using a paired *t*-test. Statistics were performed using the raw area under the curve values.

4.5. Regulation of P2X receptors expression by shear stress

As BzATP-induced extracellular calcium influx is increased in atheroprone conditioned HUVECs, expression of the BzATP sensitive ion channels P2X4 and P2X7 was examined in endothelial cells cultured under atheroprone or atheroprotective flow. Expression of mRNA transcripts for P2X4 and P2X7 (including alternatively spliced transcripts), under different flow conditions, was assessed in HUVEC cultured using either the ibidi or the orbital shaker system. The orbital shaker system showed an enhancement in P2X4 transcripts (atheroprone=1.475±0.1371 fold change), but a decrease in P2X7 transcript expression (atheroprone=0.4758±0.1720 fold change) under atheroprone flow conditions (Figure 4.5A). However, in the ibidi system, no change in either P2X4 (atheroprone=1.110±0.08706 fold change) or P2X7 (atheroprone=1.012±0.1029 fold change) transcripts was detected between atheroprone or atheroprotective flow (Figure 4.5B). To examine regulation of P2X4 and P2X7 at arterial sites *in vivo*, RNA was extracted from endothelial cells at atheroprotected and atherosusceptible sites of the porcine aorta; no significant difference was detected in P2X4 (atheroprone=3.230±2.127 fold change) or P2X7 (atheroprone=0.8460±0.2120 fold change) transcripts at these different sites (Figure 4.5C).

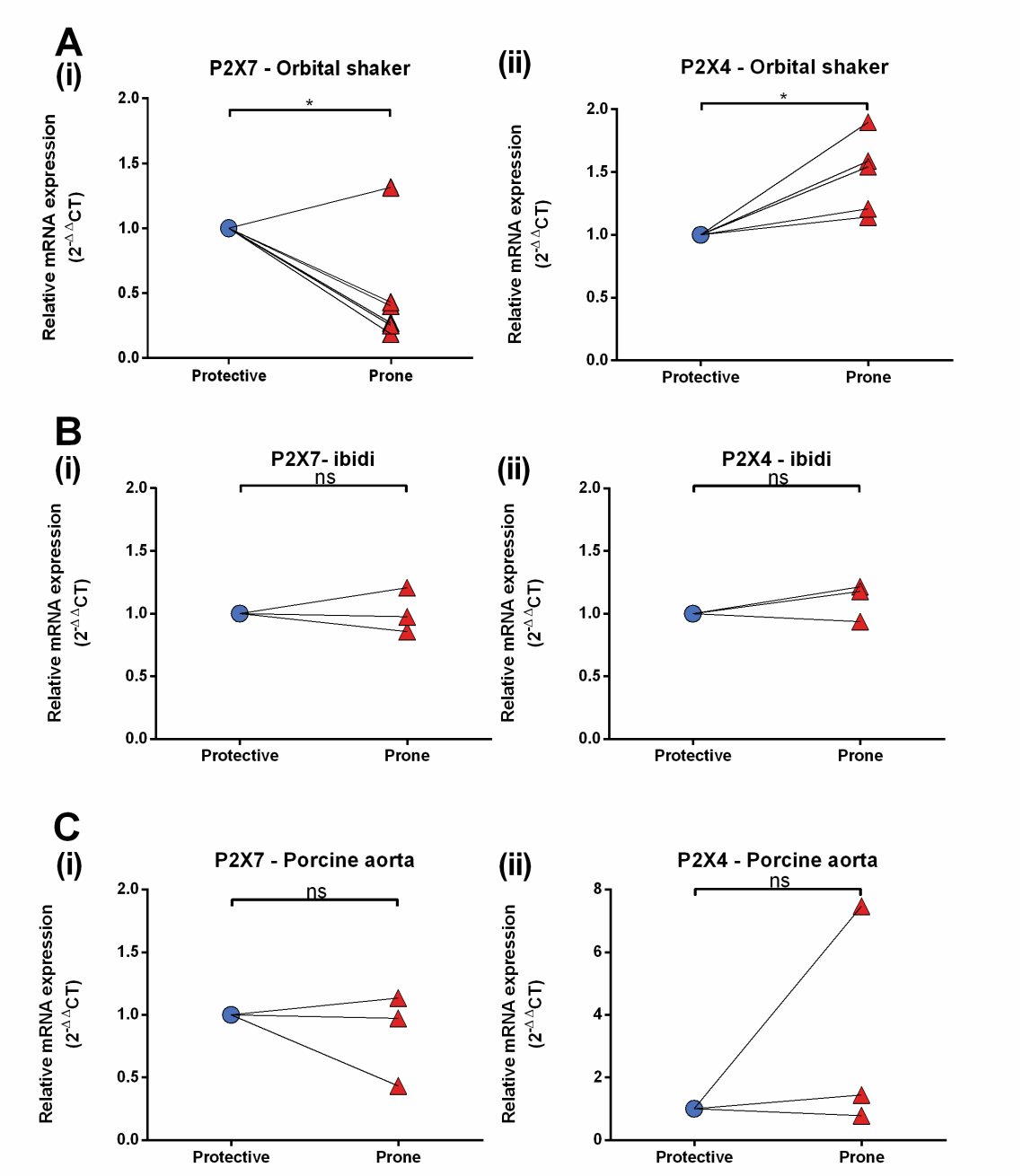

Figure 4.5 – mRNA expression of P2X4 and P2X7 is unaltered between atheroprotective and atheroprone flow.

Expression of P2X4 or P2X7 transcripts in HUVEC using the orbital shaker system (A) (n=5-6), the ibidi pump system (B) (n=3) and at sites of atheroprotective and atheroprone flow from the porcine aorta (C) (n=3). * indicates p=<0.05 using a paired *t*-test. Statistical analysis was performed on the ΔCT values.

Western blotting was used to examine protein expression of P2X4 and P2X7. The western blot for P2X7 showed two bands around the predicted size; one at 66kDa which corresponds to the unmodified amino acid weight, and one at 75kDa which corresponds to the widely reported post-translationally modified P2X7 (Nicke 2008) (Figure 4.6). P2X7 is glycosylated in the ER before trafficking to the plasma membrane via the trans-Golgi network (Robinson & Murrell-Lagnado 2013). Fully glycosylated P2X7 is therefore likely to be at the cell surface, whereas protein lacking this modification will not have been trafficked and could therefore be considered as not functional P2X7 receptors. In contrast to mRNA levels, expression of the 75kDa band for fully glycosylated P2X7 was increased in HUVEC conditioned under atheroprone flow using the ibidi (atheroprone=1.590± 0.1362 fold change) (Figure 4.6A) and orbital shaker flow systems (atheroprone=4.901±0.7806 fold change) (Figure 4.6B). Moreover, expression of the 66kDa band was up-regulated in the orbital shaker system (atheroprone=2.513±0.3057 fold change) (Figure 4.6B), but was unaltered in the ibidi system (atheroprone=0.9349±0.07662 fold change) (Figure 4.6A). This discrepancy between mRNA and protein levels could be due to several reasons. A negative feedback loop could be established, where an increase in P2X7 receptor expression downregulates *de novo* transcription. Furthermore, since P2X7 trafficking is a very slow process (Robinson & Murrell-Lagnado 2013), protein stabilisation may occur under atheroprone flow resulting in reduced degradation, subsequently enhancing protein expression regardless of the mRNA changes. P2X4 was also up-regulated under atheroprone flow in the ibidi flow system but to a smaller extent than for P2X7 (atheroprone=1.347±0.08501 fold change) (Figure 4.7A), while no significant difference was observed using the orbital shaker (atheroprone=1.235±0.09563 fold change) (Figure 4.7B).

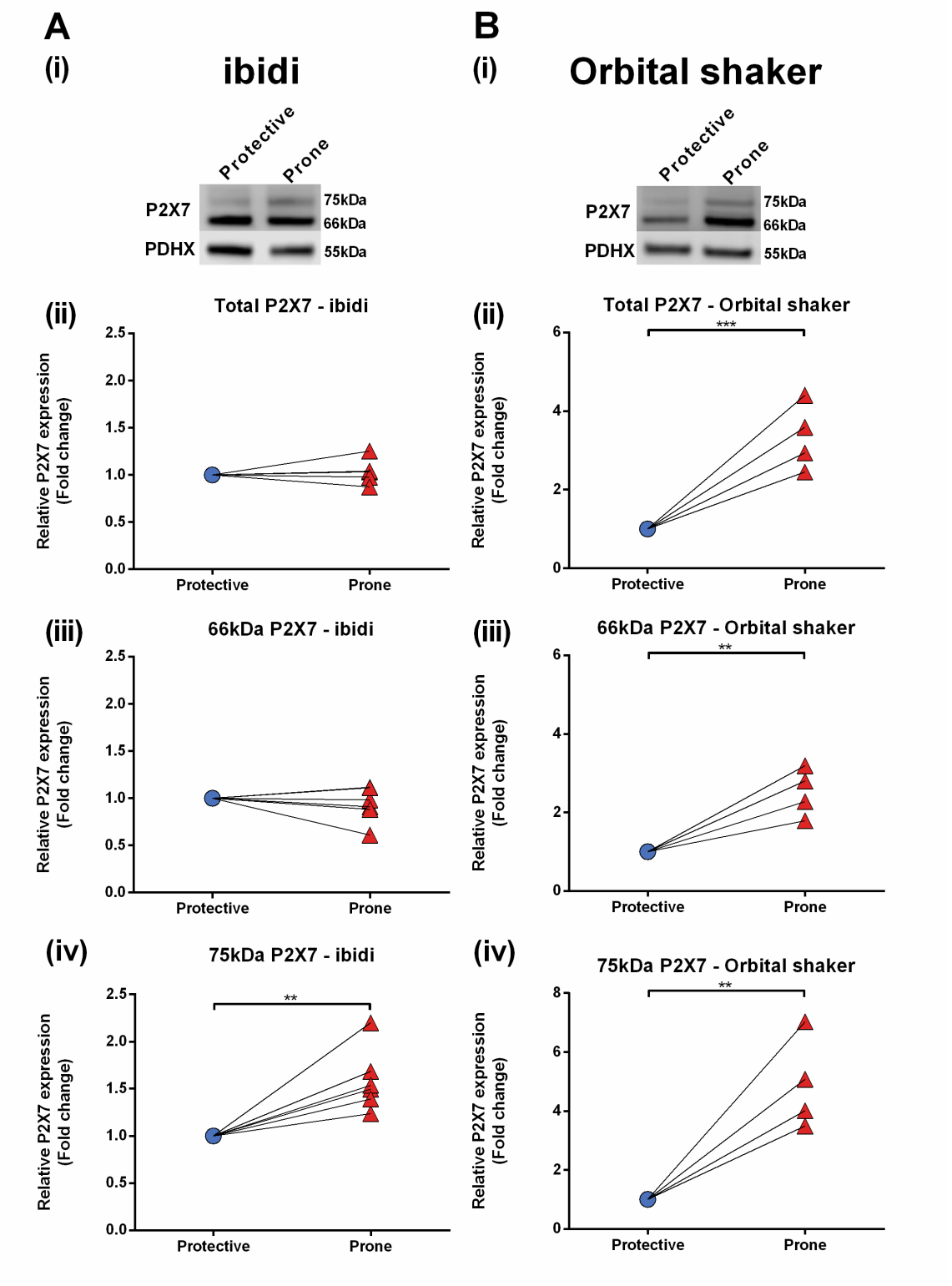

Figure 4.6 – P2X7 receptor protein expression is enhanced under atheroprone flow.

(A) Representative immunoblots for P2X7 on HUVEC lysate preconditioned with atheroprotective or atheroprone flow using the ibidi (Ai) or orbital shaker (Bi) flow systems. (Aii-Aiv) Densitometry of the 66kDa and 75kDa P2X7 bands and their combined total using the ibidi system (n=6). (Bii-Biv) Densitometry of the 66kDa and 75kDa P2X7 bands and their combined total using the orbital shaker system (n=4). ** indicates p=<0.01 and *** indicates p=<0.001 using a paired *t*-test. Statistical analysis was performed on the raw densitometry values normalised to PDHX.

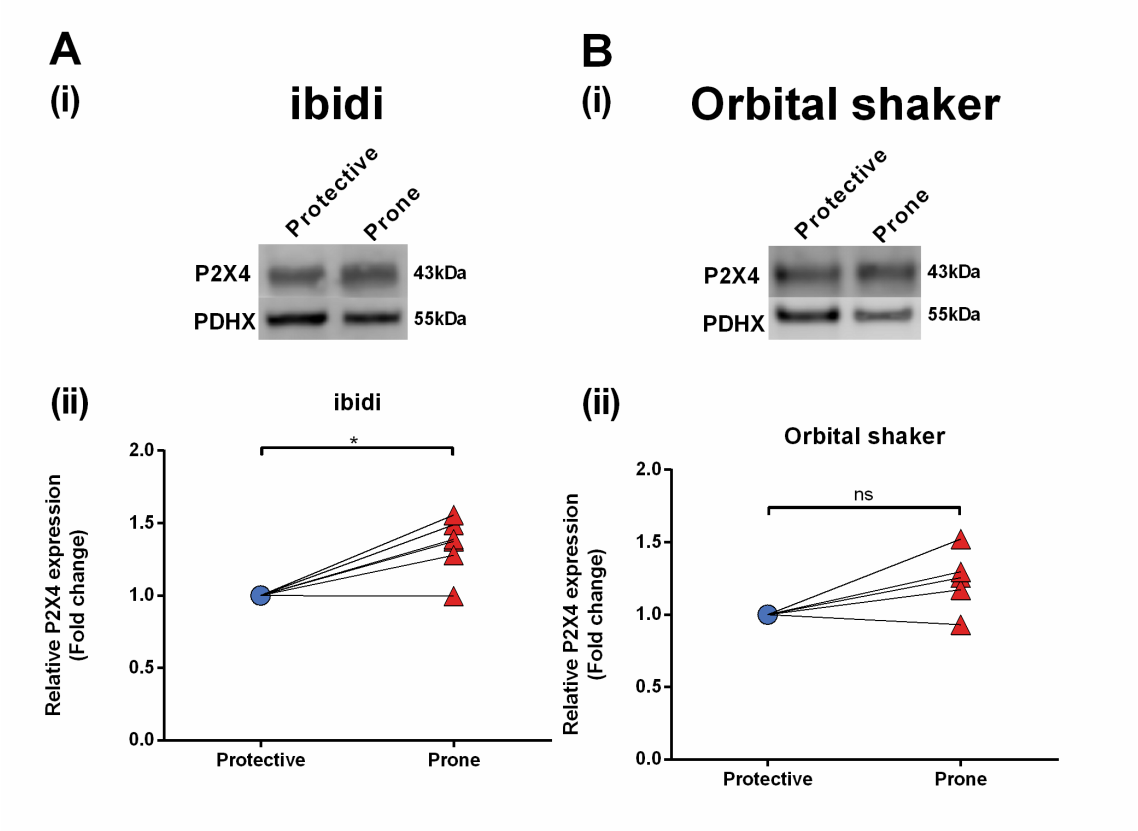

Figure 4.7 – Protein expression of P2X4 is enhanced by atheroprone flow in the ibidi system.

(A) Representative immunoblots for P2X4 on HUVEC lysate preconditioned with atheroprotective or atheroprone flow using the ibidi (Ai) or orbital shaker (Bi). (Aii) Densitometry of P2X4 using the ibidi system (n=6). (Bii) Densitometry P2X4 using the orbital shaker system (n=4). * indicates p=<0.05 using a paired *t*-test. Statistical analysis was performed on the raw densitometry values normalised to PDHX.

Expression of endothelial P2X7 protein was then assessed *in vivo* at atheroprotected and atherosusceptible sites in the murine aorta by *en face* immunostaining and confocal laser scanning microscopy (Figure 4.8). Specific regions of the mouse aorta have been mapped by computation fluid dynamics where the outer curvature, exposed to high shear stress, is considered an atheroprotected site, and the inner curvature, exposed to disturbed flow is an atheroprone site (Suo et al. 2007). The endothelial specific antigen CD31 was co-stained to assess P2X7 expression exclusively in the endothelium. Matching the protein data collected from HUVEC, endothelial P2X7 receptor staining was enhanced at sites prone to atherosclerosis compared to sites protected (atheroprotective=116.7±23.46 vs atheroprone=268.7±30.01) (Figure 4.8B). As not all the P2X7 staining was observed at the cell surface, surface P2X7 receptor expression was assessed by analysing the fluorescence of P2X7 at sites co-localising with the cell surface endothelial marker CD31. As well as an increase in total P2X7 expression levels, there was a significant increase in the surface expression of P2X7 at sites of atheroprone flow (atheroprotective=0.06192±0.008861 vs atheroprone=0.1425±0.01697) (Figure 4.8C). The P2X7 antibody was identified as specific to P2X7, determined by the lack of staining of endothelial P2X7 in the descending aorta of $P2X7^{-/-}$ mice (Figure 4.8D). In summary, endothelial P2X7 receptor expression is increased under atheroprone flow conditions in two complementary *in vitro* models and *in vivo.*

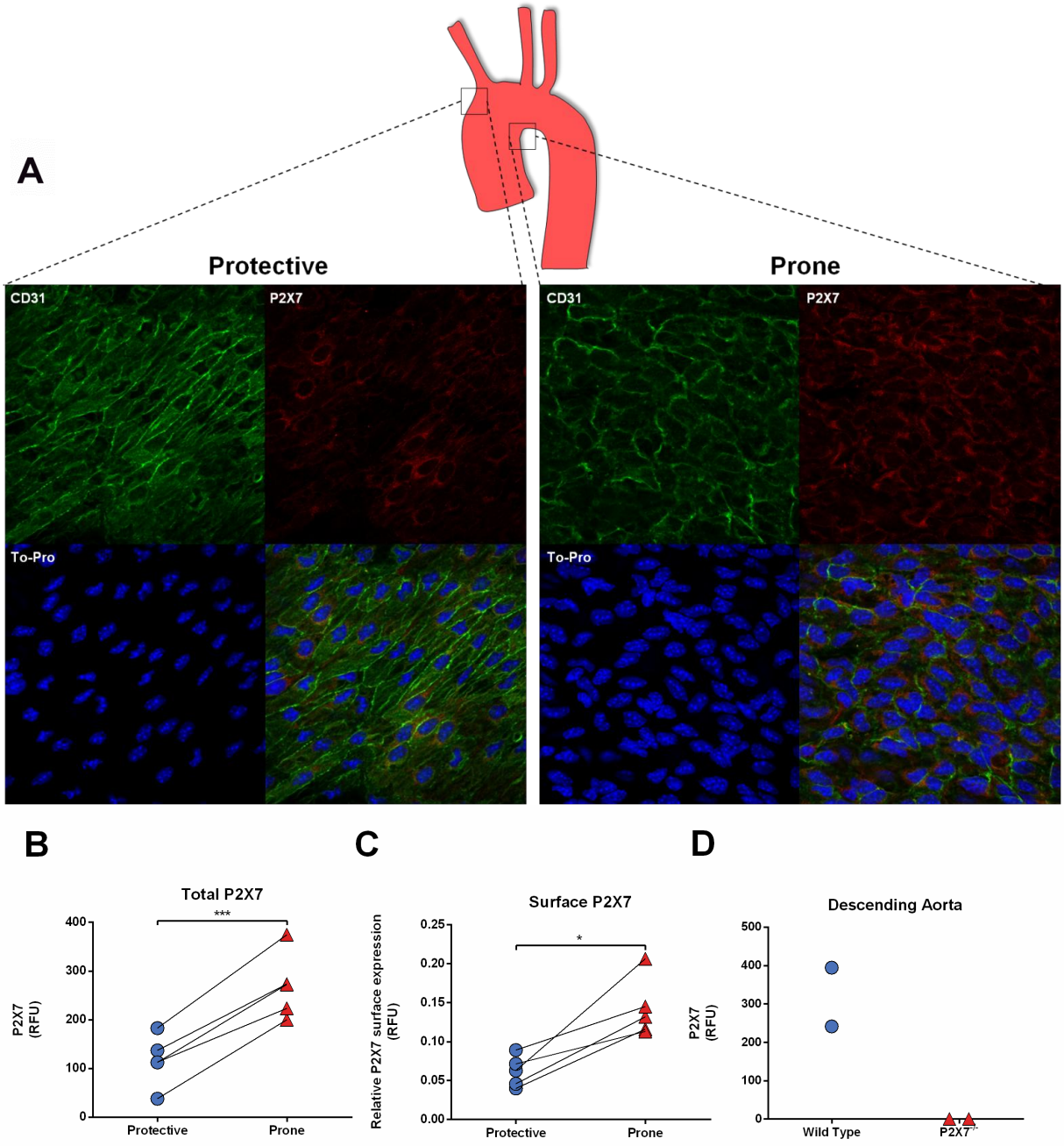

Figure 4.8 - Endothelial P2X7 receptor expression is enhanced *in vivo* at sites of atheroprone flow in the murine aortic arch.

(A) Representative *en face* immunostaining for P2X7 (red) on wildtype C57BL/6 mice at atheroprotective (outer curvature) and atheroprone (inner curvature) sites of the aorta. Endothelial cells were identified by staining with CD31 (green) and cell nuclei were stained using To-Pro (blue). (B) P2X7 expression was analysed by measuring the relative fluorescent intensity at sites of protected or prone to atherosclerosis (n=5). (C) Surface expression was measured by measuring P2X7 fluorescence at sites co-localised with the endothelial cell surface marker CD31 (n=5). (D) P2X7 fluorescence obtained from *en face* immunostaining of the endothelium from the descending aorta of wild-type or P2X7$^{-/-}$ mice (BALB/c) (n=2). Relative fluorescent intensities for P2X7 were corrected against the relative fluorescent intensity of IgG performed on the descending aorta. * indicates p=<0.05 and *** indicates p=<0.001 using a paired *t*-test.

4.6 Expression of P2X4 and P2X7 protein regulators in the endothelium

A number of proteins have been identified to influence P2X4 and P2X7 receptor activity; expression of these regulators was examined in HUVEC cultured under flow. Expression of caveolin was investigated as they are the major structural component of caveolae. Caveolin-1 has been shown to localise with P2X7 and regulate P2X7 responses (Barth et al. 2008; Gangadharan et al., 2015). Moreover, endothelial caveolae are the proposed site of shear stress-induced ATP release and subsequent calcium signalling (Yamamoto et al., 2011). Expression of caveolin-1 mRNA and protein was unaltered between atheroprone and atheroprotective flow in HUVEC cultured using the ibidi pump system (atheroprone mRNA=0.9939±0.1055 fold change; atheroprone protein=1.015±0.1696 fold change) (Figure 4.9A). Expression of caveolin-1 transcripts was significantly increased under atheroprone flow using the orbital shaker system (atheroprone=1.522±0.1180 fold change), but this did not occur post-translationally as protein levels remained unaltered (atheroprone=1.004±0.06073 fold change) (Figure 4.9B). Similar to caveolin-1, expression of caveolin-2 was unaltered by different flow patterns (atheroprone=0.9034±0.07814 fold change) (Figure 4.10A). The F_1/F_0 ATP synthase, a source of shear stress induced ATP release (Yamamoto et al. 2007) has enhanced cell surface expression under oscillatory flow patterns (Fu et al., 2011), but total expression levels were unchanged (atheroprone=1.043±0.03166 fold change) (Figure 4.10B). Pannexin-1 transcripts were examined as they can act as a cell membrane pore in which ATP can be released extracellularly in response to mechanical stimuli (Bao et al. 2004) and is considered responsible for P2X7 dependent pore formation and subsequent membrane permeabilisation (Pelegrin & Surprenant 2006). However, expression of pannexin-1 was unaltered between atheroprotective and atheroprone flow patterns in the ibidi (atheroprone=1.708±0.6220 fold change) and orbital shaker system (atheroprone=1.090±0.1569 fold change) (Figure 4.11). Heat

Shock Protein 90 has also been documented to interact with P2X7 (Kim et al., 2001), but mRNA and protein expression levels were unaltered by flow for both HSP90α (atheroprone mRNA=1.153±0.1076 fold change; atheroprone protein=1.036±1.524 fold change) and HSP90β (atheroprone mRNA=1.058±0.1229 fold change; atheroprone protein=1.105±0.1640 fold change) (Figure 4.12). Therefore, these interacting proteins were not examined further as their expression was not flow-sensitive.

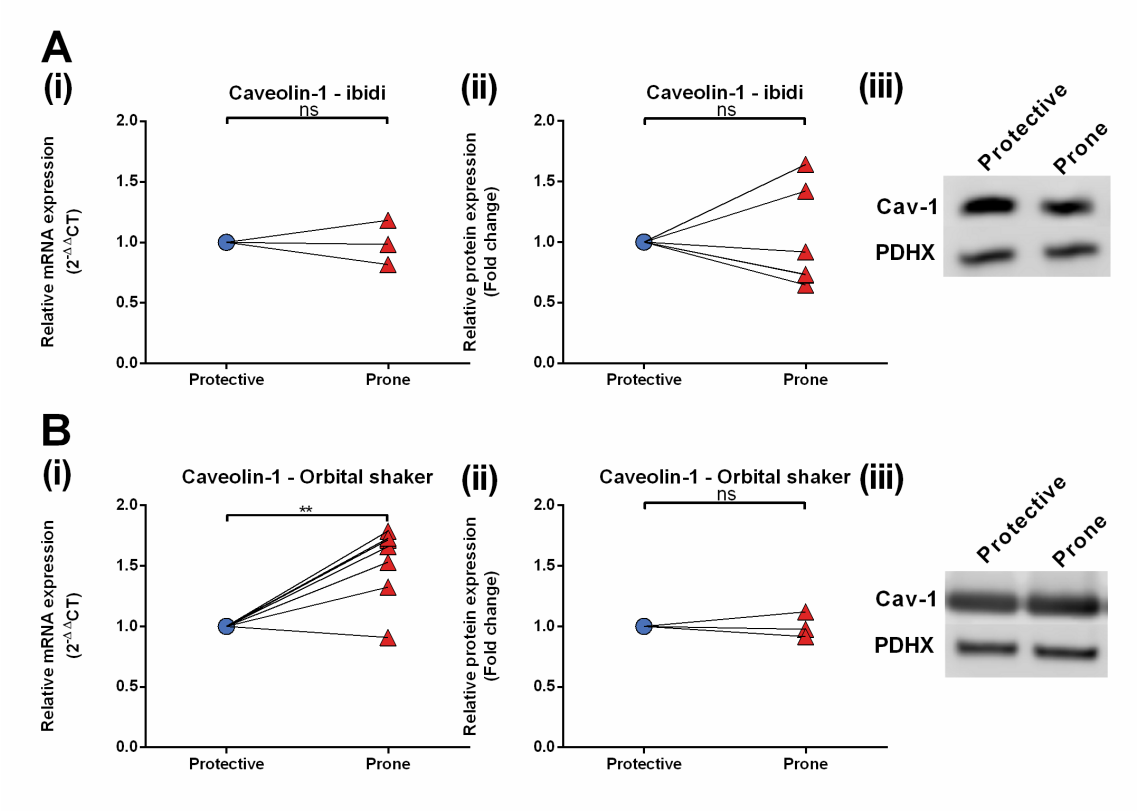

Figure 4.9 – Caveolin-1 expression is unaltered between atheroprotective and atheroprone flow in the ibidi system.

(A) Expression of Caveolin-1 in HUVEC conditioned under atheroprotective flow or atheroprone flow in the ibidi flow system (n=3-6). (B) Expression of Caveolin-1 in HUVEC conditioned under atheroprotective flow or atheroprone flow in the orbital shaker system (n=7-3). ** indicates p=<0.01 using a paired *t*-test. Statistical analysis was performed on the ΔCT for qPCR or raw densitometry values normalised to PDHX for western blotting.

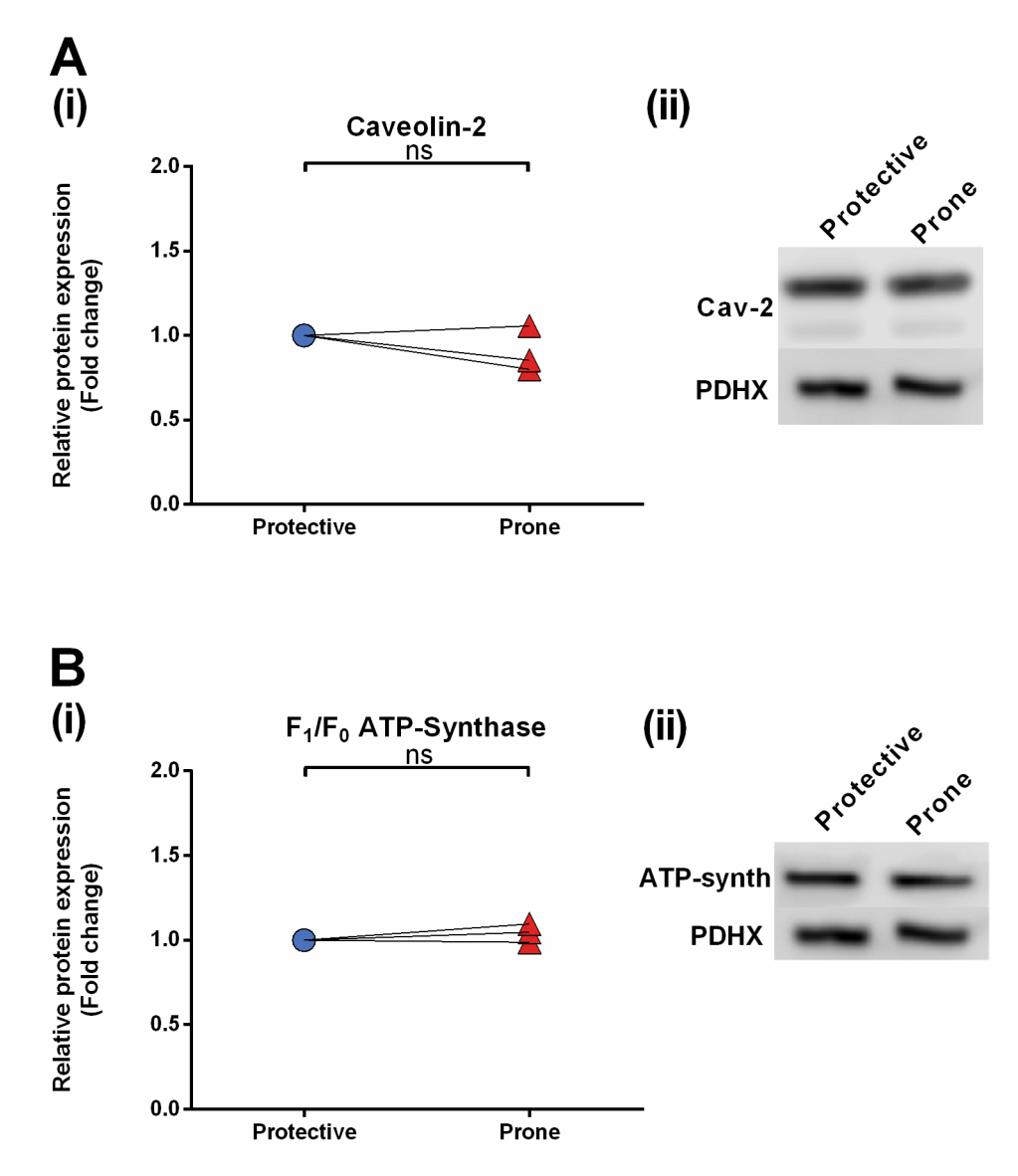

Figure 4.10 – Caveolin-2 and F_1/F_0 ATP-Synthase expression is unaltered between atheroprotective and atheroprone flow in the ibidi system.

(A) Expression of Caveolin-2 in HUVEC conditioned under atheroprotective flow or atheroprone flow in the ibidi flow system (n=3). (B) Expression of the β subunit of the F_1/F_0 ATP synthase in HUVEC conditioned under atheroprotective flow or atheroprone flow in the ibidi system (n=3). Statistical analysis was performed on the raw densitometry values normalised to PDHX.

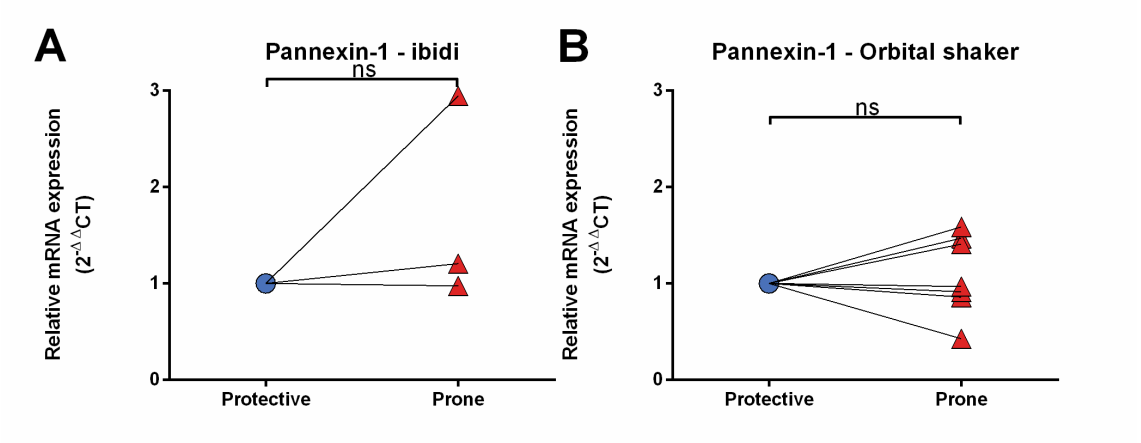

Figure 4.11 – Pannexin-1 mRNA expression is unaltered between atheroprotective and atheroprone flow.

(A) Expression of Pannexin-1 in HUVEC conditioned under atheroprotective flow or atheroprone flow in the ibidi flow system (n=3). (B) Expression of Pannexin-1 in HUVEC conditioned under atheroprotective flow or atheroprone flow in the orbital shaker system (n=7). Statistical analysis was performed on the ΔCT values.

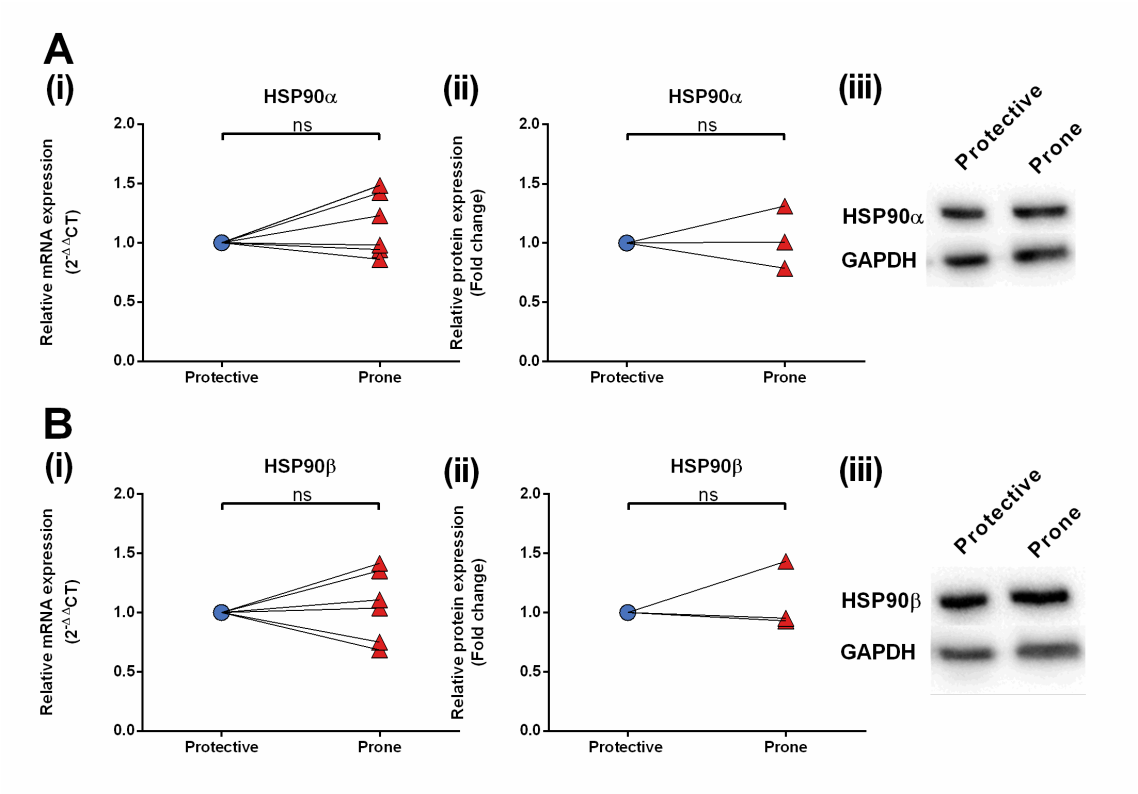

Figure 4.12 – Heat Shock Protein 90 expression is unaltered between atheroprotective and atheroprone flow in the orbital shaker system.

(A) Expression of HSP90α in HUVEC conditioned under atheroprotective flow or atheroprone flow in the orbital shaker system system (n=6-3). (B) Expression of HSP90β in HUVEC conditioned under atheroprotective flow or atheroprone flow in the orbital shaker system system (n=6-3). Statistical analysis was performed on the ΔCT for qPCR or raw densitometry values normalised to PDHX for western blotting.

4.7 Alternative splice variants of P2X7 are expressed in the endothelium

P2X7 has an additional level of regulation post-transcriptionally through alternative splicing events. At the time of these studies, NCBI Genbank contained the sequences for 11 alternatively spliced human P2X7 variants (P2X7a-P2X7j), with several studies reporting that these variants exhibited differential functions from classical P2X7 responses (Sluyter & Stokes 2011). Of particular interest is the existence of several P2X7 splice variants containing a premature stop codon, resulting in the loss of the extended intracellular C-terminal tail which is considered responsible for many of its inflammation signalling mechanisms (Costa-Junior et al. 2011). As studies on P2X7 in endothelial cells have previously reported an absence of several P2X7 unique responses following stimulation, such as pore formation (Ramirez & Kunze 2002), cell membrane blebbing and apoptosis (Wilson et al., 2007), it was hypothesised that alternative splicing might explain these endothelial specific differences. To determine which P2X7 splice variants were expressed in the endothelium, the deposited sequences from NCBI were aligned to identify splice variant-specific sequences, created by unique exon-exon junctions or retained introns (Figures 4.13). This allowed specific primers to be designed for 9 out of 11 possible P2X7 variants, but it was impossible to design primers specific to only P2X7b and P2X7a (full length, “classical”) as these contained no unique sequences. These primers were used for PCR on cDNA generated from HUVEC mRNA and resolved via agarose gel electrophoresis. Positive reactions were validated by sequencing of the PCR product . This allowed identification of P2X7c, P2X7e, P2X7h, P2X7i and P2X7j, but not P2X7d, P2X7f, P2X7g in HUVEC. Negative results were confirmed by performing further reactions at a range of different annealing temperatures to exclude non-specific PCR products. A summary of the results of these experiments is shown in table 4.2, revealing expression of P2X7 alternatively spliced variants in the endothelium.

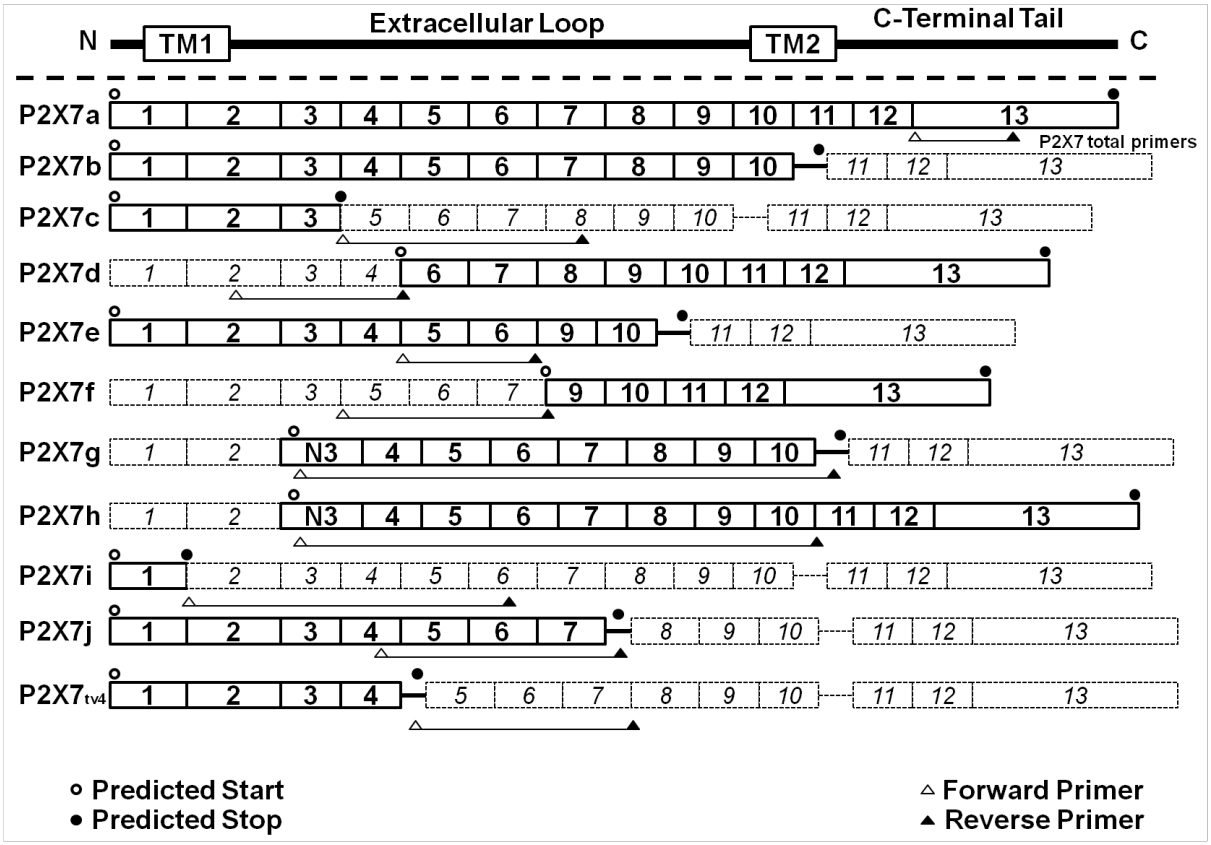

Figure 4.13 – Schematic showing regions allow P2X7 splice variant specific primers design.

P2X7 transcripts are split up into 13 exons, which are differentially spliced. The P2X7 receptor contains intracellular N and C terminals and one large extracellular loop. Exons are roughly alligned with the protein schematic to represent the effect of alternative splicing on the translated P2X7 protein. Bold segments are translated whereas faded out segments are not. Thin black lines show retained introns. Forward and reverse primers are shown to highlight the design of splice variant specific primer sets based on unique exon-exon boundaries or retained introns. Genbank accession numbers; P2X7a (GQ180122.1), P2X7b (AY847298.1), P2X7c (AY847299.1), P2X7d (AY847300.1), P2X7e (AY847301.1), P2X7f (AY847302.1), P2X7g (AY847303.1), P2X7h (AY847304.1), P2X7i (NM_177427.2), P2X7j (DQ399293.1), P2X7tv4 (NR_033950.1).

Splice Variant	Product in Gel	Confirmed by Sequencing
P2X7a	-	-
P2X7b	-	-
P2X7c	✓	✓
P2X7d	✘	✘
P2X7e	✓	✓
P2X7f	✘	✘
P2X7g	✘	✘
P2X7h	✓	✓
P2X7i	✓	✓
P2X7j	✓	✓
P2X7tv4	✓	✓

Table 4.2 - Summary table of P2X7 splice variants expressed in the endothelium

Splice variant specific primers outlined in Figure 4.15 and 4.16 were used for identification of endothelial expressed splice variants. - indicates that it was impossible to design a splice variant specific primer set for that variant.

An additional primer set was also designed which spanned the entire P2X7 transcript. Since this primer pair spanned the entire mRNA sequence, any differences in splicing resulting in a change of transcript length would be resolved as a different sized band. The predicted length of different sized P2X7 transcripts using these primers is shown in Figure 4.14A. This reaction was performed on HUVEC cultured under flow using the orbital shaker system to determine if splicing events were altered by shear stress. Splicing events were altered between donors with some bands only present under certain conditions (Figure 4.14A). Interestingly, the two strongest bands were present in all donors and the ratio of these two bands appeared to change with flow (Figure 4.16B). The upper band was more intense than the lower band in endothelial cells cultured under atheroprotective flow (upper=65.55±3.371 vs lower=34.45±3.371), but the lower band was more intense than the top band in static endothelial cells (upper=36.53±4.775 vs lower=63.47±4.775). Under atheroprone flow, the intensity of these bands was roughly the same (upper=52.87±4.721 vs lower=47.13±4.721). Based on the size of these bands, it is tempting to speculate that the upper band is P2X7b and the lower band is P2X7a, as these are the most studied variants. However, there are 5 different variants expressed in the endothelium that would also appear between 1000bps and 1200bps so it is possible that other variants could be involved. Nevertheless, this suggests that P2X7 alternative splicing events are altered between atheroprotective and atheroprone flow conditions.

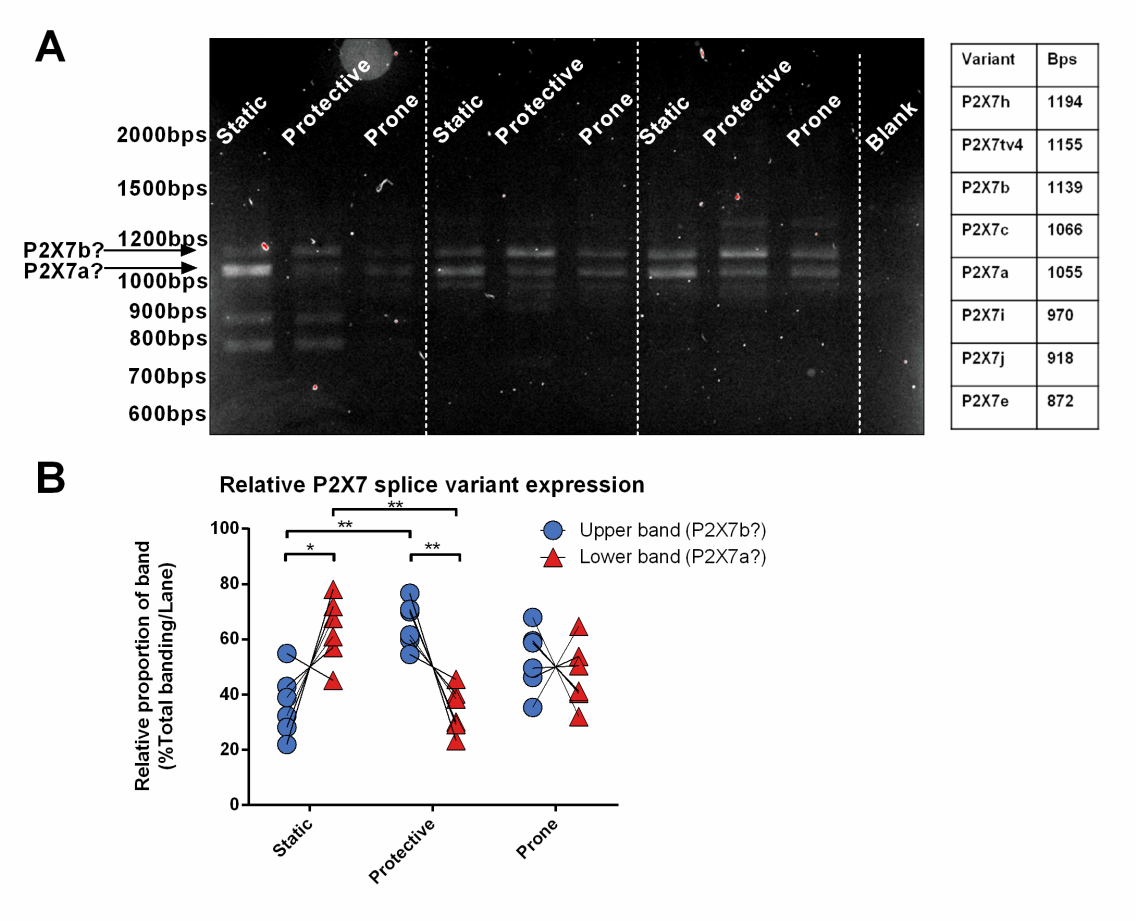

Figure 4.14 – P2X7 splicing events are altered by flow in HUVEC cultured using the orbital shaker system.

(A) Agarose gel electrophoresis on PCR products generated by a primer set spanning the entire P2X7 transcript on 3 HUVEC donors. The table represents the predicted length of P2X7 splice variant products and the arrows represent potential P2X7a and P2X7b transcripts. (B) Relative proportions of the upper and lower bands within the lane, predicted to be P2X7b and P2X7a respectively. (n=6). * indicates p=<0.05 and ** indicates p=<0.01 using a two way ANOVA.

As most alternatively spliced P2X7 variants are predicted to be subjected to non-sense mediated decay (Genbank), identification of variants at the protein level is important. As alternative splicing is proposed to induce dramatic changes in P2X7 structure, an approach using antibodies targeting the N-terminus, the extracellular region and the C-terminus was performed as, in combination, it would allow identification of all variants.

A schematic demonstrating the theoretical discrimination of P2X7 splice variants by antibodies targeting different regions of P2X7 is shown in Figure 4.15. Antibodies targeting the extracellular domain and C-terminus produced bands via western blotting, whereas N-terminus targeting antibodies did not work (Figure 4.16). Extracellular and C-terminus targeting antibodies were validated by pre-adsorption with blocking peptides, showing specificity for most bands. Moreover, P2X7 knockdown with a pool of 4 siRNAs, which should target all alternatively spliced variants, caused a reduction in several bands determining specificity of the extracellular targeting antibody for several bands produced by western blotting (95kDa=0.6623±0.2455; 75kDa=0.4377±0.1443; 66kDa=0.5235±0.1380; 33kDa=0.3976±0.1055; 17kDa=0.8077±0.3101; 14kDa=0.8758±0.2195 fold change) (Figure 4.17), suggesting that these bands are indeed variants of P2X7. However, it was impossible to determine which band corresponded to which variants as band size did not correlate with the predicted amino acid weight. Several variants still contain key residues identified as sites for post-translational modifications, suggesting that these could still be modified and explain the differences in size. However, as P2X7a, the major P2X7 receptor variant studied, was up-regulated under atheroprone flow conditions (Figure 4.6), efforts were focused on studying P2X7 functionality and subsequent downstream effects rather than alternative splicing as our laboratory was not experienced in the appropriate techniques to study alternative splicing further. In summary, P2X7 splice variants are expressed in the endothelium, with splicing events proposed to alter between flow conditions.

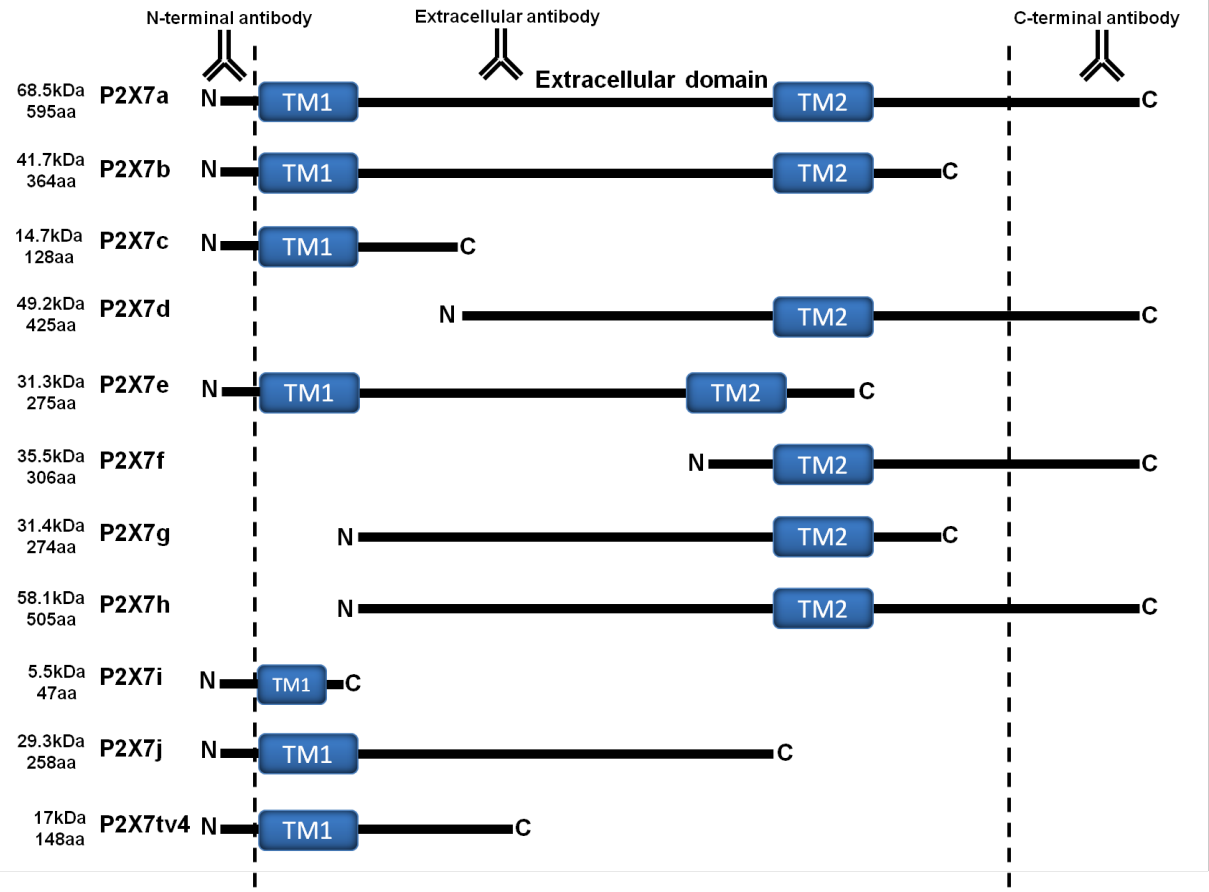

Figure 4.15– Schematic proposing a method to distinguish between different translated human P2X7 splice variants.

Alternative splicing events result in changes in the regions of P2X7 translated. Antibodies targeting the N-terminus should bind to P2X7a, P2X7b, P2X7c, P2X7e, P2X7i, P2X7j and P2X7tv4. Antibodies targeting the extracellular domain should detect P2X7a, P2X7b, P2X7e, P2X7g, P2X7h and P2X7j. Antibodies targeting the C-terminus should bind to P2X7a, P2X7d, P2X7f and P2X7h. The predicted molecular weight and amino acid (aa) length of each variant is displayed to the right of the schematic. The different molecular weight and antibody specificities can be used in combination to identify expression of specific variants.

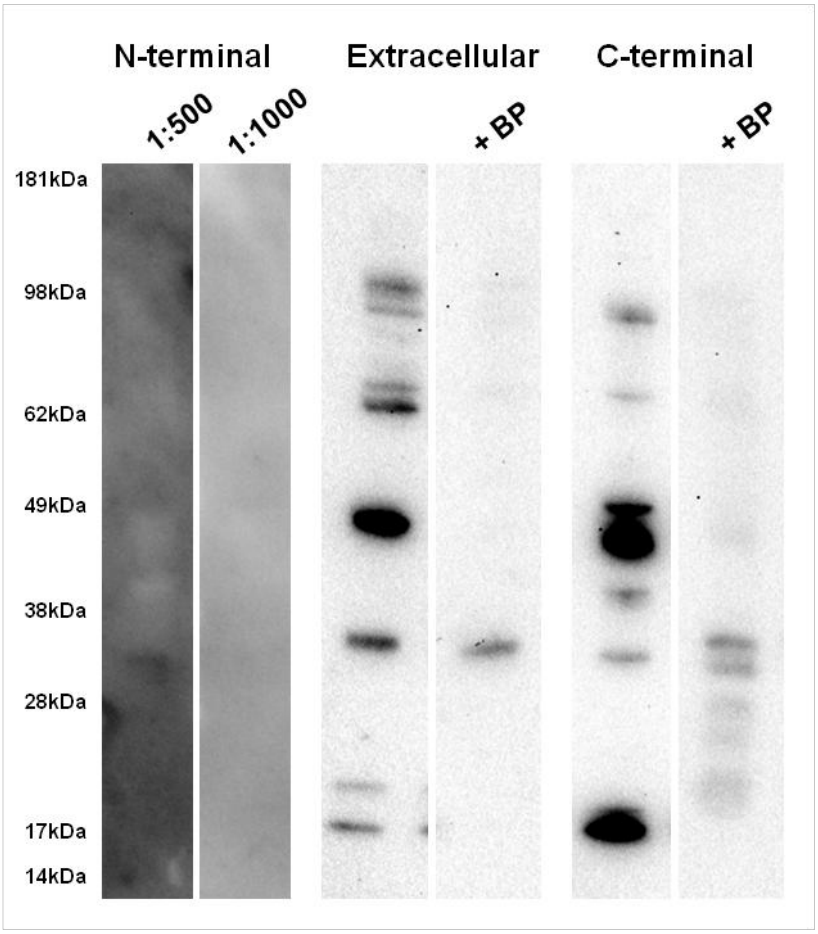

Figure 4.16 – Comparison of P2X7 antibodies on static HUVEC lysate raised against different regions of the P2X7 protein.

Immunoblot using commercial P2X7 antibodies raised against the N-terminal, extracellular domain or C-terminal. The N-terminal antibody was tested at 2 different concentrations, 1:500 and 1:1000. Extracellular and C-terminal antibody specificity was assessed by pre-incubation with blocking peptides (+BP), which blocked the fragment antigen-binding (Fab) region of the antibody.

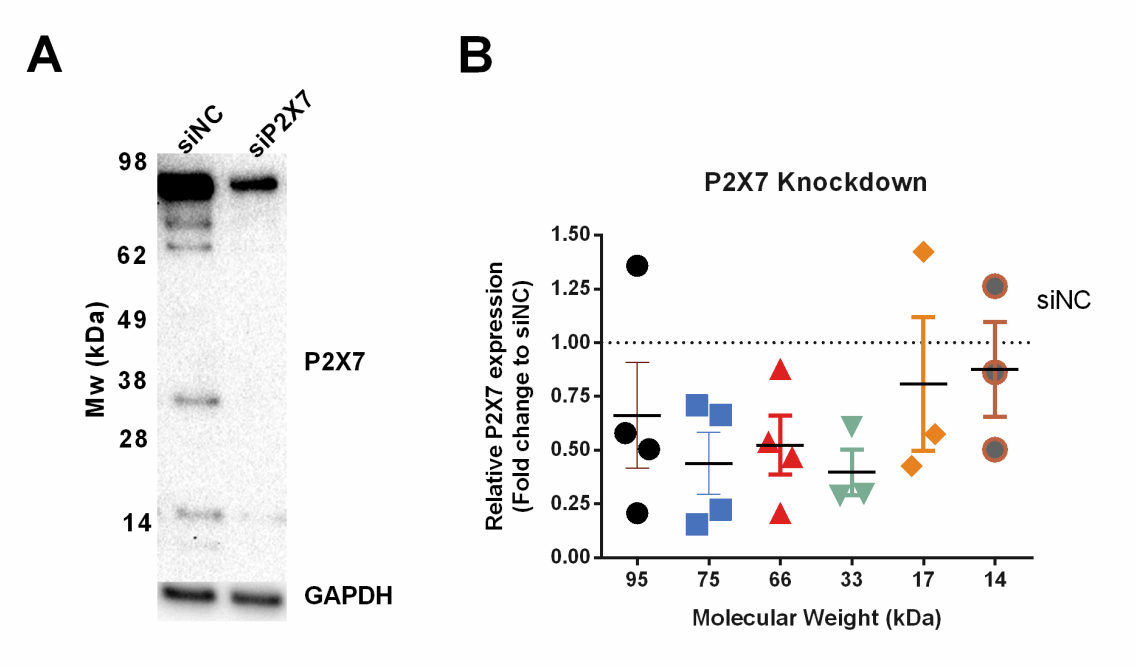

Figure 4.17– P2X7 knockdown in HUVEC reduces the intensity of several bands detected by the extracellular antibody

(A) Representative immunoblot for P2X7 in static HUVEC, transfected with non-coding siRNA (siNC) or siRNA targeting P2X7 (siP2X7). (B) Quantification of different molecular weight bands (n=3-4). The dotted line indicates the intensity of these bands in non-coding siRNA transfected cells. Values are ± SEM.

4.8 Conclusions

P2X7 receptors were activated in HUVEC following 300μM BzATP stimulation after preconditioning under atheroprone flow, but not atheroprotective flow. Expression of P2X7 was enhanced in two complementary *in vitro* models of atheroprone flow and at atherosusceptible sites *in vivo* of the murine aorta. Conversely, P2X4 receptor function, as assessed by calcium influx and specific antagonists, could not be detected in atheroprone flow conditioned HUVEC, despite a moderate enhancement in P2X4 expression. Expression of potential interacting or regulatory proteins of P2X7 remained largely unchanged. Alternatively spliced transcript variants were detected for P2X7 in the endothelium; expression of these variants appears to be differentially regulated between atheroprotective and atheroprone flow.

4.9 Discussion and future work

This data demonstrates that there is a selective role for P2X receptors in endothelial cells under atheroprone flow, which is absent under atheroprotective flow. P2X7 receptors were up-regulated and P2X7 receptor activity was detected in HUVEC under atheroprone flow. Conversely, P2X4 activity was not detected in HUVEC preconditioned with atheroprone flow, despite the fact that it is the most abundantly expressed P2 receptor in endothelial cells (Yamamoto et al. 2000; Wang et al. 2002) and was slightly up-regulated by atheroprone flow. A reason for this could be that surface expression of P2X4 has been shown to be low in this cell type. Previous data from our group suggests that cell surface P2X4 expression is almost absent in unstimulated static cultures of HUVEC, and is trafficked to the plasma membrane in response to inflammatory stimuli (Wilson et al. 2007). P2X4 has also been shown to localise predominantly to lysosomes in endothelial cells (Qureshi et al. 2007) and could have an intracellular role which is entirely different to that of a cell surface ion channel. Moreover, due to the lack of studies using the commercially available P2X4 antagonist PSB-12062, it is unclear if it is completely effective as a full inhibitor of P2X4 receptor

activity. Indeed, in the published study that identified PSB-12062, they note that the drug has a maximal inhibition of 68% (Hernandez-Olmos et al. 2012). The non-commercially available modified derivative PSB-12253 has been shown to be particularly potent at the endothelial P2X4 receptor (Sathanoori et al. 2015; Sathanoori et al. 2015), but unfortunately for this study we did not receive permission for receipt of this compound since it was subject to commercial development by the PI, Dr Christa Müller, at the time we made this request (Hernandez-Olmos et al. 2012). Therefore, these results suggest that P2X4 activity is absent under atheroprone flow, but this evidence is not unequivocal, particularly considering that up to half of the BzATP-mediated extracellular calcium influx response was not inhibited by the P2X7 antagonist or suramin. Insensitivity to suramin is characteristic of P2X4 and P2X7 receptor responses.

Most of these studies were performed *in vitro* on HUVEC, a relatively immature venule endothelial cell. However, P2X7 expression was also increased at atheroprone sites in arterial endothelial cells *in vivo* by *en face* immunostaining of the murine aortic arch, suggesting our findings translate *in vivo.* Furthermore, *in vitro* P2X7 receptor activity was only detected under atheroprone flow conditions, which correlated with the increased cell surface expression of P2X7 at atherosusceptible sites of the murine aorta. This suggests that P2X7 trafficking to the cell surface may in part explain the increased P2X7 receptor activity. Enhanced P2X7 receptor expression occurred at the same sites *in vivo* in addition to diminished CD39 expression (Kanthi et al. 2015) and enhanced F_1/F_0 ATP synthase (Fu et al. 2011) previously reported, suggesting up-regulated ATP signalling and activation of P2X7 occurs at sites of atheroprone flow. However, all these studies, including this one, were performed in C57BL/6 mice, which contain a single nucleotide polymorphism (SNP) in the P2X7 receptor (P451L) resulting in reduced P2X7 channel function (Adriouch et al. 2002). However, this polymorphism does not alter surface protein expression (Young et al. 2006; Sorge et al. 2012) and

therefore the expression data collected should be unaffected. Since this polymorphism (P451L) is not prevalent in the human population, future *in vivo* experiments examining the functional role of endothelial P2X7 should be performed in a murine model which does not contain this SNP such as BALB/c mice to fully understand the role of P2X7. Moreover, recently a $P2X7^{-/-}$ mouse strain has been generated on a BALB/c background. Compared to wild-type, these mice were shown to exhibit larger P2X7-dependent differences than those on the C57BL/6 background, which was proposed to be due to the lack of the SNP P451L (Gartland 2012; Syberg et al. 2012). Furthermore, these BALB/c $P2X7^{-/-}$ mice were also shown to be completely deficient in endothelial P2X7 receptors in this chapter by *en face* immunostaining of the aorta, making these mice ideal for functional studies on endothelial P2X7.

Alternatively spliced P2X7 transcripts were identified in HUVEC using splice variant specific primers. In agreement, data mining of RNA-seq datasets revealed expression of sequences matching the retained intron transcribed in P2X7b, P2X7c, P2X7e, and P2X7g in HUVEC (NCBI Gene Expression Omnibus - GSM1009635). In my study, an up-regulation of P2X7 transcripts was present under atheroprotective flow using the orbital shaker system, but an enhancement of the 66kDa and 75kDa P2X7a protein was seen under atheroprone flow. This discrepancy could be as a result of alternative splicing, as qPCR amplified all alternatively spliced P2X7 variants, whereas western blotting exclusively focused on P2X7a expression. Therefore, it is possible that some alternatively spliced P2X7 transcript variants are differentially regulated, with some variants up-regulated under atheroprotective flow but with P2X7a enhanced under atheroprone flow. Indeed, experiments performed with primers spanning the entire coding sequence of P2X7 suggested that alternative splicing events were altered by flow, but requires further investigation. If possible, analysis of only P2X7a transcripts would reveal if the enhanced protein expression of P2X7a is due to increased transcription or via a post-translational mechanism, such as decreased turnover. It is

tempting to speculate that atheroprotective flow could evoke an up-regulation of P2X7 splice variants which antagonise P2X7a. For example P2X7j transcripts were identified in HUVEC and previous studies have shown that P2X7j exhibited a severe deficiency in calcium influx and actually functions as a dominant negative regulator of P2X7a (Feng et al. 2006). Despite observable expression of P2X7, calcium influx in response to ATP was absent in HUVEC preconditioned under atheroprotective flow. This suggests that additional mechanisms of regulation are present and a change in the ratio of P2X7 transcript variants may be in part responsible. In addition, the majority of P2X7 splice variants have not been characterised fully and it is currently unknown what their functions are. Since it is unknown if these alternatively spliced P2X7 variants are translated, future studies could use mass spectrometry to identify endogenous P2X7 splice variants at a protein level in the endothelium. The results from this would direct functional studies of individual splice variants using over-expression studies in P2 receptor absent cell lines, such as the 1321N1 astrocytoma cell line. Progressing these studies into *in vivo* murine models is however difficult, since the human P2X7 splice variants discussed here (P2X7b-j) are not present in mice, with several murine specific P2X7 splice variants expressed instead (Sluyter & Stokes 2011). Therefore, any regulation occurring by alternative splicing will be different between human and murine models and must be taken into account.

Expression levels of caveolin-1, caveolin-2, F_1/F_0 ATP-synthase, Pannexin-1 and HSP90 were unchanged between atheroprone and atheroprotective flow conditions. However the subcellular localisation and phosphorylation states of these proteins was not assessed. Pannexin-1 channels have been reported to mediate ATP release in response to mechanical stimuli (Bao et al. 2004). Protein expression of pannexin-1 between atheroprotective and atheroprone flow was not assessed as transcript levels were unchanged, but it is possible that protein levels, cell surface expression or phosphorylation events may be modulated by flow. Indeed, TNF induces ATP release

through phosphorylation of Pannexin-1 channels in endothelial cells, whilst total expression levels of Pannexin-1 remained unchanged (Lohman et al. 2015). F_1/F_0 ATP synthase, which produces shear stress induced ATP (Yamamoto et al. 2007), exhibits increased cell surface expression in endothelial cells cultured under atheroprone flow conditions and at sites of atheroprone flow *in vivo* (Fu et al. 2011), suggesting subcellular location changes under flow. Similarly expression of caveolin-1 and 2 were unaltered between atheroprone and atheroprotective flow but reports indicate that caveolin-1 expression (Qin et al. 2016) and surface expression (Fu et al. 2011) is enhanced under atheroprone flow and is responsible for some aspects of atheroprone flow signalling (Sun et al. 2016). The results presented here may differ compared to those previously published due to differences in flow models and time points measured. Indeed, in this work, the induction of several genes differed between the orbital shaker and ibidi flow systems. Since different *in vitro* models mimic different aspects of atheroprone flow, it is plausible that the models used in these studies may provide flow conditions resulting in caveolin-1 induction, whereas ours do not. Moreover, HUVEC in our studies were exposed and pre-conditioned to flow for 72 hours, whereas studies which report caveolin-1 enhancement subjected endothelial cells for flow for less than 24 hours (Fu et al. 2011; Qin et al. 2016). It is plausible that this extended time point modulates and stabilises caveolin-1 levels. Nevertheless, since these interacting / regulatory proteins themselves have several points of regulation, their involvement in regulating P2X responses under shear stress conditions cannot be excluded. However, these results demonstrate that, if they do play a role, this is not at a transcriptional level. Further evidence from the other chapters in this thesis do indicate that some potential regulators of P2X7 are altered under flow. Expression of CD39 (Figure 3.6) and EMP2 (Figure 6.11), which are proposed to negatively regulate P2X7 responses, is enhanced under atheroprotective flow conditions, suggesting they may be involved in suppressing P2X7 responses under such conditions and are exciting targets for further research.

Chapter 5

P2X7 receptors contribute to shear stress-induced inflammatory signalling

5.1 Introduction

The previous chapters have shown that under atheroprone flow conditions, there is an enhancement in the expression of P2X7 receptors and that P2X7 receptor activity was detected exclusively in atheroprone flow conditioned HUVEC in response to stimulation with exogenous ATP. This P2X7 activity was absent in HUVEC preconditioned to atheroprotective flow. Therefore, it was proposed that P2X7 receptors were active under atheroprone flow conditions and contributed towards the pro-inflammatory phenotype of these cells. P2X7 receptors and atheroprone flow are both known to induce inflammatory signalling but these mechanisms have not been linked directly in endothelial cells. One aspect of atheroprone flow induced pro-inflammatory signalling occurs through activation of mitogen activated protein kinases (MAPKs) and NF-κB signalling leading to production of pro-inflammatory gene transcripts, such as monocyte chemoattractant protein-1 (MCP-1), E-selectin, intercellular adhesion molecule 1 (ICAM-1) and interleukin-8 (IL-8) (Chiu & Chien 2011). The up-regulation of these proteins promotes the recruitment and adhesion of circulating blood monocytes, which then transmigrate through the endothelium where they can further contribute towards atherosclerosis development (Libby 2002). These signalling pathways have been documented to be activated by P2X7 in other systems and cell types, such as the generation of reactive oxygen species (Suh et al. 2001), MAPK signalling (Skaper et al. 2009) and activation of the NF-κB subunit p65 (Ferrari et al. 1997). Moreover, application of exogenous ATP to endothelial cells has been shown to induce inflammatory genes (Figure 1.7), which has been proposed to be co-ordinated in part by P2X7 (von Albertini et al. 1998; Goepfert et al. 2000) . Therefore the role of P2X7 on atheroprone flow induced inflammatory signalling was examined.

5.2 Hypothesis

P2X7 receptor activity contributes to the pro-inflammatory phenotype of endothelial cells exposed to atheroprone flow by activating MAPK and NF-κB signalling.

5.3 Aims

1) Assess the involvement of P2X7 in cytokine-induced inflammation in endothelial cells.

2) Examine the effect of P2X receptor antagonists on the induction of atheroprone flow associated inflammatory genes.

3) Determine the role of P2X receptors in the activation of MAP kinases and NF-κB under atheroprone flow.

5.4 Endothelial P2X7 involvement in the TNF/IFNγ induced inflammatory response

P2X7 receptor expression and function was up-regulated in endothelial cells under inflammatory conditions (Figure 3.3). The Wilson lab has previously shown that 48 hours treatment with TNF and IFNγ up-regulates P2X7 expression in HUVEC (Wilson et al. 2007). Cytokines, including TNF and IFNγ, play an important role in perpetuating the inflammatory response during atherosclerosis development (Libby 2002). Therefore, endothelial genes associated with inflammation and atherosclerosis were examined in TNF/IFNγ stimulated endothelial cells and the role of P2X7 in this response was determined using P2X7 specific antagonists. In these experiments a large increase in P2X7 receptors was observed as shown previously (Figure 3.3A). Vascular cell adhesion molecule 1 (VCAM-1) and monocyte chemoattractant protein 1 (MCP-1) are inflammatory genes which have been associated with atherosclerosis development (Cybulsky et al. 2001; Aiello et al. 1999). TNF and IFNγ stimulation enhanced VCAM-1 (162.7±8.571 fold) and MCP-1 (17.25±2.119 fold) expression and this up-regulation was reduced, but not significantly, with P2X7 antagonism (VCAM-1: AZ1060620=81.43±12.34 fold; MCP-1: AZ1060620=9.441±1.011 fold) (Figure 5.1). These experiments were limited to a small number of replicates, so it is possible that a larger sample size might demonstrate a statistically significant reduction in TNF/IFNγ induced inflammatory gene expression in the presence of this P2X7 antagonist. These data suggest that endothelial P2X7 receptors may contribute to cytokine-induced vascular inflammation. Since P2X7 has already been reported to induce inflammatory gene expression in static endothelial cell cultures after inflammatory stimuli (Sathanoori et al. 2015), further efforts were focused on determining the potential role of endothelial P2X7 in inflammatory signalling under atheroprone flow conditions, as this has not been previously examined.

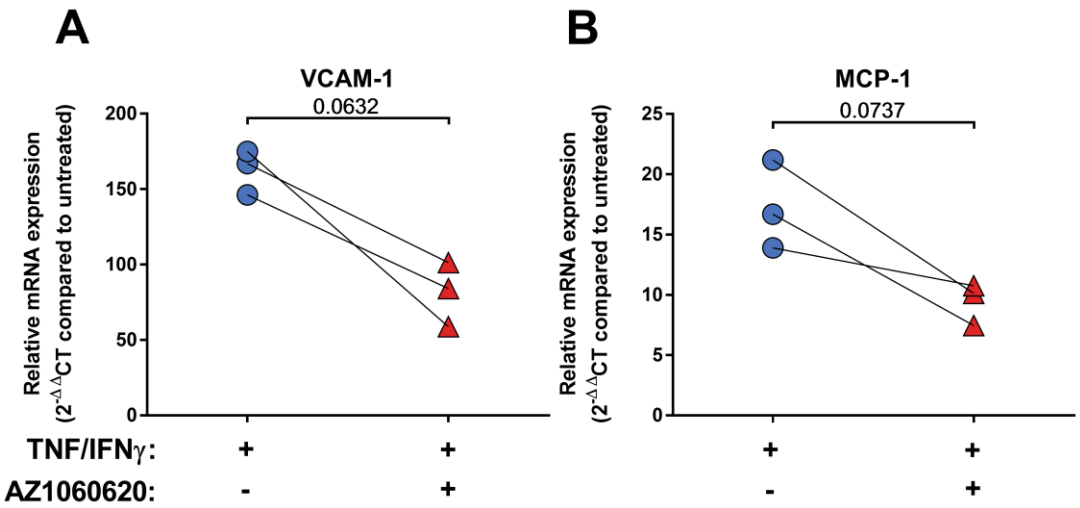

Figure 5.1 – TNF and IFNγ induced VCAM-1 and MCP-1 expression may be altered by P2X7 inhibition.

Incubation with 10ng/ml TNF and 100ng/ml IFNγ for 48 hours induces the expression of P2X4 and P2X7 mRNA and protein in static HUVEC. (A) Expression of VCAM-1 in static HUVEC stimulated with TNF/IFNγ ± AZ10606120 (10μM) (n=3). (B) Expression of MCP-1 in static HUVEC stimulated with TNF/IFNγ ± AZ10606120 (10μM) (n=3). Samples were compared for significance using a paired *t*-test. Statistical analysis was performed on the ΔCT values.

5.5 P2X7 inhibition attenuates atheroprone flow-induced adhesion molecule and chemokine expression

Work from this project demonstrates that P2X7 receptor activity is up-regulated in atheroprone flow exposed endothelial cells compared to atheroprotective flow exposed cells. In addition, the ATPase CD39 is downregulated under atheroprone flow conditions. Therefore we tested whether endogenous ATP signalling is up-regulated under atheroprone flow conditions and activates P2X7 or P2X4-mediated inflammatory signalling, by culturing HUVEC in the presence of the P2X7 antagonist A438079 or the P2X4 antagonist PSB-12062.

Initially, qPCR was performed to determine expression of a range of reported flow-induced genes under atheroprone or atheroprotective flow using the ibidi pump system to identify which genes are up-regulated using this model. However, many genes that have been previously reported to be differentially regulated between atheroprone and atheroprotective flow were not significantly altered between these flow conditions. The lack of statistical significance in these experiments was likely due to the low number of donors tested and variation in expression between donors. Endothelial nitric oxide synthase (eNOS) is a well-documented atheroprotective factor responsible for nitric oxide production and subsequent vasodilation (SenBanerjee et al. 2004). eNOS expression appeared to decrease under atheroprone flow compared to atheroprotective flow (atheroprone=0.4959±0.09313 fold change), (Figure 5.2A). MCP-1, a well-documented atheroprone flow induced factor responsible for monocyte recruitment (Papadopoulou et al. 2008; Gerszten et al. 1999), appeared to be slightly up-regulated, but not significantly, under atheroprone flow (atheroprone=1.746±0.3192 fold change) (Figure 5.2B). Several reported flow sensitive genes however did not change between these flow conditions, including IL-6 (atheroprone=1.073±0.1787 fold change) (Figure 5.2C), ICAM-1 (atheroprone=0.8780±0.3369 fold change) (Figure 5.2D), KLF2 (atheroprone=0.9449±0.3176 fold change) (Figure 5.2E), VCAM-1

(atheroprone=0.8255±0.1620 fold change) (Figure 5.2F) and RelA (atheroprone=1.284±0.3355 fold change) (Figure 5.2G). Interestingly, expression of Interleukin-8 (atheroprone=3.662±1.352 fold change) (Figure 5.2H) and E-selectin (atheroprone=2.946±0.8361 fold change) (Figure 5.2I) was significantly increased under atheroprone flow.

Since E-selectin and IL-8 were up-regulated under atheroprone flow, the effects of P2X4 and P2X7 antagonists were tested on the induction of E-selectin and IL-8. Interestingly, P2X7 antagonism significantly reduced the induction of IL-8 (DMSO=3.662±1.352 vs P2X7i=1.530±0.3494 fold change to atheroprotective) (Figure 5.3Ai) and E-selectin (DMSO=2.946±0.8361 vs P2X7i=1.386±0.4036 fold change to atheroprotective) (Figure 5.3Bi) under atheroprone flow conditions. P2X4 inhibition also impacted the induction of IL-8 (P2X4i=2.329±0.5884 fold change to atheroprotective) (Figure 5.3Aii), but not E-selectin (P2X4i=2.546±0.5372 fold change to atheroprotective) (Figure 5.3Bii)

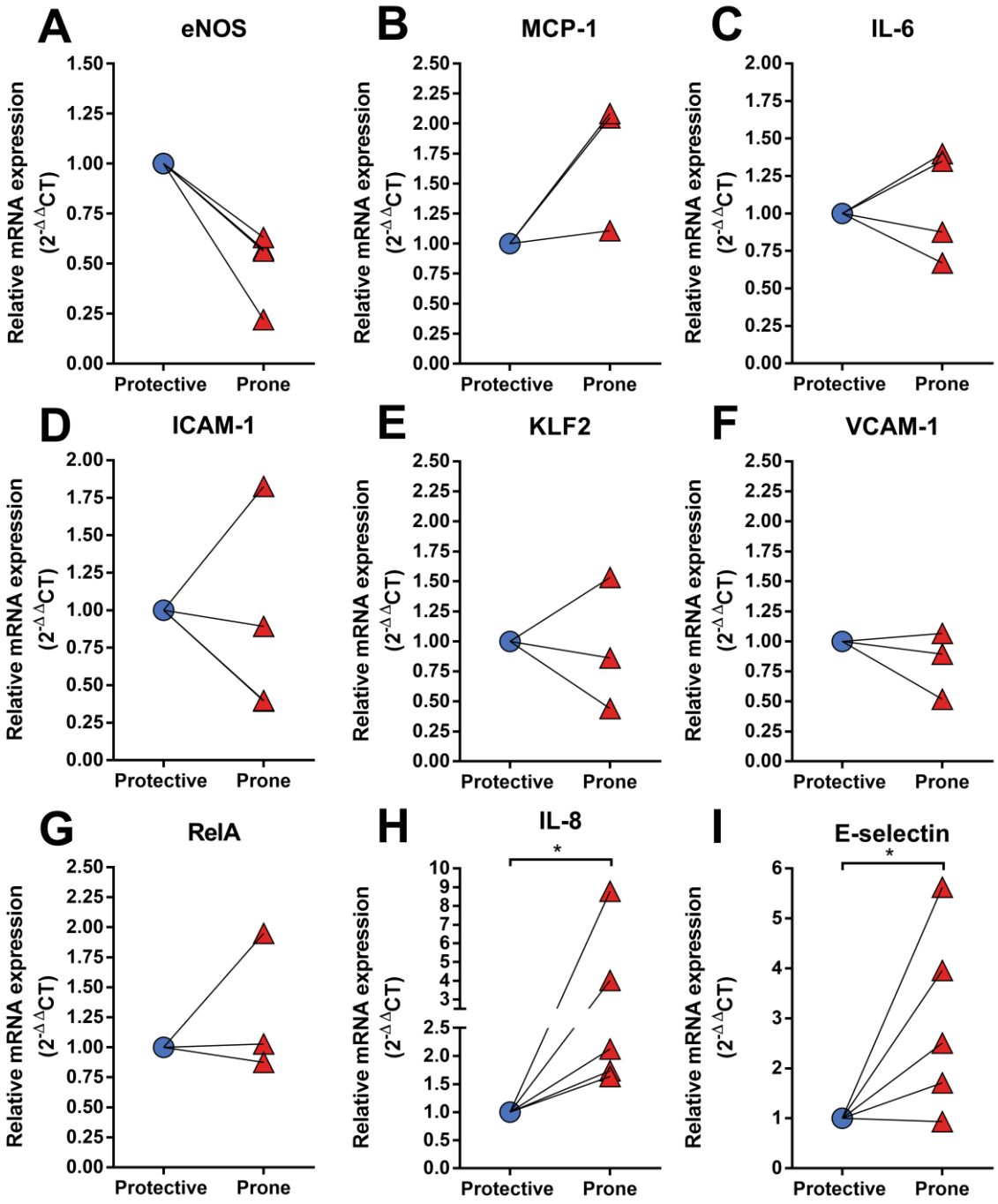

Figure 5.2 – Examining the induction of flow sensitive genes using the ibidi flow system.

qPCR analysis of reported flow sensitive gene expression in HUVEC cultured with the ibidi system for: eNOS (A) (n=4); MCP-1 (B) (n=3); IL-6 (C) (n=4); ICAM-1 (D) (n=3); KLF-2 (E) (n=4); VCAM-1 (F) (n=3); RelA (G) (n=3); IL-8 (H) (n=5); and E-selectin (I) (n=5). Samples were compared for significance using a paired *t*-test. * indicates p=<0.05. Statistical analysis was performed on the ΔCT values.

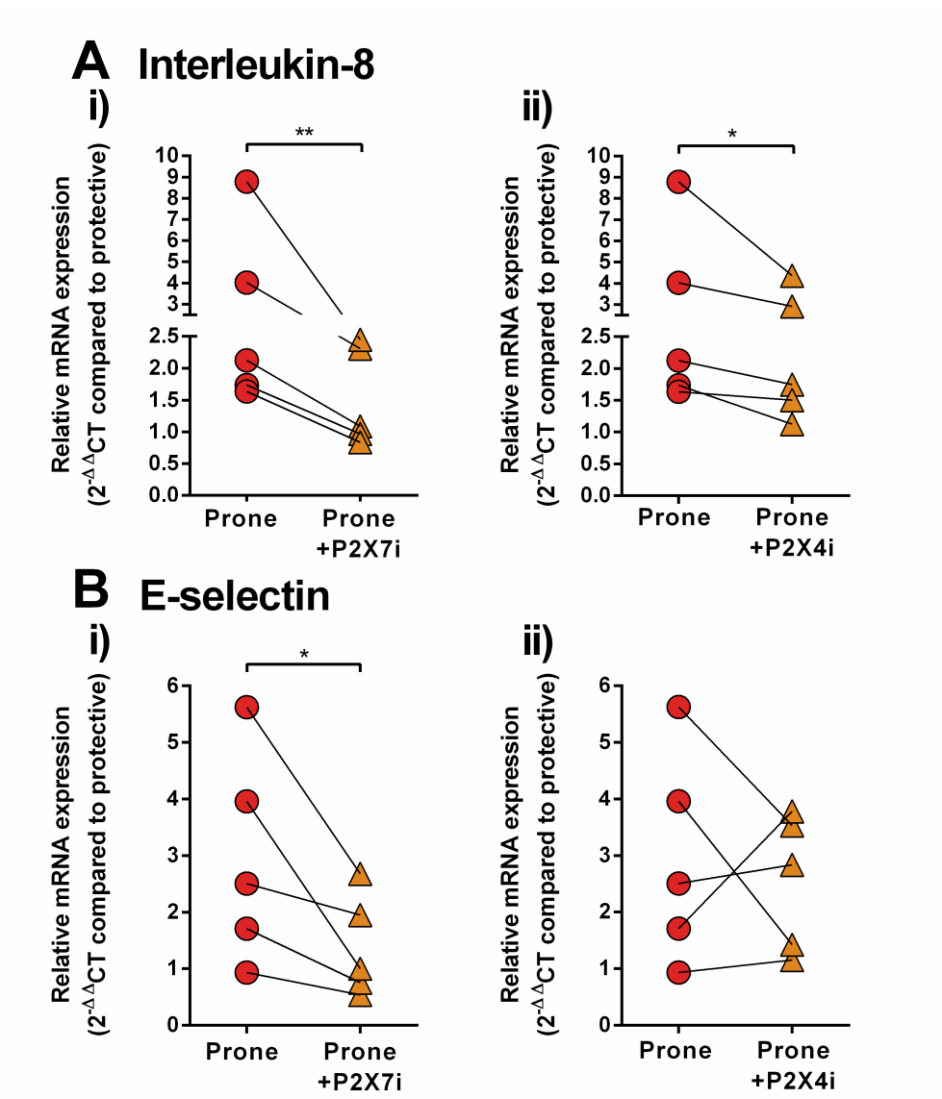

Figure 5.3 – IL-8 and E-selectin induction by atheroprone flow is reduced by P2X7 inhibition.

qPCR analysis of Interleukin-8 (A) and E-selectin (B) in HUVEC cultured under atheroprone flow ± 10μM A438079 (P2X7i) (i) or 10μM PSB-12062 (P2X4i) (ii) (n=5). Statistical analysis was performed on the ΔCT values. * indicates p=<0.05 and ** indicates p=<0.01 using a paired *t*-test.

Since P2X7 and P2X4 inhibition reduced the atheroprone flow induction of IL-8 transcripts, IL-8 secretion was tested by performing an IL-8 ELISA on the cell culture supernatants from these studies. This was possible as the ibidi system cultures a single population of endothelial cells under one flow condition. In agreement with the qPCR analysis, IL-8 release from HUVEC was significantly enhanced under atheroprone flow (atheroprone=1.617±0.09502 fold change) (Figure 5.4A). This increase, was significantly reduced by ~50% by P2X7 inhibition (P2X7i=1.375±0.07074 fold change to protective) (Figure 5.4B), but unaltered by P2X4 antagonism (P2X4i=1.475±0.1253 fold change to protective) (Figure 5.4C). Therefore, despite some inconsistencies in the induction of some atheroprone flow associated genes in the ibidi system, expression of E-selectin and IL-8 was identified as P2X7-dependent under atheroprone flow. Since IL-8 release was attenuated by P2X7 antagonism, the release of other pro-inflammatory cytokines was assessed. However, release of IL-6 (atheroprone=1.029±0.09541 fold change) (Figure 5.5A) and MCP-1 (atheroprone=0.8668±0.09395 fold change) (Figure 5.5B) was unaltered between atheroprotective and atheroprone flow. IL-1α and IL-1β release was examined in ibidi concentrated supernatants. IL-1α release appeared to be higher under atheroprone flow conditions, but was not significant (atheroprone=1.650±0.4868 fold change) (Figure 5.5C). IL-1β release was not detected, as despite concentrating the samples, they were probably still too dilute to detect the low amounts of IL-1β released by HUVEC. However, 17kDa processed active IL-1β was detected in HUVEC lysate which appeared to increase under atheroprone flow conditions (atheroprone=6.046±2.316 fold change) (Figure 5.6), although this was not statistically significant. This suggests that IL-1β mediated signalling may be enhanced under atheroprone flow conditions.

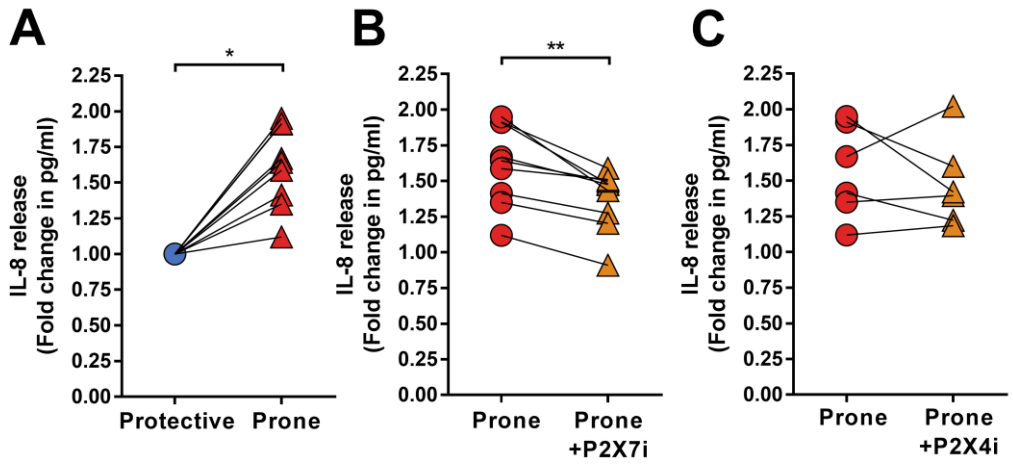

Figure 5.4 – IL-8 release under atheroprone flow is reduced by P2X7 inhibition.

(A) IL-8 protein release detected in the supernatant from HUVEC grown under atheroprotective or atheroprone flow using the ibidi system. Release of IL-8 was examined under atheroprone flow ± 10μM A438079 (P2X7i) (B) (n=9) or ± 10μM PSB-12062 (P2X4i) (C) (n=6). * indicates p=<0.05 and ** indicates p=<0.01 using a paired *t*-test, performed on pg/ml values.

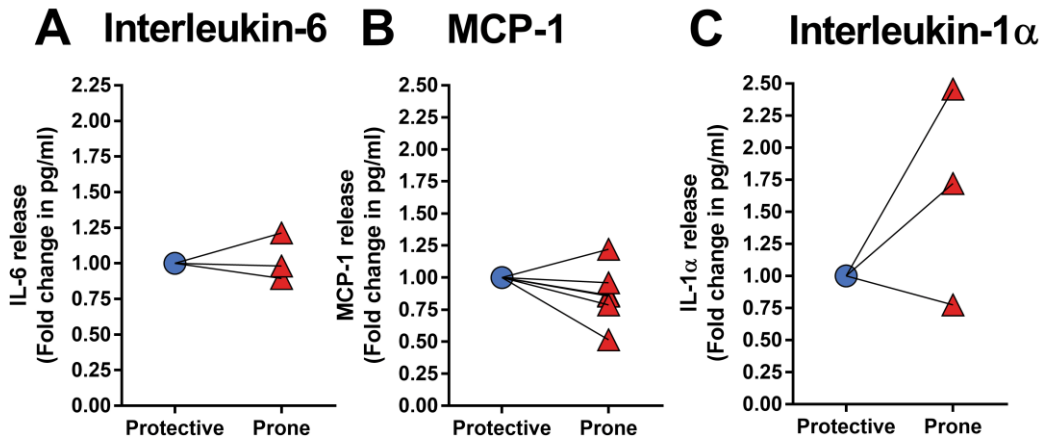

Figure 5.5 - IL-6, MCP-1 and IL-1α release is unaltered between atheroprotective and atheroprone flow in the ibidi pump system.

Release of IL-6 (A), MCP-1 (B) and IL-1α (C) from HUVEC cultured under atheroprotective or atheroprone flow using the ibidi system. Statistical significance was tested using a paired *t*-test, performed on pg/ml values.

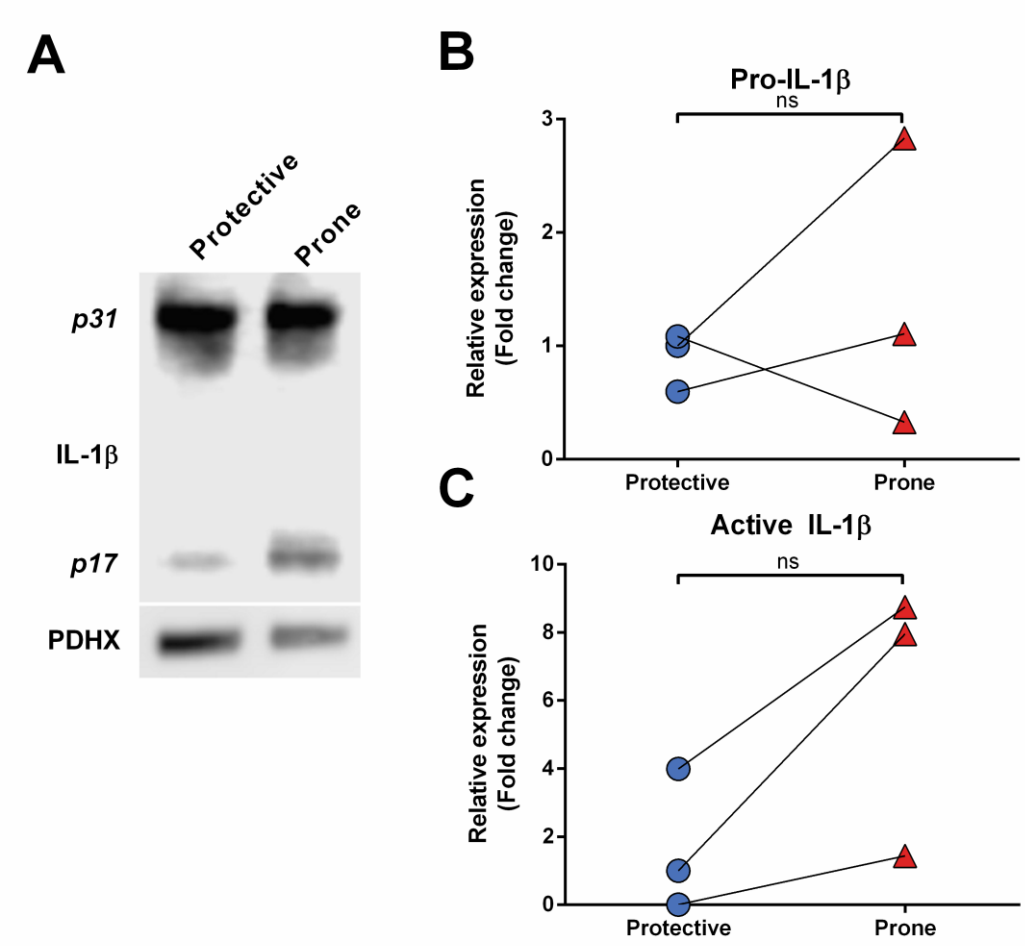

Figure 5.6 – Assessing modulation of IL-1β processing in cells cultured atheroprone flow compared to atheroprotective flow

(A) Representative western blot of IL-1β in flow conditioned HUVEC lysate. Densitometry of pro-IL-1β (p31) (B) and cleaved IL-1β (p17) (C) in HUVEC cultured under atheroprotective or atheroprone flow (n=3). Statistical analysis was tested using a paired *t*-test.

5.5 P2X7 inhibition does not alter Mitogen Activated Protein Kinase or p65 signalling

Since atheroprone flow-mediated induction of interleukin-8 and E-selectin expression were regulated by P2X7, the signalling mechanism responsible for this change in gene expression was tested. MAPK signalling has been shown to be an important pathway regulating inflammatory gene expression under atheroprone flow, including p38 (Zakkar et al. 2008), JNK and NF-κB signalling (Cuhlmann et al. 2011) (Figure1.4) . Activation of P2X7 has been associated with p38, JNK, and NF-κB signalling (Skaper et al. 2010), so the role of P2X7 in the activation of these pathways was assessed using the ibidi and orbital shaker flow systems.

The activity of the p38, ATF2 and c-Jun pathways was assessed by measuring total expression and phosphorylation levels of these proteins. Phosphorylation events activate these proteins; therefore examining phosphorylation levels provide an estimation of the amount of active signalling occuring. Comparing the level of phosphorylation to the total amount expressed, using the ratio of phosphorylated to total p38, ATF2 and c-Jun, determines if changes in these pathways are occuring through acute increases in phosphorylation events or via *de novo* transcription.

Atheroprone flow caused enhanced p38 signalling in cells cultured using the orbital shaker system (Figure 5.7A+C), but not in the ibidi system (Figure 5.7B+D). Levels of phosphorylated p38 were enhanced under atheroprone flow in the orbital shaker system, which was unaltered by P2X7 antagonism (atheroprotective=0.1379±0.03772 vs atheroprone=0.5985; P2X7i atheroprotective=0.1546±0.03183 vs P2X7i atheroprone=0.5551±0.08781). No further significant differences were identified in total p38 levels or the resulting phospho/total p38 ratio in the orbital shaker model, and no changes were identified between flow or P2X7 antagonism in the ibidi system either.

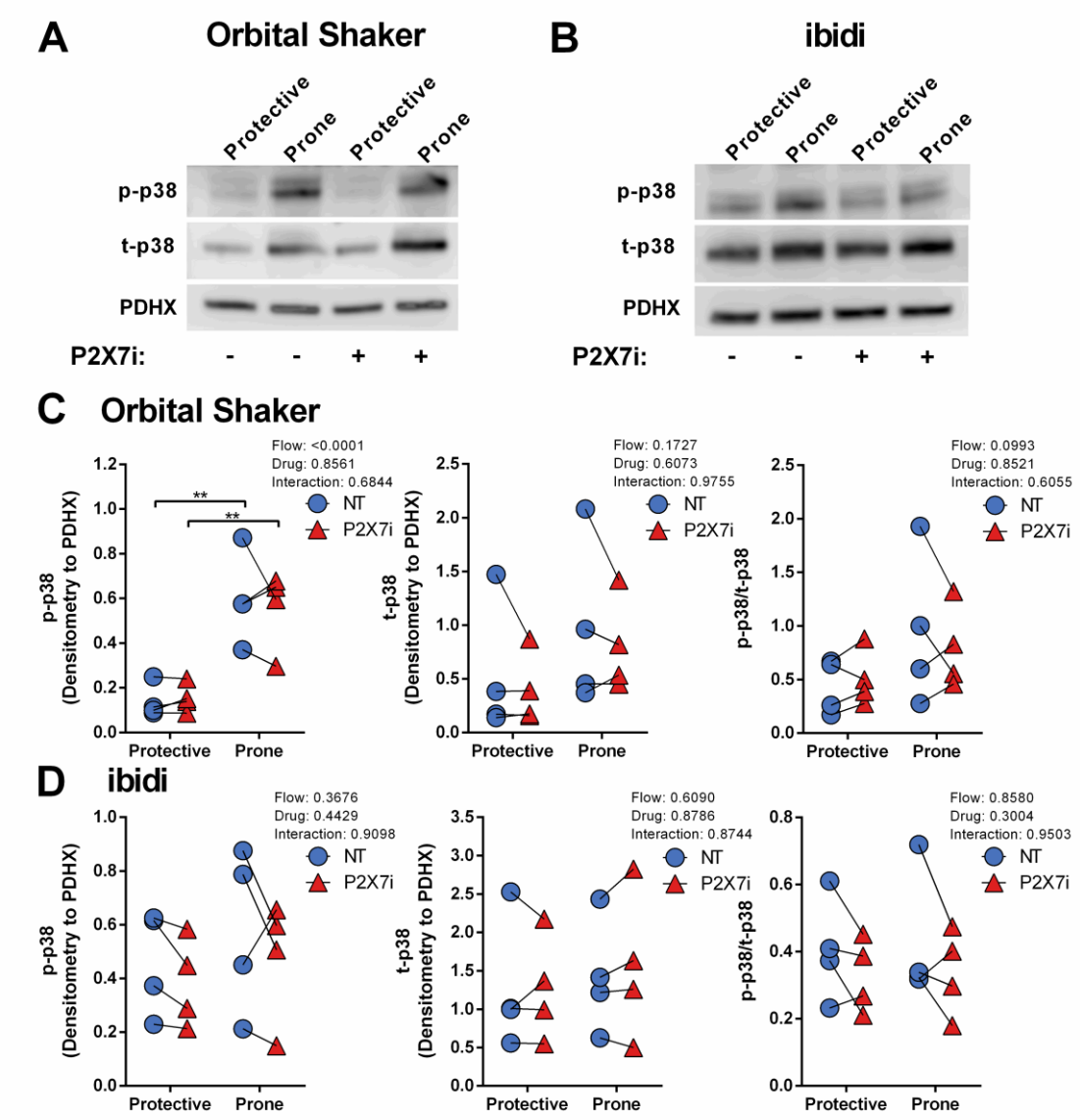

Figure 5.7 – Disturbed flow mediated induction of p38 signalling is unaltered by P2X7 inhibition.

(A) A representative western blot of p38 phosphorylation (p) and total (t) expression in HUVEC cultured using the orbital shaker system ± 10μM A438079 (P2X7i). (B) A representative western blot of p38 phosphorylation (p) and total (t) expression in HUVEC cultured using the ibidi flow system ± 10μM A438079 (P2X7i). (C) Densitometry of phosphorylated p38, total p38 and the ratio of phosphorylated/total p38 (n=4). (D) Densitometry of phosphorylated p38, total p38 and the ratio of phosphorylated/total p38 (n=4). Significance was tested using a two way ANOVA, which is displayed in the corner of each graph. ** indicates p=<0.01 using Sidak's multiple comparisons test.

p38 signalling leads to Activated Transcription Factor 2 (ATF2) activation, resulting in ATF2 phosphorylation; this was moderately increased, but not significantly, in the orbital shaker (atheroprotective=0.2167±0.04331 vs atheroprone=0.3309±0.08390) and the ibidi system (atheroprotective=0.3496±0.04886 vs atheroprone=0.4656±0.08850) under atheroprone flow (Figure 5.8). In addition, phosphorylation of the JNK activated transcription factor c-Jun was significantly enhanced under atheroprone flow in the orbital shaker system, which was not altered by P2X7 antagonism (atheroprotective=0.2720±0.02416 vs atheroprone=0.6839±0.04320; P2X7i atheroprotective=0.2502±0.02685 vs P2X7i atheroprone=0.6469±0.03940) (Figure 5.9A+C). Moreover, total expression of c-Jun was enhanced under atheroprone flow which was unaltered by P2X7 antagonism (atheroprotective=0.1156±0.02800 vs atheroprone=0.3055±0.04118; P2X7i atheroprotective=0.1167±0.03329 vs P2X7i atheroprone=0.3330±0.04396).

However, after exposure of flow and in the presence of a P2X7 antagonist for 72 hours, the ratio of phosphorylation/total expression of these proteins was largely unaffected. This suggests that these differences observed are probably due to an increase in transcription and phosphorylation, resulting in a complete up-regulation in p38 and c-Jun signalling under atheroprone rather than just acute phosphorylation events. However, antagonising P2X7 for the duration of flow conditioning did not significantly alter either the phosphorylation or expression of these proteins under flow, suggesting that the P2X7-mediated effects are not acting via this pathway.

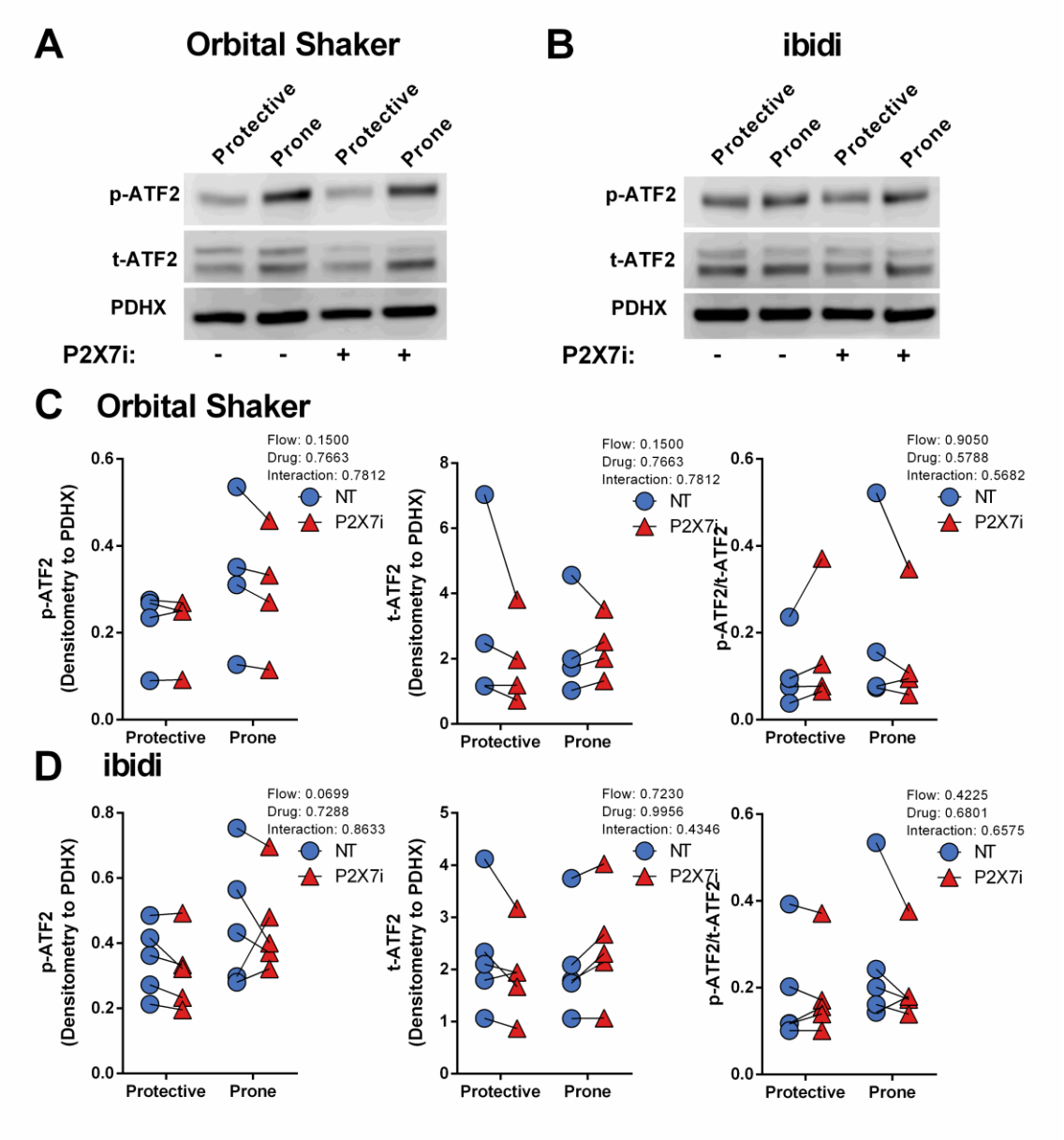

Figure 5.8 – Disturbed flow mediated induction of ATF2 signalling is unaltered by P2X7 inhibition

(A) A representative western blot of ATF2 phosphorylation (p) and total (t) expression in HUVEC cultured using the orbital shaker system ± 10μM A438079 (P2X7i). (B) A representative western blot of ATF2 phosphorylation (p) and total (t) expression in HUVEC cultured using the ibidi flow system ± 10μM A438079 (P2X7i). (C) Densitometry of phosphorylated ATF2, total ATF2 and the ratio of phosphorylated/total ATF2 (n=4). (D) Densitometry of phosphorylated ATF2 , total ATF2 and the ratio of phosphorylated/total ATF2 (n=4). Significance was tested using a two way ANOVA, which is displayed in the corner of each graph.

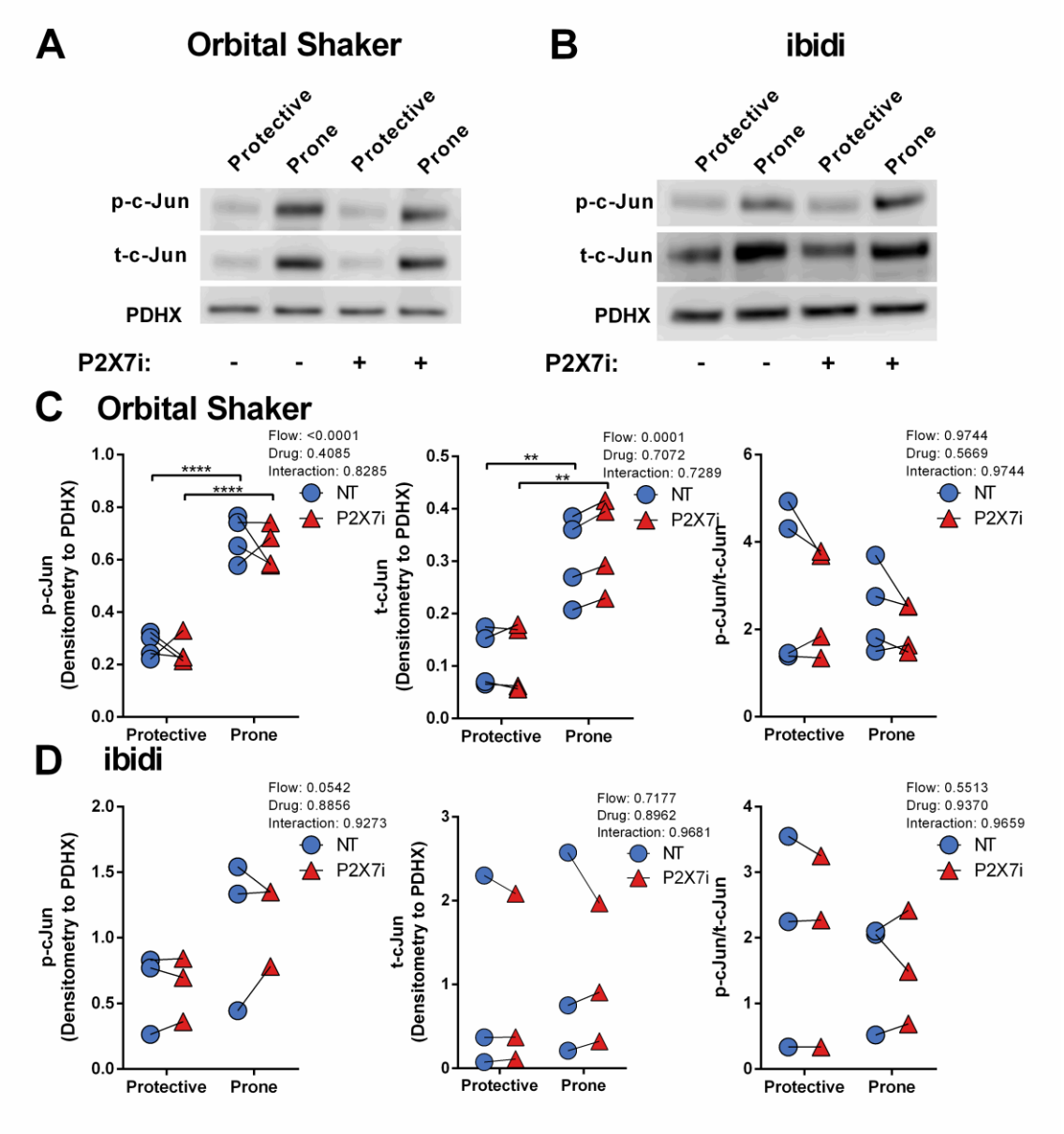

Figure 5.9 – Disturbed flow mediated induction of c-Jun signalling is unaltered by P2X7 inhibition.

(A) A representative western blot of c-Jun phosphorylation (p) and total (t) expression in HUVEC cultured using the orbital shaker system ± 10μM A438079 (P2X7i). (B) A representative western blot of c-Jun phosphorylation (p) and total (t) expression in HUVEC cultured using the ibidi flow system ± 10μM A438079 (P2X7i). (C) Densitometry of phosphorylated c-Jun, total c-Jun and the ratio of phosphorylated/total c-Jun (n=4). (D) Densitometry of phosphorylated c-Jun, total c-Jun and the ratio of phosphorylated/total c-Jun (n=4). Significance was tested using a two way ANOVA, which is displayed in the corner of each graph. ** indicates p=<0.01 and **** indicates p=<0.0001 using Sidak's multiple comparisons test.

p65, the NF-κB subunit encoded by RelA, has also been reported to be induced under atheroprone flow conditions (Van der Heiden et al. 2010). Total expression and phosphorylation (S536) of p65 was up-regulated in the disturbed flow region of the orbital shaker cultured HUVEC (total atheroprotective=0.2458±0.05120 vs total atheroprone=1.205±0.09611; phosphorylated atheroprotective=0.04108±0.01250 vs phosphorylated atheroprone=0.1023±0.006568), which was not modulated in the presence of a P2X7 antagonist (P2X7i total atheroprotective=0.2290± 0.04771, P2X7i total atheroprone=1.071± 0.07545; P2X7i phosphorylated atheroprotective=0.01077± 0.001553, P2X7i phosphorylated atheroprone=0.09011±0.01389) (Figure 5.10A+B). Expression of inhibitor of κB (IκB), a protein that is degraded upon NF-κB activation, was increased under atheroprone flow (atheroprotective=0.04224±0.006854 vs atheroprone=0.07748±0.01570), but unaltered by P2X7 inhibition (P2X7i atheroprotective=0.04474±0.004158, P2X7i atheroprone=0.08663±0.005445) (Figure 5.10A+C). The ratio of phosphorylated p65/total p65 and IκB/p65 was unaltered by P2X7 antagonism in HUVEC under atheroprotective or atheroprone flow.

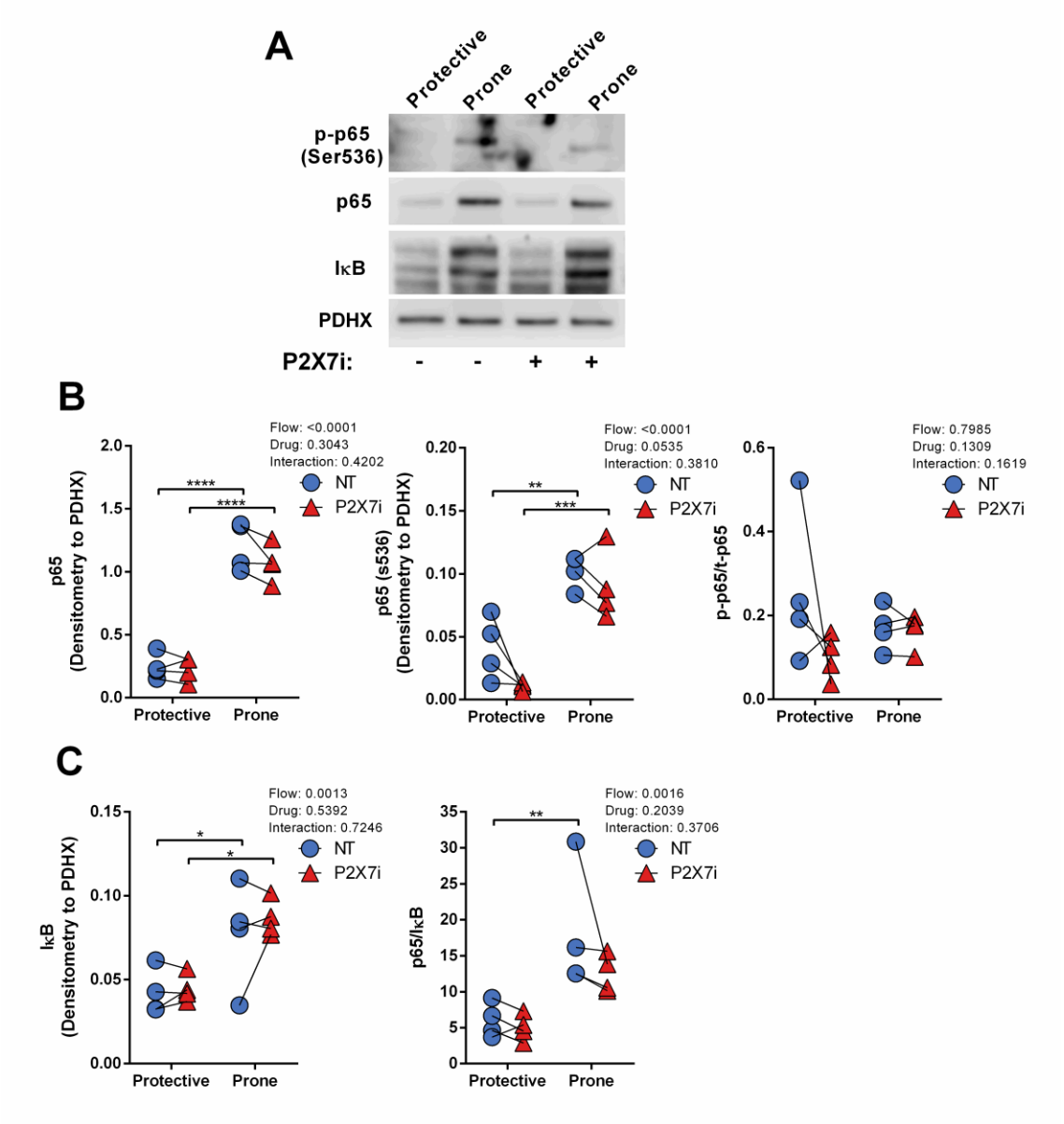

Figure 5.10 – Disturbed flow mediated induction of NF-κB signalling is unaltered by P2X7 inhibition.

(A) Representative western blot of p65 expression, phosphorylation (p) and IκB expression in HUVEC cultured under flow using the orbital shaker system. (B) Densitometry of total and phosphorylated p65 in HUVEC, with resulting p-p65/p65 ratio (n=4). (C) Densitometry of IκB expression in HUVEC, with resulting p65/IκB ratio (n=4). Significance was tested using a two way ANOVA, which is displayed in the corner of each graph.* indicates p=<0.05, ** indicates p=<0.01, *** indicates p=<0.001 and **** indicates p=<0.0001 using Sidak's multiple comparisons test.

5.6 Conclusions

Atheroprone flow induces IL-8 and E-selectin expression through activation of P2X7 receptors. The mechanism responsible for this is independent of MAPK and NF-κB signalling which unaltered by P2X7 antagonism.

5.7 Discussion and future work

The role of P2X7 in inflammatory signalling has been well established in macrophages and evidence for a similar role in endothelial cells is emerging. Recently, the role of P2X7 in atherosclerosis development has begun to be understood; $ApoE^{-/-}$ mice treated with P2X7 siRNA show a reduced atherosclerotic burden (Peng et al. 2015). Despite evidence that endothelial P2X7 is enhanced in the atherosclerotic plaque (Piscopiello et al. 2013; Peng et al. 2015), the role of endothelial P2X7 in this process has been largely overlooked. This chapter provides evidence that endothelial P2X7 could contribute to atherosclerosis initiation by regulating the expression of IL-8 and E-selectin at atherosusceptible sites.

This study is the first to examine the role of atheroprone flow on ATP signalling and subsequent inflammatory responses. No studies to date have examined ATP release or P2 receptor expression in endothelial cells under atheroprone flow conditions, but several have examined the role of cytokines. Application of exogenous inflammatory stimuli to endothelial cells such as TNF/IFNγ (Wilson et al. 2007) or high glucose/palmitate (Sathanoori et al. 2015) have been shown to induce an up-regulation in P2X7 receptor responses, resulting in an enhancement in pro-inflammatory gene expression. Moreover: LPS, TNF, glucose/palmitate, and hypoxia have all been documented to increase extracellular ATP release from endothelial cells (Bodin & Burnstock 1998; Lohman et al. 2015; Lim To et al. 2015; Sathanoori et al. 2015), suggesting a role of extracellular ATP in potentiating endothelial inflammatory responses. Indeed, This study supports these findings since P2X7 antagonism

appeared to reduce the induction of the inflammatory genes VCAM-1 and MCP-1 in TNF/IFNγ stimulated HUVEC.

IL-8 and E-selectin are important proteins that are involved in attracting (Gerszten et al. 1999) and trapping (Chiu et al. 2003) circulating monocytes to the endothelium, a key step in atherosclerosis development. P2X7 antagonism reduced the atheroprone flow driven induction of IL-8 and E-selectin. This study provides the first evidence that ATP induced IL-8 and E-selectin induction in the endothelium may be driven through P2X7 receptor activation. In support of these current findings, application of exogenous ATP has previously been shown to up-regulate E-selectin in porcine aortic endothelial cells, which was proposed to be through P2X7 receptor activation (von Albertini et al. 1998). Moreover, overexpression of the ectoATPase CD39, which also occurs under atheroprotective flow conditions (Figure 3.6.) (Kanthi et al. 2015), reduces ATP induced E-selectin production (Goepfert et al. 2000). Enhanced IL-8 expression and release has been documented to be driven by ATP in endothelial cells (Seiffert et al. 2006), which was also shown to be dependent on P2X7 receptor activation in response to high glucose/palmitate (Sathanoori et al. 2015). In addition IL-8 production was also reported to be a downstream effect of P2X7 activation in human glioma cells (Braganhol et al. 2015), prostate cancer cells (Qiu et al. 2014) and fibroblasts (Montreekachon et al. 2011). Therefore, despite not being a traditionally studied target of P2X7 responses, substantial evidence suggests P2X7 can mediate induction of IL-8 and E-selectin. It must be noted that gene expression changes were only determined in 9 flow responsive genes and therefore endothelial P2X7 may regulate additional novel targets.

Activation of endothelial P2X7 by exposure to high glucose/palmitate has been reported to induce the expression of IL-6, ICAM-1 and VCAM-1 (Sathanoori et al. 2015). These genes have established roles in atherosclerosis (Huber et al. 1999; Kitagawa et al. 2002; Cybulsky et al. 2001) and have been documented to be induced

by atheroprone flow (Chiu et al. 2003; Brooks et al. 2002). However, no change in expression of these genes was observed following P2X7 antagonism in this study. It must be noted that the induction of these genes, at least at the mRNA level using the ibidi pump system, was not observed. The discrepancies in the induction of these genes under atheroprone flow in these experiments compared to published literature could be explained as due to differences in modelling blood flow. As *in vitro* flow systems cannot perfectly mimic *in vivo* conditions, there could potentially be crosstalk with mechanosensors and circulating signalling molecules to fully co-ordinate the intracellular signalling pathways induced by flow. As such, perhaps the ibidi system does not reproduce the physiological conditions required to simulate some of the responses that occur *in vivo* and in other *in vitro* models. Therefore, it is possible that P2X7 could regulate the expression of these genes in circumstances, such as *in vivo* or under inflammatory conditions, where these genes are induced. Evidence to support this is demonstrated in our data where VCAM-1 and MCP-1 induction following TNF/IFNγ stimulation of HUVEC was lower after P2X7 antagonism. This raises the interesting possibility that P2X7 receptor activation alone is not sufficient to induce VCAM-1 and MCP-1, but is necessary for maximal expression following cytokine stimulation; this could also be true for the other inflammatory genes not induced by atheroprone flow alone. As atherosclerosis develops, the endothelium is subjected to increasing inflammatory stimuli which drives the progression of the disease (Libby 2002). Indeed, inflammatory stimuli induces the release of extracellular ATP and as such, atheroprone flow may play a role in priming the endothelium by enhancing P2X7 receptor expression and down-regulating the ATPase CD39. As a result, the combination of atheroprone flow and inflammatory stimuli could potentially lead to enhanced ATP-mediated inflammatory signalling than either alone. A similar priming mechanism is evident in the endothelium associated with NF-κB (p65) signalling. p65 expression is enhanced at atherosusceptible sites compared to atheroprotected sites. (Cuhlmann et al. 2011), which results in greatly augmented inflammatory responses

following cytokine addition (Partridge et al. 2007). Therefore, it seems plausible that other mechanisms of priming may occur, and based on the evidence discussed, this could include ATP-induced inflammatory signalling pathways. This could be tested by investigating the role of P2X7 in pro-inflammatory gene expression in endothelial cells cultured under atheroprone flow in combination with exogenous cytokines and/or their inhibitors.

Previous studies suggest that endothelial P2X7 receptor activation results in up-regulated inflammatory gene expression involving the p38 MAPK pathway (Sathanoori et al. 2015). However in this study, no statistically significant differences were observed in p38, ATF2, c-Jun or p65 signalling due to the presence of P2X7 antagonists under atheroprone flow, indicating that the P2X7 dependence of IL-8 and E-selectin expression are associated with other pathways. However, as these results were collected only for a single time-point, it is possible that the phosphorylation events contributing to these gene expression changes occurred at earlier times than tested. Indeed, in the ibidi system, enhanced p38 activity was not detected, but downstream ATF2 signalling was. Repeating this experiment at several earlier time-points would determine the kinetics of MAPK signalling in these models, and identify if P2X7 is involved in these responses. Baseline levels of p38 and phosphorylated p38 also seemed much higher under atheroprotective flow in the ibidi than the orbital shaker, suggesting that differences in the models may account for differences in p38 signalling. Furthermore, as HUVEC were incubated with the antagonist for 72 hours, it is possible that they could have compensated their response over time. Acute addition of P2X7 inhibitors could potentially reveal a role in these signalling pathways, before any compensation events would be possible. Moreover, stimulation of flow conditioned HUVEC with exogenous ATP may identify if maximal activation of P2X7 receptors triggers further or renewed induction of these pathways

P2X7 activation has been reported to activate other cellular responses which could also explain its role in the induction of IL-8 and E-selectin. P2X7 has been well established to be an activator of the NACHT, LRR and PYD domains-containing protein 3 (NLRP3) inflammasome, which is responsible for processing of the pro-inflammatory cytokines IL-1β and IL-18 (Dubyak 2012). Despite evidence suggesting endothelial cells are not potent producers of IL-1β, they secrete low levels of IL-1β under inflammatory conditions *in vitro* (Wilson et al. 2007). Atheroprone flow has been shown to drive endothelial IL-1β processing (Chen et al. 2011) and expression of the IL-1 receptor (Passerini et al. 2004). Previous work performed in the Wilson lab has demonstrated that endothelial P2X7 activation leads to IL-1β processing in stimulated HUVEC (Wilson et al. 2007). Moreover, endothelial cells have been shown to be a major source of IL-1β in atherosclerotic plaques (Galea et al. 1996). In this work, secreted IL-1β was below the ELISA detection limit in the cell culture supernatant. This could be as a result of the large amount of media required to culture HUVEC using the ibidi system, which would effectively dilute extracellular IL-1β. Since atheroprone flow only promotes a low chronic level of inflammation, it is possible that low levels of IL-1β released locally could contribute towards the pro-inflammatory state of these cells. Intracellularly there was an enhanced cleavage of IL-1β under atheroprone flow, indicating that IL-1β processing took place. Since P2X7 receptor activity is also enhanced, it is plausible that P2X7 activation could evoke IL-1β cleavage and release under atheroprone flow and that IL-8 and E-selectin up-regulation are the downstream effects of IL-1β secretion. Indeed E-selectin and IL-8 expression in HUVEC has been shown to be induced by very low levels of IL-1β (Makó et al. 2010). Interestingly, at these low concentrations, induction of IL-6 and ICAM-1 is absent (Makó et al. 2010), a feature shared with culture of HUVEC under atheroprone flow in the ibidi system. Therefore, this suggests that the large volume of media used in the ibidi pump system could dampen IL-1β signalling, as larger quantities of this cytokine are required for ICAM-1 and IL-6 induction. Furthermore, P2X7 has been reported to influence

endothelial IL-1 receptor signalling *in vivo*; brain endothelial cells up-regulate ICAM-1 through P2X7 mediated IL-1β production in a murine model of sepsis (Wang et al. 2015). Therefore, the potential role of P2X7 induced IL-1β signalling under atheroprone flow could be tested experimentally by culturing endothelial cells in the presence of the naturally occuring IL-1 receptor antagonist (IL-1ra) ± P2X7 inhibitors, which would be hypothesised to block atheroprone flow induced IL-8 and E-selectin. Likewise IL-18, another cytokine processed to its active form following P2X7 receptor activation, evokes endothelial expression of adhesion molecules and cytokines, including E-selectin and IL-8 (Morel et al. 2001; Gerdes et al. 2002). However, despite expressing the IL-18 receptor, endothelial cells do not produce IL-18 cytokines, even under inflammatory conditions (Gerdes et al. 2002). Therefore is unlikely that P2X7 is exerting its effects on E-selectin and IL-8 through IL-18 signalling.

Atheroprone flow also induces net production of reactive oxygen species (ROS) which contributes towards the pro-inflammatory phenotype (Heo et al. 2011). P2X7 has been implicated in ROS generation in other cell types (Kawano et al. 2012) and so this is another pathway requiring further investigation. Nevertheless, despite the mechanism, it is still significant that P2X7 receptors influence the atheroprone flow induction of IL-8 and E-selectin as these proteins play key roles in atherosclerosis initiation (Gerszten et al. 1999) (Chiu et al. 2003).

An important observation is that gene expression and signalling changes in response to flow are much smaller in the ibidi than in the orbital shaker model. This was particularly evident for studies examining p38 activity, where almost no difference was observed between flow conditions in the ibidi system, whereas a marked difference was seen using the orbital shaker system. Moreover, the mRNA expression of several genes that have been well described to be altered between atheroprone and atheroprotective flow conditions were found to not be significantly different using the ibidi system. This could be due to the fact that a proportion of the ibidi slide used to

culture the endothelial cells would be exposed to different shear stress and flow conditions to those set due to the geometry of the slide (Figure 5.11A). Endothelial cells lining the inlet, outlet and edges of the slide will be exposed to a shear stress pattern that varies from that defined, which may result in an inconsistent population of cells influencing the result when the whole population are isolated for mRNA and protein expression analysis. In the calcium imaging studies, recordings were only captured on cells at regions of homogenous shear stress, allowing measurement on cells only under the set flow pattern. However, this selectivity of cells was not possible for qPCR and western blotting analysis as the entire slide of cells was collected. Conversely, HUVEC lysate obtained using the orbital shaker system was collected from defined areas of the well influenced by the desired flow pattern, allowing mRNA and protein analyses on a single population of cells (Figure 5.11B). Alternatively, the different observations between flow systems could be due to differences in the flow patterns produced in the orbital shaker and ibidi system (Figure 2.3). The ibidi system lacks transverse wall shear stress under atheroprone flow and lacks pulsatile flow under atheroprotective conditions, which are both present in the orbital shaker and *in vivo*. Moreover, the orbital shaker cultures endothelial cells under atheroprotective and atheroprone flow in the same media, which does not allow separation of secreted factors across the different flow conditions. Considering this project has focused upon ATP signalling, a factor released by endothelial cells, the ibidi system was used in preference to avoid potential crosstalk of ATP signalling between atheroprotected and atheroprone conditions. Table 5.1 summarises the differences between the ibidi and orbital shaker flow systems which may be responsible for the discrepancies seen in these studies. Ultimately, future *in vivo* studies will overcome the issues obtained from these *in vitro* flow systems; the data obtained from experiments performed using *in vitro* models should however be aware of these limitations.

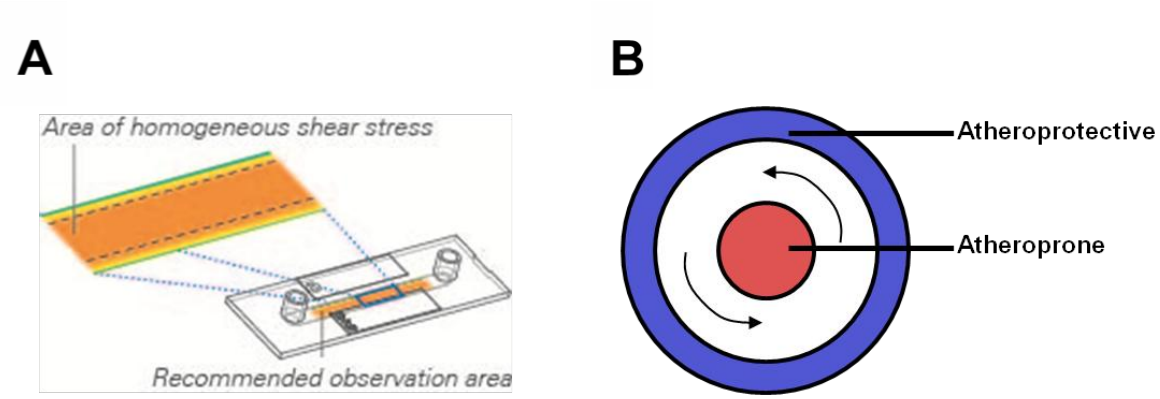

Figure 5.11 – Differences between the ibidi and orbital shaker flow systems could explain the discrepancies in mRNA and protein analyses.

(A) A schematic displaying the area of the ibidi slide influenced by homogenous shear stress. Cells lining the edges of the slide and at the inlet/outlet will not be influenced by the defined shear stress parameters. The entire slide of cells was collected for mRNA and protein analyses. (B) A schematic displaying the regions isolated from a 6 well plate using the orbital shaker system. The periphery and the centre of the well are collected individually, resulting in the collection of discrete cell populations influenced only by the desired flow pattern.

Figure A was supplied courtesy of ibidi.

Ibidi system	Orbital shaker system
Isolation of whole slide only, including cells from areas of undefined shear stresses.	Allows isolation of specific areas of the well, allowing purer isolation of atheroprone and atheroprotected regions.
Extracellular secreted products do not mix between atheroprotective and atheroprone populations.	Extracellular secreted products allow cross-talk between atheroprotective and atheroprone populations.
Atheroprotective flow = constant unidirectional high shear flow.	Atheroprotective flow = pulsatile unidirectional high shear flow.
Atheroprone flow = constant bidirectional low shear flow.	Atheroprone flow = constant multidirectional low shear flow.

Table 5.1 – A summary of the differences between the ibidi and orbital shaker flow systems.

Chapter 6

EMP2 negatively regulates the P2X7 receptor

6.1 Introduction

The previous chapters have demonstrated a role for enhanced endothelial P2X7 receptor activity under atheroprone flow conditions, which subsequently contributed towards inflammatory signalling. Furthermore, P2X7 has well documented roles in mediating inflammation via its activation in several cell types and has been implicated in numerous diseases (Sluyter & Stokes 2011; Skaper et al. 2010), and as such it is an attractive target in the treatment of many chronic inflammatory diseases (Alves et al., 2013).Therefore, identification of mechanisms regulating P2X7 receptor activity is of high therapeutic interest. Previous work from the Wilson laboratory has identified the Growth Arrest-Specific 3 (GAS3) family of proteins interacting directly with the c-terminal tail of P2X7 (Wilson et al., 2002), the region of the protein thought to be responsible for many of the unique P2X7 functions (Costa-Junior et al,. 2011). The GAS3 family consists of Epithelial Membrane Protein (EMP) 1, EMP2, EMP3 and Periphery Myelin Protein 22 (PMP22). EMP2 was found to be the strongest interacting protein of the GAS3 protein family in a yeast two hybrid performed with rat P2X7 c-terminal tail (Wilson et al., 2002). Subsequent unpublished work in the Wilson lab has shown that in HEK-293 cells, heterologously expressed P2X7 functions are enhanced when EMP2 is silenced, suggesting that EMP2 could be a novel regulator of P2X7 and a potential therapeutic target.

P2X7 responses are typically studied in macrophages, due to enhanced expression of P2X7 in these cells and its well documented relationship to activation of NLRP3 and subsequent IL-1β processing (Dubyak 2012). Conversely, endothelial P2X7 receptors remain mostly uncharacterised and as such responses following stimulation of endothelial P2X7 receptors require further investigation. Therefore, a macrophage model was initially employed to study the potential regulatory effects of EMP2 since P2X7 signalling is well characterised in this model. We hypothesise that EMP2

negatively regulates the P2X7 receptor at an endogenous level in macrophages and endothelial cells and can alter subsequent ATP-induced inflammatory signalling.

6.2 Hypothesis

EMP2 regulates P2X7 function in human primary macrophages and plays a role in suppressing endothelial P2X7 responses under atheroprotective flow.

6.3 Aims

1) Optimise EMP2 knockdown in primary human blood monocyte derived macrophages.
2) Examine the role of EMP2 knockdown on P2X7 activity in human macrophages.
3) Determine the expression of GAS3 family proteins in the endothelium under atheroprotective and atheroprone flow.

6.4 Optimisation of EMP2 knockdown in primary human macrophages

Primary human macrophages were decided to be the best model to study the regulatory role of EMP2, since endogenous P2X7 responses are well established in myeloid cells. Initially, EMP2 knockdown was optimised in primary human blood monocyte derived macrophages (MDMs). MDMs are notoriously difficult to transfect without high levels of cell death or activation. However, recently a commercial transfection reagent, Viromer green (Lipocalyx), has become available which exploits the endocytosis entry pathway into cells and as a result has been shown to be very effective on monocyte and macrophage like cells. Therefore, Viromer green was tested to see if it was an effective at silencing EMP2 in MDMs. Initially, MDMs were transfected with a non-targeting small interfering RNA chemically labelled with the fluorescent dye 6-FAM (siGLO) to see if cells effectively took up the siRNA and determine transfection efficiency (Figure 6.1). Every MDM was stained positive for the fluorescent siRNA after transfection, which was shown to be dependent on the Viromer green as intracellular staining was absent when fluorescent siRNA alone was added, highlighting that the macrophages alone are not phagocytosing the siRNA.

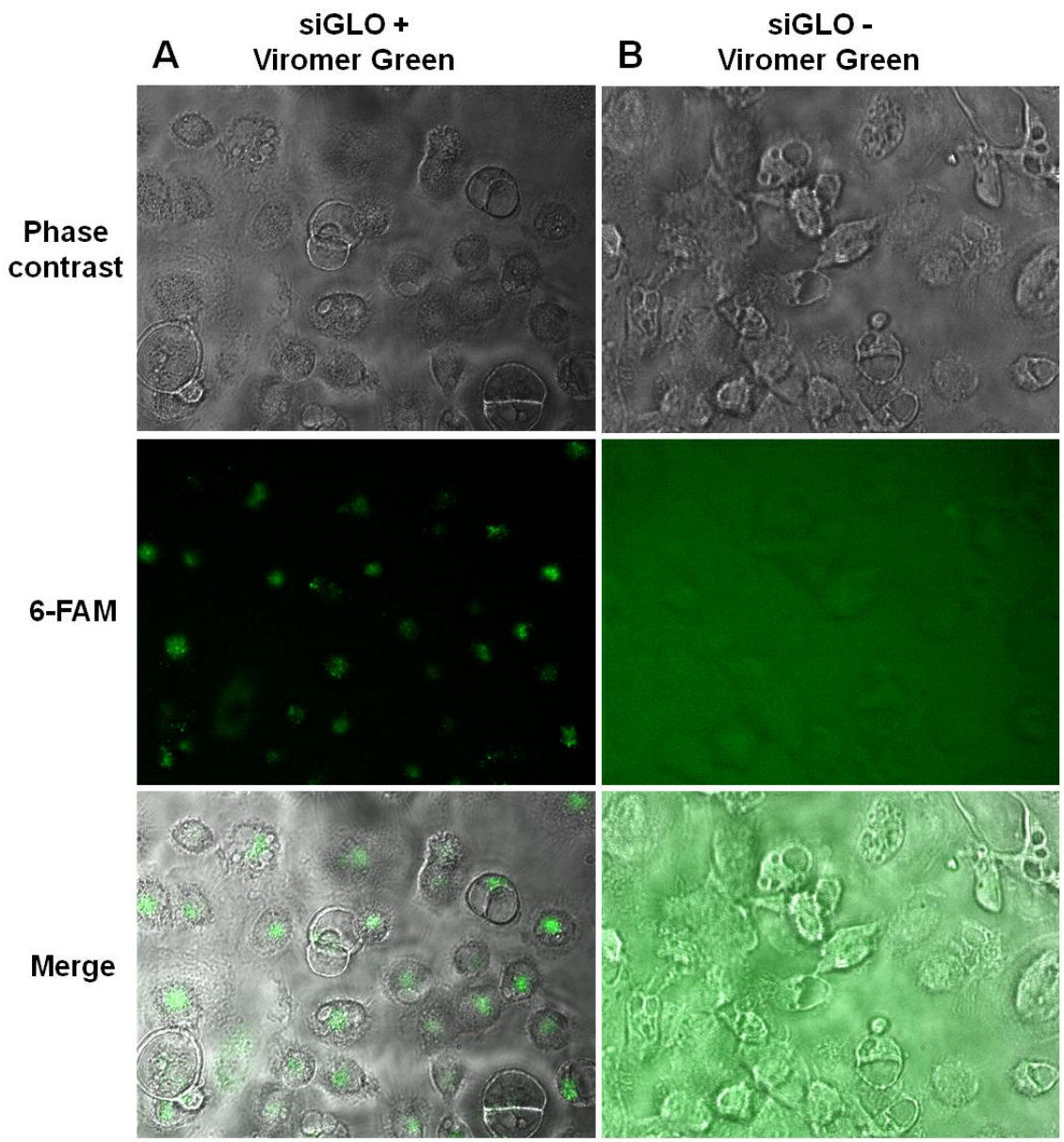

Figure 6.1 – Viromer green efficiently transfects human blood monocyte derived macrophages.

Representative images of human blood monocyte derived macrophages (MDMs) 48 hours after treatment with fluorescent 6-FAM conjugated siRNA (siGLO) packaged in Viromer green particles (A) or alone (B). 6-FAM fluorescence was measured by exposure of MDMs to 488nM. Transfection efficiency was determined to be 100% as every cell imaged was positive (n=2).

As Viromer green was highly efficient at transfecting MDMs, EMP2 knockdown using EMP2 targeting siRNA (siEMP2) or non-targeting siRNA (siNC) was assessed. After 48 hours from transfection, a ~65% reduction in EMP2 mRNA transcript was observed (siEMP2=0.3458±0.04091 fold change) (Figure 6.2). In order to assess EMP2 protein expression following EMP2 knockdown, western blotting for EMP2 was initially optimised. Two commercially available antibodies were tested on HEK-293 cells transiently over-expressing EMP2. This identified the c-terminal targeted EMP2 antibody as a suitable antibody to examine EMP2 expression using western blotting, whereas the human protein atlas (HPA) antibody did not detect EMP2 over-expressed in HEK-293 cells (Figure 6.3A). However, when the c-terminal antibody was used on MDM lysate, several bands appeared which were not reduced in response to knockdown. EMP2 is heavily post-translationally modified with glycans, increasing the molecular weight of EMP2 (Wang et al., 2001). Therefore, N-linked glycans were removed using PNGase-F to identify EMP2, as removal of glycosylated residues would cause a shift in molecular weight. However, despite a shift in heterologously expressed EMP2 in HEK293 lysates, the existing bands in MDMs did not change size following PNGase treatment (Figure 6.3B). Interestingly though, an extra band did appear at around 14kDa (close to the predicted weight of EMP2 at 19kDa) which was reduced after EMP2 knockdown. Quantification of this band from subsequent knockdowns revealed a consistent reduction of ~65% (siEMP2=0.3783±0.02924 fold change) (Figure 6.4), similar to that of EMP2 transcripts. Therefore, this band was considered to be EMP2 as the other bands did not change in response to EMP2 knockdown or shift following deglycosylation treatment. Therefore, at an endogenous level, antibody binding to EMP2 appears to be blocked by glycosylation, but removing N-linked glycans allowed visualisation of EMP2 expression by western blotting. In conclusion, EMP2 could be consistently silenced in MDMs and was subsequently used to assess the role of EMP2 in P2X7 regulation.

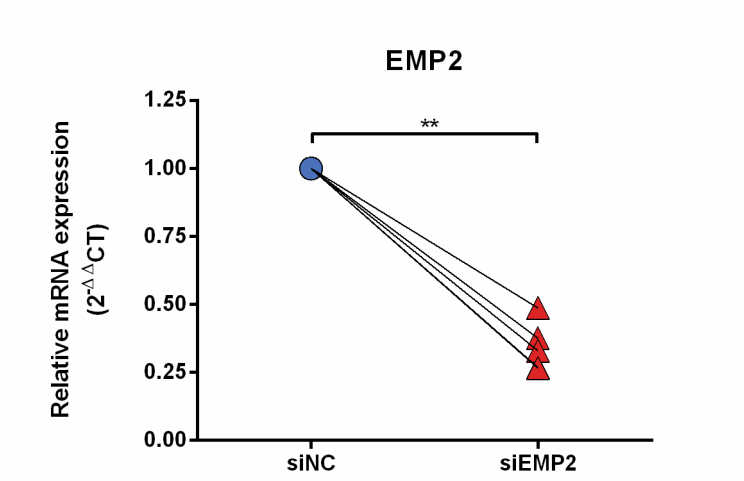

Figure 6.2 – EMP2 mRNA is reduced following EMP2 knockdown.

qPCR analysis of EMP2 in human blood monocyte derived macrophages treated with non-targeting siRNA (siNC) or EMP2 siRNA (siEMP2) (n=5). Expression was normalised to HPRT. Statistics were performed on the ΔCT values. ** indicates p=<0.01 using a paired *t*-test.

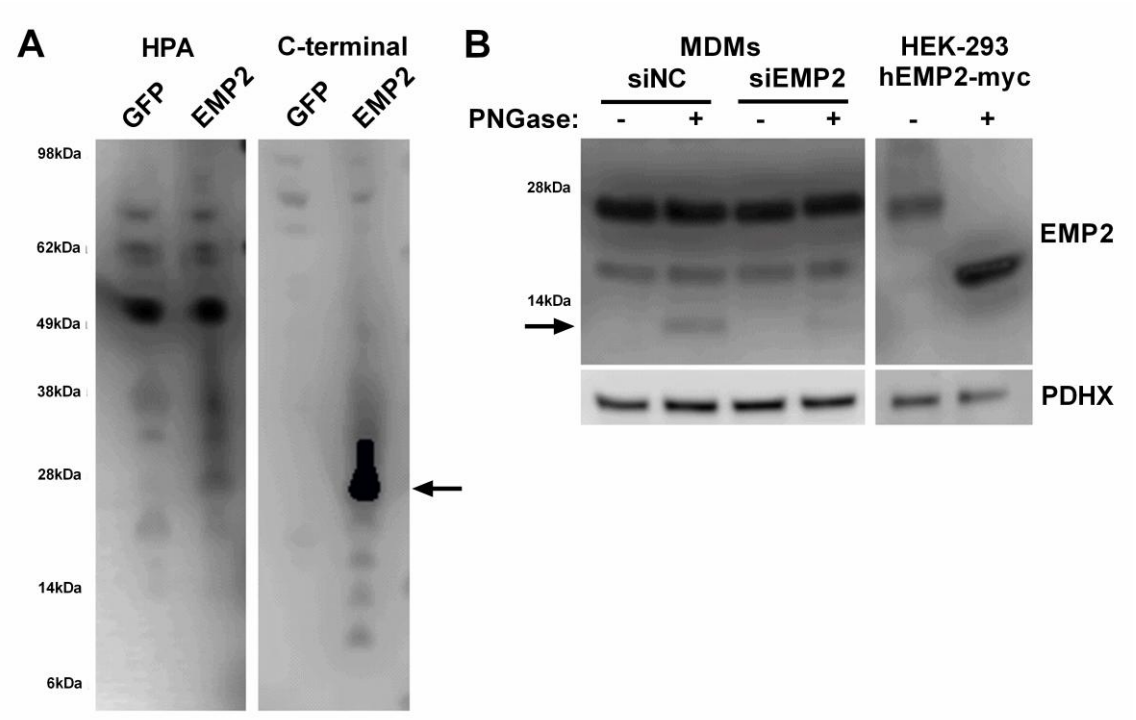

Figure 6.3 – Optimisation of western blotting for EMP2.

(A) Immunoblot for EMP2 on HEK-293 lysate overexpressing GFP or EMP2-myc using two commercially available EMP2 antibodies from the human protein atlas (HPA) or Sigma (C-terminal). (B) Immunoblot for EMP2 using the C-terminal EMP2 antibody on siNC or siEMP2 treated human blood monocyte derived macrophages (MDM) or HEK-293 hEMP2-myc lysates ±PNGase-F. Arrows point to bands proposed to be EMP2.

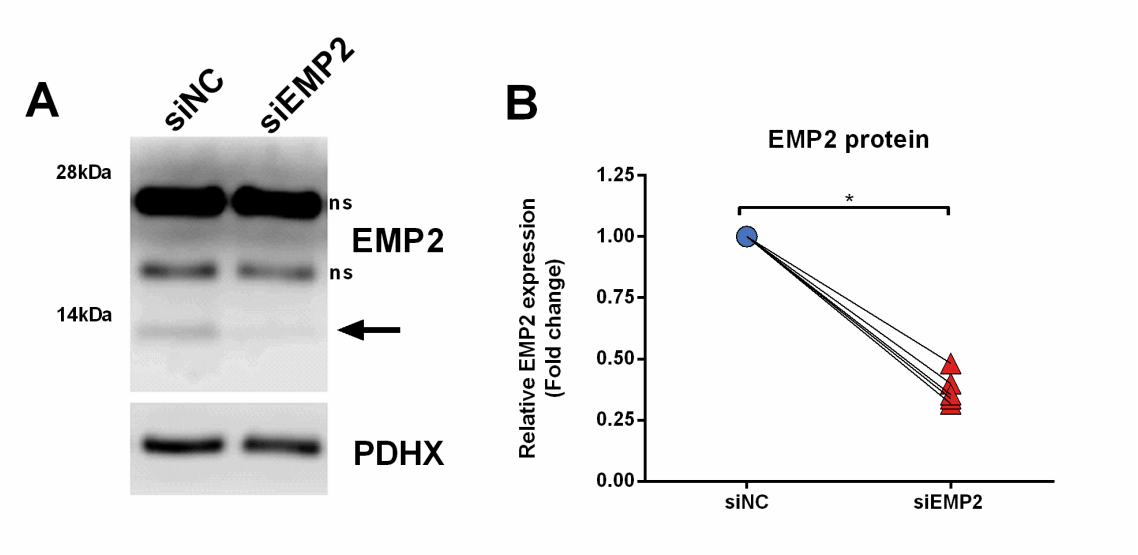

Figure 6.4 – EMP2 protein is reduced following EMP2 knockdown.

(A) Representative western of deglycosylated non-targeting (siNC) or EMP2 (siEMP2) targeted siRNA treated human bMDMs lysates. Arrow represents bands corresponding to EMP2. (B) Fold change in EMP2 protein expression following siNC or siEMP2 treatment (n=5). Statistics were performed on densitometry of EMP2 normalised to GAPDH. * indicates p=<0.05 using a paired *t*-test. The arrow points to the proposed band for EMP2. ns = non-specific bands.

6.5 EMP2 negatively regulates P2X7-mediated calcium responses

As calcium influx is the first step in P2X7 receptor activation, the effect of EMP2 knockdown on live cell calcium imaging responses to 300μM BzATP was initially tested (Figure 6.5). EMP2 knockdown (siEMP2) produced a significantly increased calcium response compared to the non-targeting control (siNC), which was present immediately after BzATP addition and persisted through all time points tested (siNC=82.47±6.256 vs siEMP2=101.8±7.745) (Figure 6.5A). This increase was also revealed by analysing the area under the curve of the BzATP-induced calcium response (siNC=4516±150.9 vs siEMP2=5665±208.9). This enhancement was lost when MDMs were stimulated with BzATP in the presence of the P2X7 antagonist A438079 hydrochloride (siNC+P2X7i=2802±84.67 vs siEMP2+P2X7i=3220±283.0). Therefore, it was concluded that EMP2 negatively regulates P2X7-mediated calcium responses in MDMs.

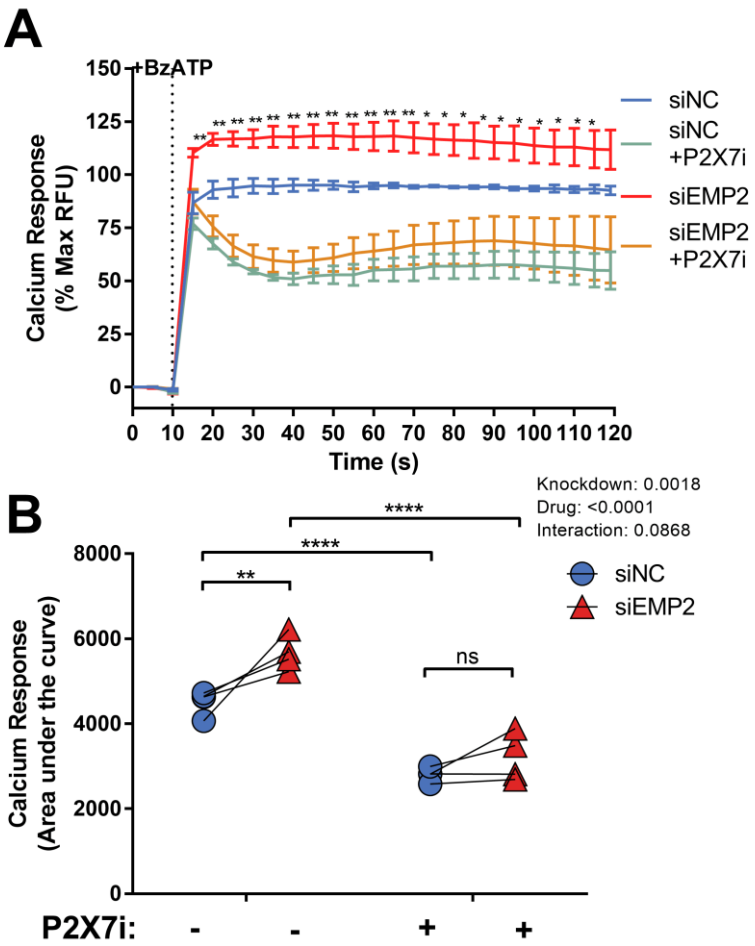

Figure 6.5 – EMP2 knockdown enhances P2X7 mediated calcium influx in human MDMs.

(A) Averaged calcium responses from siNC or siEMP2 transfected human MDMs ± 10μM A438079 (P2X7i) and analysed by measuring the area under the curve (B) (n=4). Responses were normalised to the max response recorded from siNC treated cells. Significance was tested using a two way ANOVA, which is displayed in the corner of B. * indicates p=<0.05, ** indicates p=<0.01 and **** indicates p=<0.0001. Statistical tests in (A) only shown between siNC and siEMP2. Values are ± SEM.

6.6 EMP2 positively regulates P2X7-mediated pore formation

As well as calcium influx, P2X7 activation leads to an increase in cell permeability through formation of a ≈900 dalton pore in the plasma membrane. This pore is large enough for cell membrane impermeable nucleic acid dyes, such as YO-PRO and ethidum bromide, to enter the cell and bind to nucleic acids. Therefore, measurement of nucleic acid dye accumulation in cells over time, following ATP stimulation, provides an effective reporter of P2X7 activation. Moreover, unlike calcium influx, dye uptake in response to ATP is considered P2X7 specific. EMP2 knockdown initially showed no difference in dye uptake kinetics, but was found to be significantly decreased at all time points after 10 minutes of BzATP stimulation (siNC+BzATP= 42.91±8.783 vs siEMP2+BzATP=34.42±7.429) (Figure 6.6A). The total area under the curve was also significantly decreased in EMP2 knockdown (siNC+BzATP=646.2±69.09 vs siEMP2+BzATP=523.7±59.27) (Figure 6.6B). No significant dye uptake was seen in unstimulated cells or in response to BzATP when incubated with the P2X7 antagonist A438079, (siNC+BzATP+P2X7i= 2.359±0.9854; siEMP2+BzATP+P2X7i= 1.491±0.5930) indicating that P2X7 activation was responsible for the dye uptake. In contrast to the increased calcium response, dye uptake was reduced following EMP2 knockdown. Therefore, this suggests that EMP2 has a differential role in regulating P2X7, where some P2X7 responses are positively modulated and some negatively, by EMP2 inhibition.

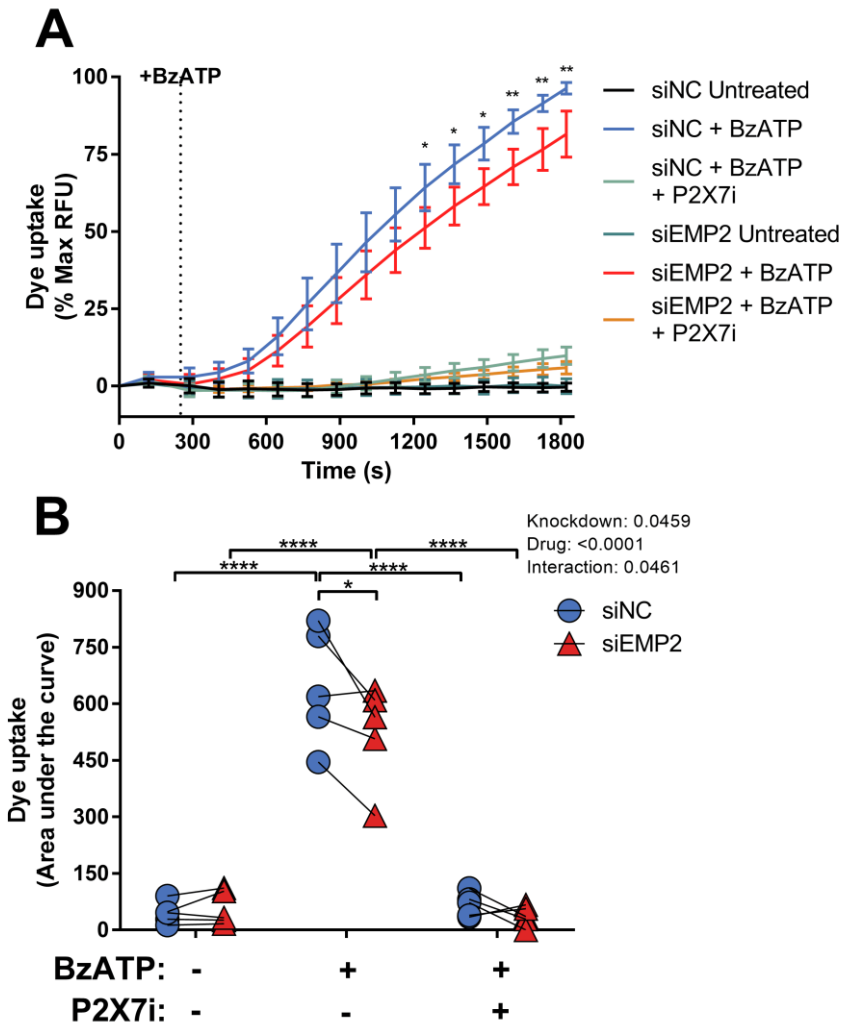

Figure 6.6 – P2X7 mediated small pore formation is reduced following EMP2 knockdown.

(A) Average response of BzATP-induced YO-PRO-1 dye uptake in siNC or siEMP2 treated human MDMs ± 10μM A438079 (P2X7i). Responses were normalised to the max response recorded from siNC treated cells. (B) Area under the curve of the YO-PRO-1 dye uptake response. (n=5). Significance was tested using a two way ANOVA, which is displayed in the corner of B. * indicates p=<0.05, ** indicates p=<0.01 and *** indicates p=<0.001. Statistical tests in (A) only shown between siNC + BzATP and siEMP2 + BzATP. Values are ± SEM.

6.7 Assessment of the role of EMP2 in P2X7-mediated IL-1β release

In monocytic cells, P2X7 receptor stimulation activates the NLRP3 inflammasome, which leads to IL-1β processing and release. Therefore, BzATP-induced IL-1β release was measured in EMP2 silenced human MDMs. These cells were primed by a 3 hour incubation with 1ng/ml LPS followed by a 30 minute stimulation with 300μM BzATP. IL-1β levels in the cell supernatants were then measured by ELISA to determine if IL-1β release is altered with EMP2 knockdown. BzATP treatment induced IL-1β release, which was blocked by pretreatment with the P2X7 antagonist A438079, demonstrating a P2X7 requirement in this response (Figure 6.7A). However, no significant differences were seen between siNC and siEMP2 treated MDMs, but there appeared to be a reduction in IL-1β release in BzATP stimulated MDMs silenced for EMP2 (siEMP2+BzATP=72.82%±11.09). Moreover, LPS alone stimulated MDMs appeared to have an increase in IL-1β release after EMP2 knockdown, but this was also found not to be statistically significant (siNC+LPS=15.52±4.945 vs siEMP2+LPS=43.40±14.86). IL-1β is originally synthesised as an inactive propeptide (p31) which is cleaved to its active form (p17) before release from the cell. In order to see if IL-1β processing or release was altered following EMP2 knockdown, western blotting for IL-1β was performed on MDM lysate following BzATP treatment. Preliminary studies examining this appear to show that cleaved IL-1β levels appear to be higher inside the cell following EMP2 knockdown (Figure 6.7B), suggesting that IL-1β release, and not processing, may be altered. However, these experiments were only performed a limited number of times and did show any statistically significant differences. Nevertheless, these data indicate that EMP2 may alter IL-1β release but require further study.

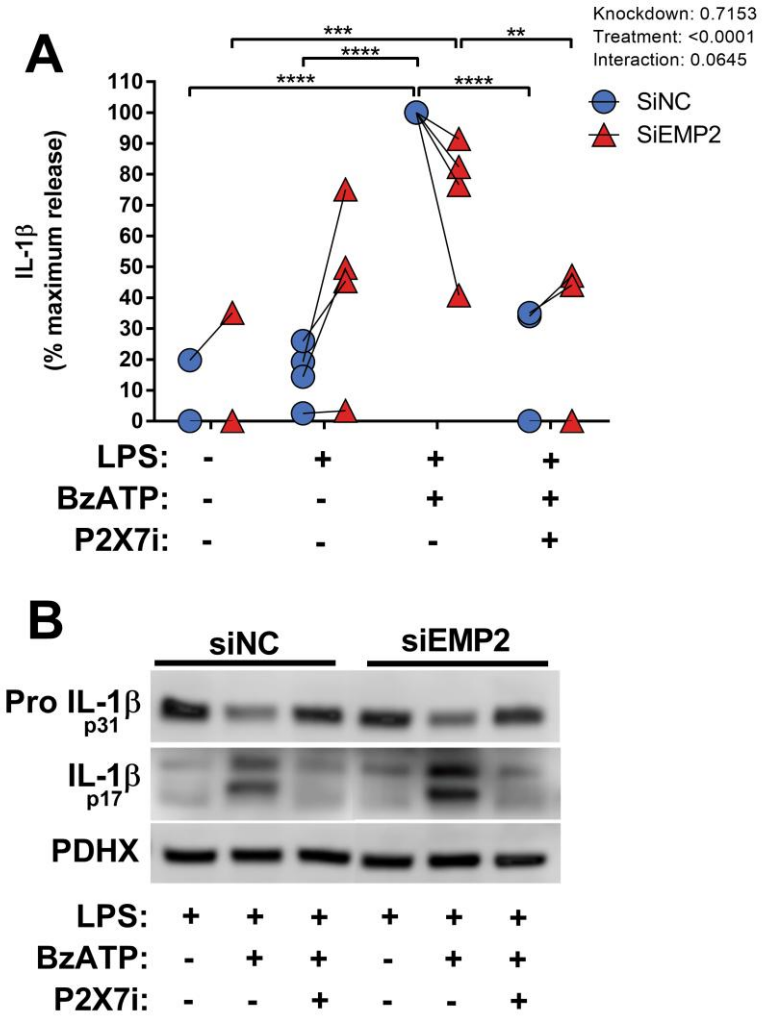

Figure 6.7 – Examining the effect of EMP2 knockdown on P2X7-dependent processing and release of IL-1β.

(A) Measurement of P2X7 dependent IL-1β released into the cell culture supernatant from human siNC or siEMP2 treated MDMs. MDMs were primed with 1ng/ml LPS for 3 hours before stimulation with 300μM BzATP ± 10μM A438079 (P2X7i) (n=4). (B) Representative western blot of IL-1β processing in siNC or siEMP2 treated MDM lysates. Significance was tested using a two way ANOVA, which is displayed in the corner of A. ** indicates p=<0.01, *** indicates p=<0.001 and **** indicates p=<0.0001.

6.8 EMP2 does not alter P2X7 expression within lipid rafts

P2X7 receptor activity is influenced by plasma membrane cholesterol, with P2X7 expressed in lipid rafts exhibiting reduced dye uptake and ion channel activity (Robinson et al., 2014). Downstream P2X7 signalling has also been proposed to be altered between raft and non-raft plasma membrane segments (Garcia-Marcos et al. 2006). P2X7 is thought to be expressed partly in lipid raft rich caveolae through an association with the caveolae structural protein caveolin-1 (Barth et al., 2007, 2008; Gangadharan et al., 2015). EMP2 has been associated with regulating caveolin-1 expression and trafficking (Forbes et al., 2007; Wadehra et al., 2004). Therefore, it was hypothesised that EMP2 could be influencing P2X7 receptor activity by altering caveolae expression of P2X7.

EMP2 differentially regulated P2X7 dependent calcium influx and pore formation. In order to identify mechanisms responsible for EMP2 modulation of these responses, P2X7 receptor expression in lipid rafts was assessed. The ratio of raft and non-raft P2X7 in siNC or siEMP2 transfected MDMs was examined by crudely isolating 1% Triton X-100 soluble (non-raft) and insoluble (raft) lysates (Figure 6.8). Insoluble fragments were assessed by immunoblotting for caveolin-2, a lipid raft marker. Matching the large P2X7 mediated dye uptake and calcium response observed in MDMs, the majority of P2X7 was expressed in Triton X-100 soluble non-raft fractions. However the ratio of soluble to insoluble P2X7 was unaltered by EMP2 knockdown (siNC soluble=82.70%±4.964 vs siEMP2 soluble=84.86%±4.794), suggesting that the regulatory effects of EMP2 are not mediated by altering P2X7 localisation to lipid rafts.

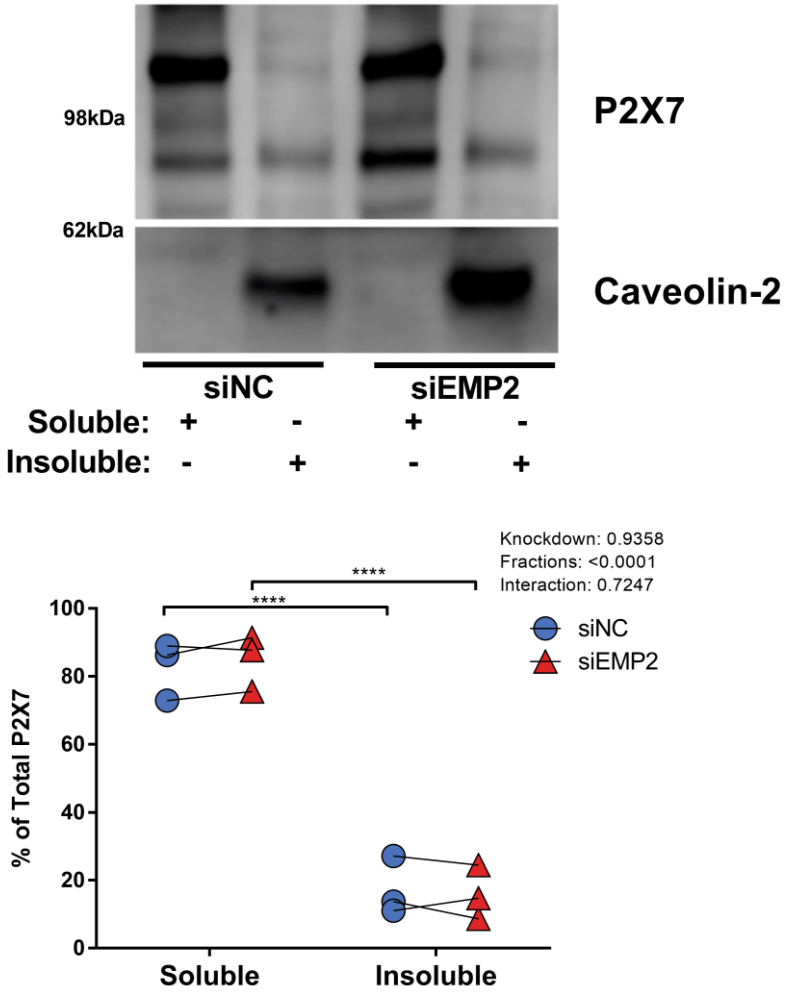

Figure 6.8 – P2X7 trafficking between 1% Triton X-100 soluble and insoluble plasma membrane microdomains is unaltered by EMP2 knockdown.

(A) Representative western blot of P2X7 and caveolin-2 in Triton X-100 soluble and insoluble lysates from siNC or siEMP2 treated MDMs. (B) The percentage of P2X7 expressed in Triton X-100 soluble and insoluble fractions determined from densitometry. Significance was tested using a two way ANOVA, which is displayed in the corner of B. **** indicates p=<0.0001.

6.9 Assessment of EMP2 expression in endothelial cells under flow

The previous chapters demonstrated that P2X7 function was up-regulated in endothelial cells cultured under atheroprone flow conditions. Since EMP2 regulates P2X7 function in MDMs, we hypothesised that EMP2, and other members of the growth arrest-specific 3 (GAS3) family, may be altered in endothelial cells subjected to different flow conditions. Initially, expression of all members of the GAS3 family was examined by qPCR. Expression of EMP2, EMP3 and Peripheral Myelin Protein 22 (PMP22) was significantly enhanced under atheroprotective flow using the orbital shaker system (atheroprone; EMP1=0.5205±0.1761 fold change; EMP2=0.4590± 0.03201 fold change; EMP3=0.3027±0.09343 fold change; PMP22=0.4764±0.08910 fold change) (Figure 6.9), and EMP2 and PMP22 were also significantly enhanced in the ibidi system (atheroprone; EMP1=1.251±0.6151 fold change; EMP2=0.2179± 0.05152 fold change; EMP3=0.5873±0.2277 fold change; PMP22=0.5829±0.0536 fold change) (Figure 6.10). All EMP family members showed a trend towards increased expression under atheroprotective flow conditions, except for EMP1 in the ibidi system. Expression of EMP2 was then examined at the protein level. Similarly to the westerns blots performed on MDMs, deglycosylation with PNGase-F was necessary for clear identification of EMP2 (Figure 6.11A). Moreover, the strongest band in the HUVEC lysate was the same size as the band that appears in MDMs after deglycosylation treatment. In agreement with the qPCR analysis, EMP2 protein expression was enhanced under atheroprotective flow in both the ibidi and orbital shaker flow system (ibidi atheroprotective=1.728±0.2953 vs atheroprone=0.9007±0.2173; orbital atheroprotective=0.5546±0.07913 vs atheroprone=0.2722±0.03572) (Figure 6.11B,C). Therefore, high shear stress induces the expression of EMP family members and may contribute to atheroprotective traits.

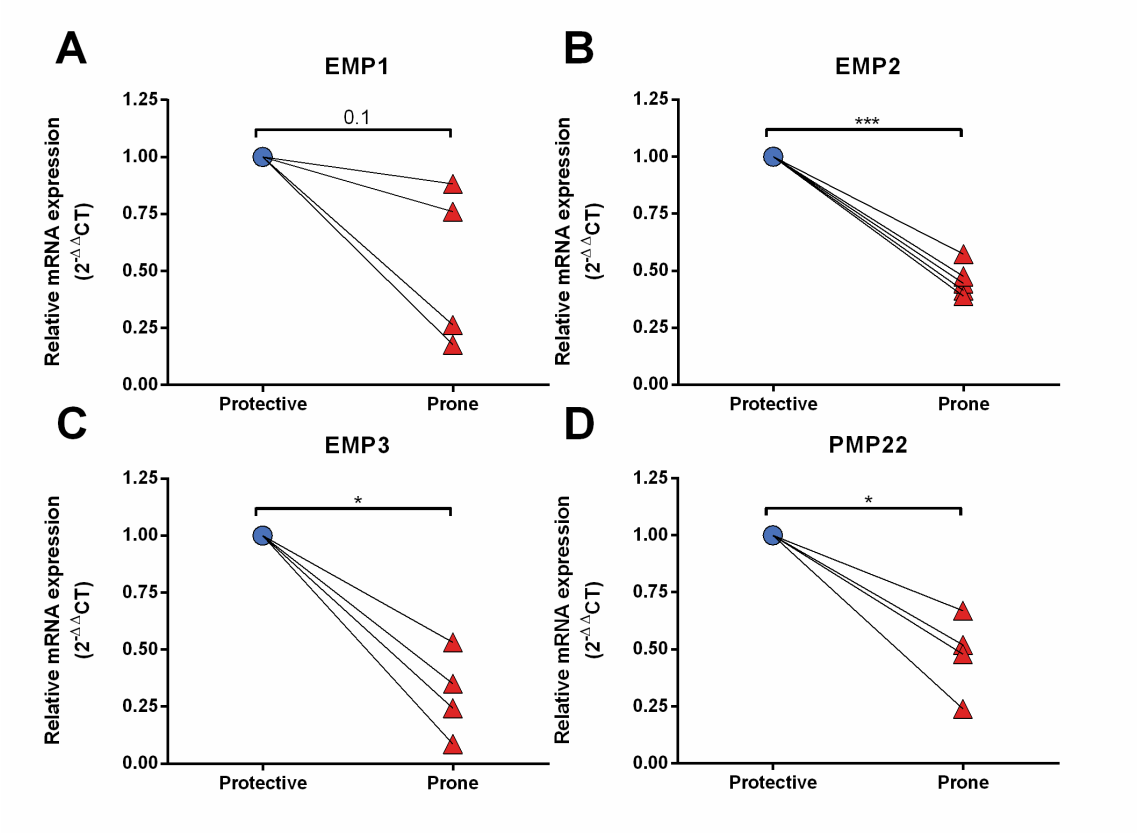

Figure 6.9 – Expression of Growth arrest-specific-3 (GAS3) family proteins in HUVEC from the orbital shaker system of flow.

qPCR analysis of Epithelial Membrane Protein (EMP) 1, EMP2, EMP3 and Peripheral Myelin Protein 22 (PMP22) from the periphery or centre of an orbited 6 well plate. n=4 for EMP1, EMP3 and PMP22, n=5 for EMP2. Statistical analysis was performed on the ΔCT values. * indicates p=<0.05 and *** indicates p=<0.001 using a paired *t*-test.

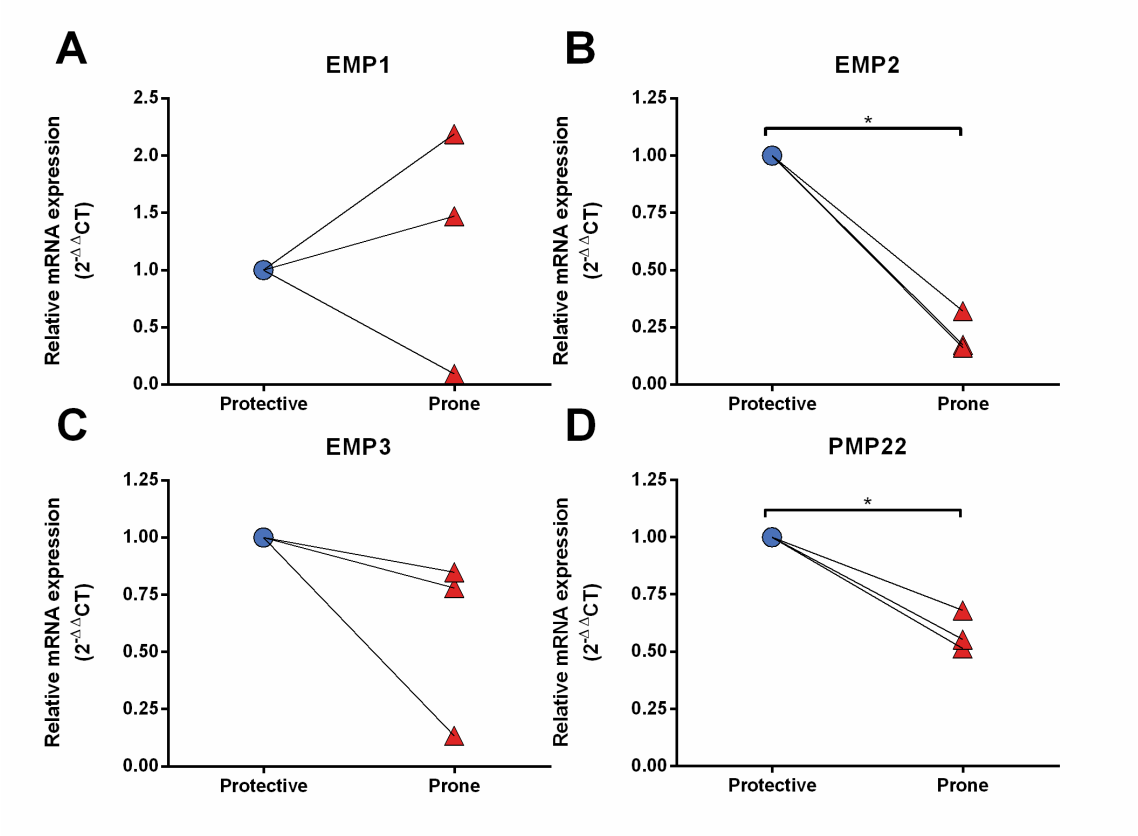

Figure 6.10 – Expression of Growth arrest-specific-3 (GAS3) family proteins in HUVEC from the ibidi system of flow.

qPCR analysis of Epithelial Membrane Protein (EMP) 1, EMP2, EMP3 and Peripheral Myelin Protein 22 (PMP22) from HUVECs cultured using the ibidi system (n=3). Statistical analysis was performed on the ΔCT values. * indicates p=<0.05 using a paired *t*-test.

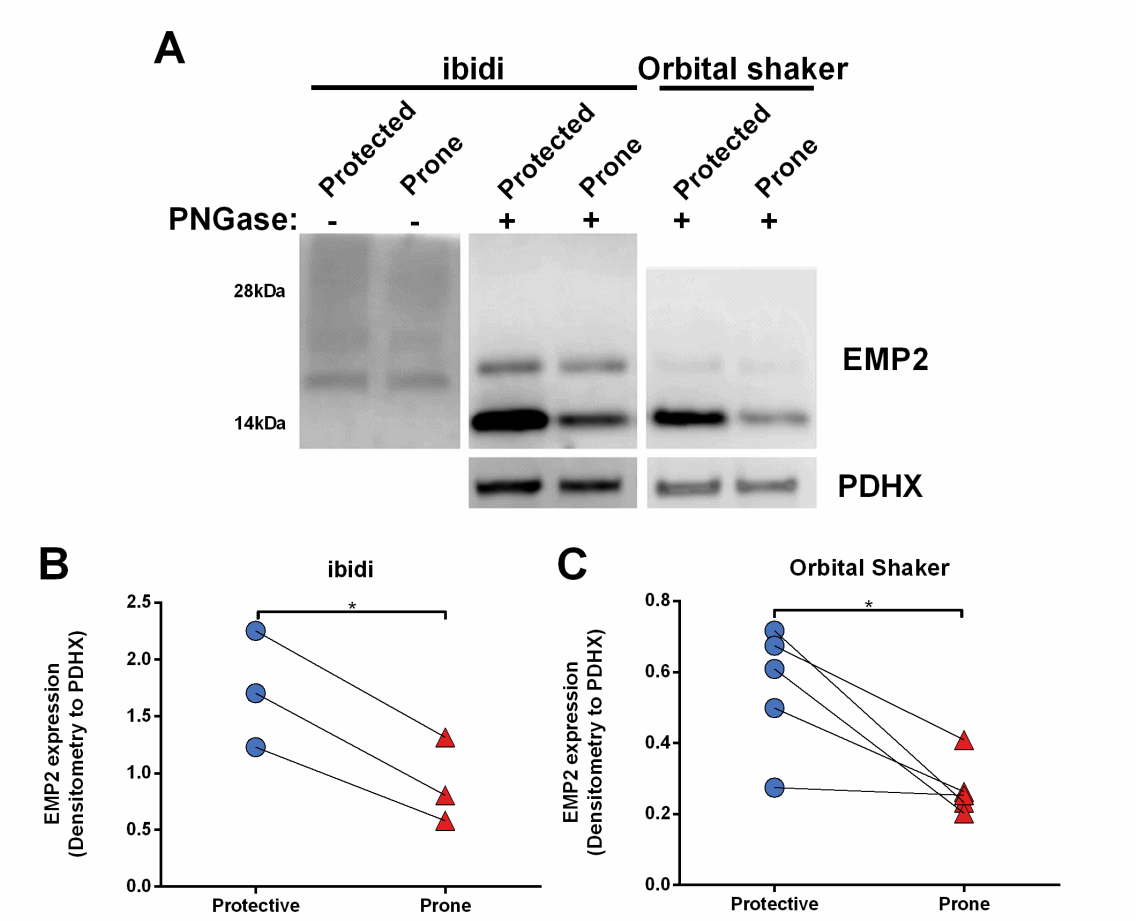

Figure 6.11 – Protein expression of EMP2 in HUVEC is enhanced under atheroprotective flow patterns.

(A) Representative western blot for EMP2 in HUVEC under atheroprotective flow or atheroprone flow using the ibidi or orbital shaker systems. Comparisons between glycosylated and deglycosylated (± PNGase) samples were also performed using samples from the ibidi system. (B) Densitometry of EMP2 expression from the ibidi pump system (n=3) (C) Densitometry of EMP2 expression from the orbital shaker system (n=5). Statistical analysis was performed on the raw densitometry values normalised to PDHX. * indicates p=<0.05 using a paired *t*-test.

6.10 Conclusions

EMP2 has been previously identified by our group as a interacting protein of exogenously expressed rat P2X7 (Wilson et al., 2002). By manipulating endogenous EMP2 levels in human blood monocyte derived macrophages (MDMs), a cell type which expresses high levels of P2X7, a differential regulatory role was identified for EMP2 on P2X7 responses. EMP2 knockdown in human MDMs enhanced P2X7-mediated calcium responses, but slightly decreased pore formation. P2X7 dependent IL-1β processing and release was not significantly altered, following EMP2 knockdown. These differential responses were determined to not be due to altered P2X7 trafficking between lipid rich rafts and non-raft plasma membrane, as P2X7 expression between Triton X-100 soluble and insoluble fractions did not alter with EMP2 knockdown. Moreover, the GAS3 family proteins were also up-regulated in the endothelium when cultured under atheroprotective flow, indicating that they might play a role in the atheroprotective phenotype of endothelial cells.

6.11 Discussion and future work

EMP2 is a relatively poorly characterised protein, with currently only 68 PubMed entries under EMP2, and only one study linking P2X7 and EMP2. However it has been implicated with a range of disease states, particularly cancer, where EMP2 has been identified to regulate the balance between cell apoptosis and proliferation. These data presented here also suggests that EMP2 is also a regulator of ATP-induced P2X7 receptor signalling.

The Wilson group first identified EMP2 interacting with the C-terminal tail of the rat P2X7 receptor (Wilson et al., 2002). In the same study, EMP2 overexpression in HEK-293 cells resulted in uncontrolled cell blebbing and eventual cell death, suggesting EMP2 plays a role in mediating plasma membrane dynamics. Furthermore, unpublished data by our group has also shown that P2X7-dependent blebbing in HEK-

293 cells is almost abolished following EMP2 knockdown. This could also explain the results obtained in MDMs, where P2X7 induced pore formation was reduced following EMP2 knockdown. IL-1β release from human MDMs was also potentially reduced by EMP2 knockdown, but requires further study. As IL-1β release is dependent on P2X7 pore formation and membrane permeabilisation (Marques-da-Silva et al., 2011; Martín-sánchez et al., 2016; Pelegrin & Surprenant, 2006) and is released in part by microvesicles (MacKenzie et al. 2001), it is tempting to speculate that EMP2 knockdown may be altering these mechanisms at the plasma membrane, subsequently modulating IL-1β release. Moreover, P2X7 is a non-selective cation channel and upon activation mediates the influx of Na^+ and Ca^{2+} and the efflux of K^+. P2X7 dependent calcium influx was increased by EMP2 knockdown, suggesting increased ion channel activity. As K+ efflux and not membrane permeabilisation is thought to activate the NLRP3 inflammasome (Munoz-Planillo et al. 2013), it would be interesting to see if EMP2 knockdown enhances P2X7 dependent NLRP3 inflammasome activation and IL-1β cleavage inside the cell. Preliminary studies examining this suggest that cleaved IL-1β levels increase following EMP2 silencing, but requires further repeats. In addition, only a few aspects of P2X7 activation have been studied, with EMP2 involvement of other pathways still unknown, such as cell death, reactive oxygen species generation and mitogen activated protein kinase (MAPK) signalling.

EMP2 has been shown to be a regulator of caveolin-1 expression, a component of lipid rich caveolae. However, we suggest that the effects observed from EMP2 knockdown are not because of changes in P2X7 trafficking between lipid rich raft domains as no differences were seen in P2X7 expression between Triton X-100 soluble and insoluble fractions. In osteoblasts, P2X7 activation leads to internalisation of caveolin-1 (Gangadharan et al. 2015) suggesting stimulation of P2X7 could lead to alterations in plasma membrane microdomains. Therefore raft P2X7 expression could potentially change in response to stimulation and repeating this experiment following ATP

stimulation may provide different results than those obtained here in unstimulated MDMs. EMP2 also regulates the plasma membrane expression of several integrins (Wadehra et al., 2005; Wadehra et al., 2002), and as such, trafficking of P2X7 to the plasma membrane could also be altered. However unpublished data from our lab using the monocytic-like cell line THP-1 indicates that P2X7 surface expression is unaltered by EMP2 knockdown, but this should also be verified in MDMs.

It is also worth noting that expression of the other GAS3 family members was not assessed after EMP2 knockdown and it is possible that compensatory up-regulation of EMP1, EMP3 or PMP22 may mask identifying a role for EMP2 in some processes. Their high level of sequence similarity and shared ability to bind to P2X7 (Wilson et al. 2002) suggests that some functions may be overlapping and gives concern for some level of redundancy. Therefore, expression of all members of the GAS3 family should be examined after EMP2 knockdown. Furthermore, future work should include knockdowns of every GAS3 family member in MDMs to further evaluate their roles in P2X7 regulation. EMP3 in particular is expressed greatly in peripheral blood leukocytes (Taylor & Suter 1996), a precursor of macrophages, and may be an additional regulator of myeloid P2X7. Once their relationship has been fully characterised, *in vivo* studies could then explore therapeutic benefits for modulating EMP family proteins in chronic inflammatory diseases associated with P2X7 dysfunction. However, no EMP2$^{-/-}$ mouse has been currently generated, but inhibitory diabodies against the EMP2 protein have been shown to have efficacy *in vitro* (Morales et al. 2012) and potentially could be used in future *in vivo* studies.

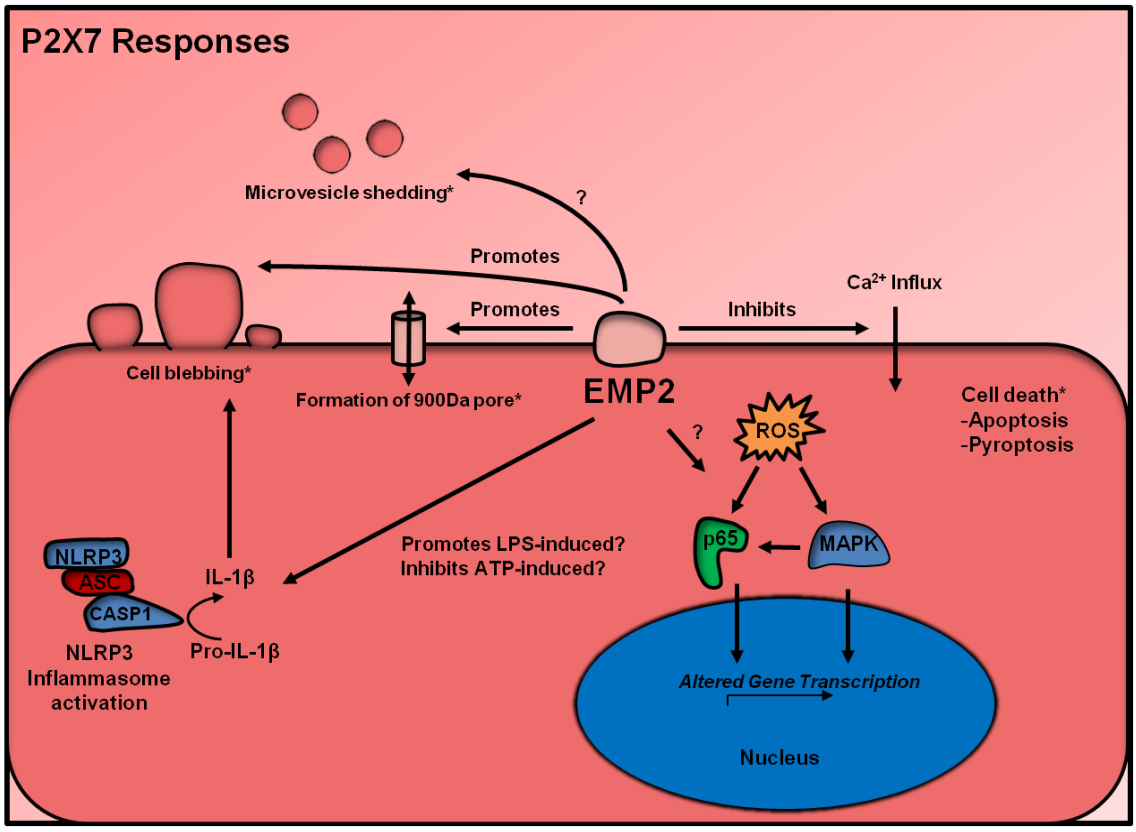

Figure 6.12 – A schematic describing the identified roles of EMP2 on P2X7 responses.

EMP2 differentially modulates P2X7-induced cellular responses. In HEK-293 cells, EMP2 modulated P2X7 mediated cell blebbing. In human monocyte derived macrophages, EMP2 negatively regulated ATP-induced calcium influx, but promoted P2X7-pore formation. EMP2 did not significantly alter IL-1β processing and release in this study, but further investigation is required. The role of EMP2 on P2X7-mediated ROS, NF-κB, MAPK signalling, microvesicle shedding and cell death is also currently unknown and requires further investigation.

This brief study of EMP2 in the endothelium revealed that the GAS3 family proteins are up-regulated under atheroprotective flow conditions. Interestingly, EMP2 was also identified as a shear sensitive target in an RNA-Seq dataset performed by Hanjoong Jo's lab (Ni et al. 2010), with a 50% down-regulation in endothelial EMP2 transcripts after partial carotid ligation, which generates atheroprone flow along the entire carotid artery *in vivo*. Therefore EMP2 may well be regulating endothelial cell signalling in response to shear stress. EMP2 regulates caveolin-1 (Wadehra et al. 2004; Forbes et al. 2007; Wan et al. 2016) and integrins (Wadehra et al., 2002, 2005) which are both considered as mechanosensitive pathways in endothelial cells (Yu et al. 2006; Shyy & Chien 2002). EMP2 knockdown in HUVEC up-regulates caveolin-1 expression (Gee et al. 2014) and caveolin-1 expression has also been reported to increase under atheroprone flow (Fu et al. 2011; Qin et al. 2016), which correlates with the decrease in EMP2 expression observed in this work. Therefore, the role endothelial EMP2 plays in endothelial signalling associated with mechano-sensing should be further investigated. Endothelial EMP2 can be efficiently knocked down by siRNA (data not shown); since EMP2 expression is augmented under atheroprotective flow conditions, atheroprotective signalling pathways should be studied, such as Akt and Erk signalling leading to eNOS generation, as these have been shown to be caveolin-1 dependent (van der Meer et al., 2009). Furthermore, the previous chapters also describe an enhancement in P2X7 receptor activity under atheroprone flow, the flow condition which decreases EMP2 expression. As EMP2 regulates P2X7 in MDMs, it is tempting to speculate that the decreased P2X7 signalling under atheroprotective flow could be controlled in part by enhanced EMP2 expression. It will be interesting to determine whether EMP2 silencing in endothelial cells cultured under atheroprotective flow results in increased P2X7 activity.

In summary, at an endogenous level in human macrophages, EMP2 regulates aspects of P2X7 signalling. The impact of this in physiology and disease should be studied further in an attempt to identify novel therapeutics.

Chapter 7

General Discussion

Extracellular ATP has been well established for its role in mediating vasodilation and atheroprotection of the vasculature. However, accumulating evidence points to a role for extracellular ATP in mediating endothelial inflammation (Figure 1.7). Several recent studies propose that regulation of extracellular ATP is altered at sites of the arterial tree, with regions influenced by atheroprone flow exhibiting ATP dysregulation (Kanthi et al. 2015; Fu et al. 2011). Endothelial cells at sites of the vasculature influenced by atheroprone flow also present a pro-inflammatory phenotype (Warboys et al. 2011; Chiu & Chien 2011). Therefore this study tested the hypothesis that ATP signalling was altered in endothelial cells at atherosusceptible regions and contributes towards their pro-inflammatory state. Atheroprone flow was found to enhance endothelial calcium responses to ATP through an increase in extracellular calcium influx and a decrease in CD39-mediated ATPase activity. Further experiments identified an up-regulation in the surface expression of the ATP-gated P2X7 ion channels under atheroprone flow conditions, which were found to be responsible for this calcium influx. Furthermore, inhibition of P2X7 resulted in a reduction in atheroprone flow-mediated inflammatory gene expression, specifically IL-8 and E-selectin. The hypothesis is therefore supported and provides a basis for further investigation into the role of extracellular ATP and endothelial P2X7 receptors in atherosclerosis initiation using a $P2X7^{-/-}$ murine model.

7.1 Main conclusions

- Endothelial cells influenced by atheroprone flow were more responsive to ATP stimulation, exhibiting larger calcium responses than those conditioned under atheroprotective flow. Enhanced CD39 activity was found to be partly responsible for the reduced calcium response under atheroprotective flow.
- Extracellular calcium influx in response to ATP was present only in atheroprone flow conditioned HUVEC and was found to be mediated by ATP-gated P2X7 ion channels.
- P2X7 receptor expression was enhanced under atheroprone flow conditions *in vitro* and was responsible for atheroprone flow mediated IL-8 and E-selectin induction. Endothelial P2X7 receptor expression was also found to be enhanced at the cell surface at atherosusceptible regions of the murine aorta.

7.2 ATP signalling is altered at sites of atheroprone flow

Existing literature has already extensively described the role of ATP signalling regulating nitric oxide production following acute atheroprotective flow; this study aimed to investigate the role of ATP in inflammatory signalling under atheroprone flow. The data obtained in this study has determined that ATP signalling is altered between endothelial cells influenced by atheroprotective or atheroprone flow patterns. As a result, a model of ATP signalling in endothelial cells under these flow patterns can be proposed (Figure 7.1). Shear stress induces the extracellular release of ATP, which activates nearby purinergic receptors. Under atheroprotective flow conditions these receptors include P2Y2 (Wang et al. 2015; Wang et al. 2016; Sathanoori et al. 2016) and P2X4 (Yamamoto et al. 2003; Sathanoori et al. 2015), their activation resulting in eNOS activity and nitric oxide (NO) production. Extracellular ATP is tightly regulated by the ectonucleotidases CD39 (Figure 3.6; Kanthi et al. 2015) and CD73 (Li et al. 2010), limiting concentrations of ATP and preventing inflammation associated with ATP signalling (Goepfert et al. 2000). Furthermore, adenosine generated from ATP

hydrolysis can activate A_2 receptors (Hein & Kuo 1999; Sobrevia et al. 1997; Ohta et al. 2013) further enhancing NO production. This strict regulation of extracellular ATP is attenuated under atheroprone flow conditions due to diminished expression of CD39 (Figure 3.6; Kanthi et al. 2015), suggesting that ATP accumulates extracellularly. Cell surface expression of the P2X7 receptor is enhanced and is subsequently activated by atheroprone flow to promote the expression of IL-8 and E-selectin, facilitating leukocyte recruitment. The mechanism preceding this gene expression change is currently unknown, but likely candidates are through direct activation of NF-κB (p65) or MAPK (p38, JNK) signalling, or indirectly through reactive oxygen species (ROS) generation or NLRP3 activation and subsequent IL-1β signalling. Furthermore, P2X7-mediated inflammatory signalling may be further inhibited under atheroprotective flow due to increased expression of negative regulators such as EMP2 and alternatively spliced P2X7 variants. Therefore, targeting this dysregulation of ATP signalling at sites of atheroprone flow conditions may provide a novel therapeutic approach for the development of preventative medicines against atherosclerosis development.

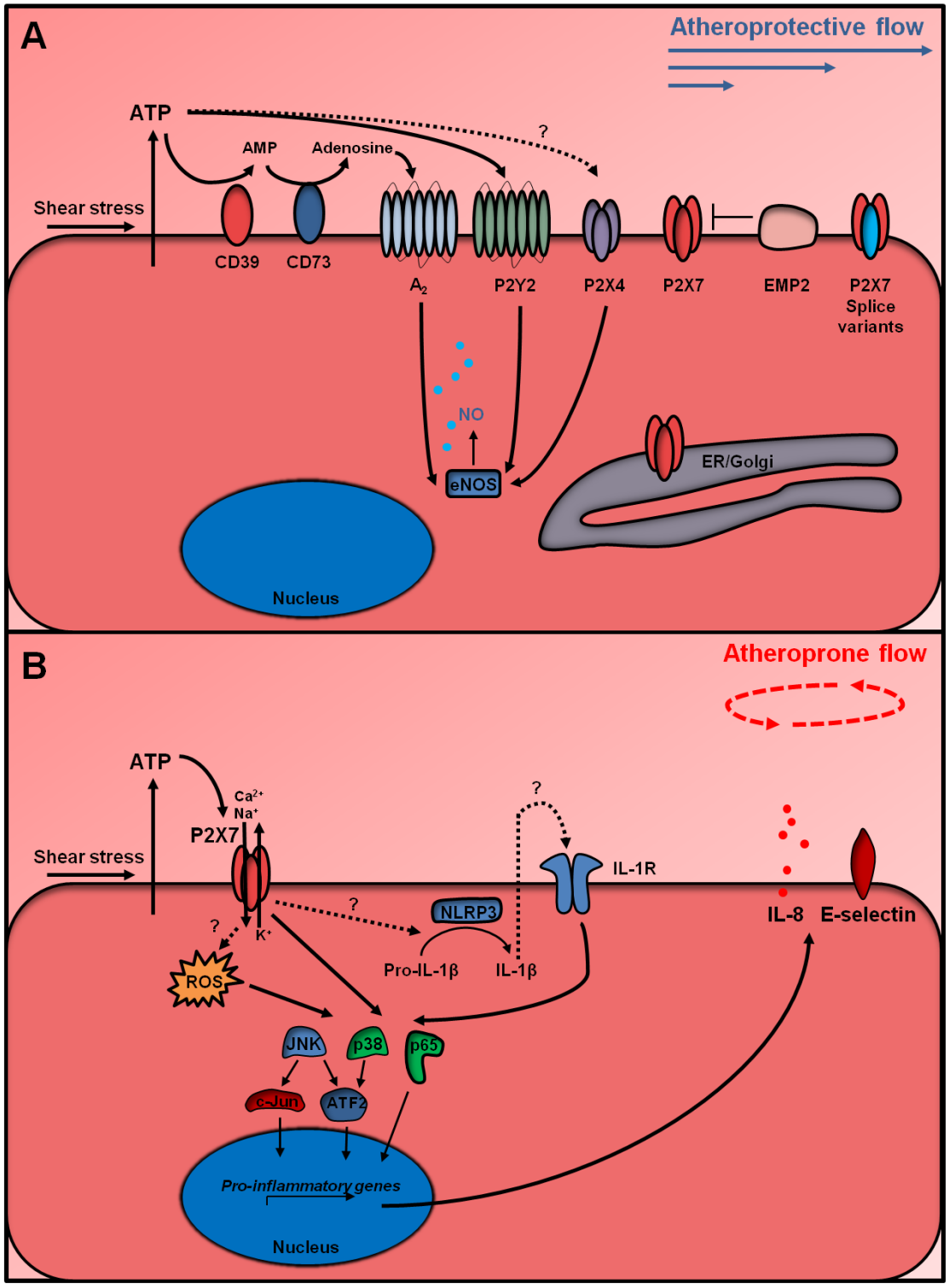

Figure 7.1 - A proposed model of altered endothelial ATP signalling between sites of the vasculature influenced by atheroprotective or atheroprone flow.

Shear stress induces ATP release which exerts different effects on endothelial cells under atheroprotective or atheroprone flow. (A) Under atheroprotective flow, ATP activates P2Y2 receptors and perhaps P2X4 receptors, inducing nitric oxide (NO) production. ATP is also hydrolysed by CD39 and CD73 to adenosine, which activates A_2 receptors, inducing NO production. P2X7 responses are inhibited by reduced surface expression and by negative regulators including EMP2 and alternatively spliced P2X7 variants. (B) Under atheroprone flow, decreased CD39 expression results in reduced ATP hydrolysis. P2X7 receptor expression is increased and is activated by increased ATP levels, up-regulating IL-8 and E-selectin expression thereby facilitating leukocyte attraction and adhesion. This up-regulation may occur through direct activation of JNK, p38 and p65, or indirectly through reactive oxygen species generation (ROS) or increased IL-1β processing and subsequent signalling.

7.3 Limitations of this study

Although the work in this thesis provides an insight into ATP signalling at sites of disturbed flow, it must be acknowledged that there are several limitations in this study. The majority of this research was performed *in vitro* using HUVEC, which despite allowing high throughput, does not completely replicate the conditions where atherosclerosis develops. In humans, atherosclerosis occurs within the arterial system, such as in the coronary arteries, suggesting that performing these studies using arterial cells rather than venule cells would be a more suitable. Recent evidence suggests however that both arterial and venule isolated endothelial cells lose their arteriovenous identity after a couple of weeks of *in vitro* culture (Aranguren et al. 2013), suggesting that the importance of using arterial cells *in vitro* may not as useful as anticipated. Nevertheless, I was able to observe expression of P2X7 from *in vitro* cultured human coronary artery endothelial cell (HCAEC) lysate (data not shown) and I observed enhanced endothelial P2X7 expression at atherosusceptible regions of the murine aorta, suggesting that my *in vitro* HUVEC work does translate to *in vivo* arterial models.

The majority of this work was performed using *in vitro* flow models which, despite simulating atheroprotective and atheroprone conditions, do not fully reproduce flow patterns that occur *in vivo* conditions. In order to address this, two *in vitro* flow models, that simulate different aspects of atheroprotective and atheroprone flow, were used when appropriate to further validate my findings. An additional point is that these *in vitro* systems only cultured endothelial cells, and therefore did not examine the potential impact from the surrounding cell types that form the vessel. Shear stress has been reported to regulate the underlying vascular smooth muscle cells (VSMC) (Qiu et al. 2014) and substantial cross-talk has also been identified between endothelial cells and VSMC under shear stress conditions, altering the phenotype of both endothelial cells and VSMC (Qi et al. 2011). Furthermore, these surrounding cells could be additional sources of extracellular ATP, further altering endothelial ATP signalling.

Circulating platelets, erythrocytes and monocytes all release ATP extracellularly in the bloodstream, which is proposed to act on endothelial P2 receptors (Hopkins 2015). Single culture *in vitro* studies also do not take into account circulating inflammatory mediators, such as low density lipoprotein (LDL) and cytokines, which are thought to contribute to the focal nature of atherosclerosis through mass-transport (Caro 2009; Warboys et al. 2011). Therefore, endothelial cell behaviour and ATP signalling could be vastly different between single endothelial cultures compared to *in vivo* arteries.

These limitations can ultimately be addressed by moving these studies into an *in vivo* atherosclerosis model, as this would full elucidate the role of ATP-P2X7 signalling in atherosclerosis under completely physiological conditions.

7.4 P2X7 as a therapeutic target.

P2X7 responses were seen exclusively in atheroprone flow-conditioned endothelial cells; this activation evoked an enhancement of the pro-atherosclerotic IL-8 and E-selectin. Furthermore, recent studies provide evidence that P2X7 promotes atherosclerosis development (Piscopiello et al. 2013; Peng et al. 2015), and is also responsible for endothelial dysfunction following high glucose and palmitate exposure (Sathanoori et al. 2015), which are conditions that occur under the pro-atherosclerotic disease diabetes mellitus. Finally, a loss of function polymorphism in the P2X7 receptor (A1513C, rs3751143) has been associated with a reduced risk of ischemic heart disease and ischemic stroke occurrence in humans (Gidlöf et al. 2012). Therefore, P2X7 is emerging as an attractive target in preventative therapeutics against atherosclerosis. P2X7 exhibits features that make it an optimal drug target (Bakheet & Doig 2009), including its plasma membrane expression making it readily accessible by small molecule drugs. Its activity is apical in the inflammatory signalling pathway (upstream of IL-1 release and of key transcriptional changes), suggesting that inhibition of P2X7 may attenuate multiple downstream pathways, maximising the potential to prevent disease progression.

P2X7 receptors have already been extensively studied as a potential therapeutic target due to their association with mediating inflammatory responses. As a result, several antagonists have been identified that efficiently inhibit P2X7 responses and have been proven effective in a range of preclinical murine and rodent models of disease (Bartlett et al. 2014; Alves et al. 2013). Moreover, very recently clinical trials have begun assessing the efficacy of two P2X7 inhibitors in humans, AZD9056 and CE-224,535 (Stock et al. 2012; Keystone et al. 2012; Eser et al. 2015). Despite being tolerated and exhibiting no serious side effects, these compounds had no significant benefit in treating rheumatoid arthritis and only a slight benefit in treating Crohn's disease, indicating a need for development of clinically effective P2X7 antagonists. However, it could also be proposed that the lack of efficacy of these drugs is because P2X7 activity does not predominate in these conditions. P2X7 is thought to mediate development of rheumatoid arthritis by inducing IL-1β release (Baroja-Mazo & Pelegrín 2012) and recent studies have found that anakinra, an antagonist of the IL-1 receptor, is less effective at treating rheumatoid arthritis than anti-TNF treatments (Nixon et al. 2007). Nevertheless, since preclinical studies with more recently developed P2X7 inhibitors are providing promising data (Bartlett et al. 2014), this suggests that in the near future, clinically appropriate P2X7 receptor antagonists will be available for human use and repurposing these drugs for the treatment of additional diseases would reduce both the time and cost. Additionally, since a loss of function polymorphism in P2X7 (A1513C, rs3751143) was identified to reduce risk or cardiovascular disease (Gidlöf et al. 2012), it would be interesting to perform retrospective analysis on patients taking P2X7 inhibitors to identify whether they also exhibited reduced cardiovascular disease risk. Furthermore, recently several natural compounds have been reported to potently modulate P2X7 responses (Faria et al. 2012) providing further opportunities for the development of a new generation of selective antagonists and allosteric modulators which may be more effective clinically. Interestingly, some of these natural compounds have already been associated with protection against cardiovascular disease. For

example, the anti-inflammatory compound colchicine, which has been reported to inhibit P2X7 dye uptake responses (Marques-da-Silva et al. 2011), has been reported to reduce the risk of adverse events in patients with established cardiovascular disease (Verma et al. 2015).

In addition to proposing the potential benefits of inhibiting P2X7 as a therapeutic treatment, it is important to consider the potential impact P2X7 antagonism may have on other systems. Activation of P2X7 is beneficial in numerous biological processes which would be impacted upon in these treatments. P2X7 is predominantly expressed on cells of hematopoietic origin, such as macrophages, and is considered an important regulator of inflammatory signalling following injury or infection due to its association with IL-1β processing and release (Ferrari et al. 2006; Dinarello 2004), suggesting that inhibiting P2X7 could suppress appropriate acute inflammatory responses. Indeed, a loss of function single nucleotide polymorphism (SNP) of P2X7 (A1513C) in humans has been linked to increased susceptibility to tuberculosis (Fernando et al. 2007; Ge & Chen 2016) and toxoplasmosis (Jamieson et al. 2010). P2X7 function is also essential for healthy bone development, by stimulating osteoblast proliferation and mineralisation (Panupinthu et al. 2008) and is a critical regulator of bone development in mice (Syberg et al. 2012; Gartland 2012). A Loss of function SNP (R307Q) in P2X7 has been associated with decreased bone mineral density in post-menopausal women (Gartland et al. 2012). These examples signify the potential side-effects that may occur following P2X7 inhibition; however P2X7 is becoming an increasingly investigated target proposed to regulate numerous disease processes and therefore it is likely that inhibition of P2X7 would impact additional biological processes not mentioned here (Sluyter & Stokes 2011; Skaper et al. 2009).

Another therapeutic approach could be to target the dysregulation of extracellular ATP under atheroprone flow. Since shear stress-induced ATP release is important in mediating vasodilation at atheroprotected sites, targeting the release of ATP may

actually exacerbate atherosclerosis. However, approaches to enhance activity of the ectoATPase CD39 under atheroprone flow may prove effective in preventing ATP dysregulation. CD39 overexpression *in vitro* has been shown to remove ATP-induced inflammatory effects (Imai et al. 2000; Goepfert et al. 2000) and is considered to been a negative regulator of P2X7 responses (Kuhny et al. 2014). Moreover, murine CD39 loss of function mutants have been reported to have exacerbated atherosclerosis (Kanthi et al. 2015) and pulmonary arterial hypertension (Helenius et al. 2015), demonstrating the protective nature of CD39 in vascular function. Unfortunately, to date no allosteric enhancers of CD39 have been reported, which makes directly targeting CD39 currently impossible. However, recent technological advances have provided a mechanism to selectively target inflamed endothelial cells, such as those at atherosusceptible sites, through VCAM-1 (Kheirolomoom et al. 2015) and E-selectin (Ma et al. 2016) targeted nanoparticles. These nanoparticles are capable of delivering micro-RNAs (miRNAs) or anti-sense miRNAs specifically to inflamed endothelial cells and aim to restore endothelial function. CD39 up-regulation under atheroprotective flow patterns has been determined to be as a result of increased KLF2 signalling (Kanthi et al. 2015), a key transcription factor considered essential for mediating atheroprotection (SenBanerjee et al. 2004; van Thienen et al. 2006). Interestingly, KLF2 expression has also been identified to be suppressed by miRNA-92a under atheroprone flow (Wu et al. 2011), and delivery of the corresponding anti-miRNA could prevent atheroprone flow mediated endothelial dysfunction by up-regulating numerous atheroprotective factors, including CD39. Indeed, studies examining the efficacy of inhibiting miRNA-92a have shown promising results in mediating increased protection of the vasculature (Liu et al. 2016; Daniel et al. 2014). Alternatively, vascular gene therapy could be performed to directly over-express CD39, amongst other atheroprotective genes, in the endothelium. Vascular gene therapy exploits viruses to deliver genetic material to cells (*in vivo* or *ex vivo)* and has already been proven to be safe and provide clinical benefits (Dishart et al. 2003), providing additional future therapeutic treatment strategies

7.5 Future studies

This study provides the first evidence that atheroprone flow regulates P2X7 receptor activity, and is necessary for atheroprone-induced inflammatory signalling. However, many questions remain unanswered and require further investigation.

Atheroprone flow-mediated up-regulation of IL-8 and E-selectin was found to be dependent in part on P2X7 receptor activity. Although this finding is significant in regards to regulating atherosclerosis development, the mechanism by which P2X7 mediates this up-regulation requires further examination. P2X7 receptor activity was specific to atheroprone flow conditions, and since P2X7 is capable of coordinating a range of intracellular responses (Skaper et al. 2010), there is likely additional P2X7 dependent responses occurring which remain to be elucidated. Atheroprone flow promotes: cleavage of caspase-3 (Chaudhury et al. 2010); generation of reactive oxygen species (ROS) (De Keulenaer et al. 1998); and NLRP3 activation leading to IL-1β release (Xiao et al. 2013). These have also all been reported to occur downstream of P2X7 in other cell types (Skaper et al. 2010; Suh et al. 2001). Therefore, investigation into additional P2X7 receptor signalling pathways is necessary to fully understand its role in endothelial cells under atheroprone flow.

Recent evidence suggests that P2X7 is a regulator of atherosclerosis development (Piscopiello et al. 2013; Peng et al. 2015; Sathanoori et al. 2015). The evidence in this thesis expands on this and therefore, the contribution to P2X7 in murine models of atherosclerosis is a critical area for future research beyond this project. Previous assessment of P2X7 in atherosclerosis was performed by intravenous (IV) injection of P2X7 siRNA into $ApoE^{-/-}$ mice on a C57BL/6 background, which demonstrated that P2X7 was pro-atherosclerotic (Peng et al. 2015). This approach however may not fully represent the role that P2X7 plays in atherosclerosis, as C57BL/6 mice contain a SNP (P451L) which reduces P2X7 responses (Adriouch et al. 2002; Syberg et al. 2012), as well as performing these studies with a only partial P2X7 knockout. Therefore,

atherosclerosis development should be modelled in P2X7 $^{-/-}$ mice on a BALB/c background, which do not contain P451L. As no genetic atherosclerosis model, such as ApoE$^{-/-}$ or LDLR$^{-/-}$, currently exists on a BALB/c background, a novel approach for atherosclerosis can be utilised by IV injection of an adenoassociated virus containing a gain of function mutated version of proprotein convertase subtilisin/kexin type 9 (rAAV8-D377Y-mPCKS9), which has shown to be efficacious in our department in C57BL/6 mice (Mahmoud et al. 2016). Furthermore, since myeloid cells are considered the predominant P2X7 expressing cells, these studies would benefit from being performed in endothelial specific P2X7$^{-/-}$ mice using Cre-Lox recombination technology. However, it is time and cost expensive to generate such mutants, and alternatively bone marrow transplant studies using readily available global P2X7$^{-/-}$ mice could quickly elucidate the role of myeloid and non-myeloid P2X7 in atherosclerosis. Ultimately, it would also be very useful to assess the efficacy of P2X7 antagonists as a preventative medicine of atherosclerosis development in murine models, as this would serve to model long-term therapeutic strategies in man. Moreover, as mentioned previously, several P2X7 receptor antagonists have already passed preclinical assessment, enabling these studies to proceed quickly.

In summary, this study contributes to the expanding evidence that endothelial P2X7 receptors promote endothelial dysfunction under inflammatory conditions. Since endothelial dysfunction is important in the development of several diseases, further research into the role of endothelial P2X7 receptors could provide a novel and accessible therapeutic approach to the treatment of many vascular diseases, including atherosclerosis.

8. References

Adinolfi, E. et al., 2010. Trophic activity of a naturally occurring truncated isoform of the P2X7 receptor. *FASEB*, 24(9), pp.3393–404.

Adriouch, S. et al., 2002. Cutting edge: a natural P451L mutation in the cytoplasmic domain impairs the function of the mouse P2X7 receptor. *Journal of Immunology*, 169(8), pp.4108–4112.

Aiello, R.J. et al., 1999. Monocyte chemoattractant protein-1 accelerates atherosclerosis in apolipoprotein E-deficient mice. *Arteriosclerosis, Thrombosis and Vascular Biology*, 19(1079–5642), pp.1518–1525.

von Albertini et al., 1998. Extracellular ATP and ADP activate transcription factor NF-kappa B and induce endothelial cell apoptosis. *Biochemical and Biophysical Research Communications*, 248(3), pp.822–9.

Allsopp, R.C. & Evans, R.J., 2015. Contribution of the juxtatransmembrane intracellular regions to the time course and permeation of ATP-gated P2X7 Receptor ion channels. *Journal of Biological Chemistry*, 290(23), pp.14556–14566.

Alves, L.A. et al., 2013. Physiological roles and potential therapeutic applications of the P2X7 receptor in inflammation and pain. *Molecules*, 18(9), pp.10953–72.

Antigny, F. et al., 2011. Thapsigargin activates Ca2+ entry both by store-dependent, STIM1/Orai1-mediated, and store-independent, TRPC3/PLC/PKC-mediated pathways in human endothelial cells. *Cell Calcium*, 49(2), pp.115–127.

Antonio, L.S. et al., 2011. P2X4 receptors interact with both P2X2 and P2X7 receptors in the form of homotrimers. *British Journal of Pharmacology*, 163(5), pp.1069–77.

Antonioli, L. et al., 2013. CD39 and CD73 in immunity and inflammation. *Trends in Molecular Medicine*, 19(6), pp.355–367.

Aranguren, X.L. et al., 2013. Unraveling a novel transcription factor code determining the human arterial-specific endothelial cell signature. *Blood*, 122(24), pp.3982–92.

Bakheet, T.M. & Doig, A.J., 2009. Properties and identification of human protein drug targets. *Bioinformatics*, 25(4), pp.451–457.

Bao, L., Locovei, S. & Dahl, G., 2004. Pannexin membrane channels are mechanosensitive conduits for ATP. *FEBS letters*, 572(1–3), pp.65–8.

Baroja-Mazo, A. & Pelegrín, P., 2012. Modulating P2X7 Receptor Signaling during Rheumatoid Arthritis: New Therapeutic Approaches for Bisphosphonates. *Journal of Osteoporosis*, 2012, p.408242.

Barth, K. et al., 2007. Caveolin-1 influences P2X7 receptor expression and localization in mouse lung alveolar epithelial cells. *The FEBS journal*, 274(12), pp.3021–33.

Barth, K. et al., 2008. Characterization of the molecular interaction between caveolin-1 and the P2X receptors 4 and 7 in E10 mouse lung alveolar epithelial cells. *The International Journal of Biochemistry & Cell Biology*, 40(10), pp.2230–9.

Bartlett, R., Stokes, L. & Sluyter, R., 2014. The P2X7 Receptor Channel: Recent Developments and the Use of P2X7 Antagonists in Models of Disease. *Pharmacological Reviews*, 66(3), pp.638–675.

Bender, S.B. et al., 2011. Functional contribution of P2Y1 receptors to the control of coronary blood flow. *Journal of Applied Physiology*, 111, pp.1744–1750.

Bennett, M.R., Sinha, S. & Owens, G.K., 2016. Vascular Smooth Muscle Cells in Atherosclerosis. *Circulation Research*, 118(4), pp.692–702.

Berk, B.C., 2008. Atheroprotective signaling mechanisms activated by steady laminar flow in endothelial cells. *Circulation*, 117(8), pp.1082–1089.

Bodin, P. & Burnstock, G., 2001. Evidence that release of adenosine triphosphate from endothelial cells during increased shear stress is vesicular. *Journal of Cardiovascular Pharmacology*, 38(6), pp.900–8.

Bodin, P. & Burnstock, G., 1998. Increased release of ATP from endothelial cells during acute inflammation. *Inflammation Research*, 47(8), pp.351–354.

Boumechache, M. et al., 2009. Analysis of assembly and trafficking of native P2X4 and P2X7 receptor complexes in rodent immune cells. *The Journal of Biological Chemistry*, 284(20), pp.13446–54.

Braganhol, E. et al., 2015. Nucleotide receptors control IL-8/CXCL8 and MCP-1/CCL2 secretions as well as proliferation in human glioma cells. *Biochimica et Biophysica Acta*, 1852(1), pp.120–130.

Brizzolara, A.L. & Burnstock, G., 1991. Endothelium-dependent and endothelium-independent vasodilatation of the hepatic artery of the rabbit. *British Journal of Pharmacology*, 103(1), pp.1206–1212.

Brooks, A.R., Lelkes, P.I. & Rubanyi, G.M., 2002. Gene expression profiling of human aortic endothelial cells exposed to disturbed flow and steady laminar flow. *Physiological Genomics*, 9(February 2002), pp.27–41.

Buchheiser, A. et al., 2011. Inactivation of CD73 promotes atherogenesis in apolipoprotein E-deficient mice. *Cardiovascular Research*, 92(2), pp.338–347.

Burm, S.M. et al., 2016. ATP-induced IL-1β secretion is selectively impaired in microglia as compared to hematopoietic macrophages. *Glia*, 64, pp.2231–2246.

Burnstock, G., 2016. P2X ion channel receptors and inflammation. *Purinergic Signalling*, 12(1), pp.59–67.

Buvinic, S., Briones, R. & Huidobro-Toro, J.P., 2002. P2Y(1) and P2Y(2) receptors are coupled to the NO/cGMP pathway to vasodilate the rat arterial mesenteric bed. *British Journal of Pharmacology*, 136(6), pp.847–856.

Cancel, L.M. et al., 2016. Endothelial glycocalyx, apoptosis and inflammation in an atherosclerotic mouse model. *Atherosclerosis*, 252, pp.136–146. Available at: http://dx.doi.org/10.1016/j.atherosclerosis.2016.07.930.

Caro, C.G., Fitz-Gerald, J.M. & Schroter, R.., 1971. Atheroma and arterial wall shear: Observation, correlation and proposal of a shear dependent mass transfer mechanism for atherogenesis. *Proceedings of the Royal Society of London*, 177(1046), pp.133–159.

Caro, G.G., 2009. Discovery of the role of wall shear in atherosclerosis. *Arteriosclerosis, Thrombosis, and Vascular Biology*, 29(2), pp.158–161.

Chang, W.-C. et al., 2007. All-or-none activation of CRAC channels by agonist elicits graded responses in populations of mast cells. *Journal of Immunology*, 179(8), pp.5255–5263.

Chaudhury, H. et al., 2010. c-Jun N-terminal kinase primes endothelial cells at atheroprone sites for apoptosis. *Arteriosclerosis, Thrombosis, and Vascular Biology*, 30(3), pp.546–53.

Cheewatrakoolpong, B. et al., 2005. Identification and characterization of splice variants of the human P2X7 ATP channel. *Biochemical and Biophysical Research Communications*, 332(1), pp.17–27.

Chen, L.-J., Wang, W.-L. & Chiu, J.-J., 2016. Vascular Endothelial Mechanosensors in Response to Fluid Shear Stress. In S. Chien, A. J. Engler, & P. Y. Wang, eds. *Molecular and Cellular Mechanobiology*. Springer International Publishing, pp. 29–56.

Chen, Z. et al., 2011. Endothelial dysfunction: the role of SREBP-induced NLRP3 inflammasome in atherosclerosis. *Current Opinion in Lipidology*, 4(164), pp.339–349.

Chiu, J.J. et al., 2003. Analysis of the effect of disturbed flow on monocytic adhesion to endothelial cells. *Journal of Biomechanics*, 36(12), pp.1883–1895.

Chiu, J.J. & Chien, S., 2011. Effects of disturbed flow on vascular endothelium: pathophysiological basis and clinical perspectives. *Physiol Rev*, 91(1), pp.327–387.

Civelek, M. et al., 2009. Chronic endoplasmic reticulum stress activates unfolded protein response in arterial endothelium in regions of susceptibility to atherosclerosis. *Circulation Research*, 105(5), pp.453–461.

Coddou, C. et al., 2011. Activation and Regulation of Purinergic P2X. *Pharmacological Reviews*, 63(3), pp.641–683.

Communi, D. et al., 2000. Advances in signalling by extracellular nucleotides: The role and transduction mechanisms of P2Y receptors. *Cellular Signalling*, 12(6), pp.351–360.

Communi, D., Robaye, B. & Boeynaems, J.M., 1999. Pharmacological characterization of the human P2Y11 receptor. *British Journal of Pharmacology*, 128, pp.1199–1206.

Costa-Junior, H.M., Sarmento Vieira, F. & Coutinho-Silva, R., 2011. C terminus of the P2X7 receptor: treasure hunting. *Purinergic Signalling*, 7(1), pp.7–19.

Coutinho-Silva, R. & Persechini, P.M., 1997. P2Z purinoceptor-associated pores induced by extracellular ATP in macrophages and J774 cells. *The American Journal of Physiology*, 273(6 Pt 1), pp.C1793-800.

Cuhlmann, S. et al., 2011. Disturbed blood flow induces RelA expression via c-Jun N-terminal kinase 1: a novel mode of NF-κB regulation that promotes arterial inflammation. *Circulation Research*, 108(8), pp.950–9.

Cybulsky, M.I. et al., 2001. A major role for VCAM-1, but not ICAM-1, in early atherosclerosis. *Journal of Clinical Investigation*, 107(10), pp.1255–1262.

D'hondt, C., Himpens, B. & Bultynck, G., 2013. Mechanical stimulation-induced calcium wave propagation in cell monolayers: the example of bovine corneal endothelial cells. *Journal of Visualized Experiments*, 77, p.e50443.

Daniel, J.M. et al., 2014. Inhibition of miR-92a improves re-endothelialization and prevents neointima formation following vascular injury. *Cardiovascular Research*, 103(4), pp.564–572.

Dawicki, D.D. et al., 1995. Extracellular nucleotides stimulate leukocyte adherence to cultured pulmonary artery endothelial cells. *American Journal of Physiology Lung Cellular and Molecular Physiology*, 268(12), pp.666–673.

Dinarello, C., 2004. Unraveling the NALP-3/IL-1B Inflammasome : a big lesson from a small mutation. *Immunity*, 20, pp.243–244.

Dishart, K.L. et al., 2003. Gene therapy for cardiovascular disease. *Journal of Biomedicine & Biotechnology*, 2003(2), pp.138–148.

Donnelly-Roberts, D.L. et al., 2009. Mammalian P2X7 receptor pharmacology: comparison of recombinant mouse, rat and human P2X7 receptors. *British Journal of Pharmacology*, 157(7), pp.1203–14.

Dubyak, G.R., 2012. P2X7 receptor regulation of non-classical secretion from immune effector cells. *Cellular Microbiology*, 14(11), pp.1697–1706.

von Eckardstein, A. & Rohrer, L., 2009. Transendothelial lipoprotein transport and regulation of endothelial permeability and integrity by lipoproteins. *Current opinion in lipidology*, 20(3), pp.197–205

Erb, L. et al., 2006. P2 receptors: Intracellular signaling. *Pflugers Arch*, 452(5), pp.552–562.

Faria, R. et al., 2012. Action of natural products on p2 receptors: a reinvented era for drug discovery. *Molecules*, 17(11), pp.13009–25.

Feng, Y.-H. et al., 2006. A truncated P2X7 receptor variant (P2X7-j) endogenously expressed in cervical cancer cells antagonizes the full-length P2X7 receptor through hetero-oligomerization. *The Journal of Biological Chemistry*, 281(25), pp.17228–37.

Fernando, S.L. et al., 2007. A polymorphism in the P2X7 gene increases susceptibility to extrapulmonary tuberculosis. *American Journal of Respiratory and Critical Care Medicine*, 175(4), pp.360–366.

Ferrari, D. et al., 1997. Extracellular ATP activates transcription factor NF-kB through the P2Z purinoreceptor by selectively targeting NF-kB p65 (RelA). *The Journal of Cell Biology*, 139(7), pp.1635–1643.

Ferrari, D. et al., 2006. The P2X7 receptor: a key player in IL-1 processing and release. *Journal of Immunology*, 176(7), pp.3877–83.

Florian, J.A. et al., 2003. Heparan Sulfate Proteoglycan Is a Mechanosensor on Endothelial Cells. *Circulation Research*, 93(10), pp.e136–e142.

Forbes, A. et al., 2007. The tetraspan protein EMP2 regulates expression of caveolin-1. *The Journal of biological chemistry*, 282(36), pp.26542–51.

Forrester, T. & Lind, A.R., 1969. Identifcation of Adenosine Triphosphate in Human Plasma and the Concentration in the Venous Effluent of Forearm Muscles Before, During and After Sustained Contraction. *Thermal exchanges of the human body in extreme heat.*, 204, pp.347–364.

Fountain, S.J., 2013. Primitive ATP-activated P2X receptors: discovery, function and pharmacology. *Frontiers in Cellular Neuroscience*, 7, pp.2007–2013.

Fu, Y. et al., 2011. A novel mechanism of γ/δ T-lymphocyte and endothelial activation by shear stress: the role of ecto-ATP synthase β chain. *Circulation Research*, 108(4), pp.410–7.

Galea, J. et al., 1996. Interleukin-1ß in Coronary Arteries of Patients With Ischemic Heart Disease. *Arteriosclerosis, Thrombosis and Vascular Biology§*, 16(8), pp.1000–1006.

Gangadharan, V. et al., 2015. Caveolin-1 regulates P2X7 receptor signaling in osteoblasts. *American Journal of Physiology: Cell Physiology*, 308(1), pp.C41-50.

Garcia-Marcos, M. et al., 2006. Coupling of two pools of P2X7 receptors to distinct intracellular signaling pathways in rat submandibular gland. *Journal of Lipid Research*, 47(4), pp.705–14.

Gartland, A., 2012. P2X receptors in bone. *WIRE Membrane Transport and Signalling*, 1, pp.221–227.

Gartland, A. et al., 2012. Polymorphisms in the P2X7 receptor gene are associated with low lumbar spine bone mineral density and accelerated bone loss in post-menopausal women. *European Journal of Human Genetics*, 20(5), pp.559–64.

Gasparics, Á. et al., 2016. When the endothelium scores an own goal: endothelial cells actively augment metastatic extravasation through endothelial-mesenchymal transition. *American Journal of Physiology - Heart and Circulatory Physiology*, 310, pp.1055–1063.

Ge, H.B. & Chen, S., 2016. A meta-analysis of P2X7 gene-1513A/C polymorphism and pulmonary tuberculosis susceptibility. *Human Immunology*, 77(1), pp.126–130.

Gee, H.Y. et al., 2014. Mutations in EMP2 cause childhood-onset Nephrotic syndrome. *American Journal of Human Genetics*, 94(6), pp.884–890.

Genetos, D.C. et al., 2005. Fluid shear-induced ATP secretion mediates prostaglandin release in MC3T3-E1 osteoblasts. *Journal of Bone and Mineral Research*, 20(1), pp.41–9.

Genetos, D.C. et al., 2011. Purinergic signaling is required for fluid shear stress-induced NF-κB translocation in osteoblasts. *Experimental Cell Research*, 317(6), pp.737–44.

Gerdes, N. et al., 2002. Expression of Interleukin (IL)-18 and functional IL-18 receptor on human vascular endothelial cells, smooth muscle cells, and macrophages: Implications for atherogenesis. *Journal of Experimental Medicine*, 195(2), pp.245–257.

Gerszten, R.E. et al., 1999. MCP-1 and IL-8 trigger firm adhesion of monocytes to vascular endothelium under flow conditions. *Nature*, 398, pp.718–723.

Gicquel, T. et al., 2015. IL-1β production is dependent on the activation of purinergic receptors and NLRP3 pathway in human macrophages. *FASEB Journal*, 29(10), pp.4162–4173.

Gidlöf, O. et al., 2012. A common missense variant in the ATP receptor P2X7 is associated with reduced risk of cardiovascular events. *PloS one*, 7(5), p.e37491.

Gifford, S.M. et al., 2004. Functional characterization of HUVEC-CS: Ca2+ signaling, ERK 1/2 activation, mitogenesis and vasodilator production. *The Journal of Endocrinology*, 182(3), pp.485–99.

Gödecke, S. et al., 2012. Thrombin-induced ATP release from human umbilical vein endothelial cells. *American Journal of Physiology: Cell Physiology*, 302(6), pp.C915-23.

Goepfert, C. et al., 2000. CD39 modulates endothelial cell activation and apoptosis. *Molecular Medicine*, 6(7), pp.591–603.

Gonçalves Da Silva, C. et al., 2009. Mechanism of purinergic activation of endothelial nitric oxide synthase in endothelial cells. *Circulation*, 119(6), pp.871–879.

Gonnord, P. et al., 2008. Palmitoylation of the P2X7 receptor, an ATP-gated channel, controls its expression and association with lipid rafts. *FASEB*, 23(3), pp.795–805.

Gouverneur, M. et al., 2006. Vasculoprotective properties of the endothelial glycocalyx: Effects of fluid shear stress. *Journal of Internal Medicine*, 259(4), pp.393–400.

Govindan, S. & Taylor, C.W., 2012. P2Y receptor subtypes evoke different Ca2+ signals in cultured aortic smooth muscle cells. *Purinergic Signalling*, 8(4), pp.763–777.

Gudipaty, L. et al., 2001. Regulation of P2X(7) nucleotide receptor function in human monocytes by extracellular ions and receptor density. *American Journal of Physiology: Cell Physiology*, 280(4), pp.C943-53.

Guns, P.-J.D.F. et al., 2006. Endothelium-dependent relaxation evoked by ATP and UTP in the aorta of P2Y2-deficient mice. *British Journal of Pharmacology*, 147(5), pp.569–74.

Guns, P.-J.D.F. et al., 2005. Pharmacological characterization of nucleotide P2Y receptors on endothelial cells of the mouse aorta. *British Journal of Pharmacology*, 146(2), pp.288–95.

Guo, C. et al., 2007. Evidence for functional P2X4/P2X7 heteromeric receptors. *Molecular Pharmacology*, 72(6), pp.1447–1456.

Hajra, L. et al., 2000. The NF-kappa B signal transduction pathway in aortic endothelial cells is primed for activation in regions predisposed to atherosclerotic lesion formation. *Proceedings of the National Academy of Sciences of the United States of America*, 97(16), pp.9052–7.

Hansson, G.K. & Libby, P., 2006. The immune response in atherosclerosis: a double-edged sword. *Nature Reviews*, 6, pp.508–519.

Harkness, R.A., Coade, S.B. & Webster, A.D.B., 1984. ATP, ADP and AMP in plasma from peripheral venous blood. *Clinica Chimica Acta*, 143(2), pp.91–98.

Hechler, B. et al., 2008. Reduced atherosclerotic lesions in P2Y1/Apolipoprotein E double-knockout mice: The contribution of non-hematopoietic-derived P2Y 1 receptors. *Circulation*, 118(7), pp.754–763.

Van der Heiden, K. et al., 2010. Role of nuclear factor kappaB in cardiovascular health and disease. *Clinical Science*, 118(10), pp.593–605.

Hein, T.W. & Kuo, L., 1999. cAMP-independent dilation of coronary arterioles to adenosine : role of nitric oxide, G proteins, and K(ATP) channels. *Circulation Research*, 85(7), pp.634–642.

Heine, P. et al., 1999. Functional characterization of rat ecto-ATPase and ecto-ATP diphosphohydrolase after heterologous expression in CHO cells. *European Journal of Biochemistry*, 262(1), pp.102–107.

Helenius, M.H. et al., 2015. Suppression of endothelial CD39/ENTPD1 is associated with pulmonary vascular remodeling in pulmonary arterial hypertension. *American Journal of Physiology: Lung Cellular and Molecular Physiology*, 308(10), pp.L1046-57.

Heo, K.-S., Fujiwara, K. & Abe, J., 2011. Disturbed-Flow-Mediated Vascular Reactive Oxygen Species Induce Endothelial Dysfunction. *Circulation Journal*, 75(12), pp.2722–2730.

Hernandez-Olmos, V. et al., 2012. N-substituted phenoxazine and acridone derivatives: Structure-activity relationships of potent P2X4 receptor antagonists. *Journal of Medicinal Chemistry*, 55(22), pp.9576–9588.

Hjermann, I. et al., 1981. Effect of Diet and Smoking Intervention on the Incidence of Coronary Heart Disease. *The Lancet*, 318(8259), pp.1303–1310.

Hopkins, P.N., 2015. Molecular Biology of Atherosclerosis. *Physiological Reviews*, 93, pp.1317–1542.

Hopwood, A.M. & Burnstock, G., 1987. ATP mediates coronary vasoconstriction via P2x-purinoceptors and coronary vasodilatation via P2y-purinoceptors in the isolated perfused rat heart. *European Journal of Pharmacology*, 136(1), pp.49–54.

Huber, S. a et al., 1999. Interleukin-6 exacerbates early atherosclerosis in mice. *Arteriosclerosis, Thrombosis and Vascular Biologyoscler Thromb Vasc Biol*, 19, pp.2364–2367.

Hung, S.-C. et al., 2013. P2X4 assembles with P2X7 and Pannexin-1 in gingival epithelial cells and modulates ATP-induced reactive oxygen species production and inflammasome activation. *PloS one*, 8(7), p.e70210.

Imai, M. et al., 2000. CD39 modulates IL-1 release from activated endothelial cells. *Biochemical and Biophysical Research Communications*, 270(1), pp.272–8.

Jabs, M., Ferrell, W.J. & Robb, H.J., 1977. Microdetermination of Plasma ATP and Creatine Phosphate Concentrations with a Luminescence Biometer. *Clinical Chemistry*, 23(12), pp.2254–2257.

Jacobson, K. a., Jarvis, M.F. & Williams, M., 2002. Purine and Pyrimidine (P2) Receptors as Drug Targets. *Journal of Medicinal Chemistry*, 45(19), pp.4057–4093.

Jafarnejad, M. et al., 2015. Measurement of shear stress-mediated intracellular calcium dynamics in human dermal lymphatic endothelial cells. *American Journal of Physiology: Heart and Circulatory Physiology*, 308(7), pp.H697-706.

Jamieson, S.E. et al., 2010. Evidence for associations between the purinergic receptor P2X(7) (P2RX7) and toxoplasmosis. *Genes and Immunity*, 11(5), pp.374–83.

Jarvis, M.F. & Khakh, B.S., 2009. ATP-gated P2X cation-channels. *Neuropharmacology*, 56(1), pp.208–215.

Kaczmarek-Hájek, K. et al., 2012. Molecular and functional properties of P2X receptors--recent progress and persisting challenges. *Purinergic Signalling*, 8(3), pp.375–417.

Kanjanamekanant, K., Luckprom, P. & Pavasant, P., 2014. P2X7 receptor-Pannexin1 interaction mediates stress-induced interleukin-1 beta expression in human periodontal ligament cells. *Journal of Periodontal Research*, 49, pp.595–602.

Kanthi, Y. et al., 2015. Flow-dependent expression of ectonucleotide tri(di) phosphohydrolase-1 and suppression of atherosclerosis. *Journal of Clinical Investigation*, 125(8), pp.3027–3036.

Kawano, A. et al., 2012. Regulation of P2X7-dependent inflammatory functions by P2X4 receptor in mouse macrophages. *Biochemical and Biophysical Research Communications*, 420(1), pp.102–7.

Kennedy, C. et al., 2000. ATP, an agonist at the rat P2Y4 receptor, is an antagonist at the human P2Y4 receptor. *Molecular Pharmacology*, 57, pp.926–931.

De Keulenaer, G.W. et al., 1998. Oscillatory and steady laminar shear stress differentially affect human endothelial redox state: Role of a superoxide-producing NADH Oxidase. *Circulation Research*, 82(10), pp.1094–1101.

Keystone, E.C. et al., 2012. Clinical evaluation of the efficacy of the P2X7 purinergic receptor antagonist AZD9056 on the signs and symptoms of rheumatoid arthritis in patients with active disease despite treatment with methotrexate or sulphasalazine. *Annals of the Rheumatic Diseases*, 71(10), pp.1630–1635.

Kheirolomoom, A. et al., 2015. Multifunctional nanoparticles facilitate molecular targeting and miRNA delivery to inhibit atherosclerosis in ApoE-/- mice. *ACS Nano*, 9(9), pp.8885–8897.

Kim, M. et al., 2001. Proteomic and functional evidence for a P2X7 receptor signalling complex. *The EMBO Journal*, 20(22), pp.6347–58.

Kitagawa, K. et al., 2002. Involvement of ICAM-1 in the progression of atherosclerosis in APOE-knockout mice. *Atherosclerosis*, 160(2), pp.305–310.

Koo, A., Dewey, C.F. & García-Cardeña, G., 2013. Hemodynamic shear stress characteristic of atherosclerosis-resistant regions promotes glycocalyx formation in cultured endothelial cells. *American journal of physiology. Cell physiology*, 304(2), pp.C137-46.

Korenaga, R. et al., 2000. Sp1-mediated downregulation of P2X 4 receptor gene transcription in endothelial cells exposed to shear stress. *American Journal of Physiology: Heart and Circulatory Physiology*, 280, pp.2214–2221.

Koziak, K. et al., 2000. Palmitoylation Targets CD39/Endothelial ATP Diphosphohydrolase to Caveolae. *Journal of Biological Chemistry*, 275(3), pp.2057–2062. Available at: http://www.jbc.org/cgi/doi/10.1074/jbc.275.3.2057 [Accessed October 1, 2014].

Kügelgen, I. Von, 2008. Pharmacology of mammalian P2X- and P2Y-receptors. *Biotrend Reviews*, 3(9), pp.1–12.

Kuhny, M. et al., 2014. CD39 is a negative regulator of P2X7-mediated inflammatory cell death in mast cells. *Cell Communication and Signaling*, 12(40), pp.1–13.

Kukley, M. et al., 2004. Ecto-nucleotidases and nucleoside transporters mediate activation of adenosine receptors on hippocampal mossy fibers by P2X7 receptor agonist 2'-3'-O-(4-Benzoylbenzoyl)-ATP. *Journal of Neuroscience*, 24(32), pp.7128–7139.

Li, J. et al., 1998. Adenosine A2a receptors increase arterial endothelial cell nitric oxide. *Journal of Surgical Research*, 80, pp.357–364.

Li, J. et al., 2005. The P2X7 nucleotide receptor mediates skeletal mechanotransduction. *The Journal of Biological Chemistry*, 280(52), pp.42952–9.

Li, Y. et al., 2016. SIRT1 inhibits inflammatory response partly through regulation of NLRP3 inflammasome in vascular endothelial cells. *Molecular Immunology*, 77, pp.148–156.

Libby, P., 2002. Inflammation in atherosclerosis. *Arteriosclerosis, Thrombosis, and Vascular Biology*, 32(9), pp.2045–51.

Lim To, W.K., Kumar, P. & Marshall, J.M., 2015. Hypoxia is an effective stimulus for vesicular release of ATP from human umbilical vein endothelial cells. *Placenta*, 36(7), pp.759–766.

Liu, H. et al., 2016. Inhibition of miR-92a may protect endothelial cells after acute myocardial infarction in rats: Role of KLF2/4. *Medical Science Monitor*, 22, pp.2451–2462.

Lohman, A.W. et al., 2015. Pannexin 1 channels regulate leukocyte emigration through the venous endothelium during acute inflammation. *Nature Communications*, 6, p.7965.

Lytton, J., Westlin, M. & Hanley, M.R., 1991. Thapsigargin inhibits the sarcoplasmic or endoplasmic reticulum Ca-ATPase family of calcium pumps. *Journal of Biological Chemistry*, 266(26), pp.17067–17071.

Ma, S. et al., 2016. E-selectin-targeting delivery of microRNAs by microparticles ameliorates endothelial inflammation and atherosclerosis. *Scientific Reports*, 6(22910), pp.1–11.

MacKenzie, A. et al., 2001. Rapid secretion of interleukin-1β by microvesicle shedding. *Immunity*, 15(5), pp.825–835.

Mahmoud, M.M. et al., 2016. TWIST1 integrates endothelial responses to flow in vascular dysfunction and atherosclerosis. *Circulation Research*, 119(3), pp.450–462.

Makó, V. et al., 2010. Proinflammatory activation pattern of human umbilical vein endothelial cells induced by IL-1β, TNF-α, and LPS. *Cytometry Part A*, 77(10), pp.962–970.

Mankus, C. et al., 2011. Corneal epithelium expresses a variant of P2X(7) receptor in health and disease. *PloS One*, 6(12), p.e28541.

Marques-da-Silva, C. et al., 2011. Colchicine inhibits cationic dye uptake induced by ATP in P2X2 and P2X7 receptor-expressing cells: implications for its therapeutic action. *British Journal of Pharmacology*, 163(5), pp.912–26.

Martín-sánchez, F. et al., 2016. Inflammasome-dependent IL-1 β release depends upon membrane permeabilisation. *Cell Death and Differentiation*, 23, pp.1219–1231.

van der Meer, A.D. et al., 2009. Lowering caveolin-1 expression in human vascular endothelial cells inhibits signal transduction in response to shear stress. *International Journal of Cell Biology*, 2009, p.532432.

Mercier, N. et al., 2012. Impaired ATP-induced coronary blood flow and diminished aortic NTPDase activity precede lesion formation in apolipoprotein E-deficient mice. *American Journal of Pathology*, 180(1), pp.419–428.

Montreekachon, P. et al., 2011. Involvement of P2X7 purinergic receptor and MEK1/2 in interleukin-8 up-regulation by LL-37 in human gingival fibroblasts. *Journal of Periodontal Research*, 46(3), pp.327–337.

Morales, S.A. et al., 2012. Anti-EMP2 diabody blocks epithelial membrane protein 2 (EMP2) and FAK mediated collagen gel contraction in ARPE-19 cells. *Experimental Eye Research*, 102, pp.10–16.

Morel, J.C.M. et al., 2001. A Novel Role for Interleukin-18 in Adhesion Molecule Induction through NF-kappaB and Phosphatidylinositol (PI) 3-Kinase-dependent Signal Transduction Pathways. *Journal of Biological Chemistry*, 276(40), pp.37069–37075.

Munoz-Planillo, R. et al., 2013. K+ Efflux is the common trigger of NLRP3 inflammasome activation by bacterial toxins and particulate matter. *Immunity*, 38(6), pp.1142–1153.

Nakamura, M. et al., 2006. Cell-surface-localized ATP detection with immobilized firefly luciferase. *Analytical Biochemistry*, 352(1), pp.61–67.

Nayler, W.G., 1995. Atherosclerosis and Endothelial Damage : A Brief Overview. *Cardiovascular Drugs and Therapy*, 9, pp.25–30.

Newton, K. & Dixit, V.M., 2012. Signaling in innate immunity and inflammation. *Cold Spring Harbor perspectives in biology*, 4(3), p.a006049.

Ni, C.-W. et al., 2010. Discovery of novel mechanosensitive genes in vivo using mouse carotid artery endothelium exposed to disturbed flow. *Blood*, 116(15), pp.e66-73.

Nicke, A., 2008. Homotrimeric complexes are the dominant assembly state of native P2X7 subunits. *Biochemical and Biophysical Research Communications*, 377(3), pp.803–8.

Nie, K. et al., 2005. CD39-associated high ATPase activity contribute to the loss of P2X7-mediated calcium response in LCL cells. *Leukemia Research*, 29(11), pp.1325–1333.

Nixon, R., Bansback, N. & Brennan, A., 2007. The efficacy of inhibiting tumour necrosis factor α and interleukin 1 in patients with rheumatoid arthritis: A meta-analysis and adjusted indirect comparisons. *Rheumatology*, 46(7), pp.1140–1147.

North, R.A., 2002. Molecular physiology of P2X receptors. *Physiological Reviews*, 82(4), pp.1013–67.

North, R.A. & Surprenant, A., 2001. Pharmacology of cloned P2X receptors. *Annual Reviews of Pharmacology and Toxicology*, 40, pp.563–80.

Ohta, M. et al., 2013. Ecto-5′-nucleotidase, CD73, is an endothelium-derived hyperpolarizing factor synthase. *Arteriosclerosis, Thrombosis, and Vascular Biology*, 33(3), pp.629–636.

Oliveira, S.D.D.S., Coutinho-Silva, R. & Silva, C.L.M., 2013. Endothelial P2X7 receptors' expression is reduced by schistosomiasis. *Purinergic Signalling*, 9(1), pp.81–9.

Panupinthu, N. et al., 2008. P2X7 receptors on osteoblasts couple to production of lysophosphatidic acid: A signaling axis promoting osteogenesis. *Journal of Cell Biology*, 181(5), pp.859–871.

Papadopoulou, C. et al., 2008. The role of the chemokines MCP-1, GRO-α, IL-8 and their receptors in the adhesion of monocytic cells to human atherosclerotic plaques. *Cytokine*, 43(2), pp.181–186.

Partridge, J. et al., 2007. Laminar shear stress acts as a switch to regulate divergent functions of NF-kappaB in endothelial cells. *FASEB*, 21(13), pp.3553–61.

Passerini, A.G. et al., 2004. Coexisting proinflammatory and antioxidative endothelial transcription profiles in a disturbed flow region of the adult porcine aorta. *Proceedings of the National Academy of Sciences of the United States of America*, 101(8), pp.2482–7.

Pelegrin, P. & Surprenant, A., 2006. Pannexin-1 mediates large pore formation and interleukin-1beta release by the ATP-gated P2X7 receptor. *The EMBO Journal*, 25(21), pp.5071–82.

Peng, K. et al., 2015. P2X7R is involved in the progression of atherosclerosis by promoting NLRP3 inflammasome activation. *International Journal of Molecular Medicine*, 35, pp.1179–1188.

Pfleger, C. et al., 2012. Detection of caveolin-3/caveolin-1/P2X7R complexes in mice atrial cardiomyocytes in vivo and in vitro. *Histochemistry and cell biology*, 138(2), pp.231–41.

Piscopiello, M. et al., 2013. P2X7 receptor is expressed in human vessels and might play a role in atherosclerosis. *International Journal of Cardiology*, 168(3), pp.2863–2866.

Plendl, J. et al., 1996. Isolation and characterization of endothelial cells from different organs of fetal pigs. *Anatomy and Embryology*, 194(5), pp.445–56.

Qi, Y. et al., 2011. PDGF-BB and TGF-β1 on cross-talk between endothelial and smooth muscle cells in vascular remodeling induced by low shear stress. *Proceedings of the National Academy of Sciences of the United States of America*, 108, pp.1908–1913.

Qian, S. et al., 2016. Deletion of P2Y2 receptor reveals a role for lymphotoxin- α in fatty streak formation. *Vascular Pharmacology*, 85, pp.11–20.

Qin, W.D. et al., 2016. Notch1 inhibition reduces low shear stress-induced plaque formation. *International Journal of Biochemistry and Cell Biology*, 72, pp.63–72.

Qiu, J. et al., 2014. Biomechanical regulation of vascular smooth muscle cell functions: from in vitro to in vivo understanding. *Journal of the Royal Society: Interface*, 11, p.20130852.

Qiu, Y. et al., 2014. P2X7 mediates ATP-driven invasiveness in prostate cancer cells. *PLoS One*, 9(12), pp.1–22.

Qureshi, O.S. et al., 2007. Regulation of P2X4 receptors by lysosomal targeting, glycan protection and exocytosis. *Journal of Cell Science*, 120(Pt 21), pp.3838–49.

Ralevic, V. & Burnstock, G., 1998. Receptors for purines and pyrimidines. *Pharmacological Reviews*, 50(3), pp.413–492.

Ramirez, A.N. & Kunze, D.L., 2002. P2X purinergic receptor channel expression and function in bovine aortic endothelium. *American journal of physiology: Heart and Circulatory Physiology*, 282(6), pp.H2106-16.

Raqeeb, A. et al., 2011. Purinergic P2Y2 receptors mediate rapid Ca2+ mobilization, membrane hyperpolarization and nitric oxide production in human vascular endothelial cells. *Cell Calcium*, 49(4), pp.240–248.

Robinson, L.E. et al., 2014. Plasma membrane cholesterol as a regulator of human and rodent P2X7 receptor activation and sensitization. *The Journal of Biological Chemistry*, 289(4), pp.31983–31994.

Robinson, L.E. & Murrell-Lagnado, R.D., 2013. The trafficking and targeting of P2X receptors. *Frontiers in Cellular Neuroscience*, 7, p.233.

Roy, B., Haupt, L.M. & Griffiths, L.R., 2013. Review: Alternative splicing (AS) of genes as an approach for generating protein complexity. *Current Genomics*, 14(3), pp.182–94.

Rudijanto, A., 2007. The role of vascular smooth muscle cells on the pathogenesis of atherosclerosis. *Acta Medica Indonesiana*, 39(2), pp.86–93.

Sabala, P. et al., 1993. Thapsigargin: potent inhibitor of Ca2+ transport ATP-ase of endoplasmic and sarcoplasmic reticulum. *Acta Biochemica Polonica*, 40(3), pp.309–319.

Sakaki, H. et al., 2013. P2X4 receptor regulates P2X7 receptor-dependent IL-1β and IL-18 release in mouse bone marrow-derived dendritic cells. *Biochemical and Biophysical Research Communications*, 432(3), pp.406–11.

Sathanoori, R. et al., 2016. P2Y2 receptor modulates shear stress-induced cell alignment and actin stress fibers in human umbilical vein endothelial cells. *Cellular and Molecular Life Sciences*, pp.1–16.

Sathanoori, R. et al., 2015. Shear stress modulates endothelial KLF2 through activation of P2X4. *Purinergic Signalling*, 11(1), pp.139–53.

Sathanoori, R. et al., 2015. The ATP receptors P2X7 and P2X4 modulate high glucose and palmitate-induced inflammatory responses in endothelial cells. *PloS One*, 10(5), p.e0125111.

Schachter, J.B. & Harden, T.K., 1997. An examination of deoxyadenosine 5'(alpha-thio)triphosphate as a ligand to define P2Y receptors and its selectivity as a low potency partial agonist of the P2Y1 receptor. *British Journal of Pharmacology*, 121(2), pp.338–44.

Schroder, K. & Tschopp, J., 2010. The Inflammasomes. *Cell*, 140(6), pp.821–832.

Seiffert, K. et al., 2006. ATPgammaS enhances the production of inflammatory mediators by a human dermal endothelial cell line via purinergic receptor signaling. *The Journal of Investigative Dermatology*, 126(5), pp.1017–1027.

SenBanerjee, S. et al., 2004. KLF2 Is a novel transcriptional regulator of endothelial proinflammatory activation. *The Journal of Experimental Medicine*, 199(10), pp.1305–15.

Serbanovic-Canic, J. et al., 2016. Zebrafish Model for Functional Screening of Flow-Responsive Genes. *Arteriosclerosis, Thrombosis, and Vascular Biology*, p.ATVBAHA.116.308502.

Shishikura, Y. et al., 2016. Extracellular ATP is involved in dsRNA-induced MUC5AC production via P2Y2R in human airway epithelium. *Respiratory research*, 17(1), p.121.

Shyy, J.Y.J. & Chien, S., 2002. Role of integrins in endothelial mechanosensing of shear stress. *Circulation Research*, 91(9), pp.769–775.

Skaper, S.D., Debetto, P. & Giusti, P., 2009. P2X(7) Receptors in Neurological and Cardiovascular Disorders. *Cardiovascular Psychiatry and Neurology*, 2009, p.861324.

Skaper, S.D., Debetto, P. & Giusti, P., 2010. The P2X7 purinergic receptor: from physiology to neurological disorders. *FASEB*, 24(2), pp.337–45.

Sluyter, R. & Stokes, L., 2011. Significance of P2X7 receptor variants to human health and disease. *Recent Patents on DNA & Gene Sequences*, 5(1), pp.41–54. Available at: http://www.ncbi.nlm.nih.gov/pubmed/21303345.

Smedlund, K. & Vazquez, G., 2008. Involvement of native TRPC3 proteins in ATP-dependent expression of VCAM-1 and monocyte adherence in coronary artery endothelial cells. *Arteriosclerosis, Thrombosis, and Vascular Biology*, 28(11), pp.2049–55.

Sobrevia, L., Yudilevich, D.L. & Mann, G.E., 1997. Activation of A2-purinoceptors by adenosine stimulates L-arginine transport (system y+) and nitric oxide synthesis in human fetal endothelial cells. *The Journal of Physiology*, 499(1), pp.135–40.

Solini, A. et al., 1999. Human primary fibroblasts in vitro express a purinergic P2X7 receptor coupled to ion fluxes, microvesicle formation and IL-6 release. *Journal of Cell Science*, 112, pp.297–305.

Sorge, R.E. et al., 2012. Genetically determined P2X7 receptor pore formation regulates variability in chronic pain sensitivity. *Nature Medicine*, 18(4), pp.595–599.

Stachon, P. et al., 2016. Extracellular ATP induces vascular inflammation and atherosclerosis via P2Y2 in mice. *Arteriosclerosis, Thrombosis, and Vascular Biology*, p.ATVBAHA.115.307397.

Stachon, P. et al., 2014. P2Y6 deficiency limits vascular inflammation and atherosclerosis in mice. *Arteriosclerosis, Thrombosis, and Vascular Biology*, 34(10), pp.2237–2245.

Stock, T.C. et al., 2012. Efficacy and safety of CE-224,535, an antagonist of P2X7 receptor, in treatment of patients with rheumatoid arthritis inadequately controlled by methotrexate. *Journal of Rheumatology*, 39(4), pp.720–727.

Suh, B.C. et al., 2001. P2X7 nucleotide receptor mediation of membrane pore formation and superoxide generation in human promyelocytes and neutrophils. *Journal of Immunology*, 166(11), pp.6754–63.

Sun, X. et al., 2016. Activation of integrin α5 mediated by flow requires its translocation to membrane lipid rafts in vascular endothelial cells. *Proceedings of the National Academy of Sciences*, 113(3), p.201524523.

Suo, J. et al., 2007. Hemodynamic shear stresses in mouse aortas: Implications for atherogenesis. *Arteriosclerosis, Thrombosis, and Vascular Biology*, 27(2), pp.346–351.

Surprenant, a et al., 1996. The cytolytic P2Z receptor for extracellular ATP identified as a P2X receptor (P2X7). *Science*, 272(5262), pp.735–8.

Syberg, S. et al., 2012. Genetic background strongly influences the bone phenotype of P2X7 receptor knockout mice. *Journal of Osteoporosis*, 2012.

Taylor, E.M. et al., 1989. The effects of adenosine triphosphate and related purines on arterial resistance vessels in vitro and in vivo. *European Journal of Pharmacology*, 161, pp.121–133.

Taylor, V. & Suter, U., 1996. Epithelial membrane protein-2 and epithelial membrane protein-3: Two novel members of the peripheral myelin protein 22 gene family. *Gene*, 175(1–2), pp.115–120.

van Thienen, J. V. et al., 2006. Shear stress sustains atheroprotective endothelial KLF2 expression more potently than statins through mRNA stabilization. *Cardiovascular Research*, 72(2), pp.231–240.

Townsend, N. et al., 2015. *Cardiovascular Disease Statistics 2015*,

Verma, S. et al., 2015. Colchicine in cardiac disease: a systematic review and meta-analysis of randomized controlled trials. *BMC Cardiovascular Disorders*, 15(1), p.96.

Virginio, C. et al., 1999. Kinetics of cell lysis, dye uptake and permeability changes in cells expressing the rat P2X7 receptor. *The Journal of Physiology*, 519(2), pp.335–346.

Visovatti, S.H. et al., 2016. Purinergic dysregulation in pulmonary hypertension. *American Journal of Physiology: Heart and Circulatory Physiology*, 311(1), pp.H286–H298.

Wadehra, M. et al., 2005. Epithelial membrane protein-2 regulates surface expression of αvβ3 integrin in the endometrium. *Developmental Biology*, 287(2), pp.336–345.

Wadehra, M. et al., 2002. The tetraspan protein epithelial membrane protein-2 interacts with β1 integrins and regulates adhesion. *Journal of Biological Chemistry*, 277(43), pp.41094–41100.

Wadehra, M., Goodglick, L. & Braun, J., 2004. The tetraspan protein EMP2 modulates the surface expression of caveolins and glycosylphosphatidyl inositol-linked proteins. *Molecular Biology of the Cell*, 15, pp.2073–2083.

Wan, X. et al., 2016. Loss of Epithelial Membrane Protein 2 aggravates podocyte injury via upregulation of Caveolin-1. *Journal of the American Society of Nephrology*, 27, pp.1066–1075.

Wang, C.X. et al., 2001. Epithelial membrane protein 2, a 4-transmembrane protein that suppresses B-cell lymphoma tumorigenicity. *Blood*, 97(12), pp.3890–3895.

Wang, H. et al., 2015. P2RX7 sensitizes Mac-1/ICAM-1-dependent leukocyte-endothelial adhesion and promotes neurovascular injury during septic encephalopathy. *Cell Research*, 25(6), pp.674–690.

Wang, L. et al., 2002. P2 receptor expression profiles in human vascular smooth muscle and endothelial cells. *Journal of Cardiovascular Pharmacology*, 40(6), pp.841–53.

Wang, S. et al., 2016. Endothelial cation channel PIEZO1 controls blood pressure by mediating flow-induced ATP release. *Journal of Clinical Investigation*, 126(12), pp.4527–4536.

Wang, S. et al., 2015. P2Y2 and Gq /G11 control blood pressure by mediating endothelial mechanotransduction. *Journal of Clinical Investigation*, 125(8), pp.3077–3086.

Wang, T. et al., 2006. Cholesterol loading increases the translocation of ATP synthase beta chain into membrane caveolae in vascular endothelial cells. *Biochimica et Biophysica Acta*, 1761(10), pp.1182–90.

Warboys, C.M. et al., 2014. Disturbed flow promotes endothelial senescence via a p53-dependent pathway. *Arteriosclerosis, Thrombosis, and Vascular Biology*, 34(5), pp.985–95.

Warboys, C.M. et al., 2011. The role of blood flow in determining the sites of atherosclerotic plaques. *F1000 Medicine Reports*, 3(5), pp.1–8.

Weinhold, K. et al., 2010. Interaction and interrelation of P2X7 and P2X4 receptor complexes in mouse lung epithelial cells. *Cellular and Molecular Life Sciences*, 67(15), pp.2631–42.

Weisman, G.A. et al., 2006. P2 receptors in health and disease. *Biotechnology & Genetic Engineering Reviews*, 22, pp.171–95.

Wildman, S.S., Unwin, R.J. & King, B.F., 2003. Extended pharmacological profiles of rat P2Y2 and rat P2Y4 receptors and their sensitivity to extracellular H+ and Zn2+ ions. *British Journal of Pharmacology*, 140(7), pp.1177–86.

Wilson, H.L. et al., 2002. Epithelial membrane proteins induce membrane blebbing and interact with the P2X7 receptor C terminus. *The Journal of Biological Chemistry*, 277(37), pp.34017–23.

Wilson, H.L. et al., 2007. P2X receptor characterization and IL-1/IL-1Ra release from human endothelial cells. *British Journal of Pharmacology*, 151(1), pp.115–27.

Wilson, H.L. et al., 2004. Secretion of intracellular IL-1 receptor antagonist (type 1) is dependent on P2X7 receptor activation. *Journal of Immunology*, 173(2), pp.1202–8.

Wu, W. et al., 2011. Flow-dependent regulation of krüppel-like factor 2 is mediated by MicroRNA-92a. *Circulation*, 124(5), pp.633–641.

Wyatt, A.W. et al., 2002. Early activation of the p42/p44MAPK pathway mediates adenosine-induced nitric oxide production in human endothelial cells: a novel calcium-insensitive mechanism. *FASEB*, 16(12), pp.1584–1594.

Xiao, H. et al., 2013. Sterol regulatory element binding protein 2 activation of NLRP3 inflammasome in endothelium mediates hemodynamic-induced atherosclerosis susceptibility. *Circulation*, 128(6), pp.632–642.

Xingjuan, C. et al., 2016. Endothelial Cell–Specific Deletion of P2Y $_2$ Receptor Promotes Plaque Stability in Atherosclerosis-Susceptible ApoE-Null Mice. *Arteriosclerosis, Thrombosis, and Vascular Biology*, p.ATVBAHA.116.308561.

Yamamoto, K. et al., 2003. Endogenously released ATP mediates shear stress-induced Ca2+ influx into pulmonary artery endothelial cells. *American Journal of Physiology: Heart and Circulatory Physiology*, 285(2), pp.H793-803.

Yamamoto, K. et al., 2000. Fluid shear stress activates Ca2+ influx into human endothelial cells via P2X4 purinoceptors. *Circulation Research*, 87(5), pp.385–391.

Yamamoto, K. et al., 2006. Impaired flow-dependent control of vascular tone and remodeling in P2X4-deficient mice. *Nature Medicine*, 12(1), pp.133–7.

Yamamoto, K. et al., 2007. Involvement of cell surface ATP synthase in flow-induced ATP release by vascular endothelial cells. *American Journal of Physiology: Heart and Circulatory Physiology*, 293, pp.H1646–H1653.

Yamamoto, K. et al., 2000. P2X(4) receptors mediate ATP-induced calcium influx in human vascular endothelial cells. *American Journal of Physiology: Heart and Circulatory Physiology*, 279(1), pp.H285-92.

Yamamoto, K. et al., 2011. Visualization of flow-induced ATP release and triggering of Ca2+ waves at caveolae in vascular endothelial cells. *Journal of Cell Science*, 124(20), pp.3477–83.

Young, M.T., Pelegrin, P. & Surprenant, A., 2006. Identification of Thr283 as a key determinant of P2X7 receptor function. *British Journal of Pharmacology*, 149(3), pp.261–268.

Yu, J. et al., 2006. Direct evidence for the role of caveolin-1 and caveolae in mechanotransduction and remodeling of blood vessels. *Journal of Clinical Investigation*, 116(5), pp.1284–1291.

Zakkar, M. et al., 2008. Increased endothelial mitogen-activated protein kinase phosphatase-1 expression suppresses proinflammatory activation at sites that are resistant to atherosclerosis. *Circulation Research*, 103(7), pp.726–32.

Zernecke, A. et al., 2006. CD73/Ecto-5′-nucleotidase protects against vascular inflammation and neointima formation. *Circulation*, 113(17), pp.2120–2127.